

THE EFFECT OF ACTIVE SUSPENSION CONTROL
ON VEHICLE RIDE BEHAVIOUR

by

Magdy Bekhit Abdou Abdel Hady

B.Sc., M.Sc., Mech. Eng.

A dissertation submitted in accordance with
the requirements for the degree of
Doctor of Philosophy

Department of Mechanical Engineering
The University of Leeds

November 1989

ABSTRACT

This work is concerned with a theoretical investigation into the ride behaviour of actively suspended vehicles. It is based on the concept of developing control laws for active suspension systems fitted to full vehicle models and then comparing the performances of competing systems using a fair basis for comparison. A review of published work was revealed the need for further work on active control laws for full vehicle models. Theoretical techniques necessary to generate random road profiles and various methods for evaluating vehicle ride response are explained. This is followed by an evaluation of the performance of the passive suspension systems. Techniques for obtaining control laws for an active suspension implemented at all four wheel stations of a vehicle are outlined. It is shown that the classical control law based on ignoring the correlation between the road inputs can be replaced by one which involves limited state feedback and includes the effect of the wheelbase time delay. Performance of this system is better than the system which ignores the time delay and almost as good as that of the full state feedback active system with time delay. In addition, it is much more attractive in terms of its practical implementation. The general strategy of keeping seat accelerations, dynamic tyre load under control and the fore/aft and lateral dynamic tyre load transfers is used, within the realistic design constraint of a specified amount of available working space. The effect of road surface representation, including the cross correlation and the measurement errors in deriving the control laws is examined. Finally the performances of all the active suspensions considered are compared with those obtained from passive systems and conclusions and recommendations for future work are made.

ACKNOWLEDGEMENTS

I would like to express my most sincere gratitude to **Dr. D.A. Crolla**, for his constant guidance, friendliness, encouragement and his most invaluable suggestions and comments during the research work. I would also like to thank **Mr. D. Horton** for all his help and assistance, and in particular for the use of his excellent plot package.

I would also like to express my deep gratitude and thanks to the **Egyptian Government** who made this scholarship available and financially supported me throughout the period of this study.

My thanks are also extended to all the academic staff and the secretaries of the Mechanical Engineering Department at Leeds University for their help and kindness.

Special gratitude and appreciation are due to my wife and my children Ahmed, Shereen and my family for their patience, understanding and support through the years of this research.

To the Soul of My Father

TABLE OF CONTENTS

| | Page |
|---|------|
| ABSTRACT | i |
| ACKNOWLEDGEMENTS | ii |
| TABLE OF CONTENTS | iv |
| | |
| Chapter 1 : INTRODUCTION AND REVIEW OF PREVIOUS | |
| WORK | 1 |
| 1.1 Introduction | 1 |
| 1.2 Review of previous work | 4 |
| 1.2.1 Mathematical models of vehicle and road surface | 4 |
| 1.2.2 Passive suspension systems | 7 |
| 1.2.3 Active suspension systems | 9 |
| 1.2.4 Comparison studies of the various suspension systems | 15 |
| 1.3 Critical summary and conclusions | 17 |
| | |
| Chapter 2 : FUNDAMENTALS OF MODELLING VEHICLE RIDE | |
| BEHAVIOUR | 23 |
| 2.1 Introduction | 23 |
| 2.2 Generation of random road profiles | 24 |
| 2.3 Equations of motion | 26 |
| 2.4 Analysis of linear systems | 31 |
| 2.4.1 Frequency response | 31 |
| 2.4.2 Response to amplitude spectral density ground inputs | 33 |
| 2.5 Non-linear analysis | 35 |

| | |
|---|-----------|
| 2.6 Output variables | 36 |
| 2.7 System response calculation and computational procedure | 38 |
| 2.8 Concluding remarks | 39 |
| Chapter 3 : PASSIVE SUSPENSION SYSTEMS | 45 |
| 3.1 Introduction | 45 |
| 3.2 Results | 47 |
| 3.3 Discussions of results | 48 |
| 3.4 The effect of passive system adaptation | 52 |
| 3.3 Concluding remarks | 54 |
| Chapter 4 : APPLICATION OF LINEAR CONTROL THEORY TO VEHICLE PROBLEMS | 79 |
| 4.1 Introduction | 79 |
| 4.2 Uncorrelated road input case | 82 |
| 4.2.1 Full state information available | 82 |
| 4.2.1.1 Filtered white noise case | 82 |
| 4.2.1.2 Integrated white noise case | 85 |
| 4.2.2 Limited state feedback available | 86 |
| 4.2.2.1 Gradient search method | 86 |
| 4.2.2.2 Kalman filter algorithm | 88 |
| 4.3 Correlated road input case | 89 |
| 4.3.1 Full state information available | 89 |
| 4.3.1.1 Filtered white noise case | 89 |
| 4.3.1.1.1 Correlation between the right and left tracks | 89 |
| 4.3.1.1.2 Time delay between the front and rear wheels | 91 |

| | |
|---|------------|
| 4.3.1.2 Integrated white noise case | 96 |
| 4.3.2 Limited state feedback available | 97 |
| 4.4 Computer software preparation | 98 |
| 4.5 Example solutions | 99 |
| 4.5.1 Uncorrelated road input case | 99 |
| 4.5.2 Correlated road input case | 105 |
| 4.5.3 Kalman filter algorithm | 107 |
| 4.6 Concluding remarks | 109 |
| | |
| Chapter 5 : EFFECT OF MODELLING DETAILS ON THE PERFORMANCE OF THE ACTIVELY SUSPENDED VEHICLE | 112 |
| 5.1 Introduction | 112 |
| 5.2 Effect of cross correlation | 113 |
| 5.3 Effect of time delay approximation | 116 |
| 5.3.1 Vehicle model and equations of motion | 116 |
| 5.3.2 Identification of the time delay approximation by discrete optimal control theory | 118 |
| 5.3.3 Identification of the time delay approximation by linear ride calculations | 119 |
| 5.4 Decoupled vehicle model studies | 120 |
| 5.5 Concluding remarks | 122 |
| | |
| Chapter 6 : FULL STATE FEEDBACK ACTIVE SUSPENSION SYSTEMS | 133 |
| 6.1 Introduction | 133 |
| 6.2 Equations of motion | 135 |
| 6.3 Results | 138 |
| 6.4 Discussion of results | 139 |
| 6.4.1 Effect of ground surface representation ... | 139 |

| | |
|---|---------|
| 6.4.2 Effect of various types of feedback information | 142 |
| 6.4.3 The effect of the working space available . | 143 |
| 6.4.4 The effect of wheelbase time delay | 143 |
| 6.4.5 Discussion of some of the practical limitations of the full state feedback active systems .. | 146 |
| 6.5 Active system adaptation | 149 |
| 6.6 Concluding remarks | 151 |
| Chapter 7 : LIMITED STATE FEEDBACK ACTIVE SUSPENSION SYSTEMS | 196 |
| 7.1 Introduction | 196 |
| 7.2 Equations of motion | 198 |
| 7.3 Accuracy of the calculations in the time domain | 200 |
| 7.4 Effect of the wheelbase time delay | 202 |
| 7.5 The effect of measurement errors | 203 |
| 7.6 Concluding remarks | 208 |
| Chapter 8 : PERFORMANCE COMPARISONS OF PROPOSED SYSTEMS | 233 |
| 8.1 Introduction | 233 |
| 8.2 Comparison of the performance at equal usage of working space | 235 |
| 8.2.1 Overall performance comparison | 235 |
| 8.2.2 Effect of ground description/control strategy | 236 |

| | |
|--|------------|
| 8.2.3 Effect of full/limited state feedback | 238 |
| 8.3 effect of adaptation | 239 |
| 8.4 Concluding remarks | 240 |
| Chapter 9 : CONCLUSIONS AND FUTURE WORK | 265 |
| 9.1 Conclusions | 265 |
| 9.2 Future work | 275 |
| NOMENCLATURE | 277 |
| REFERENCES | 283 |

CHAPTER 1

INTRODUCTION AND REVIEW OF PREVIOUS WORK

1.1 Introduction.

The main functions of an automotive suspension system are to provide vehicle support, stability and directional control during handling manoeuvres and to provide effective isolation from road disturbances. These different tasks result in conflicting design requirements. Directional control and stability require a suspension that is neither very stiff nor very soft. Insensitivity to external loads requires a stiff suspension, whereas good ride comfort demands a soft suspension.

Passive suspension systems (encountered in the majority of current vehicles) consist of conventional elements such as coil or leaf springs and viscous dampers. In most of these systems, neither the rates of the spring nor the dampers are capable of being changed by external signals. Hence, the designer is faced with the problem of choosing fixed values of suspension stiffness and damping parameters, which inevitably involves a difficult compromise in view of the wide range of conditions over which a vehicle operates. Therefore, more recent developments of passive suspension systems have involved self-levelling systems and/or adjustable dampers. Furthermore, with recent advances in micro electronics and actuators, there has been an upsurge of

interest in the concept of active suspension control.

In the active systems, actuators are fitted in place of, or in addition to, the usual passive elements. The actuators operate in response to force demand signals generated from a microprocessor on the basis of measured information about the vehicle response and the road input. Thus, these systems require external power sources, measuring and sensing instruments, signal conditioning and amplifying devices. Active suspensions offer the potential for being adapted to the quality of the road surface, vehicle speed and different safety and comfort requirements, with the choice being selected either by the driver or by an adaptive control algorithm embodied in a microcomputer.

Advances in modern computer facilities either in the hardware design or in the preparation of software, provide a good opportunity for theoretical analysis to be used as an aid to practical system design. This enables the study of the effects of parameter changes at the design stage and hence reduces the development costs. At the University of Leeds, Horton [1988] developed a suite of computer programs called VDAS for solving both linear and non-linear vehicle ride and handling problems. In this package, several options are available covering most computational schemes of interest such as eigensolutions, frequency responses, responses to idealised ground inputs and simulation in the time domain. Some other large computer programs such as MEDYNA [1986] and ADAMS [1984] are also available. These packages can be used to deal with

complex simulations which involve multibody systems with large numbers of degrees of freedom as well as the simple vehicle models.

Theoretical investigations in vehicle system dynamics are based on mathematical models. The mathematical models can be obtained either by application of the fundamental laws of physics to an idealised representation of the real technical system or by evaluation of measurements performed on the real technical system itself or on parts of it. The quality of the theoretical results is only as good as the underlying mathematical model. Thus, the mathematical models must be as complete and accurate as necessary. On the other hand, from the computational point of view these models must be simple and easy to handle as possible. In general, the dynamic analysis of deterministic and random vehicle vibrations and the consequences especially to ride comfort requires consideration of the following factors. The first one is the modelling of vehicle and road roughness, the second point is the prediction of vehicle response to road excitations, the third one is the prediction of passenger response to vibration exposure and the final one is the optimisation of the suspension systems. In addition, when actively controlled systems are under investigation, the development of control strategies will need to be considered.

In the next sections, the first three subproblems are discussed, then some of the studies concerning the analysis

and the optimisation of the passive and active suspension systems are reviewed. Finally, the critical summary and concluding remarks obtained from this review are outlined.

1.2 Review of previous work.

1.2.1 Mathematical models of vehicle and road surface.

Consider first, the mathematical description of the road surface. Actual road surface measurements have been described statistically by simple spectral density formulation. A commonly employed model for the road surface considers the amplitude to be Gaussian, having a power spectral density of the form:

$$psd(\lambda) = \frac{R_c}{\lambda^\kappa} \quad \dots(1.1)$$

where λ is the wavenumber (cycle/m) and R_c is the road roughness coefficient. Values of R_c corresponding to different road surfaces can be found in Robson [1979]. The exponent κ may range typically between 1.5 and 3, and some formulae for $psd(\lambda)$ have different values of κ for different ranges of wavenumber. The spectral density given in (1.1) is not valid at very low wavenumbers and some modifications to the spectrum at low wavenumbers have been proposed. In these, a cutoff wavenumber λ_0 is included such that $psd(\lambda)$ is constant for $\lambda < \lambda_0$. If the same surface is now traversed at a constant forward speed V , then equation (1.1) may be re-written as:

$$psd(f) = R_c V^{\kappa-1} / f^\kappa \quad \dots(1.2)$$

where f is the frequency (cycle/sec). For the optimisation problem discussed later the exponent κ is assumed to be 2. Hence equation (1.2) becomes:

$$psd(f) = R_c V / f^2 \quad \dots(1.3)$$

This equation represents the power spectral density of an integrated white noise. Other excitation models which are given by stationary Gaussian coloured noise processes obtained from a white noise process $w(t)$ by means of a shape filter are widely used. Clear examples of using first and third order shaping filters appear in Hac [1985] and [1987] respectively. Finally, the road surface irregularities may be presented in the time domain by applying the inverse Fourier transform to the spectral density function (1.1). Techniques for generating single random profile and two correlated parallel tracks are given in Cebon and Newland [1983].

During the past twenty years a number of linear and non-linear suspension models have been proposed to study the effect of suspension design on ride and handling improvements. The models range in complexity from simple quarter vehicle models to complex multi degree of freedom models. The following assumptions are made in deriving the equations of motion of the linear suspension models. The sprung mass is considered to be a rigid body as are similarly all unsprung masses. The available working space is large enough so that the suspension always operates without contacting the bump stops. The tyres are assumed to be in constant contact with the road surface and are modelled as linear springs (sometimes damping elements

are included). The front and rear suspensions are modelled as linear spring and damper units with the possible addition of anti-roll bars.

Healey et al [1977] studied the validity of some of these linear models using actual measured road roughness profiles. The linear models were the 2 d.o.f. quarter car model, the bounce and pitch 4 d.o.f. half vehicle model and the three dimensional 7 d.o.f. vehicle model. In their study, the roughness inputs and the acceleration at the body connection points were measured for different quality roadways. Using these measurements, they showed that the seven degree of freedom model predicts more accurately the vehicle acceleration in the low frequency range (up to 10 Hz). They attributed the discrepancies which appeared over 10 Hz to excitation from tyre unevenness.

The next problem is to combine the input, described either in the frequency or time domain, with the vehicle model to obtain the output of interest. A good and clear review of this part is given in Horton [1986]. Most details about this problem can be found in the next chapter.

The last stage in developing ride models is the prediction of the passenger response to vibration exposure. This is necessary since the human body itself has a vibrating structure, recognizing vibrations of the same strength but with various frequencies differently. This means that between physical measures and subjective perception there exists a frequency transfer function. The well-known ISO curves were

developed in [1974] to attempt to characterise the effect of vibration on human beings. In the case of evaluating the driver's seat accelerations in the frequency domain, the frequency weighting shown in Fig. 1.1 may be applied to the output spectral densities. In the case of time domain simulations, two alternative methods are available. The first method is based on using shaping filters. The parameters of these shaping filters depend on the direction of the acceleration. According to the International Standard ISO 2631 [1974] the frequency response of the shaping filter for the longitudinal acceleration exposure of the human body is given by Fig. 1.2. The filter equations and parameters can be found in Muller [1982]. The second method is based on processing the time histories of the accelerations into the frequency domain to give spectral densities to which the standard ISO weighting functions can then be applied.

1.2.2 Passive suspension systems.

Passive suspension systems have been studied by Ryba in a series of two papers [1974 a] and [1974 b]. He first employed a two mass quarter car model [1974 a] to investigate the effect of natural frequency of the sprung mass on ride comfort, dynamic tyre load and suspension working space. He concluded that the possible improvements in ride comfort which can be achieved by a low natural frequency of the sprung mass are associated with an increase in dynamic tyre load and suspension working space. Ryba [1974 b] studied various configurations for a three mass system representation consisting of an

additional mass attached to the sprung mass and/or the unsprung mass. He concluded that it is possible to reach a high degree of ride comfort without deterioration in the contact between wheels and road by using a dynamic absorber of mass equal to the wheel mass, but incorporating an auxiliary mass equal to the unsprung mass seems to be impractical.

In a more recent paper, the two and three mass systems were studied by Sharp and Hassan [1984]. In each system two reasonable values of the unsprung masses equal to $1/8$ and $1/5$ of the sprung mass were employed. In the three mass system an absorber mass amounting only to 10% of each unsprung mass was notionally attached to the wheel mass. The optimal suspension and absorber parameters (stiffness and damping coefficients) were calculated for each absorber mass ratio by a simplex minimisation procedure. They concluded that neither the reduction of the unsprung mass nor the addition of a dynamic absorber appeared to be cost effective. This, they stated, was due to the slight improvements achieved in ride comfort and dynamic tyre load compared with the practical difficulty of fitting this dynamic absorber mass to any actual system.

Real vehicles operate over a wide range of running conditions, i.e. surfaces and speeds. It is however clear that the fixed parameter passive system must be a compromise and cannot perform as well as an adaptive system which is able to choose its parameters to match each particular running condition. In principle, the passive system could be adaptive if a number of discrete spring and damper rates could be provided. However,

from a practical point of view, it is a big problem to make the passive system adaptive. In particular an attractive method of providing a range of spring stiffnesses in practice has yet to be found. Recent developments in the suspension designs proposed by the vehicle manufacturers were reviewed by Sharp and Crolla [1987 b]. New designs involving the use of self-levelling devices and/or switchable dampers were explained and the improvements achieved from these designs were outlined. In brief, with these modifications, only modest improvements in performance were available. In other words, using concepts involving major changes of principle, e.g. active suspension systems, may be the only available way for further significant improvements.

1.2.3 Active suspension systems.

The optimisation problem of active suspension systems have been studied in many investigations. However, most of these investigations have been based on the quarter car model. Over the last few years, the subject has been reviewed by Hedrick and Wormley [1975], Morman and Giannopoulos [1982] and more recently by Goodall and Kortum [1983]. The basic ideas in the active suspension optimisation are as follows. The road surface is the source of excitation and often described as integrated or filtered white noise. Ride comfort of a vehicle can be described in terms of the body acceleration. The suspension is assumed to operate without contacting the bump stops, i.e.

within the available working space, to maintain linearity. The dynamic tyre load must be kept low for good directional control.

The active suspension problem is addressed by Thompson [1976] using the two degree of freedom quarter car model. His control strategy relies on perfect knowledge of the absolute velocities of the body and wheel as well as their positions relative to the ground. The optimal control law was derived using state space techniques for a unit step input or integrated white noise.

In Hac [1985] the two degree of freedom quarter car model was also used but the road surface was described as filtered white noise. Linear passive suspension elements (spring and damper) are fitted in parallel with the actuator. In deriving the control law, perfect measurements of all the states as well as the road input were assumed. In his analysis, it was found that the use of properly chosen passive elements in parallel to the actuator reduces the control forces without influencing the performance of the active system.

Previous investigations essentially treated the suspension design as an optimal control problem with full state feedback capabilities. One of the practical difficulties in using the active system introduced by Thompson [1976] is the need to measure the body and wheel positions relative to the road. This difficulty is due to the fact that most of the possible methods of measurements are either too expensive or do not work reliably on all the types of road surfaces. In Hac [1985],

the most important practical limitation is the need to measure the road profile height. Therefore, there has been a movement to use the concept of the limited state feedback active suspension systems. In these systems, the classical optimal control law based on full state feedback is replaced by one which involves limited state feedback - omitting, in particular, the ground input information - and one which may involve measurement errors.

Again, the problem was studied by Thompson [1984]. The quarter car model was used, but with a suspension spring of arbitrary stiffness fitted in parallel with the actuator. The control law of the limited state feedback active system was restricted by constraints involved in the selection of the performance index weighting parameters. The result achieved was the replacement of a road surface height sensor by one measuring the relative displacement. Thompson found that this simplification did not affect the performance significantly.

In more recent work, Wilson et al [1986] formulated the optimisation problem of limited state feedback active systems using a gradient search technique. In their study, the two degree of freedom quarter car model was used and the road surface was described either as integrated white noise or as filtered white noise. For the integrated white noise description, the control laws were derived after applying a standard coordinate transformation. The main advantage of their method is the avoidance of the difficulty which arose in Thompson [1984] from selecting the weighting parameters in a special way. Furthermore, different configurations of

these limited state active systems were introduced. For example, the optimal control law was found for the case in which only the difference between the body and wheel velocity is available and not their individual values. They showed that if the road surface is described as a filtered white noise the gradient search technique can be applied to the problem without the need for a coordinate transformation arising.

Although the quarter car model has proved useful for understanding control strategies, it does not reflect the coupling between the various degrees of freedom e.g. between pitch, bounce and roll. Nor does it include the correlation between the input at each side of the vehicle from two parallel tracks. Furthermore, it might be expected in principle that in controlling the rear suspension, there was some advantage to be gained from knowing in advance what had happened at the front suspension. Hence, it is necessary to use at least the 2D "bicycle" model to develop the optimal control laws of the active suspension systems. The use of the quarter car model to obtain the control law for a decoupled "bicycle" model might be expected to lead to sub-optimal control laws. Hence, the real benefits which could be available from those active systems will not be achieved. For these reasons attempts have been made to extend the control strategies using two or three dimensional vehicle models.

Thompson and Pearce [1979] used the bounce and pitch four degree of freedom vehicle model. Perfect knowledge of all the state variables was assumed in deriving the control law. It

was found that the speed dependent time delay between the road inputs at the front and rear suspensions did not affect the optimal control law. Unfortunately, this is not the optimal case. The comments about this conclusion will be discussed later.

Fruhauf et al [1986] were the first to formulate the optimisation problem of the active suspension using a three dimensional vehicle model. The inclusion of the time delay between the front and rear inputs was introduced by means of a Pade approximation of fourth order. The Kalman filter algorithm was used to estimate the states which cannot be measured directly. Furthermore, the installation of two sensors which look ahead of the front wheels was considered in deriving the control strategies and examining the vehicle response. Their results showed that the active systems dramatically reduce the seat acceleration and the dynamic tyre load when compared with the passive suspension systems. However, it is felt that the use of large working space in the active systems rather than that used by the passive one is the reason behind these unusually large improvements. In addition, the following comments and questions related to their work are made:

- 1- Some aspects of the problem formulation are not completely straightforward, and the requirements for the effective formulations of the time delay representation and the preview control strategy in deriving the control laws remain somewhat unclear.

- 2- Since the Pade approximation was used in developing the

control laws for the active systems, these systems are not optimal in the sense of optimal control theories. Hence, the question arises of how far these systems are from the optimal system ?.

Recently, Louam et al [1988] applied the discrete linear quadratic regulator theory to the four degree of freedom bounce and pitch half vehicle model. The road surface was described as integrated white noise and the time delay between the front and rear inputs was considered in deriving the control law. Their results showed that, using enough samples to reach the continuous case, the overall performance index was reduced by 25% when compared with that calculated based on Thompson's control law [1979], providing that a perfect knowledge of feed forward information relating to the road profile was available. It is however clear that the optimal control law depends on the time delay between the front and rear inputs and hence on the vehicle speed. Therefore, the conclusion derived by Thompson and Pearce [1979] which indicated that the optimal control law is speed independent is incorrect. Louam et al attributed two reasons for this wrong conclusion. Firstly, the optimal control law derived by Thompson and Pearce was constrained through the implicit assumption that it depended only on the vehicle states. Secondly, the argument leading to the conclusion of optimality requiring that the matrix $\Gamma(t)$ in the inequality (40) of Thompson and Pearce [1979] be always non-negative is not achievable. Regardless of the practical implications arising in Louam et al [1988] either from using discrete optimal

control law or introducing system states which cannot be measured directly, this work seems to be the only available optimal solution to the optimisation problem.

1.2.4 Comparison studies of the various suspension systems

Many analytical studies have been proposed to consider the benefits which could be achieved from active suspension systems over the passive suspension systems. The subject has been reviewed by Sharp and Crolla [1987 a] and [1987 b]. As in the case of developing control strategies, most of the investigations studying the benefits of the active system have been based on the quarter car model. For example Sharp and Hassan [1986] introduced a method to enable a range of active and passive suspension systems to be compared on an equitable basis, that is, equal usage of working space. In their study the full state feedback active system was found to provide the best overall performance in terms of ride behaviour but other limited state feedback and semi-active systems were found to give similar performance with potentially fewer practical problems involved in the necessary hardware. Another example appears in Crolla and Abouel-Nour [1988], where the performance indices have been extended to identify the power required in the actuators of various active systems.

However, to date few investigations based on a three dimensional vehicle model have been published. Barak and Sachs [1986] compared the performance of active and semi-active suspension systems having full state feedback, with the conventional passive system, using a three dimensional 7

d.o.f. model. The semi-active suspension was fitted with a passive suspension damper, and the control strategy was treated as a stochastic linear optimal regulator problem and perfect knowledge of all the states was assumed. They ignored the effect of the correlation between the front and rear inputs in deriving the control laws. Hence the active and semi-active systems introduced in their study are sub-optimal systems. The semi-active system was found to be superior to the passive system with performance approaching that of the fully active system. They identified a penalty cost associated with these ride comfort improvements as an increase in working space and dynamic tyre load. However, a comparison carried out on this basis is not revealing since it is impossible to weight the value of gains on some aspects of performance with losses in other areas. Indeed, only few comparative investigations carried out on an equitable basis are available. For example, Chalasani [1986 a] and [1986 b], prefers to compare the active and passive systems at equal usage of working space. Such a comparison is a justifiable one if the passive systems employed are adaptive. If a fixed parameter passive system is employed, a more equitable basis for performance comparison is by considering different vehicle operating conditions, in which the adaptive active and passive suspension systems are always able to consume all the available working space while it is impossible for the fixed parameter passive suspension to do so. This will enable the benefits from fitting an active system to a full vehicle to be accurately established.

In a parametric study, Malek and Hedrick [1986] compared the performance capabilities of different configurations of full state feedback active systems with those of a conventional passive one. As in Barak and Sachs [1986] a three dimensional 7 d.o.f vehicle model was considered, perfect knowledge of the states were assumed and the correlation between the front and rear inputs was neglected. The main limitation of their study was that only a frequency response analysis was used to evaluate the performance of the various systems. The fully active system having the control forces which were functions of the relative displacements and velocities at all four corners, as well as the absolute velocities of the sprung mass at all four corners was found to be the best performing system.

1.3 Critical summary and conclusions.

The following points are made from the above review.

1- Almost all the efforts which have been directed towards analysis and optimising the active systems were based on the quarter car model. However, this model does not reflect the coupling between the various degrees of freedom in deriving the control law. Nor does it include the cross correlation and the time delay between the road inputs. Therefore, a more realistic model, e.g. bounce and pitch half vehicle model or the three dimensional vehicle model, should be considered in designing the control strategy of the active systems. Which model is taken depends on the effect of including the roll motion and the cross correlation in deriving the control laws

on the performance of the active systems. This effect has yet to be found.

2- Few investigations based on the three dimensional vehicle model have been published. Most of these studies did not consider the time delay and cross correlation in developing the control laws of the active systems. Hence, the conclusions drawn have not changed much when compared with those obtained from using the quarter car model. Furthermore, most of the control laws in these studies assume perfect knowledge of all the state variables. Therefore, it can be established that there is a need for a more general study to design control laws for limited state feedback active systems and to examine the effect of the measurement errors on the performance of these systems.

3- In the reviewed literature there are two methods to include the wheelbase time delay in deriving the control law of the active suspension systems. The method which was introduced by Louam et al [1988] is optimal but difficult to realise. On the other hand, although the method which was introduced by Fruhauf et al [1986] is not optimal, it is a much more practical one. The future of this sub-optimal method depends on how far it is from the optimal one. However, there is no answer yet known to this question.

4- Based on the three dimensional model, there has been confusion in quantifying the benefits achieved from the active systems over the passive systems. Some authors found that the active system can dramatically improve the vehicle performance when compared with the passive system. Others, found that a well designed passive system can perform close to the active

one. Therefore, there is a need for an equitable basis comparison study. This will enable the benefits from fitting an active system to a full vehicle to be accurately established.

The aim of this work is to develop control laws for active suspension systems fitted to full vehicle models and then to compare the performances of competing systems using a fair basis for comparison. Various models, up to a seven degree-of-freedom vehicle model, are used. The time delay between the front and rear wheels is introduced in the optimisation problem by means of Pade approximation. The effect of modelling details on the performance of the actively suspended vehicle is discussed. Furthermore, the effect of including the cross correlation in deriving the control laws is examined. The general strategy of keeping lateral, longitudinal and vertical seat accelerations and the dynamic tyre load under control as well as the fore/aft and lateral dynamic tyre load transfers is used, within the realistic design constraint of a specified amount of available working space. The possibility of using limited state feedback active systems instead of the full state feedback system is considered and the effect of the measurement errors on the performance of these active systems is discussed. Two different algorithms are used to derive the control law of the limited state feedback active systems. The first one is based on the well known Kalman-Bucy filter [1961] assuming noisy measurements. The second method is based on the gradient search technique introduced by Wilson et al [1986] assuming perfect measurements. In this method, the problem formulation is

successfully modified so that the time delay is included in the optimisation problem. This, however, provides a novel strategy in developing the control laws of the limited state feedback active system. Finally the performances of all the active suspensions considered are compared with those obtained from passive systems and conclusions and recommendations for future work are made.

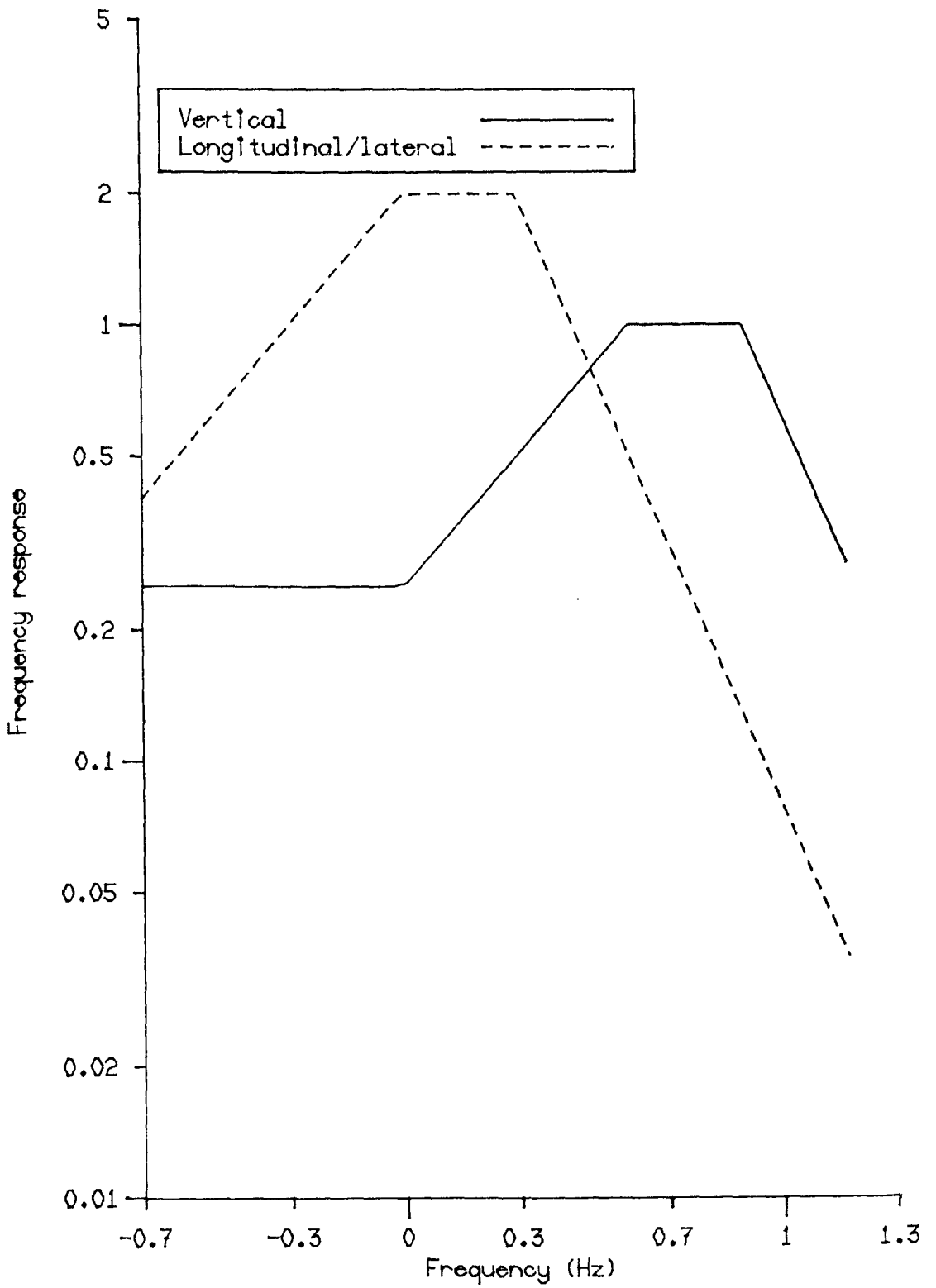


Fig. 1.1 I.S.O. 2631 weighting functions for acceleration spectra.

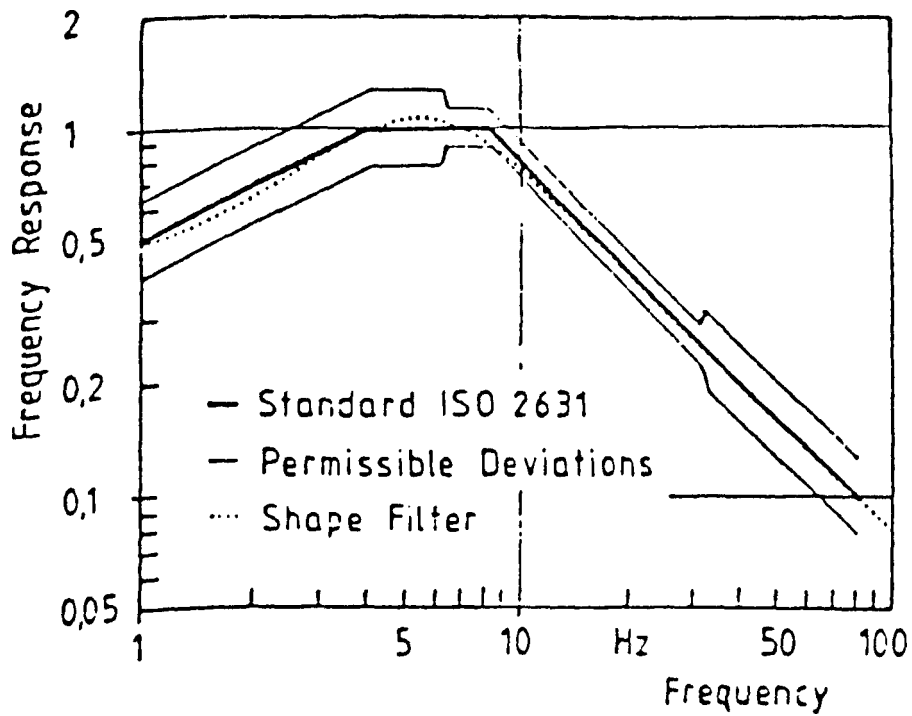


Fig. 1.2 Frequency response of a shaping filter for passenger response to longitudinal vibrations.

CHAPTER 2

FUNDAMENTALS OF MODELLING VEHICLE RIDE BEHAVIOUR

2.1 Introduction

Analysis of vehicle response to road roughness first requires a model of the road surface. Road surface height may typically be described as a random process, and techniques for describing stochastic signals have proved to be suitable as a basis for representing road profiles. For many surfaces, the amplitude spectral density is usually approximated by equation (1.1) in terms of the wave number or (1.2) in terms of the frequency. The power spectral density defined in equation (1.2) can be used directly as the input for frequency domain studies, in which the vehicle is modelled by a linear transfer function. Non-linear system studies require representing the road surface in the time domain.

The equations of motion of vehicle ride models may be formulated using either Lagrangian or Newtonian methods. In most cases, the Newtonian approach is more economic, since there are only matrix operations to be performed instead of partial differentiations in case of Lagrange's equations. If these equations are linearised, several analytical algorithms to obtain the eigensolutions, frequency responses and responses to idealised ground inputs may be used. In non-linear form, these equations may be solved to give time histories which may be subsequently processed to give spectral densities in the frequency domain.

In this Chapter, the artificial generation of random profiles necessary for vehicle simulation is discussed, the general way of writing equations of motion is outlined and example solutions based on a three dimensional vehicle model (Fig. 2.1) is given. Finally, the analysis of linear and non-linear systems is considered.

2.2 Generation of random road profiles.

A one dimensional random profile may be generated by applying the inverse discrete Fourier transform (IDFT) to the input spectral density described by equation (1.1). This method is explained in detail in Cebon and Newland [1983]. The summary of this method is as follows. The series of spot heights z_r at regular intervals along the track is given by

$$z_r = \left(\sum_{k=1}^{N_p} \sqrt{s_k} e^{i\chi_k} \right), \quad r = 1, 2, \dots, N_p \quad \dots(2.1)$$

where

$$s_k = \frac{1}{IPL} psd(\lambda_k), \quad \chi_k = \theta_k + 2\pi k r / N_p \quad \dots(2.2)$$

IPL is the input profile length (m), N_p is the number of points in the input profile and θ_k is a set of independent random phase angles uniformly distributed between 0 and 2π . These phase angles may be generated by using a random number generator routine (available for example in a NAG library subroutine G05CAF, NAG [1987] (section G05)). The wave number λ_k is related to IPL by

$$\lambda_k = (k-1)/IPL \text{ for } \lambda_k > \lambda_0, \text{ otherwise } \lambda_k = \lambda_0 \quad \dots(2.3)$$

In Fig. 2.2 a track profile which is 100 m long and contains 8192 amplitude points is shown. This profile represents a somewhat worse than average main road ($R_c = 3 \times 10^{-6}$). The exponent κ and cutoff wave number λ_o in equation (1.1) are taken equal to 2.5 and 0.01 cycle/m respectively.

However, a two track vehicle sees two separate road profiles—one for each wheel track travelled. The relationship between two parallel tracks on a surface can be expressed by the coherence, which is a function of frequency and lies between 0 and 1. This function provides a measure of the correlation between the left and right tracks (cross correlation). Various assumptions can be made about the coherence. If the coherence is taken equal unity, then the two parallel tracks are assumed to be identical. On the other hand if the coherence is taken equal zero, the two tracks are assumed to be independent. However, a more realistic assumption considers that the vehicle traverses two parallel tracks on an isotropic surface (i.e. one which looks the same statistically in all directions). This leads to a coherence which is unity at low frequencies and which decreases both with increasing frequency and increasing the track width t_w . In this case the coherence function as derived by Horton [1986] and [1988] may be defined by

$$\gamma_{ck} = Y_k K_1\{Y_k\} \quad \dots(2.4)$$

where K_1 is a modified Bessel function of the second kind and

$$Y_k = 2\pi\lambda_k t_w \quad \dots(2.5)$$

Fig. 2.3 shows the coherence function γ_c generated for $t_w = 1.54m$. Another method to generate the coherence function may be found in Cebon and Newland [1983].

Having calculated the coherence function and assuming an isotropic surface, a parallel track at distance equal to the vehicle track width away can be generated by summing two independent series y_r and x_r and which are given by

$$y_r = \left(\sum_{k=1}^{N_p} \gamma_{c_k} \sqrt{s_k} e^{ix_k} \right), \quad r = 1, 2, \dots, N_p \quad \dots(2.6)$$

$$x_r = \left(\sum_{k=1}^{N_p} \sqrt{1 - \gamma_{c_k}^2} \sqrt{s_k} e^{ix_{1k}} \right), \quad r = 1, 2, \dots, N_p \quad \dots(2.7)$$

where

$$x_{1k} = \theta_{1k} + 2\pi kr / N_p \quad \dots(2.8)$$

Here, θ_{1k} is a new set of random phase angles which are also uniformly distributed between 0 and 2π . The second track \hat{z}_r is then given by

$$\hat{z}_r = y_r + x_r \quad \dots(2.9)$$

Fig 2.4 shows the correlated track profile at a distance of 1.54 m apart from the track profile shown in Fig. 2.2.

2.3 Equations of motion.

The equations of motion of the vehicle ride models may be written in the form

$$M_{XDD} \ddot{z} = M_f F_p(z, \dot{z}, x_o, \dot{x}_o, t) + M_{f1} u(t) \quad \dots(2.10)$$

where $M_{XDD}(n \times n)$ is a matrix of masses and inertias, $M_f(n \times p)$ and $M_{f1}(n \times m)$ are the connection matrices, $z(n \times 1)$ is the vector of system coordinates, $F_p(p \times 1)$ is the passive suspension and

tyre forces, $x_o(m \times 1)$ is the road input vector and $u(m \times 1)$ is the control force vector. Consider now the case in which these models are linear and the vehicle is only passively suspended (i.e. $u=0$). The most convenient form to describe the forces F_p is

$$F_p = -M_k d_s - M_c \dot{d}_s \quad \dots(2.11)$$

where M_k and M_c are $(p \times p)$ matrices containing the stiffness and damping coefficients respectively and d_s is the relative displacement vector across the connecting elements. These displacements are related to z and x_o by

$$d_s = M_f^T z + M_{DU} x_o \quad \dots(2.12)$$

Substituting equations (2.11) and (2.12) in equation (2.10), the result may be written as

$$M_{XDD} \ddot{z} + M_{XD} \dot{z} + M_X z = M_{UD} \dot{x}_o + M_U x_o \quad \dots(2.13)$$

where

$$\begin{aligned} M_{XD} &= M_f M_c M_f^T, \quad M_X = M_f M_k M_f^T, \\ M_{UD} &= -M_f M_c M_{DU}, \quad M_U = -M_f M_k M_{DU} \end{aligned} \quad \dots(2.14)$$

The second order equations (2.13) may be transformed into $2n$ first order equations by defining new state variables $x(n_1, 1) = [z \quad \dot{z}]^T$, $n_1 = 2n$. The results may be written as

$$\dot{x} = Ax + B_2 x_o + B_3 \dot{x}_o \quad \dots(2.15)$$

where $A(n_1, n_1)$, $B_2(n_1, m)$ and $B_3(n_1, m)$ are constant matrices which are related to M_{XDD} , M_{XD} , M_X , M_{UD} and M_U by

$$A = \begin{bmatrix} 0 & I \\ -M_{XDD}^{-1} M_X & -M_{XDD}^{-1} M_{XD} \end{bmatrix}, \quad B_2 = \begin{bmatrix} 0 \\ M_{XDD}^{-1} M_U \end{bmatrix},$$

$$B_3 = \begin{bmatrix} 0 \\ M_{XDD}^{-1} M_{UD} \end{bmatrix} \quad \dots(2.16)$$

where $I =$ unit matrix ($n \times n$).

If the vehicle models involve active suspensions, i.e actuators are fitted in place of, or in addition to, the passive elements, equation (2.15) is modified as

$$\dot{x} = Ax + Bu + B_2 x_o + B_3 \dot{x}_o \quad \dots(2.17)$$

where $B(n_1, m)$ is defined as

$$B = \begin{bmatrix} 0 \\ M_{XDD}^{-1} M_{f1} \end{bmatrix} \quad \dots(2.18)$$

This form may be used directly to derive the control laws of the active systems. In Chapter 4, techniques for obtaining these control laws will be explained in detail, while the modifications in the formulation of the matrices M_{XDD} , M_{XD} , M_X , M_{UD} and M_U in equation (2.13) will be outlined throughout the text whenever necessary.

The lumped mass 7 d.o.f. model (Fig. 2.1) is used here. Modes relating to engine mounts, chassis bending and torsion may lie within or close to the frequency range of interest (0 - 15 Hz) but their inclusion would make the problem too complicated at this stage of the study. Hence, the body mass is treated as a rigid body and the vector z is defined as

$$z = [z_b \quad \theta \quad \phi \quad x_1 \quad x_3 \quad x_5 \quad x_7]^T \quad \dots(2.19)$$

The tyres are assumed to be in constant contact with the road surface and are modelled as linear springs. In the passive suspension model, the front and rear suspensions are modelled

as linear spring and damper units with the addition of anti-roll bars. With reference to Fig. 2.1, the equations of motion are

$$M_b \ddot{z}_b = F_1 + F_2 + F_3 + F_4 + u_1 + u_2 + u_3 + u_4 \quad \dots(2.20)$$

$$I_p \ddot{\theta} = -w_a(F_1 + F_2) + w_b(F_3 + F_4) - w_a(u_1 + u_2) + w_b(u_3 + u_4) \quad \dots(2.21)$$

$$I_r \ddot{\phi} = -(F_1 - F_2 + F_3 - F_4)t_s - T_f - T_r - (u_1 - u_2 + u_3 - u_4)t_s \quad \dots(2.22)$$

$$M_{wf} \ddot{x}_1 = -F_1 + F_5 - \frac{T_f}{t_w} - u_1 \quad \dots(2.23)$$

$$M_{wf} \ddot{x}_3 = -F_2 + F_6 + \frac{T_f}{t_w} - u_2 \quad \dots(2.24)$$

$$M_{wr} \ddot{x}_5 = -F_3 + F_7 - \frac{T_r}{t_w} - u_3 \quad \dots(2.25)$$

$$M_{wr} \ddot{x}_7 = -F_4 + F_8 + \frac{T_r}{t_w} - u_4 \quad \dots(2.26)$$

or

$$\begin{bmatrix} M_b & 0 & 0 & 0 & 0 & 0 & 0 & 0 \\ 0 & I_p & 0 & 0 & 0 & 0 & 0 & 0 \\ 0 & 0 & I_r & 0 & 0 & 0 & 0 & 0 \\ 0 & 0 & 0 & M_{wf} & 0 & 0 & 0 & 0 \\ 0 & 0 & 0 & 0 & M_{wf} & 0 & 0 & 0 \\ 0 & 0 & 0 & 0 & 0 & M_{wr} & 0 & 0 \\ 0 & 0 & 0 & 0 & 0 & 0 & M_{wr} & 0 \end{bmatrix} \begin{bmatrix} \ddot{z}_b \\ \ddot{\theta} \\ \ddot{\phi} \\ \ddot{x}_1 \\ \ddot{x}_3 \\ \ddot{x}_5 \\ \ddot{x}_7 \end{bmatrix} =$$

$$\begin{bmatrix} 1 & 1 & 1 & 1 & 0 & 0 & 0 & 0 & 0 & 0 \\ -w_a & -w_a & w_b & w_b & 0 & 0 & 0 & 0 & 0 & 0 \\ -t_s & t_s & -t_s & t_s & 0 & 0 & 0 & 0 & -1 & -1 \\ -1 & 0 & 0 & 0 & 1 & 0 & 0 & 0 & -1/t_w & 0 \\ 0 & -1 & 0 & 0 & 0 & 1 & 0 & 0 & 1/t_w & 0 \\ 0 & 0 & -1 & 0 & 0 & 0 & 1 & 0 & 0 & -1/t_w \\ 0 & 0 & 0 & -1 & 0 & 0 & 0 & 1 & 0 & 1/t_w \end{bmatrix} \begin{bmatrix} F_1 \\ F_2 \\ F_3 \\ F_4 \\ F_5 \\ F_6 \\ F_7 \\ F_8 \\ T_f \\ T_r \end{bmatrix} + \begin{bmatrix} 1 & 1 & 1 & 1 \\ -w_a & -w_a & w_b & w_b \\ -t_s & t_s & -t_s & t_s \\ -1 & 0 & 0 & 0 \\ 0 & -1 & 0 & 0 \\ 0 & 0 & -1 & 0 \\ 0 & 0 & 0 & -1 \end{bmatrix} \begin{bmatrix} u_1 \\ u_2 \\ u_3 \\ u_4 \end{bmatrix}$$

or

$$M_{XDD} \ddot{z} = M_f F_p + M_{f1} u$$

The displacements d_s are related to z and x_o by

$$d_s = \begin{bmatrix} 1 & -w_a & -t_s & -1 & 0 & 0 & 0 \\ 1 & -w_a & t_s & 0 & -1 & 0 & 0 \\ 1 & w_b & -t_s & 0 & 0 & -1 & 0 \\ 1 & w_b & t_s & 0 & 0 & 0 & -1 \\ 0 & 0 & 0 & 1 & 0 & 0 & 0 \\ 0 & 0 & 0 & 0 & 1 & 0 & 0 \\ 0 & 0 & 0 & 0 & 0 & 1 & 0 \\ 0 & 0 & 0 & 0 & 0 & 0 & 1 \\ 0 & 0 & -1 & -1/t_w & 1/t_w & 0 & 0 \\ 0 & 0 & -1 & 0 & 0 & -1/t_w & 1/t_w \end{bmatrix} z + \begin{bmatrix} 0 & 0 & 0 & 0 \\ 0 & 0 & 0 & 0 \\ 0 & 0 & 0 & 0 \\ 0 & 0 & 0 & 0 \\ -1 & 0 & 0 & 0 \\ 0 & -1 & 0 & 0 \\ 0 & 0 & -1 & 0 \\ 0 & 0 & 0 & -1 \\ 0 & 0 & 0 & 0 \\ 0 & 0 & 0 & 0 \end{bmatrix} x_o$$

or

$$d_s = M_f^T z + M_{DU} x_o$$

The matrices M_k and M_c in equation (2.11) are given by

$$M_k = \begin{bmatrix} K_f & 0 & 0 & 0 & 0 & 0 & 0 & 0 & 0 & 0 \\ 0 & K_f & 0 & 0 & 0 & 0 & 0 & 0 & 0 & 0 \\ 0 & 0 & K_r & 0 & 0 & 0 & 0 & 0 & 0 & 0 \\ 0 & 0 & 0 & K_t & 0 & 0 & 0 & 0 & 0 & 0 \\ 0 & 0 & 0 & 0 & K_t & 0 & 0 & 0 & 0 & 0 \\ 0 & 0 & 0 & 0 & 0 & K_t & 0 & 0 & 0 & 0 \\ 0 & 0 & 0 & 0 & 0 & 0 & K_t & 0 & 0 & 0 \\ 0 & 0 & 0 & 0 & 0 & 0 & 0 & K_r & 0 & 0 \\ 0 & 0 & 0 & 0 & 0 & 0 & 0 & 0 & K_r & 0 \\ 0 & 0 & 0 & 0 & 0 & 0 & 0 & 0 & 0 & K_r \end{bmatrix}, \quad M_c = \begin{bmatrix} C_f & 0 & 0 & 0 & 0 & 0 & 0 & 0 & 0 & 0 \\ 0 & C_f & 0 & 0 & 0 & 0 & 0 & 0 & 0 & 0 \\ 0 & 0 & C_r & 0 & 0 & 0 & 0 & 0 & 0 & 0 \\ 0 & 0 & 0 & C_t & 0 & 0 & 0 & 0 & 0 & 0 \\ 0 & 0 & 0 & 0 & C_t & 0 & 0 & 0 & 0 & 0 \\ 0 & 0 & 0 & 0 & 0 & C_t & 0 & 0 & 0 & 0 \\ 0 & 0 & 0 & 0 & 0 & 0 & C_t & 0 & 0 & 0 \\ 0 & 0 & 0 & 0 & 0 & 0 & 0 & C_r & 0 & 0 \\ 0 & 0 & 0 & 0 & 0 & 0 & 0 & 0 & C_r & 0 \\ 0 & 0 & 0 & 0 & 0 & 0 & 0 & 0 & 0 & C_r \end{bmatrix}$$

Consider now the case that the vehicle is only passively suspended. Using the matrices M_f , M_{DU} , M_k and M_c as defined above, and by using equation (2.14) it is easy to find the matrices M_{XD} , M_X and M_U . It should be mentioned that because the tyre damping coefficient is not considered, the matrix M_{UD} is a null matrix. Having these matrices available, and by using equations (2.16) and (2.18), it is easy to reduce the second order equations (2.20) to (2.26) into first order form as described by equation (2.17). In this case, because M_{UD} is a null matrix, B_3 will be also a null matrix. The elements

of A , B and B_2 for the case when the vehicle is only actively suspended may be written as follows.

$$A = \begin{bmatrix} 0 & 0 & 0 & 0 & 0 & 0 & 0 & 1 & 0 & 0 & 0 & 0 & 0 & 0 \\ 0 & 0 & 0 & 0 & 0 & 0 & 0 & 0 & 1 & 0 & 0 & 0 & 0 & 0 \\ 0 & 0 & 0 & 0 & 0 & 0 & 0 & 0 & 0 & 1 & 0 & 0 & 0 & 0 \\ 0 & 0 & 0 & 0 & 0 & 0 & 0 & 0 & 0 & 0 & 1 & 0 & 0 & 0 \\ 0 & 0 & 0 & 0 & 0 & 0 & 0 & 0 & 0 & 0 & 0 & 1 & 0 & 0 \\ 0 & 0 & 0 & 0 & 0 & 0 & 0 & 0 & 0 & 0 & 0 & 0 & 1 & 0 \\ 0 & 0 & 0 & 0 & 0 & 0 & 0 & 0 & 0 & 0 & 0 & 0 & 0 & 1 \\ 0 & 0 & 0 & 0 & 0 & 0 & 0 & 0 & 0 & 0 & 0 & 0 & 0 & 0 \\ 0 & 0 & 0 & 0 & 0 & 0 & 0 & 0 & 0 & 0 & 0 & 0 & 0 & 0 \\ 0 & 0 & 0 & 0 & 0 & 0 & 0 & 0 & 0 & 0 & 0 & 0 & 0 & 0 \\ 0 & 0 & 0 & 0 & 0 & 0 & 0 & 0 & 0 & 0 & 0 & 0 & 0 & 0 \\ 0 & 0 & 0 & \frac{-K_t}{M_{wf}} & 0 & 0 & 0 & 0 & 0 & 0 & 0 & 0 & 0 & 0 \\ 0 & 0 & 0 & 0 & \frac{-K_t}{M_{wf}} & 0 & 0 & 0 & 0 & 0 & 0 & 0 & 0 & 0 \\ 0 & 0 & 0 & 0 & 0 & \frac{-K_t}{M_{wr}} & 0 & 0 & 0 & 0 & 0 & 0 & 0 & 0 \\ 0 & 0 & 0 & 0 & 0 & 0 & \frac{-K_t}{M_{wr}} & 0 & 0 & 0 & 0 & 0 & 0 & 0 \end{bmatrix}$$

$$B = \begin{bmatrix} 0 & 0 & 0 & 0 \\ 0 & 0 & 0 & 0 \\ 0 & 0 & 0 & 0 \\ 0 & 0 & 0 & 0 \\ 0 & 0 & 0 & 0 \\ 0 & 0 & 0 & 0 \\ 0 & 0 & 0 & 0 \\ \frac{1}{M_b} & \frac{1}{M_b} & \frac{1}{M_b} & \frac{1}{M_b} \\ \frac{-w_a}{I_p} & \frac{-w_a}{I_p} & \frac{w_b}{I_p} & \frac{w_b}{I_p} \\ \frac{-t_s}{I_r} & \frac{t_s}{I_r} & \frac{-t_s}{I_r} & \frac{t_s}{I_r} \\ \frac{-1}{M_{wf}} & 0 & 0 & 0 \\ 0 & \frac{-1}{M_{wf}} & 0 & 0 \\ 0 & 0 & \frac{-1}{M_{wr}} & 0 \\ 0 & 0 & 0 & \frac{-1}{M_{wr}} \end{bmatrix}, \quad B_2 = \begin{bmatrix} 0 & 0 & 0 & 0 \\ 0 & 0 & 0 & 0 \\ 0 & 0 & 0 & 0 \\ 0 & 0 & 0 & 0 \\ 0 & 0 & 0 & 0 \\ 0 & 0 & 0 & 0 \\ 0 & 0 & 0 & 0 \\ 0 & 0 & 0 & 0 \\ 0 & 0 & 0 & 0 \\ 0 & 0 & 0 & 0 \\ 0 & 0 & 0 & 0 \\ \frac{K_t}{M_{wf}} & 0 & 0 & 0 \\ 0 & \frac{K_t}{M_{wf}} & 0 & 0 \\ 0 & 0 & \frac{K_t}{M_{wr}} & 0 \\ 0 & 0 & 0 & \frac{K_t}{M_{wr}} \end{bmatrix}$$

2.4 Analysis of linear systems.

2.4.1 Frequency response.

This section deals with the sinusoidal steady state, or the frequency response, of a system. For a system with m inputs described as

$$x_o = E e^{i\omega t} \quad \dots(2.27)$$

all the outputs will respond in the form

$$z = Z(\omega)x_o \quad \dots(2.28)$$

where $E(m \times 1)$ is the excitation amplitude vector and $Z(\omega)$ is the complex $(n \times m)$ matrix of the frequency response function. Because $\dot{z} = i\omega z$, $\ddot{z} = -\omega^2 z$ and $\dot{x}_o = i\omega x_o$, equation (2.13) may be written as

$$(-\omega^2 M_{XDD} + i\omega M_{XD} + M_X)z = (i\omega M_{UD} + M_U)x_o \quad \dots(2.29)$$

By comparing equations (2.28) and (2.29), the frequency response matrix $Z(\omega)$ can be found from

$$Z(\omega) = (-\omega^2 M_{XDD} + i\omega M_{XD} + M_X)^{-1} (M_U + i\omega M_{UD}) \quad \dots(2.30)$$

In the case of using a simple vehicle model, e.g. the quarter car model, the vector $E(1 \times 1)$ will be scalar and equal to 1. In a more realistic vehicle model, e.g. the bounce and pitch 4 d.o.f. model, the input to the rear wheel can be considered as that to the front wheel but delayed by a time $D = L/V$ ie.

$$x_{o_r} = e^{i\omega(t-D)} = x_{o_f} e^{-i\omega D} \quad \dots(2.31)$$

and hence, the input vector x_o may be written as

$$x_o = \begin{bmatrix} 1 \\ e^{-i\omega D} \end{bmatrix} e^{i\omega t} \quad \dots(2.32)$$

This formula can easily be generalised to more than two axles. In this, the sub-element E_k in the vector E can be found from

$$E_k = e^{-i\omega L_{1k}/V} \quad \dots(2.33)$$

where L_{1k} is the distance from axle 1 to axle k .

2.4.2 Response to amplitude spectral density ground inputs.

In this part, it will be shown how the input described as an amplitude spectral density can be combined with the vehicle model frequency response functions to obtain spectral densities for the output coordinates. A comprehensive account of the theory which is reviewed here may be found in Newland [1984], while example solution based on a bounce and pitch 2 d.o.f. vehicle model may be found in Horton [1986]. To indicate the strategy, consider first the three dimensional vehicle model shown in Fig. 2.1. In this model, each of the four inputs has an auto spectral density, but in addition, each two inputs generate a cross spectral density term. The general form of the input spectral density matrix is

$$S_u = s_u E^c E^T = s_u E_E \quad \dots(2.34)$$

where

$$s_u = \frac{1}{2\pi V} psd(\lambda) \quad \dots(2.35)$$

is the auto spectral density term and c denotes complex conjugate. With reference to Fig. 2.1, it can be seen that the input at the wheel No. 3 is identical to No. 1 but delayed by a time $D = L/V$. The input at the wheel No. 2 is only related to No. 1 by the coherence between the tracks while the input at the wheel No. 4 is delayed and cross correlated with the input No. 1. Hence, the four auto spectra for the input are

$$S_u(1,1) = S_u(2,2) = S_u(3,3) = S_u(4,4) = s_u \quad \dots(2.36)$$

and the cross spectra are

$$S_u(1,2) = S_u(2,1) = S_u(3,4) = S_u(4,3) = s_u \gamma_c$$

$$S_u(1,3) = S_u^c(3,1) = S_u(2,4) = S_u^c(4,2) = s_u e^{-i\omega D}$$

$$S_u(1,4) = S_u^c(4,1) = S_u(2,3) = S_u^c(3,2) = s_u \gamma_c e^{-i\omega D} \quad \dots(2.37)$$

so that the matrix E_E is given by

$$E_E = \begin{bmatrix} 1 & \gamma_c & e^{-i\omega D} & \gamma_c e^{-i\omega D} \\ \gamma_c & 1 & \gamma_c e^{-i\omega D} & e^{-i\omega D} \\ e^{i\omega D} & \gamma_c e^{i\omega D} & 1 & \gamma_c \\ \gamma_c e^{i\omega D} & e^{i\omega D} & \gamma_c & 1 \end{bmatrix} \quad \dots(2.38)$$

In the case of using the bounce and pitch half vehicle model this matrix is simplified to

$$E_E = \begin{bmatrix} 1 & e^{-i\omega D} \\ e^{i\omega D} & 1 \end{bmatrix} \quad \dots(2.39)$$

while in the case of using a single end vehicle model (bounce and roll), this matrix would become

$$E_E = \begin{bmatrix} 1 & \gamma_c \\ \gamma_c & 1 \end{bmatrix} \quad \dots(2.40)$$

The output spectral density matrix $S_x(n \times n)$ is related to the input spectral density matrix and the frequency response Z by

$$S_x = Z^c S_u Z^T \quad \dots(2.41)$$

The root mean square value of coordinate z_j in the frequency range ω_1 to ω_2 is given by

$$(\sigma_z)_j = \sqrt{\int_{\omega_1}^{\omega_2} (S_x(\omega))_{jj} d\omega} \quad \dots(2.42)$$

The r.m.s. values are therefore proportional to $\sqrt{R_c}$ and to \sqrt{V} . This relation is very useful if the linear quarter car model is employed because calculations of the r.m.s. values at a certain operating condition can simply be scaled to

to obtain the r.m.s. values at any other operating conditions. However, if the bounce and pitch half vehicle model or the three dimensional vehicle model is employed, the r.m.s. values are not simply proportional to \sqrt{V} due to the wheelbase time delay. This relationship, however, depends on the vehicle speed and the parameters.

2.5 Non-linear analysis.

In this work, all the vehicle models considered are linear including that which uses active suspension with a control law based on the Kalman filter algorithm, but in this system, the control force u is a function of the system states and the time. Hence, equation (2.17) must be solved iteratively to give the time histories of x . To indicate the algorithm, the dynamics of the system will be described by

$$\dot{x} = Ax + B_2 x_o + B_4 f_t(t) \quad \dots(2.43)$$

where $B_4(n_1, n_f)$ is constant matrix and $f_t(t)$ is a vector which contains n_f input forces which are only functions of time. From this equation it is possible to write the following difference equation

$$x_{k+1} = P_p x_k + Q_q x_{o_k} + Q_f f_{t_k} \quad \dots(2.44)$$

where

$$P_p = e^{AT} \quad , \quad Q_q = (P_p - I)A^{-1}B_2 \quad , \quad Q_f = (P_p - I)A^{-1}B_4$$

and T is the sampling time. Having the road input irregularity x_o and the forces f_t known at any time (t) , then it is possible to compute $x(t)$ as the initial condition to the system and generate the solution at small time steps T as time progress.

The matrices P_p , Q_q and Q_f need only be calculated once for any given system. Different algorithms to find these matrices are available. For the case in which the matrix A is singular, P and $(P_p - I)A^{-1}$ may be found by the expansion of the series

$$P = e^{AT} = I + AT + \frac{1}{2!} A^2 T^2 + \dots + \frac{1}{p!} A^p T^p \quad \dots(2.45)$$

$$(P_p - I)A^{-1} = T \left(I + \frac{1}{2!} AT + \frac{1}{3!} A^2 T^2 + \dots \right) \quad \dots(2.46)$$

A procedure to find the number of terms after which the series can be truncated is given in Yasundo et al [1970]. However, if A^{-1} exists, a more efficient technique to use the Pade approximation to find the matrix P_p . In this, P_p is found from

$$P_p = \frac{a_0 I - a_1 A + a_2 A^2 - \dots + \dots + a_N A^N}{a_0 I + a_1 A + a_2 A^2 + \dots + \dots + a_N A^N} \quad \dots(2.47)$$

In Chapter 4, values for the constants a_0, a_1, \dots, a_N are given for $N=2$ and $N=4$ i.e. for the second and fourth order Pade approximation.

Several other techniques for solving equation (2.43) by numerical integration e.g., Runge-Kutta-Merson method and Adams method are available in the form of the NAG library subroutines (see NAG [1987] (section D02)).

2.6 Output variables.

The n output coordinates in the state vector z and the m road inputs x_o as well as \ddot{z} , \dot{z} and \dot{x}_o may be combined into N_o output variables. The result may be written as

$$y_z = T_{XDD} \ddot{z} + T_{XD} \dot{z} + T_X z + T_{UD} \dot{x}_o + T_U x_o \quad \dots(2.48)$$

To indicate this transformation, the following example will be given. The output vector y_z is considered to contain:

1- Vertical acceleration at the driver's seat

$$\ddot{z}_x = \ddot{z}_b - X_s \ddot{\theta} + Y_s \ddot{\phi}$$

2- Lateral acceleration at the driver's seat

$$\ddot{y}_x = -Z_s \ddot{\phi}$$

3- Longitudinal acceleration at the driver's seat

$$\ddot{x}_x = Z_s \ddot{\theta}$$

4- Dynamic tyre load at front wheel (No. 1)

$$FDTL = -K_t(x_1 - x_{o1})$$

5- Dynamic tyre load at rear wheel (No. 3)

$$RDTL = -K_t(x_5 - x_{o3})$$

6- Suspension working space at front wheel (No. 1)

$$sWS_f = z_b - w_a \theta - t_s \phi - x_1$$

7- Suspension working space at rear wheel (No. 3)

$$sWS_r = z_b + w_b \theta - t_s \phi - x_5$$

8- Fore/aft tyre load transfer which is defined as

$$FDTT = (F_5 + F_6 - F_7 - F_8) / FDTT_{\max}$$

$$= -K_t(x_1 + x_3 - x_5 - x_7 - x_{o1} - x_{o2} + x_{o3} + x_{o4}) / FDTT_{\max}$$

where $FDTT_{\max}$ is the total fore/aft load transfer experienced by the vehicle when braking (or accelerating) at 0.8 g

9- Lateral tyre load transfer

$$LDTT = (-F_5 + F_6 - F_7 + F_8) / LDTT_{\max}$$

$$= -K_t(-x_1 + x_3 - x_5 + x_7 + x_{o1} - x_{o2} + x_{o3} - x_{o4}) / FDTT_{\max}$$

where $LDTT_{\max}$ is the lateral load transfer experienced by the vehicle when cornering at 0.8 g of lateral acceleration.

Hence, T_{XD} and T_{UD} are null matrices while the T_{XDD} , T_X , T_U are defined as

$$T_{XDD} = \begin{bmatrix} 1 & -X_f & Y_f & 0 & 0 & 0 & 0 \\ 0 & 0 & -Z_f & 0 & 0 & 0 & 0 \\ 0 & Z_f & 0 & 0 & 0 & 0 & 0 \\ 0 & 0 & 0 & 0 & 0 & 0 & 0 \\ 0 & 0 & 0 & 0 & 0 & 0 & 0 \\ 0 & 0 & 0 & 0 & 0 & 0 & 0 \\ 0 & 0 & 0 & 0 & 0 & 0 & 0 \\ 0 & 0 & 0 & 0 & 0 & 0 & 0 \end{bmatrix}, \quad T_X = \begin{bmatrix} 0 & 0 & 0 & 0 & 0 & 0 & 0 \\ 0 & 0 & 0 & 0 & 0 & 0 & 0 \\ 0 & 0 & 0 & 0 & 0 & 0 & 0 \\ 0 & 0 & 0 & -K_t & 0 & 0 & 0 \\ 0 & 0 & 0 & 0 & 0 & -K_t & 0 \\ 1 & -w_a & -t_f & -1 & 0 & 0 & 0 \\ 1 & w_b & -t_f & 0 & 0 & -1 & 0 \\ 0 & 0 & 0 & -KD_F & -KD_F & KD_F & KD_F \\ 0 & 0 & 0 & KD_L & -KD_L & KD_L & -KD_L \end{bmatrix},$$

$$T_U = \begin{bmatrix} 0 & 0 & 0 & 0 \\ 0 & 0 & 0 & 0 \\ 0 & 0 & 0 & 0 \\ K_t & 0 & 0 & 0 \\ 0 & 0 & K_t & 0 \\ 0 & 0 & 0 & 0 \\ 0 & 0 & 0 & 0 \\ KD_F & KD_F & -KD_F & -KD_F \\ -KD_L & KD_L & -KD_L & KD_L \end{bmatrix}$$

where $KD_F = K_t / FD_{TT_{max}}$ and $KD_L = K_t / LD_{TT_{max}}$. The new frequency response matrix Z_y is related to y_z by

$$y_z = Z_y x_o \quad \dots(2.49)$$

and using

$$z = Z x_o, \quad \dot{z} = i\omega z, \quad \ddot{z} = -\omega^2 z, \quad \dot{x}_o = i\omega x_o$$

it is easy to show that

$$Z_y = (-\omega^2 T_{XDD} + i\omega T_{XD} + T_X)Z + (i\omega T_{UD} + T_U) \quad \dots(2.50)$$

The rest of the formulae involving frequency response and outputs from spectral density may be modified by substituting Z_y for Z .

2.7 System response calculation and computational procedure.

In order to solve first the linear optimisation problem (discussed later) and then to carry out the subsequent ride

analyses in response to a random ground input for the vehicle systems, a general computer program was developed. Fig. 2.5 shows an outline flow diagram for this program indicating the major steps involved. This program is written in Fortran on the University main frame computer "AMDAHL". In preparing that program, a variety of NAG library subroutines were employed for matrix inversion (section F04), eigensolution (section F02), Bessel function of the second kind (subroutine S18ADF) and in minimising a function (subroutine E04KDF). Work is in progress to modify this program to be used on PC computers.

2.8 Concluding remarks.

The problem of generating a single profile or two correlated profiles is briefly reviewed. The equations of motion necessary for ride analysis or for the active systems optimisation problem are explained and an illustrative example based on a 7 d.o.f. is given. The analyses of linear systems in terms of the frequency response or the spectral density functions are discussed and the computational scheme of the difference equation to evaluate the time history of the outputs of interest is indicated. References to literature covering other necessary mathematical details are made. Finally, the outline flow diagram for the computer program used to carry out all the ride analysis is shown.

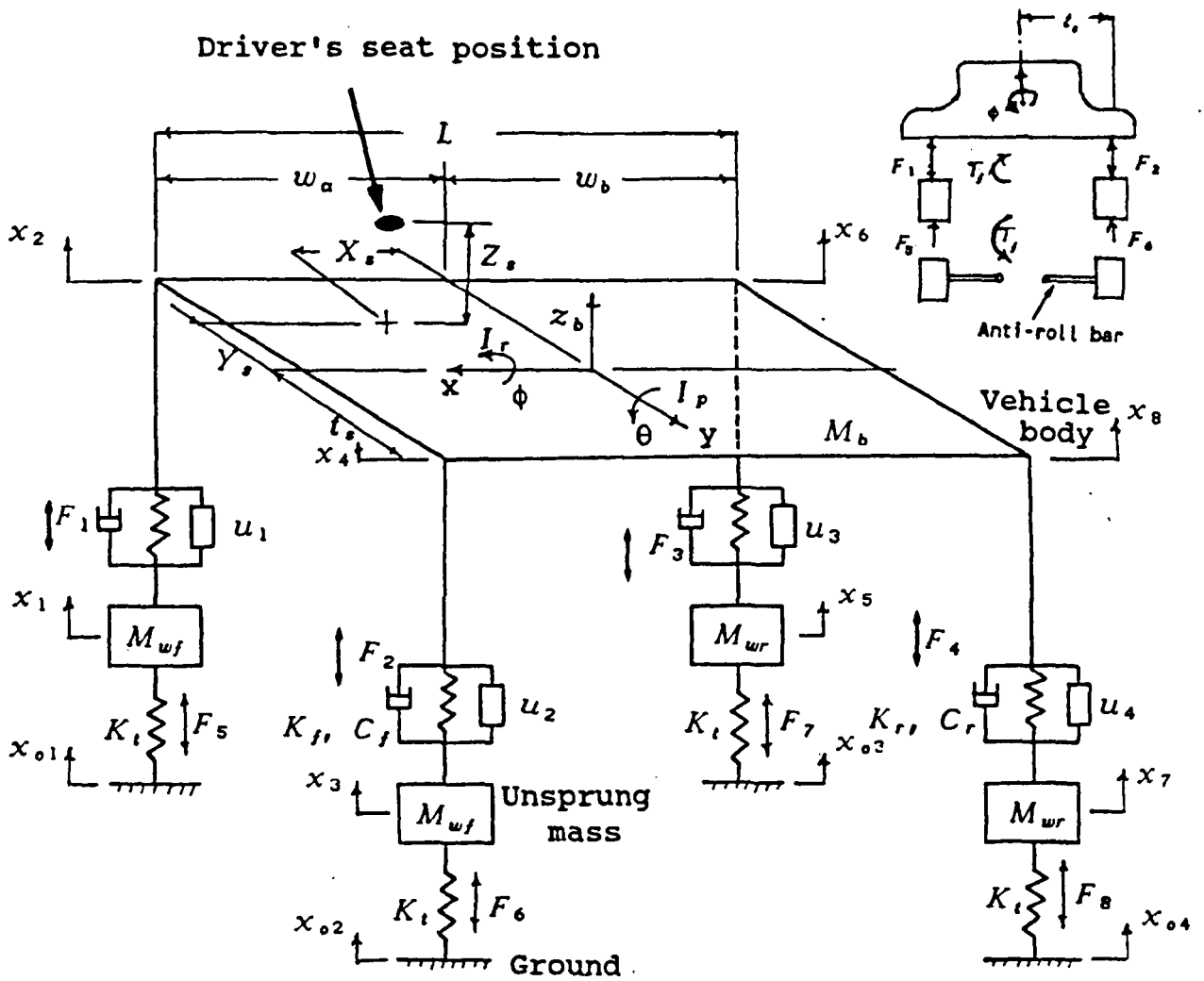


Fig. 2.1 Vehicle model

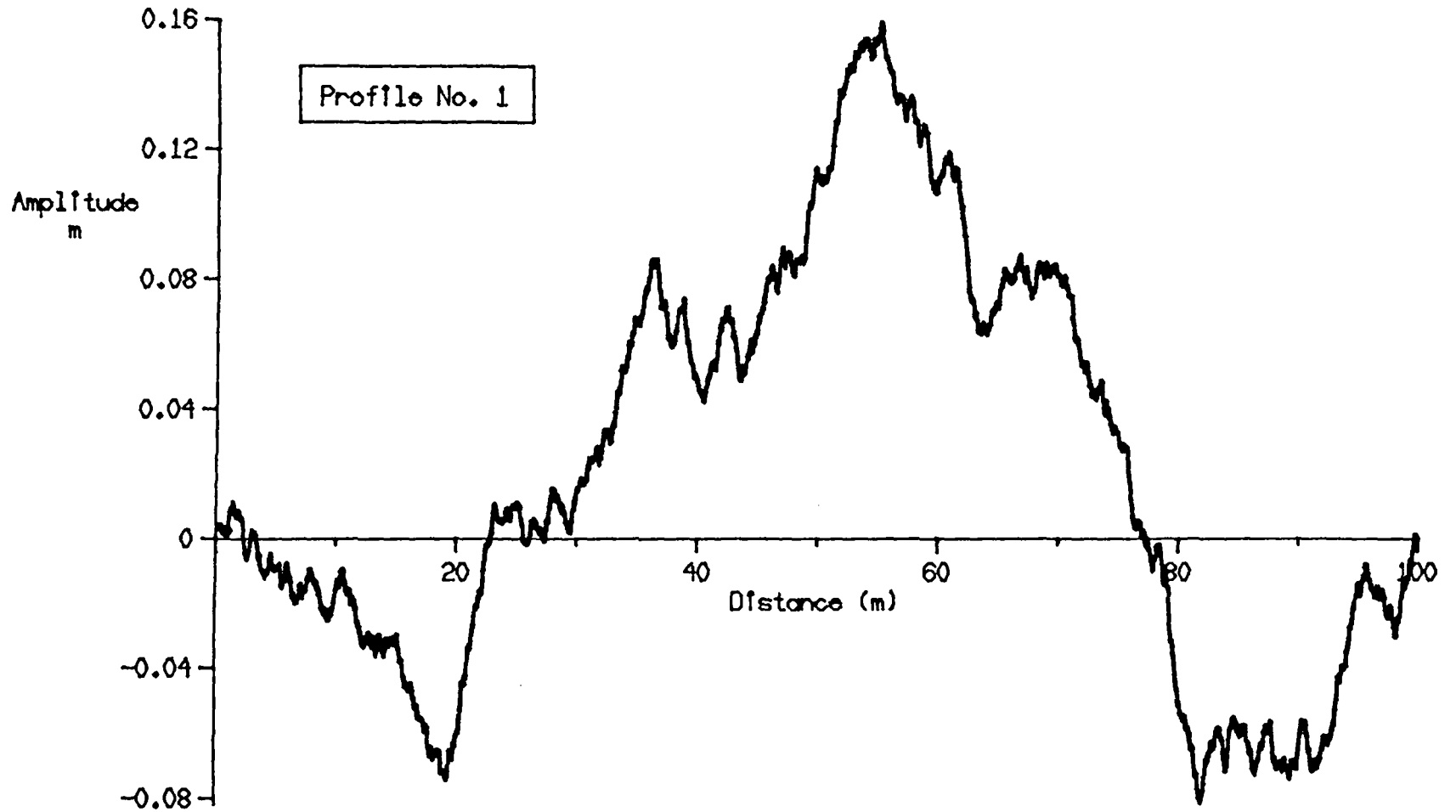


Fig. 2.2 Profile track generated by IDFT from the spectral density
 $R_s = 3 \times 10^{-6}$, $\lambda = 0.01$ cycle/m and $\kappa = 2.5$.

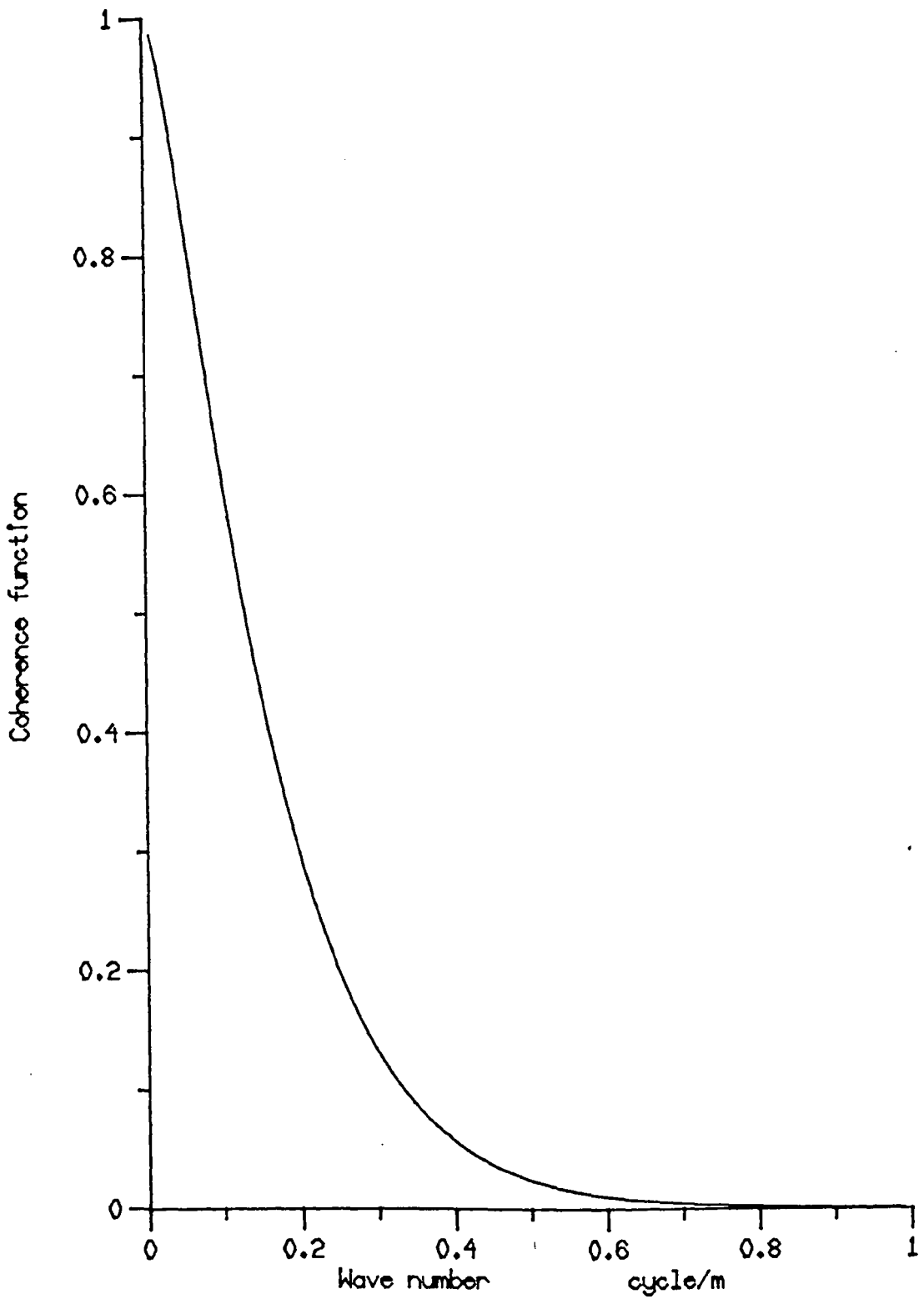


Fig. 2.3 Coherence function generated for a wheel track of 1.54 m.

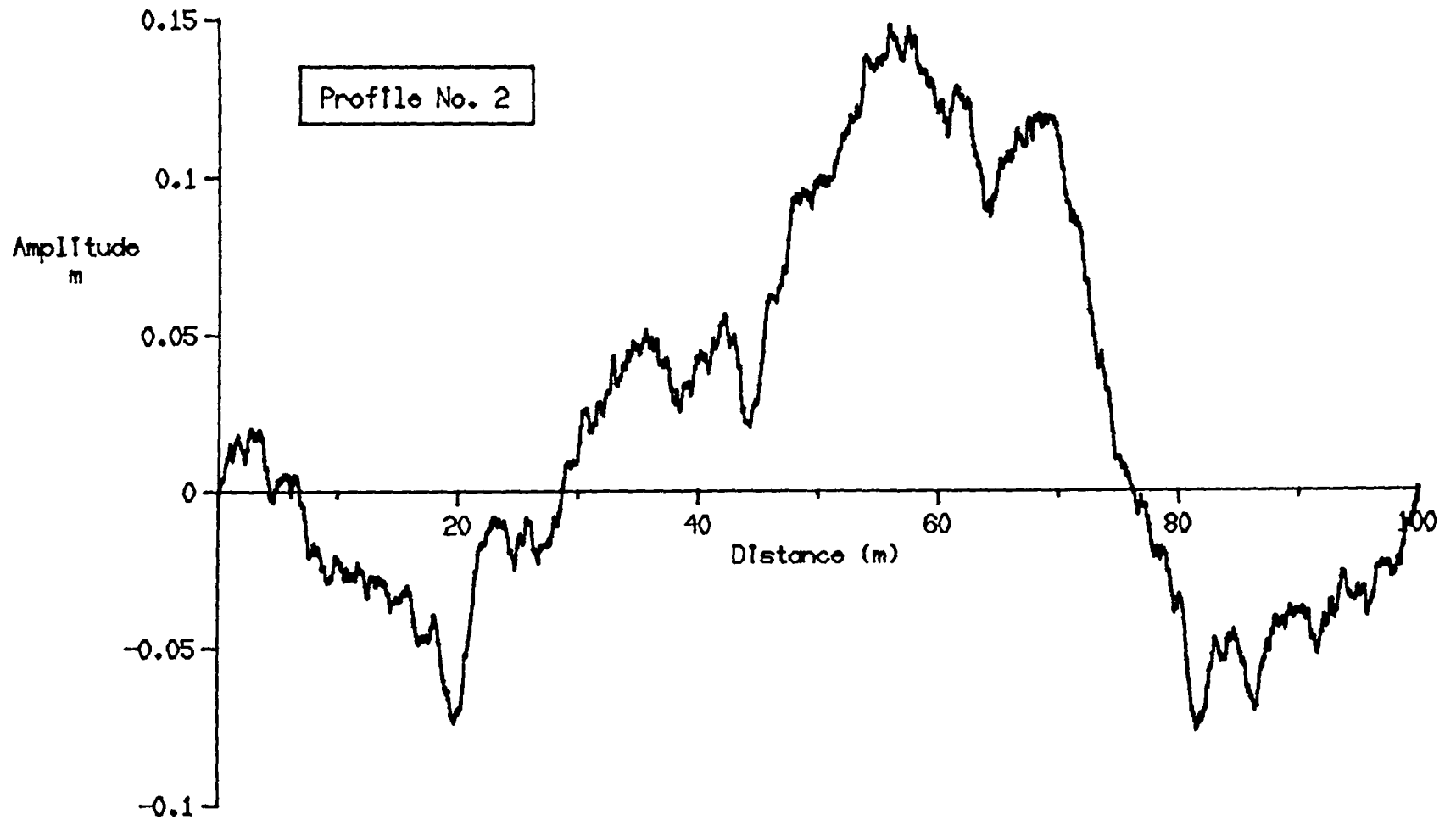


Fig. 2.4 Correlated profile track generated at 1.54 m apart from profile No. 1 shown in Fig. 2.2.

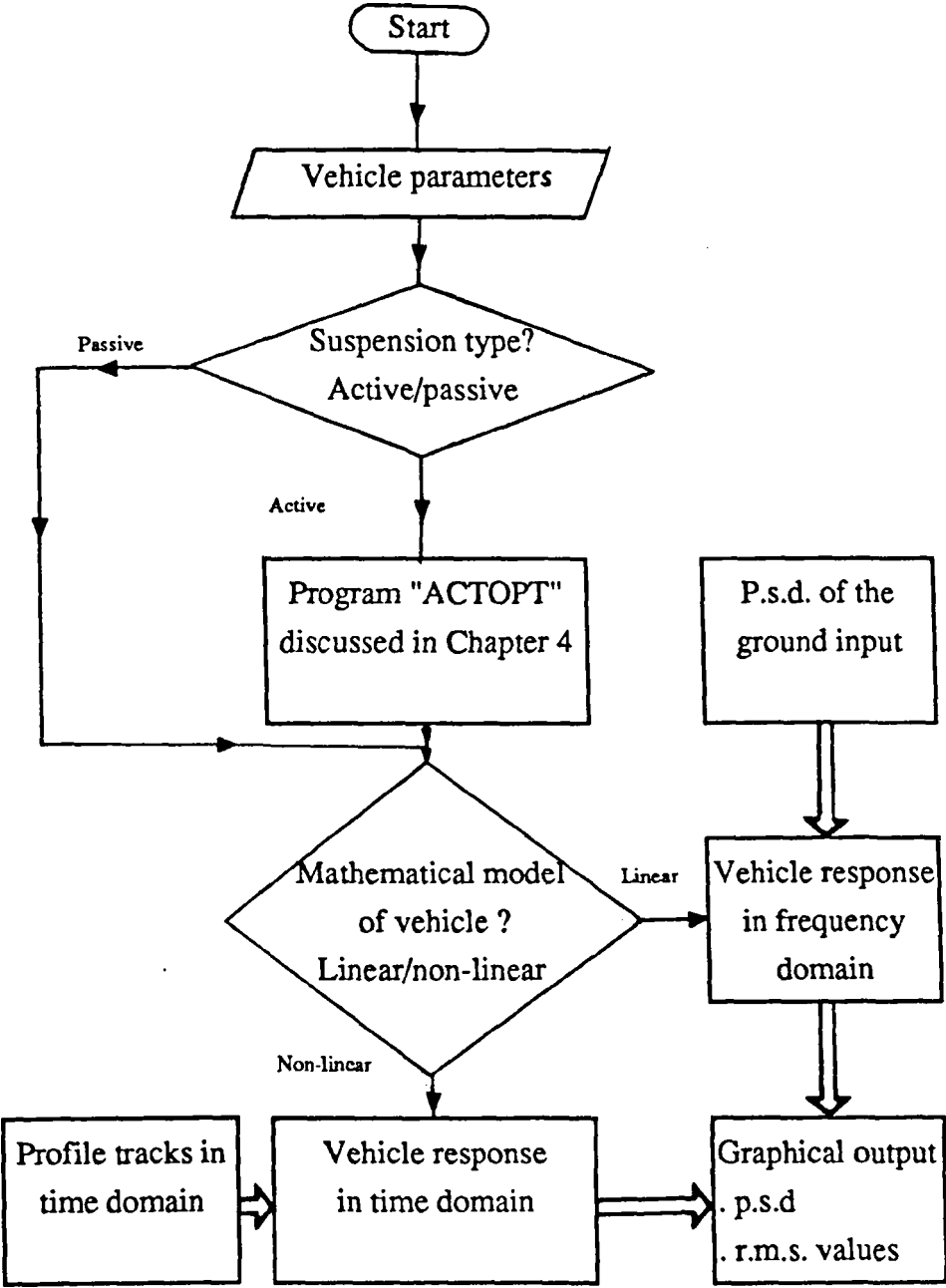


Fig. 2.5 Flow diagram of computer program for ride analysis.

CHAPTER 3

PASSIVE SUSPENSION SYSTEMS

3.1 Introduction.

The good design of passive suspensions requires a compromise between ride comfort, road holding and the vehicle attitude control. This should be achieved within the constraint of the amount of the suspension working space available. Over recent years, the analysis of the problems has been comprehensively studied using the quarter car model. Perhaps the most important conclusion obtained from these studies was that, to have a good performance of a passive system over a range of speeds and road conditions, then it must be adaptive. In other words it must be able to alter its stiffness and the damping coefficients in response to the road surface over which it is travelling. However, the primary purpose of this Chapter is to quantify the ride behaviour of the passive suspension systems so they can be used as a guide in estimating the benefits that could be achieved from using the active systems. Secondly, it is intended to provide a clear understanding of the performance properties of these systems when a three dimensional vehicle model is employed.

The equations of motion of this model (see Fig. 2.1) are given in detail in section 2.3 and the methods used to obtain the matrices M_{xDD} , M_{xD} , M_X and M_U are explained. Table 3.1 gives the parameter values used throughout this work. The spring stiffness and the damping coefficients are considered to be design parameters. Following the solution procedure described

in the last Chapter for the linear models, it is possible to generate the r.m.s. values and the spectral densities of the outputs of interest. The r.m.s. values of the ISO weighted vertical, lateral and longitudinal acceleration at the driver's seat position are considered to be measures of the ride comfort. Furthermore, the road holding ability is examined using the r.m.s. values of the dynamic tyre load calculated at the front and rear wheels. However, because a full vehicle model is used, the effect of the passive suspension design on the tyre load distribution is also studied. The r.m.s. values of the lateral dynamic tyre load transfer due to roll motion and the fore/aft dynamic tyre load transfer due to pitch motion are calculated and taken into account in the performance analysis. The elements of the output matrices T_{XDD} , T_{XD} , T_X and T_U are then similar to those given in section 2.6. In calculating these r.m.s. values, the cross correlation between the left and right tracks and the effective time delay characteristic between front and rear wheels is represented as discussed in section 2.4.2. The frequency range considered in these calculations is selected based on the assumptions used by Sharp and Hassan [1984]. In these, the low frequency limit was set at $\lambda_0 V$, where V is the vehicle speed and λ_0 is the cutoff wave number which is taken here as 0.01 cycle/m. Hence for a speed of 30 m/s the linear calculations start at 0.3 Hz. However, this assumption is a realistic one because the suspension systems cannot attempt to filter out the effects of very long wave length irregularities and the calculation of the acceleration response itself is not relevant at very low frequency. The high frequency limit has been chosen to

be 15 Hz. This value is selected because it is lower than the lowest natural frequency of the car body structure which starts around 20 Hz and because the wave length $V/15$ m for any vehicle speed considered in this work is greater than the tyre to road contact length. Hence, the representation of the tyre as a linear vertical spring is reasonably accurate. In all the results presented later either here in this Chapter or in the next Chapters, the vehicle is assumed to move straight forward with a constant speed.

3.2 Results

The results described here refer to performance analyses of the passive suspension system when a road of $R_c = 3 \times 10^{-6}$ and $\kappa = 2.5$ is traversed at 30 m/s. The r.m.s. values of the front and rear working space, front and rear dynamic tyre load, the fore/aft and lateral dynamic tyre load transfers, vertical, lateral and longitudinal seat accelerations are each calculated for different spring stiffnesses (5 KN/m to 50 KN/m in steps of 1 KN/m) and damping ratios DR (0.25 to 0.6 in steps of 0.05 and at 0.7 and 0.8). The natural frequencies fn and the damping ratios DR are defined for the front and rear suspensions as:

$$fn_f = \frac{1}{2\pi} \sqrt{\frac{K_f}{M_{B_f}}} , \quad fn_r = \frac{1}{2\pi} \sqrt{\frac{K_r}{M_{B_r}}}$$

$$DR_f = \frac{C_f/2}{\sqrt{M_{B_f}K_f}} , \quad DR_r = \frac{C_r/2}{\sqrt{M_{B_r}K_r}}$$

where

$$M_{B_f} = \frac{M_B w_b}{L} \quad , \quad M_{B_r} = \frac{M_B w_a}{L}$$

Here K_f and K_r are the front and rear stiffness coefficients, C_f and C_r are the front and rear damping coefficients, M_B is the sprung mass and w_a and w_b are the horizontal distances from body centre to the front and rear wheels respectively. The results are collected and presented in Figs. 3.1 to 3.5. Using these figures, the design and performance parameters (r.m.s. values , spring stiffness and damping ratio) of suspensions which have 2.5 and 3 cm working space r.m.s. values are read off and represented in Tables 3.2 and 3.3 and in Figs. 3.6 to 3.9. When the vehicle is in its laden static condition a typical value of total available working space would be 18 cm. Bump or rebound stop contact would occur occasionally if the r.m.s. of the working space exceeds ± 6 cm ($\pm 3 \sigma_{sws}$). Hence for these standard deviations of the working space (2.5 and 3 cm), the linear system calculations will be reasonably accurate. The spectral densities of the seat accelerations, dynamic tyre load, fore/aft and the lateral dynamic tyre load transfer of systems No. (3) and (6) described in Table 3.2 is shown in Figs 3.10 to 3.13. Finally, the effect of variation in anti-roll bar stiffness on the performance of passive system No. 6 in Table 3.2 ($K_f = 10.5$ kN/m and $K_r = 12.5$ kN/m) are shown in Figs. 3.14 and 3.15.

3.3 Discussion of results

Comments about the effect of varying the spring stiffness and damping coefficients which can be drawn from Figs. 3.1 to

Figs. 3.5 are made as follows:

1- Employing soft suspension springs always improves the seat accelerations. Reducing the damping coefficients improves the vertical and longitudinal accelerations, while to have an improvement in the lateral seat acceleration, a damping coefficient ($DR = 0.4-0.8$) should be used (see Figs. 3.4 and 3.5).

2- As the spring stiffness is reduced, the demand for the working space is increased. This demand is also substantially increased as the damping coefficient is reduced (see Fig. 3.1).

3- The best dynamic tyre load and the fore/aft and the lateral dynamic tyre load transfer can be obtained by employing a spring with K_f and K_r equal to between 15 and 20 kN/m (see Figs. 3.2 and 3.3). However, the requirements of the damping coefficient to obtain this minimum r.m.s. value in each performance category are different. The fore/aft load transfer requires low damping ($DR = 0.25$), the lateral load transfer requires high damping ($DR = 0.8$), while the dynamic tyre load requires moderate damping ($DR = 0.45$).

In practice, the working space must be restricted and hence the performance analysis of the passive system at a specific working space can be examined to study more closely the system behaviour. Consider first the case where the working space standard deviation available is 2.5 cm (see Figs. 3.6 and 3.7). The best performing system is system No. [6]. This system improves vertical, lateral and longitudinal seat accelerations and the lateral dynamic tyre load transfer by

11%, 21%, 3% and 5% respectively with some gains in the dynamic tyre load at the expense of increasing fore/aft tyre load transfer by 9% when compared with system No. 3. These improvements appear clearly as a dramatic reduction in the peaks appearing in Figs. 3.10 to 3.13 at the body resonance frequency. However, two practical problems are likely with such a soft suspension (system No. [6], $f_n = 0.79$ Hz for the front suspension and $f_n = 0.86$ Hz for the rear one); first, static deflections occurring as a result of varying payload may be too great in the absence of self-levelling, and second, control of body attitude during handling manoeuvres would be poor. Hence, a more realistic fixed parameter passive suspension design would be one of those systems having $f_n > 1$ Hz (see Figs. 3.6 and 3.7). However, employing a spring stiffness such that $f_n > 1$, and increasing the available working space improves all the performance categories but only at the expense of increasing the lateral acceleration and the lateral dynamic tyre load transfer. For example, increasing the working space from 2.5 cm (system No. 3 in Figs. 3.6 and 3.7) to 3 cm (system No. 2 in Figs. 3.8 and 3.9) improves the vertical and longitudinal seat accelerations and the fore/aft tyre load transfer by 4%, 13% and 12% respectively but at the expense of increasing the lateral acceleration and the lateral dynamic tyre load transfer by 5% and 10% respectively.

The foregoing discussion shows how it is difficult for a passive suspension system to cover the wide range of conflicting requirements unless it is adaptive. However, even

a simple enhancement such as a self-levelling facility offers significant improvements by virtue of ensuring that a softer suspension can be used without the static deflection penalty when laden and without causing a deterioration in the vehicle attitude control during handling manoeuvres. The use of stiffer anti-roll bar would be useful in controlling the vehicle attitude, but for straight running this always causes a deterioration in the roll response leading to an increase in the lateral seat acceleration. This fact is confirmed clearly in Figs. 3.14 and 3.15. In these figures, the r.m.s. values of the vertical and longitudinal seat accelerations, dynamic tyre load and the fore/aft tyre load transfer are not significantly affected by increasing the stiffness of the anti-roll bar. On the other hand, employing front and rear anti roll bars with stiffnesses $K_{rf} = 36 \text{ kN.m/rad}$ and $K_{rr} = 20 \text{ kN.m/rad}$ almost doubles the lateral seat accelerations compared with the case of setting these stiffnesses to zero.

It is interesting to compare the performance of this system which has stiff anti roll bars and soft spring stiffness with system No. 3 ($f_n = 1.22 \text{ Hz}$, $K_{rf} = 18 \text{ kN m/rad}$, $K_{rr} = 10 \text{ kN m/rad}$). The results are shown in Table 3.4. It is clear that the passive system with soft spring stiffness and stiff anti roll bars is only slightly better than the passive system with moderate spring stiffness and anti-roll bars. In other words, the advantage achieved from employing the former system in reducing the r.m.s. value of the vertical acceleration by 9% with some gains reducing the dynamic tyre load and the longitudinal acceleration are probably not worthwhile due to

the increase of the r.m.s. values of the lateral acceleration and the fore/aft tyre load transfer by 7% and 9% respectively. The previous analysis confirms the well known conclusion that in order to have a good performance of a passive system over a range of speeds and road conditions, then it must be adaptive. The performance of such a system is discussed in the next section.

3.4 The effect of passive system adaptation.

Previous comparative results have not considered the performance of the passive system as an adaptive one. Therefore, in addition to the speed 30 m/s considered above, results have been generated for the passive system when the same road surface is traversed at 10 and 20 m/s. For each speed the adaptive passive suspension system is designed so as to consume up to the maximum working space (2.5 cm is only considered), while it is impossible for the fixed parameter passive system to do so. The results presented in Table 3.7 were obtained as follows. Firstly, the passive systems of $f_n \approx 1.2$ Hz (system No. 3 in Fig. 3.6 and 3.7) is selected to represent the conventional fixed parameter passive system. The performances of this system are recalculated at 10 and 20 m/s and the results are shown in Table 3.5. Secondly, graphs similar to those in figures 3.6 and 3.7 were repeated at 10 and 20 m/s. For each vehicle speed the best adaptive passive system is selected and its design and performance properties are presented in Table 3.6. Table 3.7 summarises the percentage improvements (ie. the reduction in the r.m.s.

values) achieved from the adaptive passive system when compared with the fixed parameter one. It can be seen from the Table that significant improvements in seat accelerations and fore/aft dynamic tyre load transfer can be achieved from the adaptive passive system when compared with the fixed parameter system at 10 and 20 m/s. Also, the improvements achieved at these speeds are substantially higher than those achieved at 30 m/s where both systems consume all the working space available.

In practice, the realisation of the adaptive passive system is possible. Adjustable dampers in which the damper rate can be varied manually were commercially available many years ago. Recent developments enable this rate to be adjusted by means of an electric motor and control unit. This system typically consists of a microprocessor which receives the information on vehicle speed, steering wheel angle or their rate of change. Based on this information and a programmed control strategy, an electronic signal may be sent to a small electrical actuator (e.g. motor) to change the damper rate as required. On the other hand, it is a much bigger problem to make the spring stiffness adaptive. In principle at least, the use of a pneumatic or hydro-pneumatic suspension system with different effective air volumes could allow a range of spring stiffnesses to be used. The most important practical limitation in this system is the rate of the stiffness variation. However, if this stiffness is changed suddenly, extra dynamic forces will be introduced to the system and

hence the performance would deteriorated. More details about the adaptation of the passive system can be found in Sharp and Crolla [1987 b].

3.5 Concluding remarks.

A performance analysis of passive suspension systems on a full vehicle model has been presented. The primary purpose of this analysis was to provide a clear understanding of the performance properties of these systems when a three dimensional vehicle model is employed and to quantify the ride behaviour of these systems so they can be used as a guide in scaling the performance of the active systems.

The results show that:

- 1- Employing soft suspension with low damping coefficient always improves the vertical and longitudinal seat accelerations, while to improve the lateral seat acceleration a moderate damping coefficient should be used.
- 2- As the spring stiffness is reduced the demand for the working space is increased. This demand can be reduced by increasing the damping coefficient.
- 3- The best dynamic tyre load and the fore/aft and the lateral dynamic tyre load transfer can be obtained by employing a moderate spring stiffness ($f_n = 1$ Hz). However, the requirements of the damping coefficient in each performance category are variable. The fore/aft load transfer requires a low damping coefficient, the lateral load transfer requires a high damping coefficient, while the dynamic tyre load requires a moderate damping coefficient.

4- For a conventional passive system, increasing the design value of the available working space can always be exploited to improve the ride comfort in terms of the vertical and longitudinal accelerations and the fore/aft tyre load transfer but at the expense of increasing the lateral seat acceleration and the lateral dynamic tyre load transfer.

5- In the above four points, the conclusions concerning the vertical acceleration, dynamic tyre load and the suspension working space are similar to those obtained from the quarter car model studied by different authors (see for example, Sharp and Hassan [1984] and [1986 b]). Hence, in general the use of this simple vehicle model in studying the ride behaviour of the passive systems is very useful.

6- In studying the effect of varying the anti-roll bar stiffness, it was found that the r.m.s. values of the vertical and longitudinal seat accelerations, dynamic tyre load and the fore/aft tyre load transfer were not significantly affected by increasing the stiffness of the anti-roll bar. On the other hand, employing front and rear anti roll bars with stiffnesses $K_{rf} = 36 \text{ kN.m/rad}$ and $K_{rr} = 20 \text{ kN.m/rad}$ was found to double the lateral acceleration compared with the case of setting these stiffnesses to zero.

7- The practical limitations of using a suspension system with a soft spring were discussed. The possibility of employing a passive system with soft spring stiffness (to improve the ride comfort) and with stiff anti-roll bars (to maintain the vehicle attitude during handling manoeuvres) was examined. The comparison of the performance of this system with a system with moderate spring and anti-roll stiffnesses showed that

the improvements achieved by the former system in terms of vertical acceleration are associated with an increase in the lateral acceleration and lateral dynamic tyre load. Hence, the use of a system with soft spring and stiff anti-roll bars is not worthwhile overall.

8- Comparisons of the adaptive passive system and the fixed parameter one at different speeds shows that significant improvements in seat acceleration could be achieved from the system adaptation.

Table 3.1 Fixed vehicle parameters.

| | | |
|----------------------------|-------------------------------|--------------------------|
| $M_b = 1710 \text{ kg}$ | $K_{rr} = 18 \text{ kNm/rad}$ | $t_s = 0.595 \text{ m}$ |
| $M_{wf} = 57.5 \text{ kg}$ | $K_{rf} = 10 \text{ kNm/rad}$ | $t_w = 1.54 \text{ m}$ |
| $M_{wr} = 75 \text{ kg}$ | $K_t = 200 \text{ kN/m}$ | $X_s = -0.267 \text{ m}$ |
| $I_p = 2500 \text{ kgm}^2$ | $L = 2.69 \text{ m}$ | $Y_s = 0.432 \text{ m}$ |
| $I_r = 600 \text{ kgm}^2$ | $w_a = 1.353 \text{ m}$ | $Z_s = 0.485 \text{ m}$ |
| | $w_b = 1.337 \text{ m}$ | |

Table 3.2 Performance and design properties of the passive suspension systems calculated for 2.5 cm working space r.m.s. at 30 m/s on a road of $R_c = 3 \times 10^{-6}$.

| System | K_f | K_r | DR_f | DR_r | Root mean square values | | | | | | |
|--------|----------------|----------------|--------|--------|-------------------------|-------------|--------------|--------|--------|--------|--------|
| No. | $\frac{kN}{m}$ | $\frac{kN}{m}$ | | | \ddot{z}_x | \dot{y}_x | \ddot{x}_x | $FDTL$ | $RDTL$ | $FDTT$ | $LDTT$ |
| | | | | | m/s^2 | m/s^2 | m/s^2 | N | N | | |
| 1 | 38 | 43 | 0.30 | 0.35 | 2.05 | 1.16 | 0.68 | 1614 | 1818 | 0.218 | 0.184 |
| 2 | 30 | 33 | 0.35 | 0.40 | 1.81 | 1.01 | 0.61 | 1535 | 1765 | 0.219 | 0.177 |
| 3 | 25 | 23 | 0.40 | 0.50 | 1.67 | 0.90 | 0.55 | 1496 | 1698 | 0.223 | 0.173 |
| 4 | 21 | 20 | 0.45 | 0.55 | 1.62 | 0.84 | 0.54 | 1477 | 1687 | 0.228 | 0.171 |
| 5 | 18 | 17 | 0.50 | 0.60 | 1.58 | 0.80 | 0.53 | 1467 | 1677 | 0.232 | 0.169 |
| 6 | 10.5 | 12.5 | 0.70 | 0.70 | 1.49 | 0.71 | 0.54 | 1463 | 1666 | 0.245 | 0.165 |
| 7 | 8.5 | 9.5 | 0.80 | 0.80 | 1.46 | 0.69 | 0.53 | 1468 | 1666 | 0.249 | 0.164 |

Table 3.3 Performance and design properties of the passive suspension systems calculated for 3 cm working space r.m.s. at 30 m/s on a road of $R_c = 3 \times 10^{-6}$.

| System | K_f | K_r | DR_f | DR_r | Root mean square values | | | | | | |
|--------|----------------|----------------|--------|--------|-------------------------|--------------|--------------|--------|--------|--------|--------|
| No. | $\frac{kN}{m}$ | $\frac{kN}{m}$ | | | \ddot{z}_x | \ddot{y}_x | \ddot{x}_x | $FDTL$ | $RDTL$ | $FDTT$ | $LDTT$ |
| | | | | | m/s^2 | m/s^2 | m/s^2 | N | N | | |
| 1 | 29 | 32 | 0.25 | 0.30 | 1.79 | 1.09 | 0.54 | 1596 | 1794 | 0.191 | 0.198 |
| 2 | 23 | 25 | 0.30 | 0.35 | 1.60 | 0.94 | 0.48 | 1521 | 1711 | 0.197 | 0.191 |
| 3 | 19 | 20 | 0.35 | 0.40 | 1.49 | 0.85 | 0.46 | 1480 | 1672 | 0.203 | 0.187 |
| 4 | 15 | 16 | 0.40 | 0.45 | 1.41 | 0.78 | 0.43 | 1459 | 1654 | 0.208 | 0.185 |
| 5 | 11 | 11 | 0.50 | 0.55 | 1.34 | 0.70 | 0.42 | 1441 | 1645 | 0.218 | 0.181 |
| 6 | 9 | 9 | 0.55 | 0.60 | 1.31 | 0.67 | 0.41 | 1439 | 1647 | 0.220 | 0.182 |
| 7 | 4.5 | 5.5 | 0.80 | 0.80 | 1.28 | 0.61 | 0.41 | 1442 | 1650 | 0.229 | 0.18 |

Table 3.4 Comparison of the performance of the passive system No. 3 in Table 3.2 (which employs medium stiffness springs and anti-roll bars) and system No. 20 in Figs 6.14 and 6.15 (which employs soft springs and stiff anti-roll bars).

| System of | K_f | K_r | K_{rf} | K_{rr} | Root mean square values calculated at 30 m/s for $R_c = 3 \times 10^{-6}$ | | | | | | |
|--------------|----------------|----------------|-------------------|-------------------|---|--------------|--------------|----------|------|-------|-------|
| | $\frac{kN}{m}$ | $\frac{kN}{m}$ | $\frac{kNm}{rad}$ | $\frac{kNm}{rad}$ | \ddot{z}_x | \ddot{y}_x | \ddot{x}_x | FDTLRDTL | FDTT | LDTT | |
| | | | | | m/s^2 | m/s^2 | m/s^2 | N | N | | |
| Table 3.2 | 25 | 23 | 18 | 10 | 1.67 | 0.90 | 0.55 | 1496 | 1698 | 0.223 | 0.173 |
| Fig. 6.14 | 10.5 | 12.5 | 36 | 20 | 1.52 | 0.97 | 0.54 | 1471 | 1664 | 0.245 | 0.172 |

Table 3.5 Performance properties of the fixed parameter passive system (system No. 3 in Table 3.2) calculated at 10, 20 and 30 m/s and $R_c = 3 \times 10^{-6}$.

| Speed <i>m/s</i> | Root mean square values | | | | | | | | |
|---------------------|--|--|--|-------------------------------------|-------------------------------------|-------------------------|-------------------------|-------------|-------------|
| | \ddot{z}_x <i>m/s²</i> | \ddot{y}_x <i>m/s²</i> | \ddot{x}_x <i>m/s²</i> | <i>sws_f</i> <i>cm</i> | <i>sws_r</i> <i>cm</i> | <i>FDTL</i> <i>N</i> | <i>RDTL</i> <i>N</i> | <i>FDTT</i> | <i>LDTT</i> |
| 10 | 0.68 | 0.37 | 0.36 | 1.0 | 1.0 | 643 | 715 | 0.103 | 0.080 |
| 20 | 1.23 | 0.73 | 0.50 | 1.8 | 1.8 | 1099 | 1243 | 0.168 | 0.130 |
| 30 | 1.67 | 0.9 | 0.55 | 2.5 | 2.5 | 1496 | 1698 | 0.223 | 0.173 |

| Speed | K_f | K_r | DR_f | DR_r | Root mean square values | | | | | | | | |
|-------|----------------|----------------|--------|--------|-------------------------|--------------|--------------|---------|---------|--------|--------|--------|--------|
| m/s | $\frac{kN}{m}$ | $\frac{kN}{m}$ | | | \ddot{z}_x | \ddot{y}_x | \ddot{x}_x | sws_f | sws_r | $FDTL$ | $RDTL$ | $FDTT$ | $LDTT$ |
| | | | | | m/s^2 | m/s^2 | m/s^2 | cm | cm | N | N | | |
| 10 | 7.5 | 8.5 | 0.5 | 0.55 | 0.54 | 0.31 | 0.20 | 1.4 | 1.36 | 643 | 722 | 0.095 | 0.084 |
| 20 | 7.5 | 8.5 | 0.5 | 0.5 | 0.93 | 0.55 | 0.30 | 2.5 | 2.50 | 1084 | 1248 | 0.162 | 0.135 |
| 30 | 10.5 | 12.5 | 0.7 | 0.7 | 1.49 | 0.71 | 0.54 | 2.5 | 2.50 | 1463 | 1666 | 0.245 | 0.165 |

Table 3.6 Performance and design properties of the adaptive passive systems calculated at 10, 20 and 30 m/s and $R_c = 3 \times 10^{-6}$.

Table 3.7 Improvements achieved from the adaptive passive systems when compared with the fixed parameter one at 10, 20 and 30 m/s and $R_c = 3 \times 10^{-6}$.

| Speed <i>m/s</i> | Percentage reduction in the r.m.s. values | | | | | | |
|---------------------|---|--|--|-------------------------|-------------------------|-------------|-------------|
| | \ddot{z}_x <i>m/s²</i> | \ddot{y}_x <i>m/s²</i> | \ddot{x}_x <i>m/s²</i> | <i>FDTL</i> <i>N</i> | <i>RDTL</i> <i>N</i> | <i>FDTT</i> | <i>LDTT</i> |
| 10 | 21 | 16 | 44 | 0 | 0 | 8 | -5 |
| 20 | 25 | 25 | 40 | 1 | 0 | 3 | -4 |
| 30 | 11 | 21 | 3 | 2 | 2 | -9 | 5 |

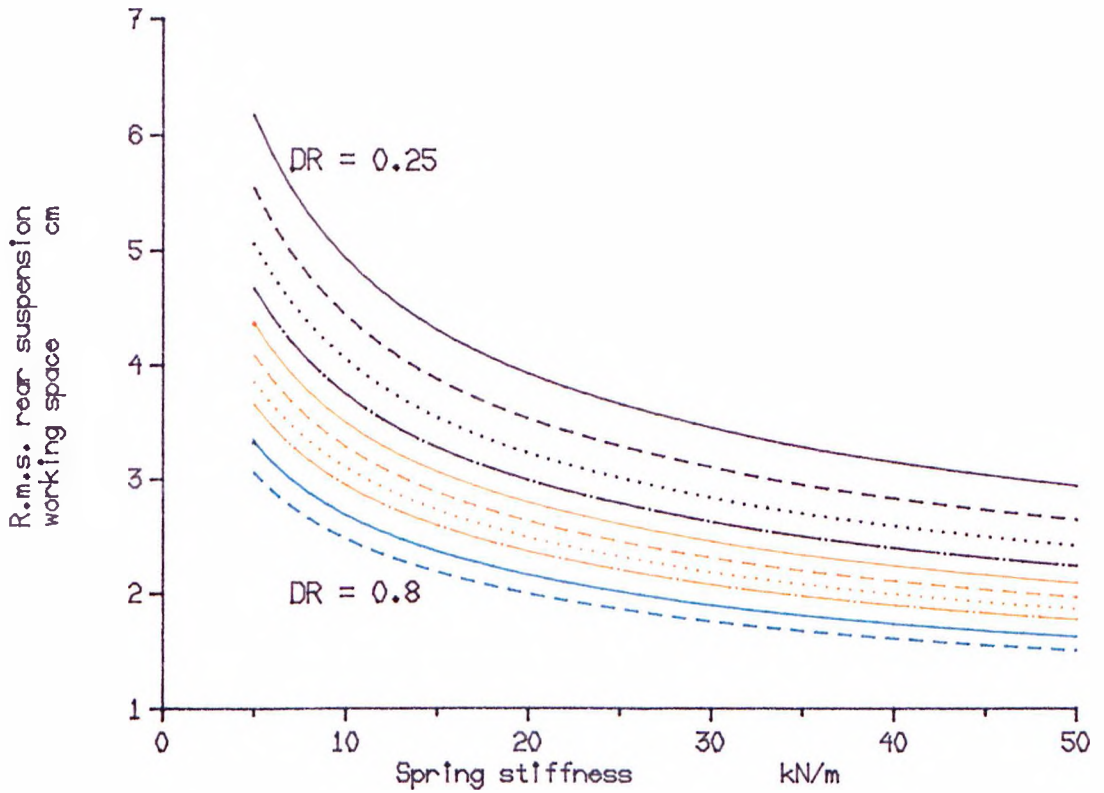
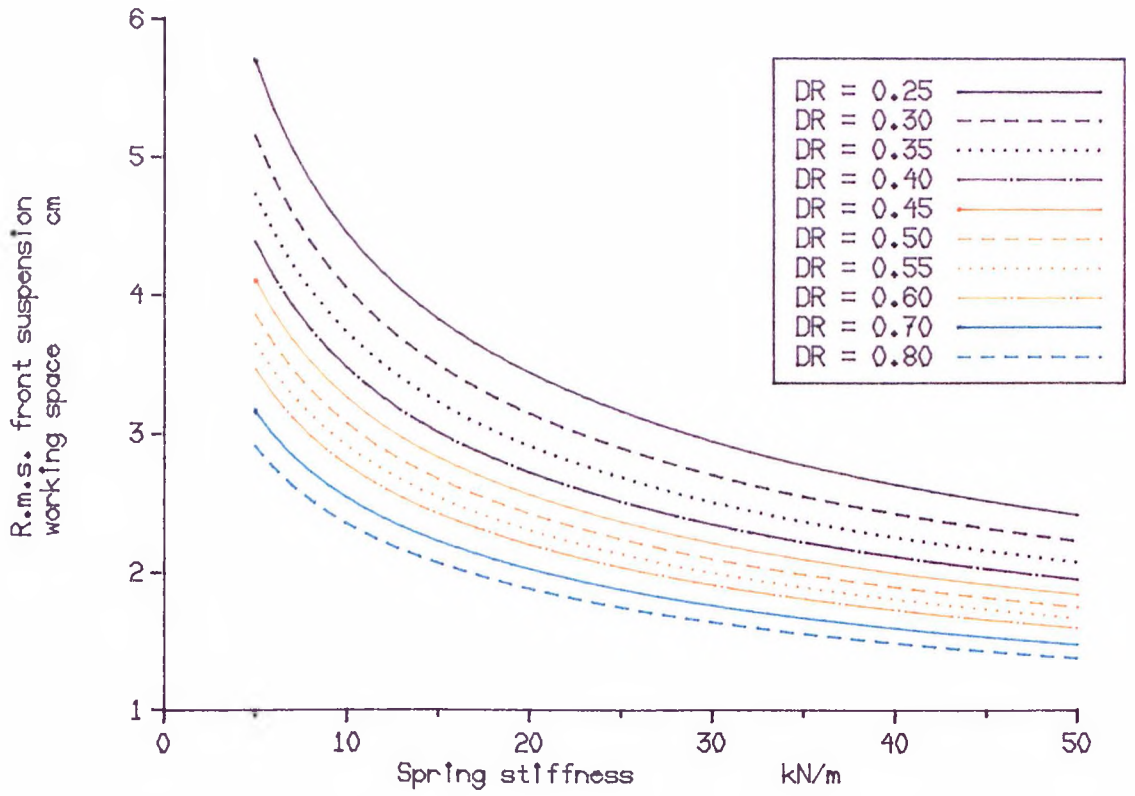


Fig. 3.1 The effect of suspension parameter variation on the r.m.s. values of the suspension working space at 30 m/s on a road of $R_0 = 3 \times 10^{-6}$.

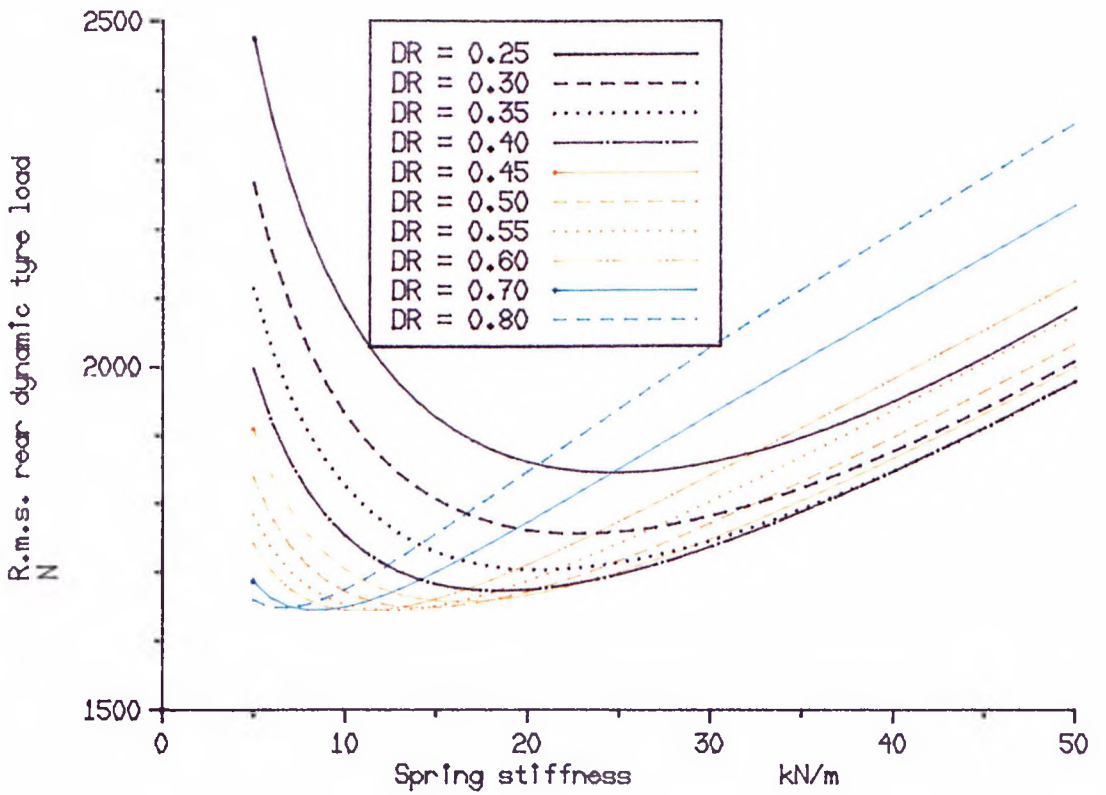
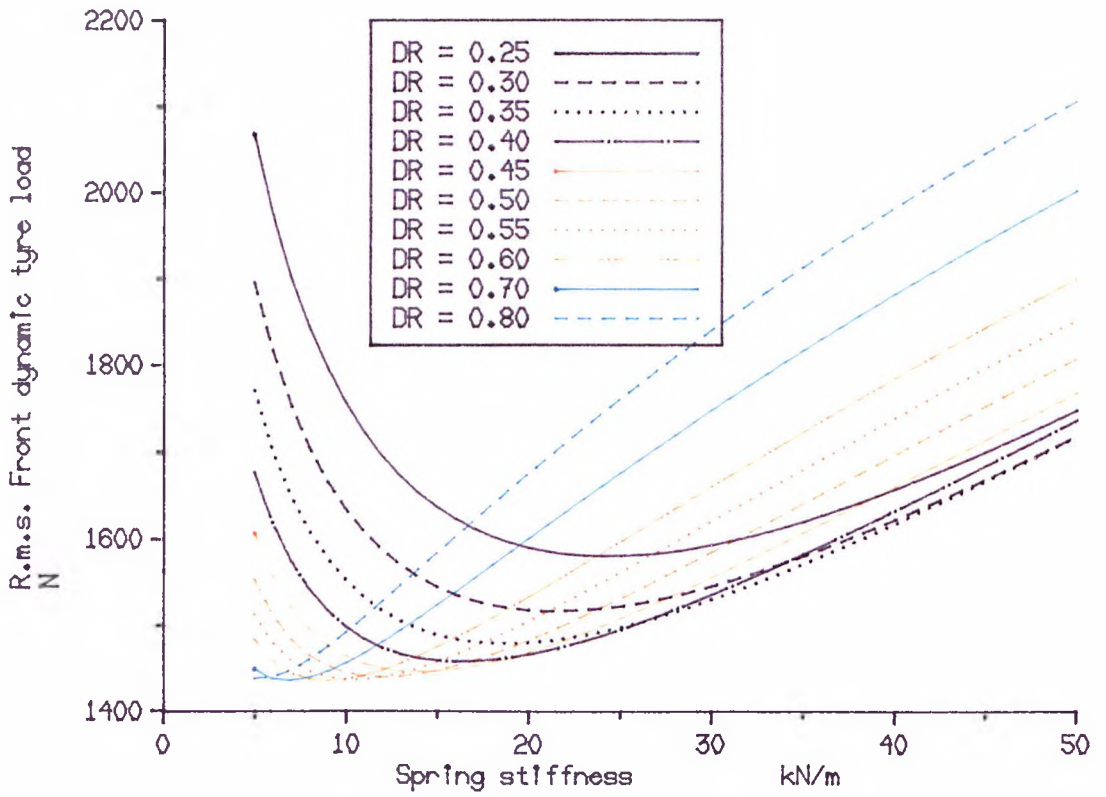


Fig. 3.2 The effect of suspension parameter variation on the r.m.s. values of the dynamic tyre load at 30 m/s on a road of $R_o = 3 \times 10^{-6}$.

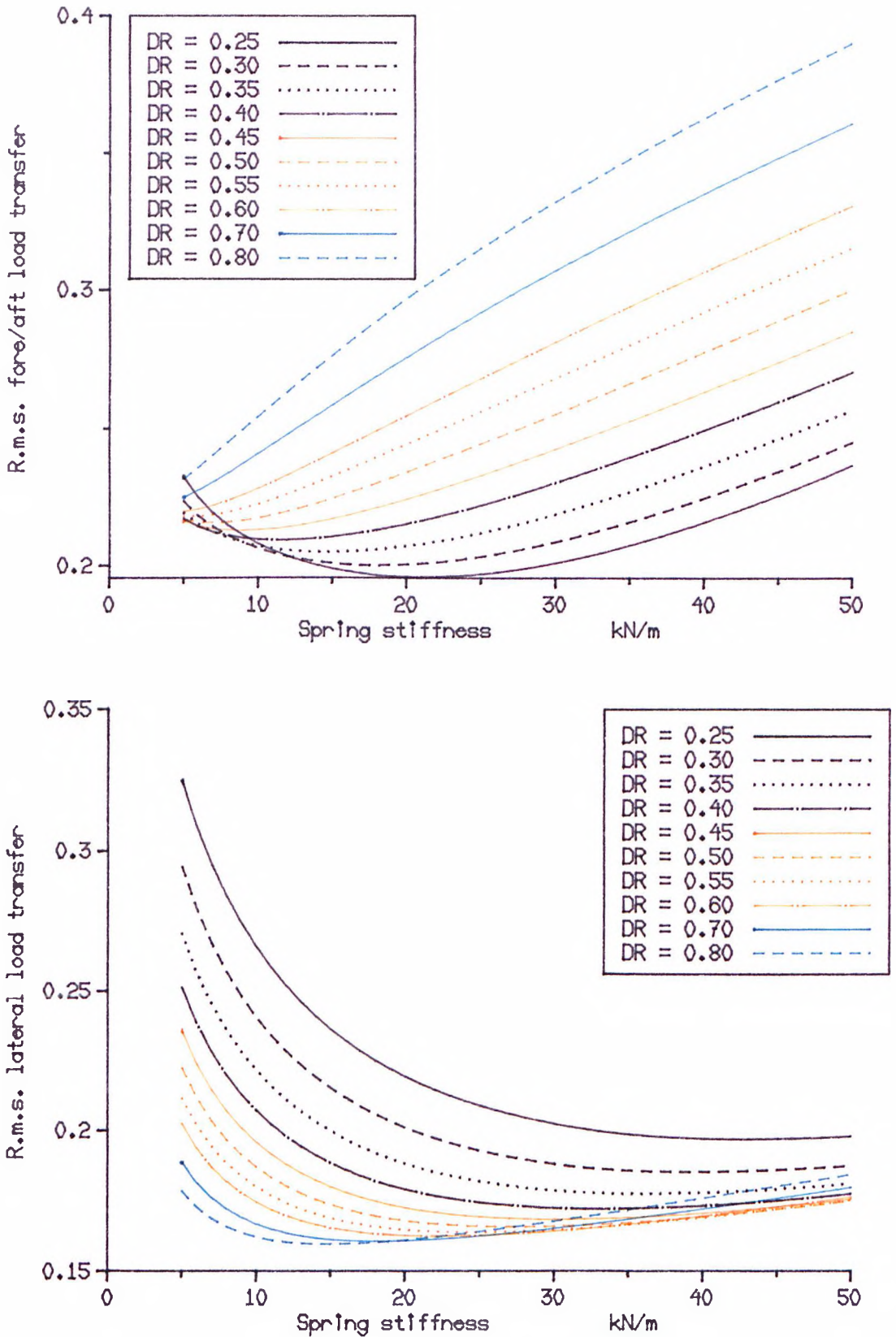


Fig. 3.3 The effect of suspension parameter variation on the r.m.s. values of the fore/aft and lateral dynamic tyre load transfer at 30 m/s on a road of $R_s = 3 \times 10^{-6}$.

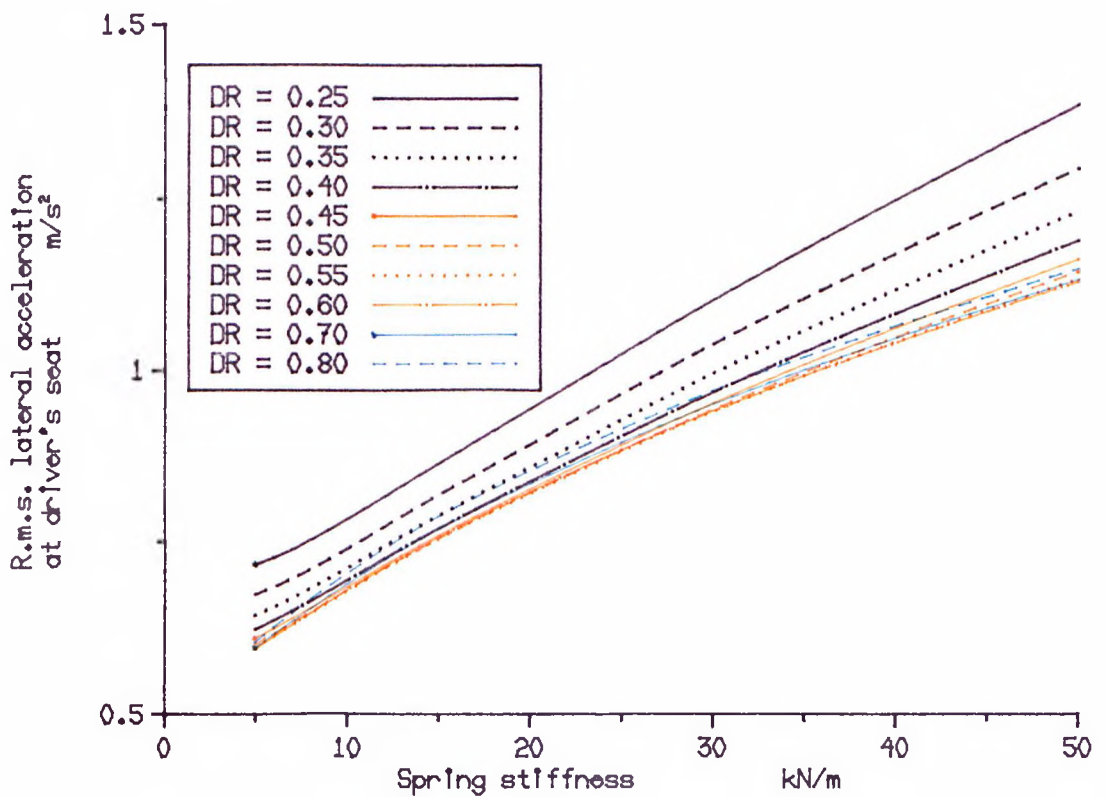
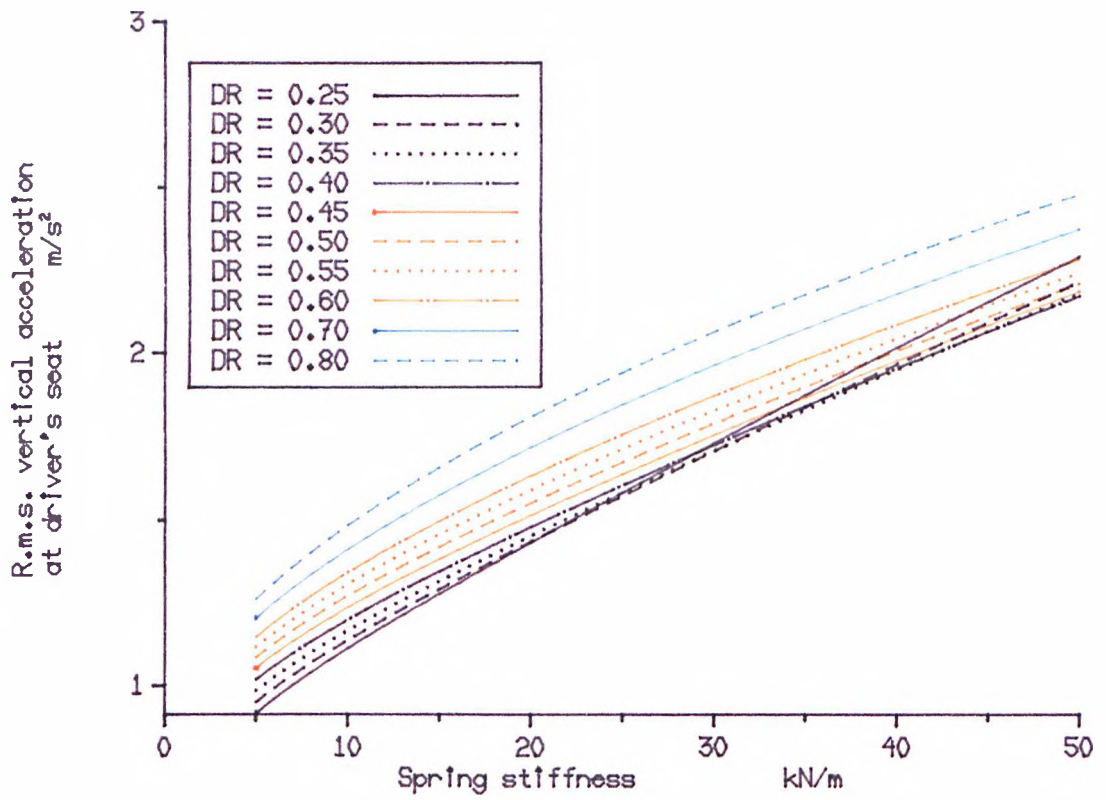


Fig. 3.4 The effect of suspension parameter variation on the r.m.s. values of the vertical and lateral accelerations at 30 m/s on a road of $R_0 = 3 \times 10^{-6}$.

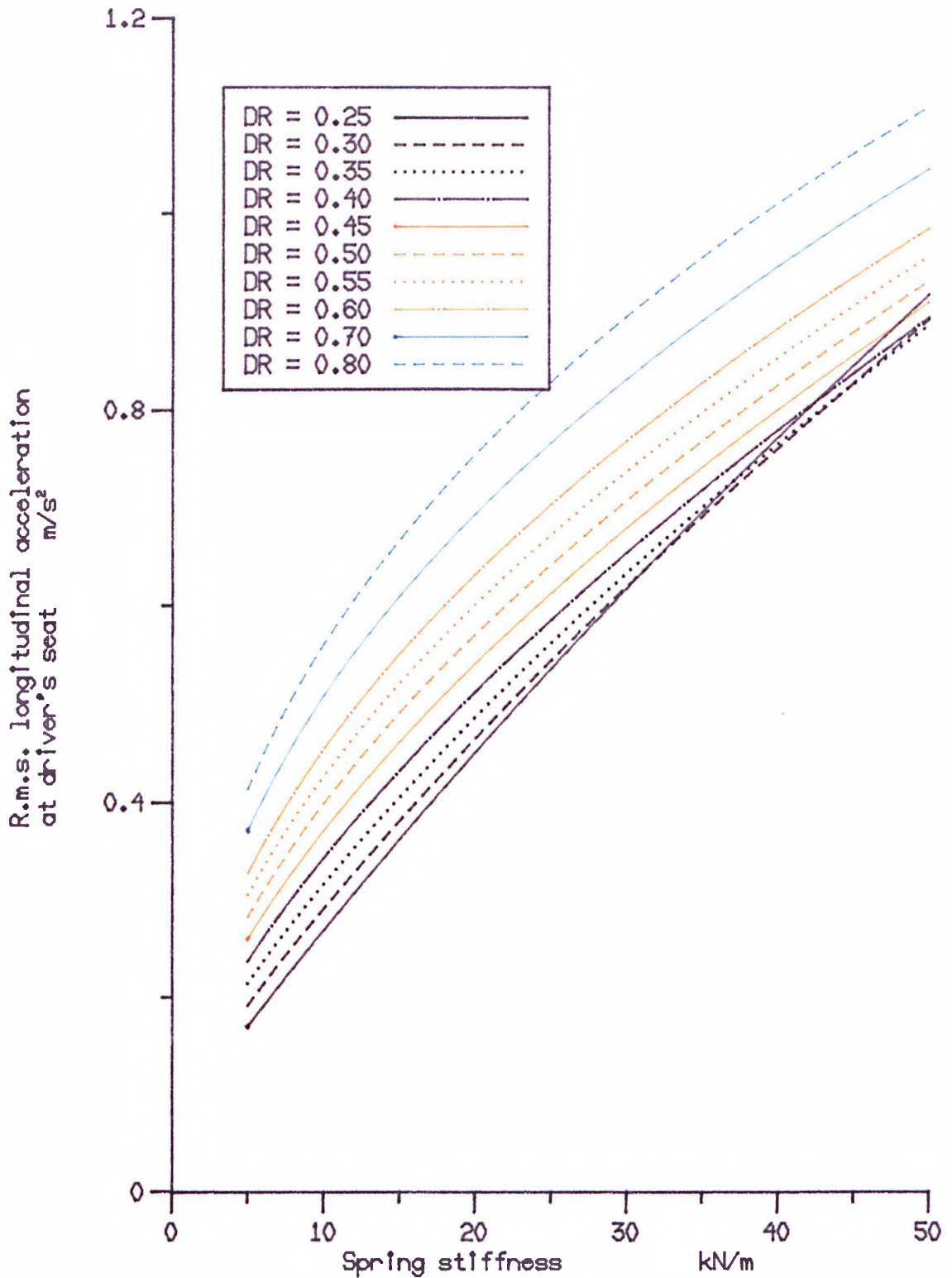


Fig. 3.5 The effect of suspension parameter variation on the r.m.s. values of the longitudinal acceleration at 30 m/s on a road of $R_0 = 3 \times 10^{-6}$.

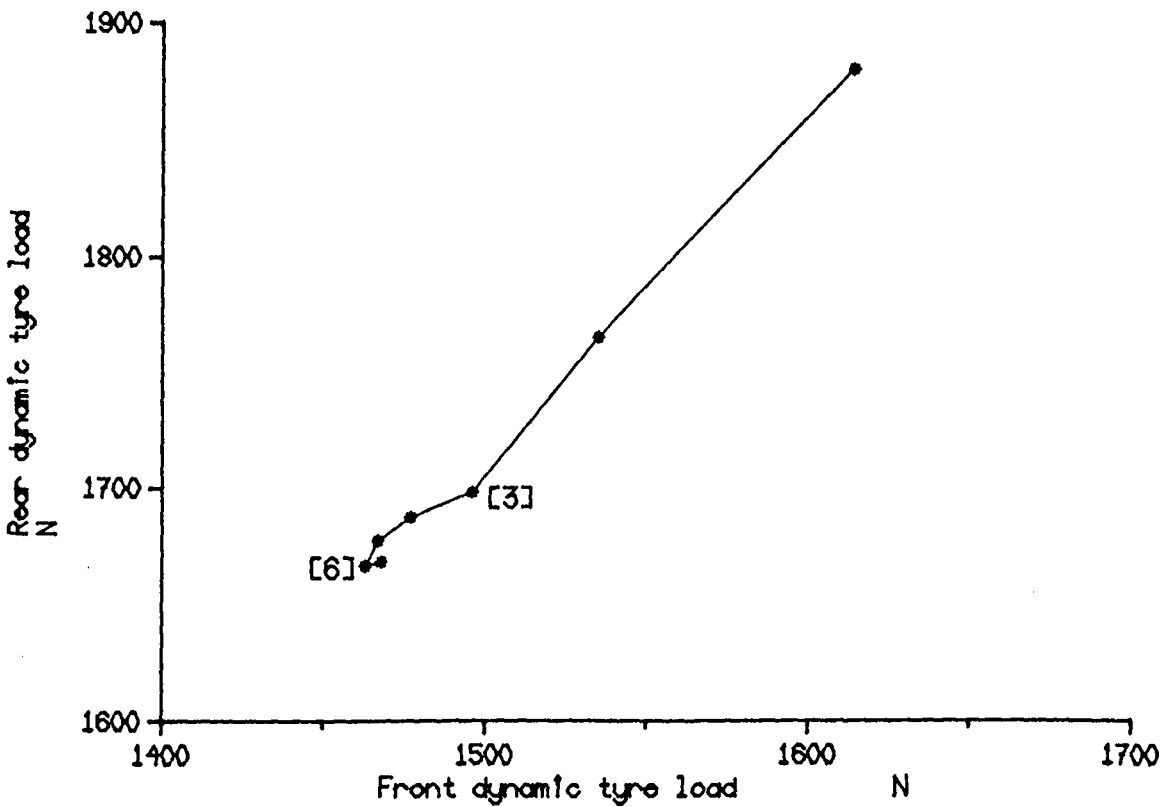
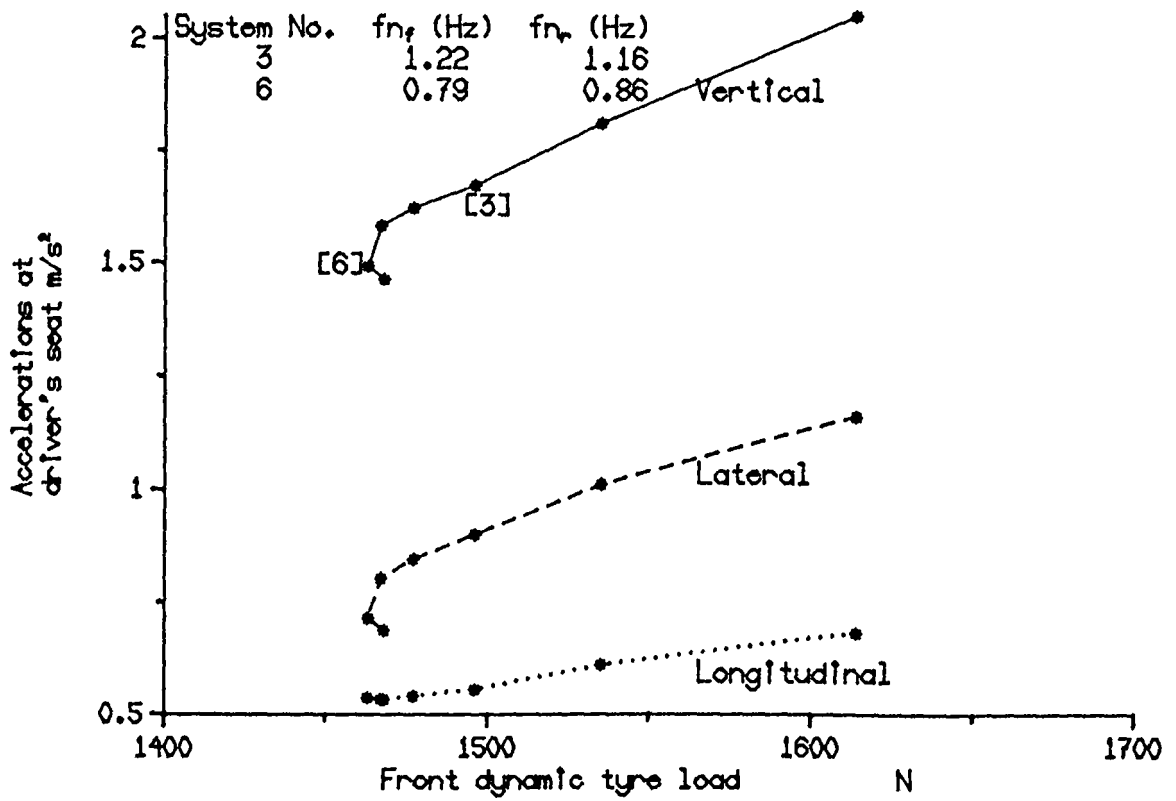


Fig. 3.6 R.m.s. values of the seat accelerations and the rear dynamic tyre load for various passive suspension systems for 2.5 cm r.m.s. working space at 30 m/s on a road of $R_0 = 3 \times 10^{-6}$.

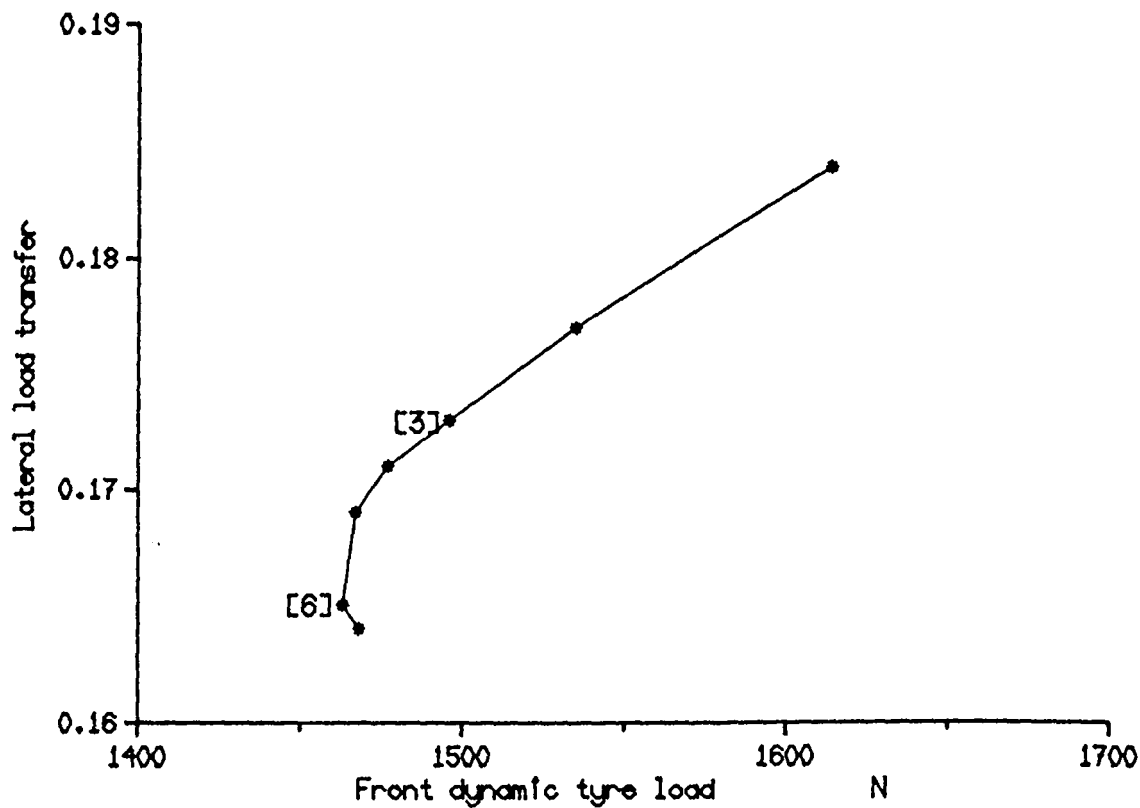
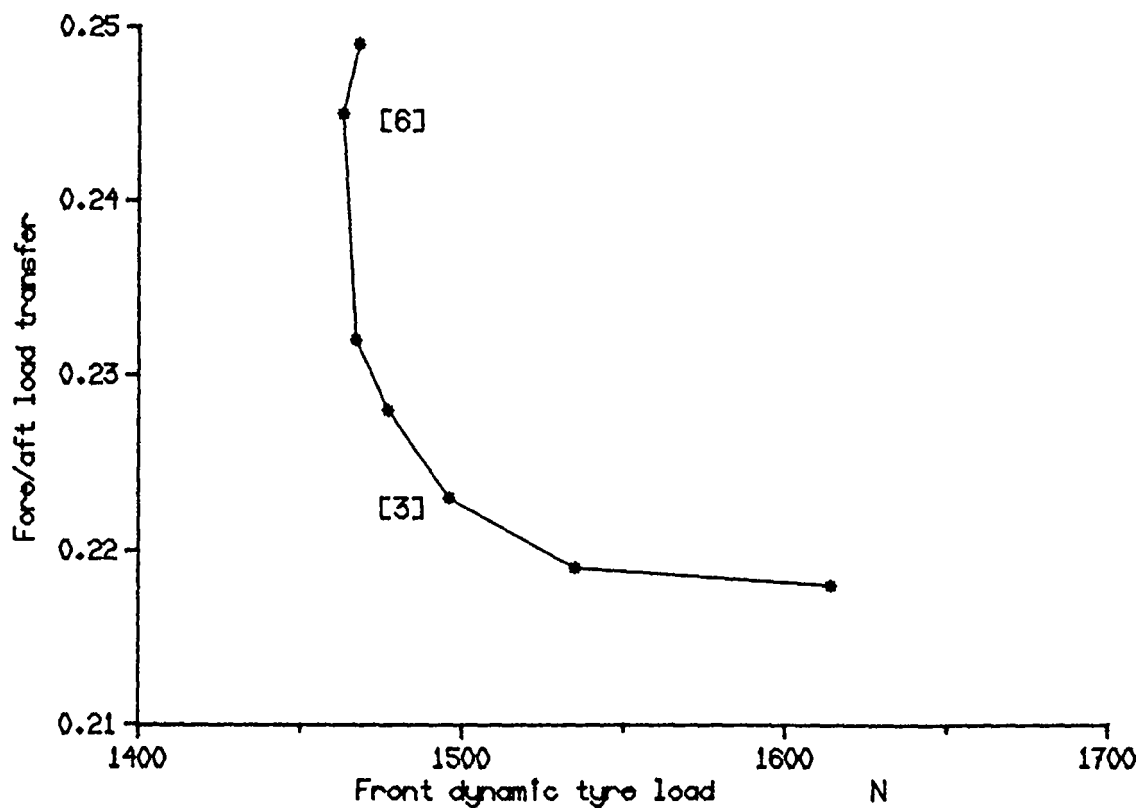


Fig. 3.7 R.m.s. values of the fore/aft and the lateral tyre load transfer for various passive suspension systems for 2.5 cm r.m.s. working space at 30 m/s on a road of $R_0 = 3 \times 10^{-6}$.

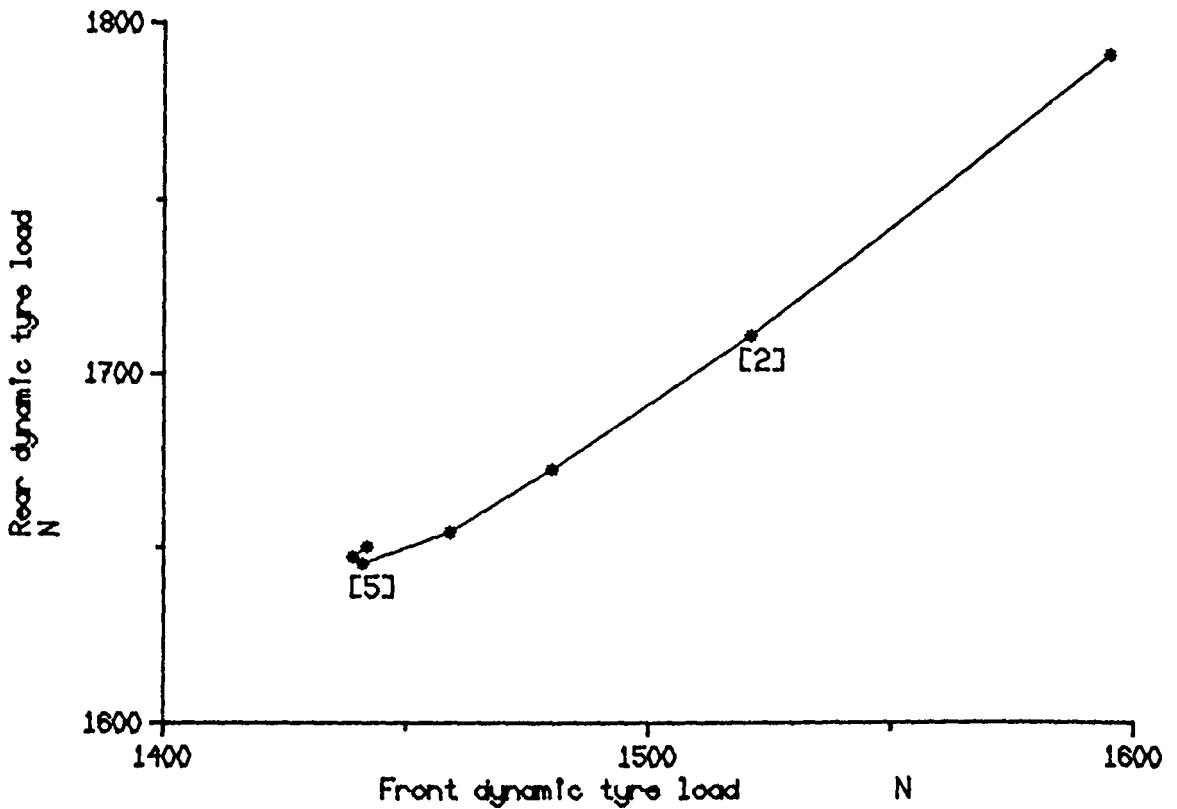
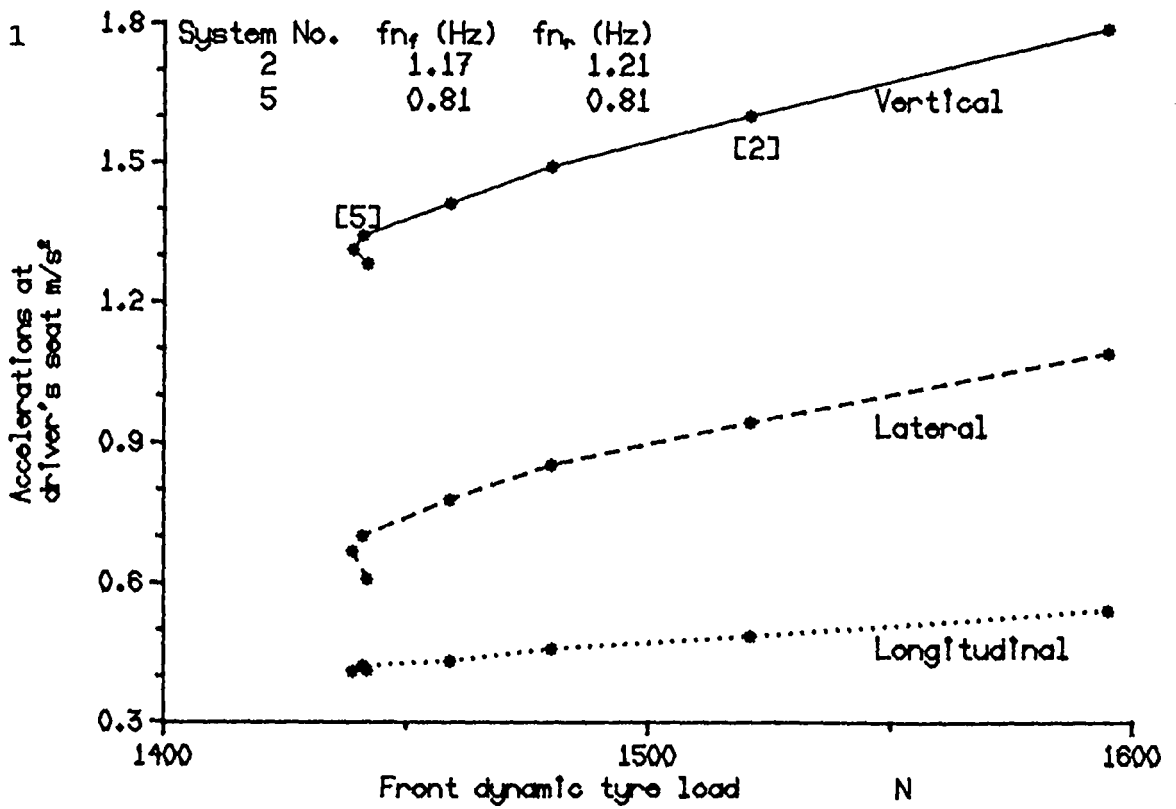


Fig. 3.8 R.m.s. values of the seat accelerations and the rear dynamic tyre load for various passive suspension systems for 3 cm r.m.s. working space at 30 m/s on a road of $R_0 = 3 \times 10^{-6}$.

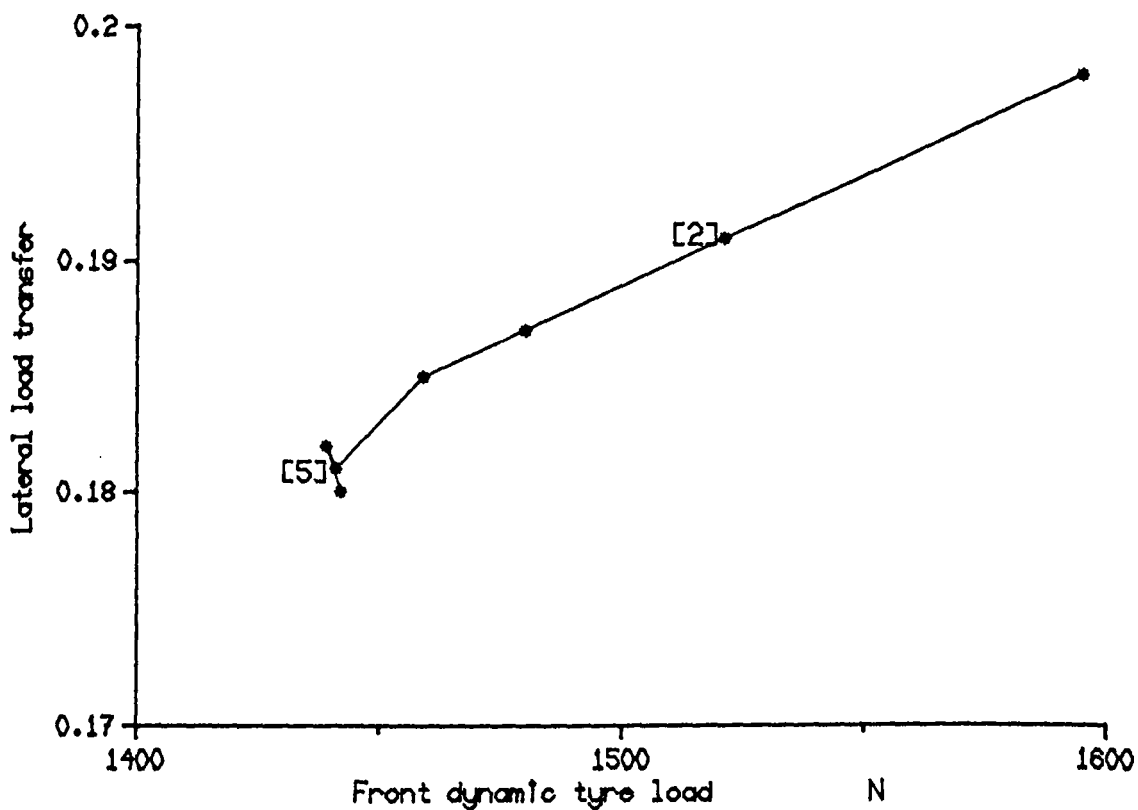
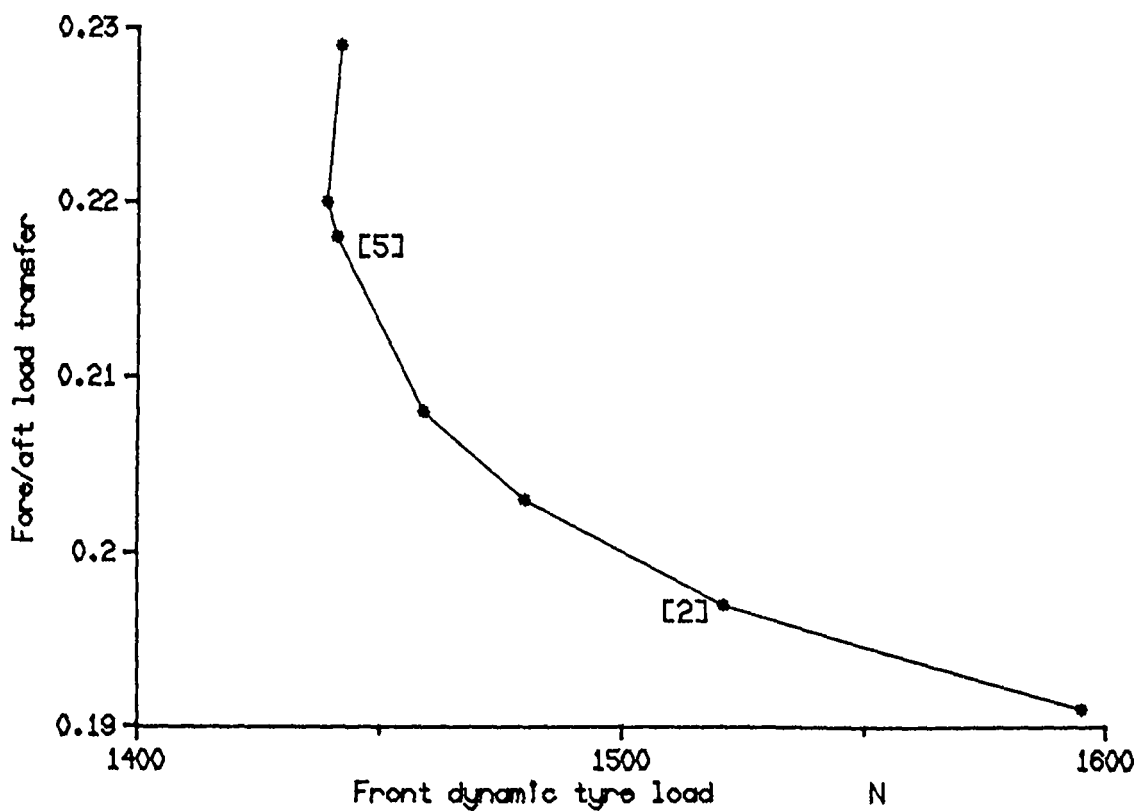


Fig. 3.9 R.m.s. values of the fore/aft and the lateral tyre load transfer for various passive suspension systems for 3 cm r.m.s. working space at 30 m/s on a road of $R_0 = 3 \times 10^{-6}$.

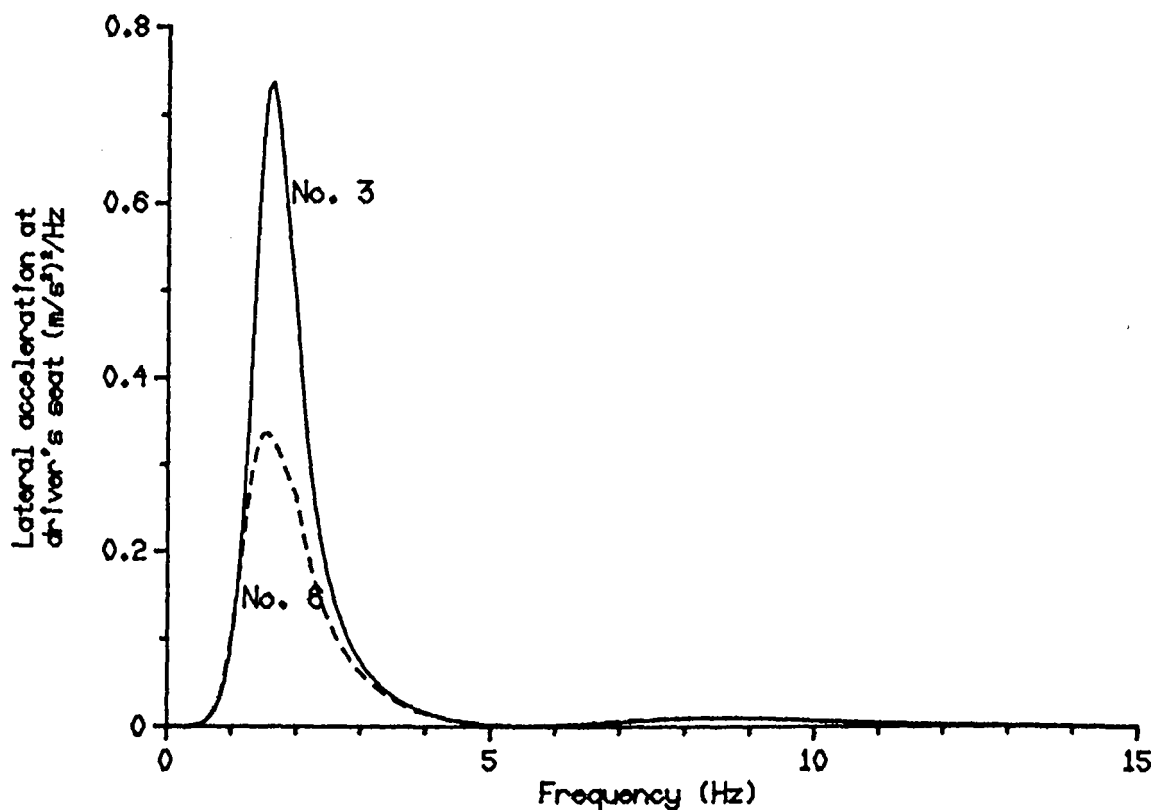
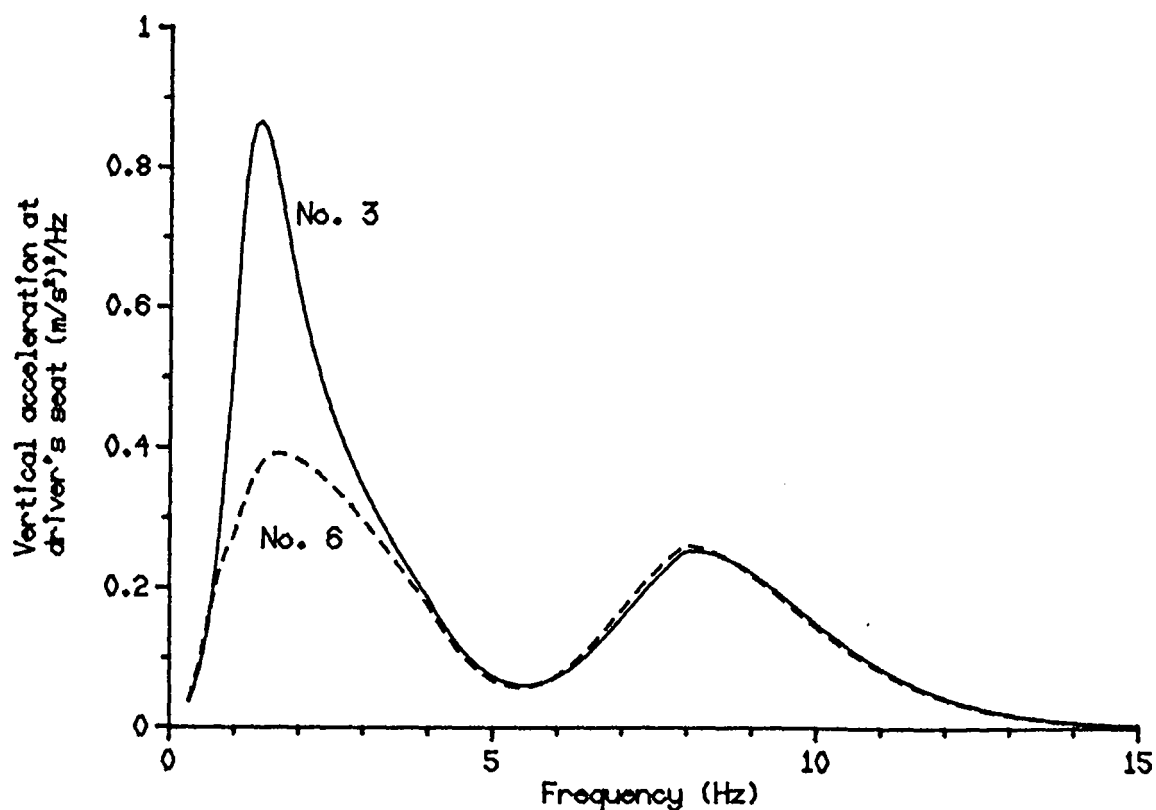


Fig. 3.10 Spectral densities of the I.S.O. weighted vertical and lateral accelerations for systems No. 3 and No. 6 for a suspension working space of 2.5 cm.

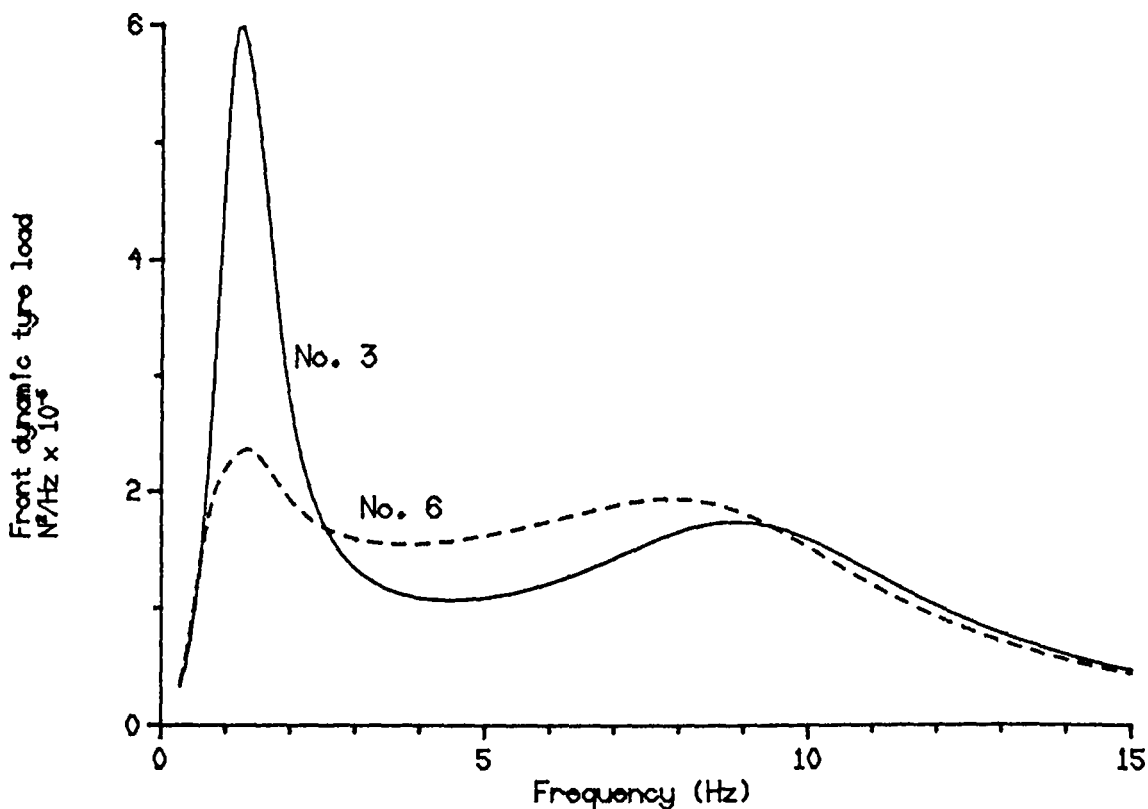
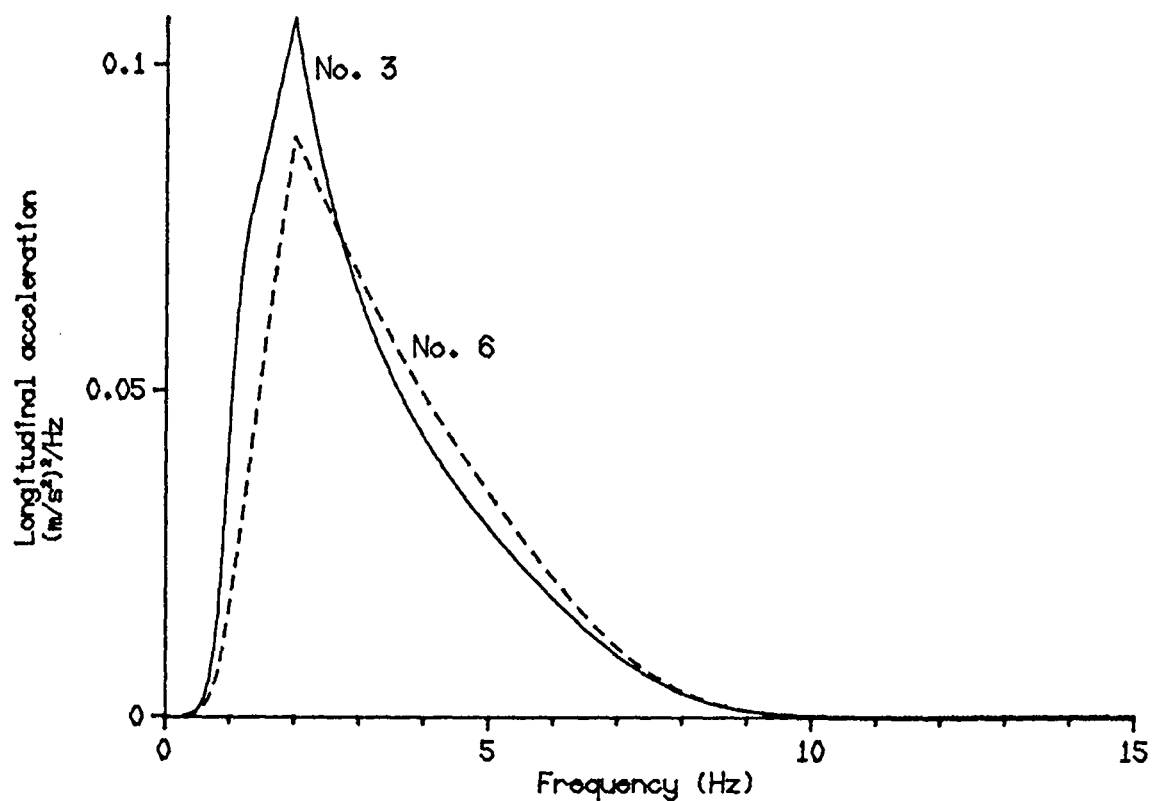


Fig. 3.11 Spectral densities of the I.S.O. weighted longitudinal acceleration and the front dynamic tyre load for systems No. 3 and No. 6 for a suspension working space of 2.5 cm.

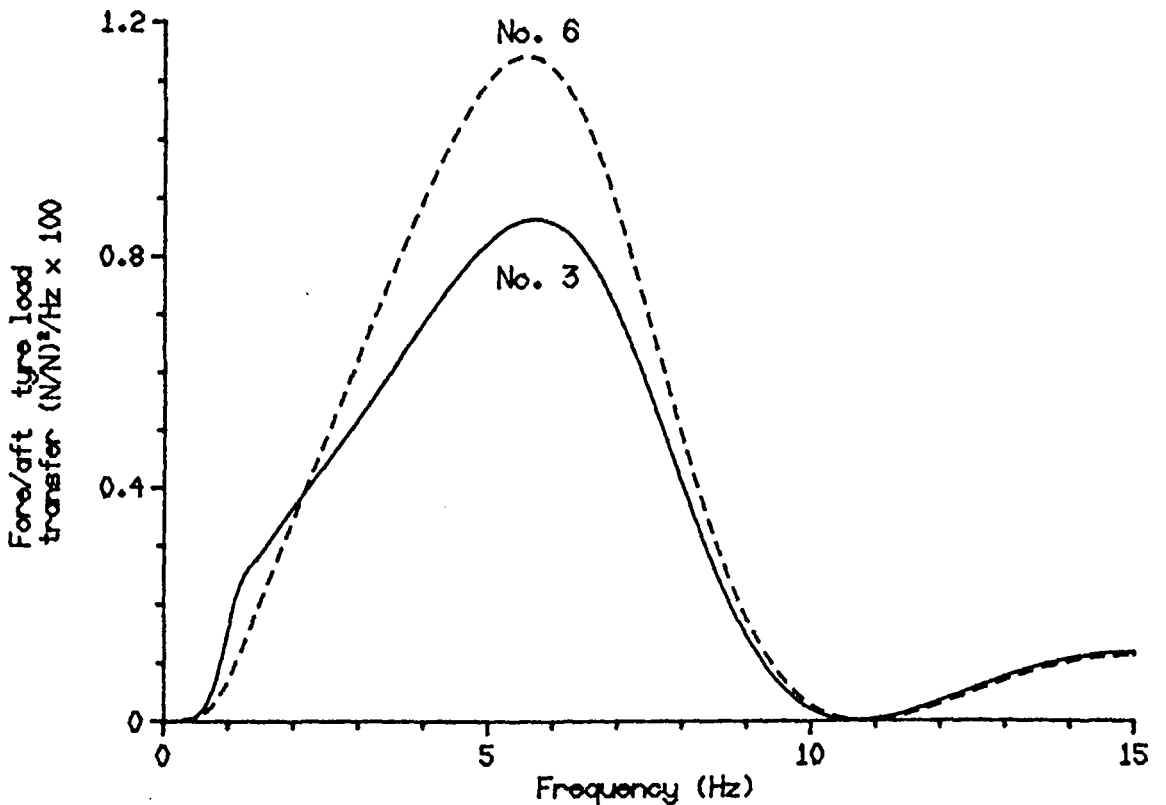
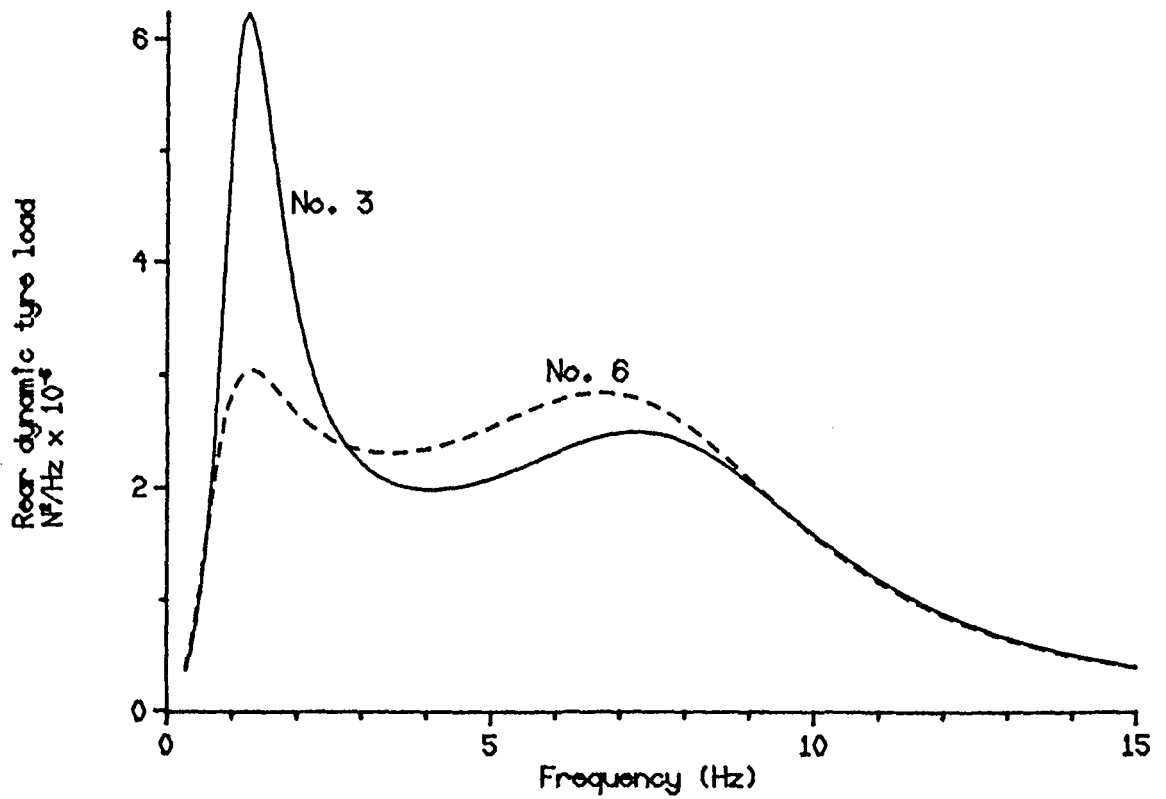


Fig. 3.12 Spectral densities of the rear dynamic tyre load and the fore/aft tyre load transfer for systems No. 3 and No. 6 for a suspension working space of 2.5 cm.

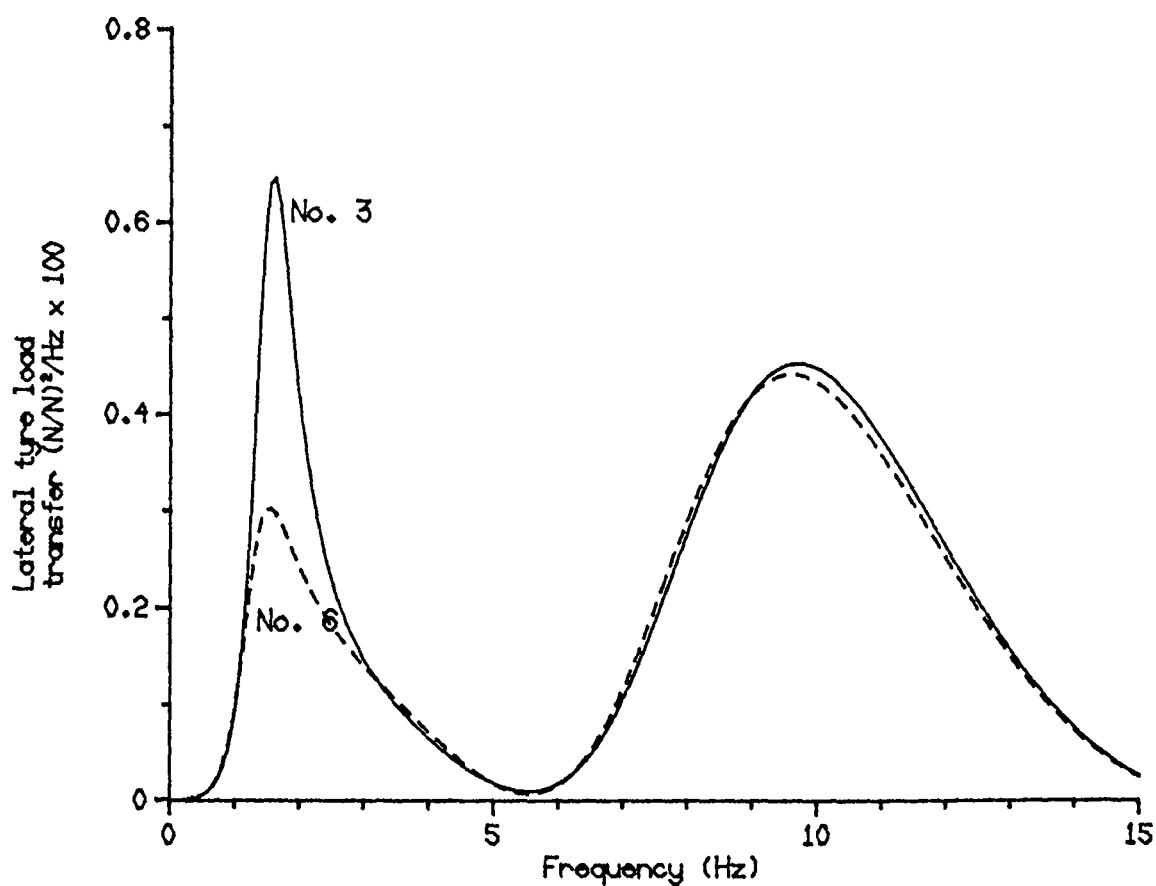


Fig. 3.13 Spectral densities of the lateral tyre load transfer for systems No. 3 and No. 6 for a suspension working space of 2.5 cm.

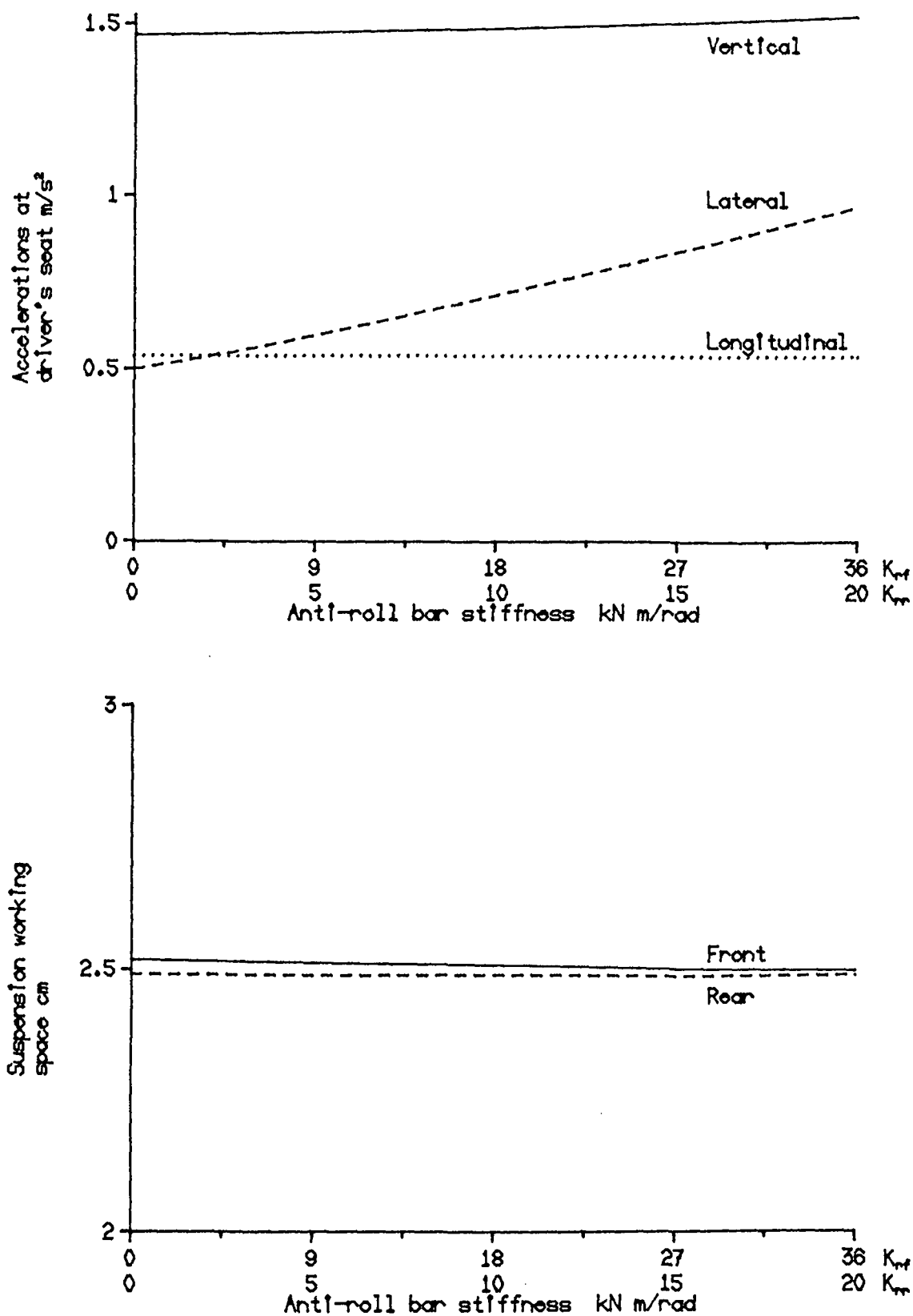


Fig. 3.14 The effect of variation in anti-roll bar stiffness on the r.m.s. values of the seat accelerations and the suspension working space for a passive system with $K_f = 10.5 \text{ kN/m}$, $K_r = 12.5 \text{ kN/m}$ and $DR = 0.7$.

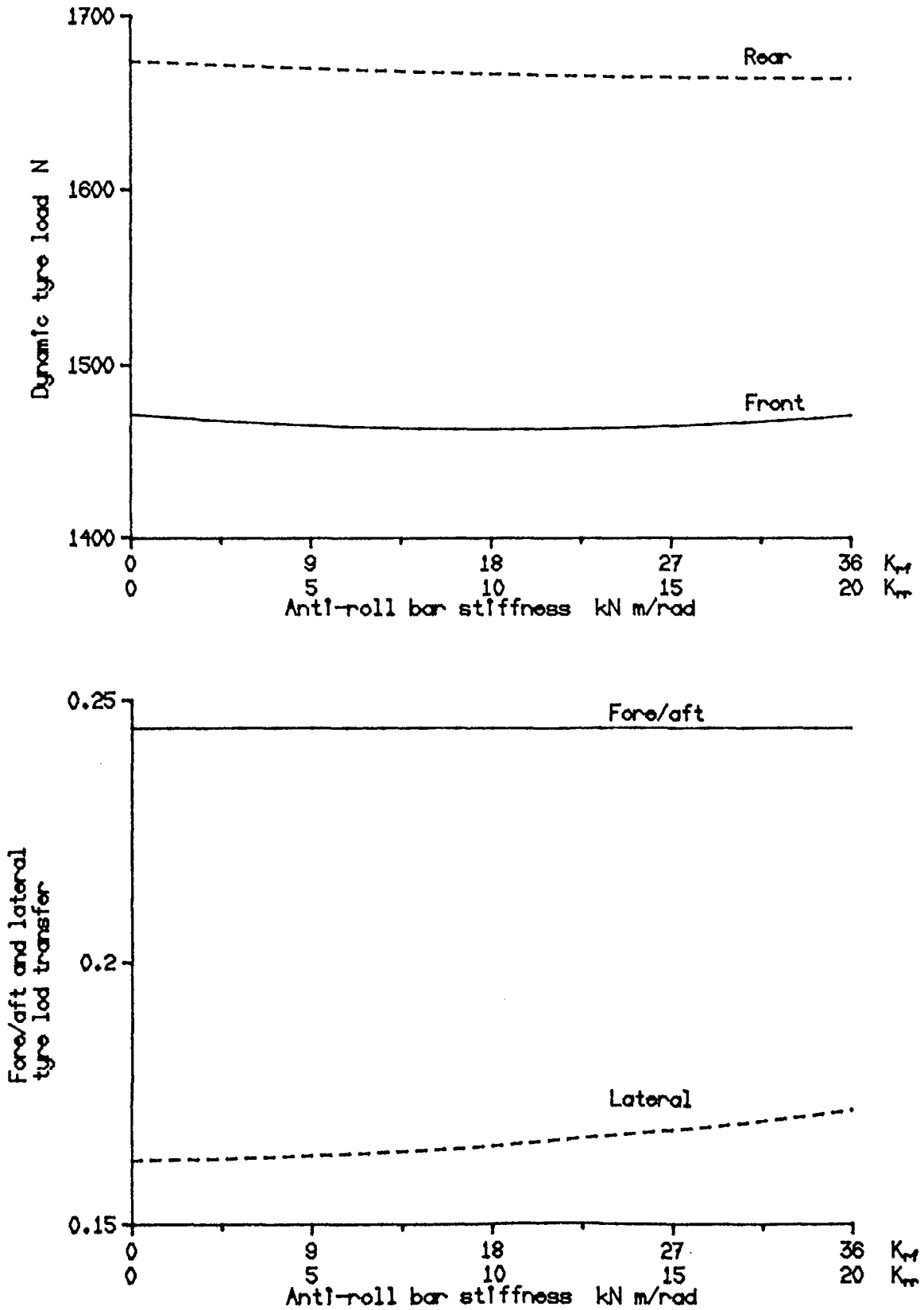


Fig. 3.15 The effect of variation in anti-roll bar stiffness on the r.m.s. values of the dynamic tyre load, lateral and fore/aft tyre load transfer for a passive system with $K_r = 10.5$ kN/m, $K_{\text{roll}} = 12.5$ kN/m and $DR = 0.7$.

CHAPTER 4

APPLICATION OF LINEAR CONTROL THEORY TO VEHICLE PROBLEMS

4.1 Introduction

Active suspension control has been comprehensively reviewed several times over recent years. In previous work, the following assumptions have commonly been made, in the problem formulation. Firstly, the vehicle model has typically been linearised and described by equations of the form:

$$\dot{x}(t) = Ax(t) + Bu(t) + B_2x_o(t) \quad \dots(4.1)$$

where $x(t)$ is the state vector ($n_1 \times 1$), $u(t)$ is control force vector ($m \times 1$), $x_o(t)$ is the road input vector ($m \times 1$), $A(n_1 \times n_1)$, $B(n_1 \times m)$ and $B_2(n_1 \times m)$ are constant matrices containing system parameters and dimensions. Secondly, the road excitation models have considered that the road surface has a displacement spectral density function described either as filtered white noise:

$$psd(\lambda) = \frac{R_c}{\lambda_o^2 + \lambda^2} \quad \dots(4.2)$$

or integrated white noise:

$$psd(\lambda) = \frac{R_c}{\lambda^2} \quad \dots(4.3)$$

where R_c is the road roughness coefficient, λ is the wave number (cycle/m) and λ_o (cutoff wave number (cycle/m)) is a constant implying that displacements remain finite for increasingly small wave numbers. Thirdly, in the majority of cases, the correlation between left/right tracks or front/rear

inputs has been ignored and hence the control strategies have been treated as standard stochastic linear optimal regulator problems. Based on these assumptions, techniques used to derive the control laws either for the full or limited state feedback active systems have been described in various publications. For example, in the case where full state feedback information is available, some of the good references are Thompson [1976] for the integrated white noise case and Hac [1985] for the filtered white noise case. In the case where only limited state feedback control is available, the most effective techniques are the gradient search method introduced by Wilson et al [1986] and the method which is based on the Kalman filter algorithm [1961] and recently applied to this field by for example, the work introduced by Abdel Hady and Crolla [1989].

However, a more realistic control law for an active suspension system fitted to a vehicle should take into account any correlation that exists between the road inputs at all four wheels. For a vehicle moving on a straight path at a constant forward speed, two types of correlation exist: (1) the correlation between the left and right tracks, and (2) the time delay between the front and rear wheels. An approach to the optimisation of a system which incorporates a time delay is to transform it into an equivalent linear one without a time delay. A possible technique using this approach is to use the Pade approximation to represent the time delay. However, another approach to the control of systems with time delays is to treat the delay terms as extra inputs to an

equivalent linear system which must then be optimised at each time step. Hence, discrete optimal control theory must be used to generate the control laws and although this method is optimal, it implies some significant practical difficulties in performing all the necessary calculations quickly enough. In the work presented here, only the first method which is based on the Pade approximation is used. One of the important features of this method is the possibility of using it either for the integrated white noise case or the filtered white noise case.

Consider now the correlation between the right and left tracks. To date, only one method has been proposed to derive a control law which accounts for this correlation and since this uses a shaping filter, it is restricted to the case of the filtered white noise input. In the work presented here, the modified first order shaping filter approach described by Rill [1983] is used to represent this correlation. However, it can be concluded from the available literature, that there is no clear formulation of a continuous control strategy which deals with both kinds of the correlation of the road inputs.

The main purpose of this Chapter is to clarify the available control strategies. Throughout the discussion, the proofs will be referred to rather than developed and emphasis will be placed to the specific conditions under which the results are obtained. For ease of reference, the control strategies relating to the case in which the correlation between the road inputs is ignored is first reviewed. At the end of the Chapter example solutions are given.

4.2 Uncorrelated road input case.

4.2.1 Full state information available.

4.2.1.1 Filtered white noise case.

The fundamental idea of this approach is that the inputs should be treated as additional states of the system. Thus, the framework for formulating and solving the control problem is the augmentation of the system states with states representing the inputs. In the case where the filtered white noise description is employed, the disturbance signals may be modelled by the following first order differential equation:

$$\dot{x}_o(t) = F_{w_1} x_o(t) + I w(t) \quad \dots(4.4)$$

where F_{w_1} is an $(m \times m)$ diagonal matrix with diagonal elements equal to $F_w = -2\pi\lambda_o V$ and the vector $w(m \times 1)$ contains m zero-mean white noise processes, which satisfy

$$E\{w(t), w^T(\tau)\} = W \delta(t - \tau) \quad \dots(4.5)$$

Combining equations (4.1) and (4.4), the result may be written as:

$$\dot{x}_a = A_1 x_a + B_1 u + B_w w \quad \dots(4.6)$$

where: $x_a = [x \ x_o]^T$, $B_1 = [B \ 0]^T$, $B_w = [0 \ I]^T$,

$$A_1 = \begin{bmatrix} A & B_2 \\ 0 & F_{w_1} \end{bmatrix}$$

and I is $(m \times m)$ identity matrix. The output equation may be written in the form:

$$y(t) = C x_a(t) \quad \dots(4.7)$$

where $y(t)$ is the output vector assuming perfect measurements and contains all the important quantities to be controlled e.g. suspension working space, dynamic tyre load, control force, pitch and roll motions etc. C is the output matrix which may be divided into two sub-matrices i.e. $C=[C_1|C_2]$, where C_1 is $(n_q \times n_1)$ and C_2 is $(n_q \times m)$. Here n_q is the number of outputs. The performance index is specified in terms of the outputs as

$$J = \int_0^{\infty} (y^T(t)Qy(t) + u^T(t)Ru(t))dt \quad \dots(4.8)$$

where $Q(n_q \times n_q)$ and $R(m \times m)$ are the weighting matrices. In this case where full state feedback information is assumed available, the optimisation problem can be summarised as follows: find the control law $u(x_a(t))$ which minimises a quadratic cost function defined by equation (4.8). The results, see for example, Bryson and Yu-Chi [1975], can be expressed by a linear control law:

$$u = Kx_a \quad \dots(4.9)$$

where K is the matrix of gains which is related to the gradient of the performance index by:

$$\partial J / \partial K = 2\{RK + B_1^T P\}X_a \quad \dots(4.10)$$

where X_a is the covariance matrix of the states x_a and can be obtained from:

$$\hat{A}_1 X_a + X_a \hat{A}_1^T + G = 0 \quad \dots(4.11)$$

where

$$\hat{A}_1 = A_1 + B_1 K \quad , \quad G = B_w W B_w^T \quad \dots(4.12)$$

Because the correlation between the road inputs is ignored here, W should be obtained from:

$$W = R_c V I \quad \dots(4.13)$$

where R_c is the road roughness coefficient and V is the vehicle speed. By setting $\partial J / \partial K = 0$, the optimal matrix K can be found from:

$$K = -R^{-1} B_1^T P \quad \dots(4.14)$$

where P can be obtained as a solution of the algebraic Riccati equation:

$$P A_1 + A_1^T P - P B_1 R^{-1} B_1^T P + C^T Q C = 0 \quad \dots(4.15)$$

However, the system considered here is not completely controllable. This is because the part of the input vector x_0 in equation (4.6) cannot be changed by applying a control force. This lack of complete controllability of the system (4.6) is discussed and proved by Wilson et al [1986]. In this case, the Riccati equation (4.15) can be solved numerically after separation of the unknown matrix P into four sub-matrices in which:

$$P = \begin{bmatrix} P_{11} & P_{12} \\ P_{12}^T & P_{22} \end{bmatrix}$$

This approach has been presented in detail by Hac [1985]. The result is the following system of equations instead of equation (4.15) :

$$P_{11} A + A^T P_{11} - P_{11} B R^{-1} B^T P_{11} + C_1^T Q C_1 = 0 \quad \dots(4.16)$$

$$P_{12} F_{w1} + (A^T - P_{11} B R^{-1} B^T) P_{12} + P_{11} B_2 + C_1^T Q C_2 = 0 \quad \dots(4.17)$$

$$P_{12}^T (A - B R^{-1} B^T P_{11}) + F_{w1}^T P_{12}^T + B_2^T P_{11} + C_2^T Q C_1 = 0 \quad \dots(4.18)$$

$$P_{22}F_{w1} + F_{w1}^T P_{22} + P_{12}^T B_2 + B_2^T P_{12} - P_{12}^T B R^{-1} B^T P_{12} + C_2^T Q C_2 = 0 \dots (4.19)$$

Once P_{11} and P_{12} are found, the control law can be found from:

$$u = K x_a = [K_x \mid K_{x_0}] x_a = -R^{-1} B^T [P_{11} \mid P_{12}] x_a \dots (4.20)$$

4.2.1.2 Integrated white noise case.

Since the spectral density function used in this part to describe the road surface is of the form $psd(\lambda) = R_c / \lambda^2$, the disturbance signal model must be:

$$\dot{x}_o = w(t) \dots (4.21)$$

and the solution of this problem can be found after transforming the states x in equation (4.1) to the new variables x_s , in which:

$$x_s = x + B_{ws} x_o \dots (4.22)$$

where $B_{ws}(n_1 \times m)$ is the transformation matrix. Detailed examples for this transformation based on the 2 d.o.f. quarter car model and the bounce and pitch 4 d.o.f. half vehicle model appear in Thompson [1976] and Thompson and Pearce [1979] respectively. An example of this transformation for the full vehicle model is given at the end of this Chapter. In general this matrix should satisfy:

$$A B_{ws} = B_2 \dots (4.23)$$

Because the matrix A is always singular, the equation (4.23) cannot be used to find B_{ws} . Nevertheless this equation provides an easy way to check the transformation especially when a large vehicle model is used. Using equations (4.21) to (4.23), equation (4.1) can be re-written as:

$$\dot{x}_s = A x_s + B u + B_{ws} w \dots (4.24)$$

The output vector in equation (4.7), the performance index in equation (4.8) and the control law in equation (4.20) become:

$$y_s = C_1 x_s \quad \dots(4.25)$$

$$J = \int_0^{\infty} (y_s^T(t) Q y_s(t) + u^T(t) R u(t)) dt \quad \dots(4.26)$$

$$u = -R^{-1} B^T P_{11} x_s = K_x x_s \quad \dots(4.27)$$

It is however, clear that only P_{11} in equation (4.16) is required to find the gain matrix K_x .

The control law (4.27) may be re-written in the form

$$u = K_x x_s = K_x (x + B_{ws} x_o) = K_x x + \hat{K}_o x_o \quad \dots(4.28)$$

This form is similar to that obtained in the previous section for the filtered white noise case except that the matrix \hat{K}_o does not depend on the vehicle speed and hence in general, $\hat{K}_o \neq K_o$.

4.2.2 Limited state feedback available.

4.2.2.1 Gradient search method

The gradient search method introduced by Wilson et al [1986] will be discussed briefly here. Consider first the case where the road surface is described as a filtered white noise. Having simplified the problem using the assumption in equation (4.13), i.e. the correlation between the road inputs is ignored, the technique can be applied to any vehicle model. This technique can be summarised as follows. The control law is related to x_a by:

$$u = K_H H x_a = K_H H [x \ x_o]^T \quad \dots(4.29)$$

where H is the matrix defining the state variables to be measured. For example if all the states can be measured except the road input displacements x_o , then the matrix $H = [I \ 0]$. Here $I(n_1 \times n_1)$ is the identity matrix and $O(n_1 \times m)$ is a null matrix. To find the optimal matrix of the feedback gains K_H the following steps must be followed:

- (i) Guess an initial value for K_H . A good first approximation which minimises computing time can be obtained if the matrix K_x appearing in equation (4.20) is used as the initial guess.
- (ii) Solve the following two "Lyapunov" equations for X_a and P

$$\hat{A}_1 X_a + X_a \hat{A}_1^T + B_w W B_w^T = 0 \quad \dots(4.30)$$

$$\hat{A}_1^T P + P \hat{A}_1 + C^T Q C + H^T K_H^T R K_H H = 0 \quad \dots(4.31)$$

The first equation is similar to equation (4.11) except that the matrix \hat{A}_1 must be found from:

$$\hat{A}_1 = A_1 + B_1 K_H H \quad \dots(4.32)$$

- (iii) Calculate the performance index and its gradient from:

$$J = \text{trace}\{P(B_w W B_w^T)\} \quad \dots(4.33)$$

$$\partial J / \partial K_H = 2[R K_H H X_a H^T + B_1^T P X_a H^T] \quad \dots(4.34)$$

- (iv) Update K_H using a gradient search routine and go to step (ii) until satisfactory convergence has been achieved.

The previous method is also valid for the integrated white noise case. Equations (4.29) to (4.34) will remain unchanged except for x_o , A_1 , B_1 , C and B_w which will be replaced by x_s , A , B , C_1 and B_{ws} respectively.

4.2.2.2 Kalman filter algorithm.

The control laws described in the previous sections assume perfect measurements of the states. In practice these measurements would be noisy and thus the performance of the active systems would suffer. The purpose of this part is to indicate how the Kalman filter algorithm can be used to design a control strategy when noisy measurements of a limited number of the states is available. Consider first the filtered white noise case i.e. the road surface is described by equation (4.3). The algorithm can be summarised as follows. First of all, the output vector $y(t)$ in equation (4.7) should be modified so that it can account for measurement errors. The result may be written as:

$$y(t) = Hx_a(t) + v_a(t) \quad \dots(4.35)$$

where $v_a(t)$ is the measurement error vector which is assumed to be white noise with covariance described by:

$$E\{v_a(t), v_a^T(\tau)\} = V_a \delta(t - \tau) \quad \dots(4.36)$$

The optimum filter algorithm is given by:

$$\dot{\hat{x}}_a = A_1 \hat{x}_a + B_1 u + K_k (y - H \hat{x}_a) \quad \dots(4.37)$$

where \hat{x}_a are the optimal estimates of the state variables x_a and K_k is the filter gain which can be found from:

$$K_k = P_o H^T V_a^{-1} \quad \dots(4.38)$$

where P_o is the filter error covariance matrix which may be found as a solution of the following Riccati equation:

$$A_1 P_o + P_o A_1^T - P_o H^T V_a^{-1} H P_o + B_w W B_w^T = 0 \quad \dots(4.39)$$

The control forces $u(t)$ and the estimation error $e_r(t)$ are then:

$$u(t) = K \hat{x}_a(t) \quad \dots(4.40)$$

$$e_r(t) = x_a(t) - \hat{x}_a(t) \quad \dots(4.41)$$

The previous method is also valid for the integrated white noise case. Equations (4.35) to (4.41) will remain unchanged except for x_a , \hat{x}_a , A_1 , B_1 and B_w which will be replaced by x_s , \hat{x}_s , A , B and B_{ws} respectively.

4.3 Correlated road input case.

4.3.1 Full state information available.

4.3.1.1 Filtered white noise case.

4.3.1.1.1 Correlation between the right and left tracks.

This part describes how the modified first order shaping filter introduced by Rill [1983] can be used to account for the correlation between the left and right tracks in deriving the control law. This algorithm was also used by Chalasani [1986 b] but only to represent this correlation in the calculation of the r.m.s. values and not in the derivation of the control law. In general this method can be summarised as follows. Firstly, the following power spectral density may be employed:

$$psd(\lambda) = \alpha_0 \left(\frac{\lambda^2 + \alpha_1}{\lambda^4 + \alpha_2 \lambda^2 + \alpha_3} \right) \quad \dots(4.42)$$

where α_0 , α_1 , α_2 and α_3 are constants depending on the shaping filter constants and the vehicle speed V . Secondly, the

displacements of the road surface at the left and right front wheels should be modelled as:

$$x_{o1} = \zeta_f - \frac{t_f}{2} \theta_f \quad \dots(4.43)$$

$$x_{o2} = \zeta_f + \frac{t_f}{2} \theta_f \quad \dots(4.44)$$

or:

$$\begin{bmatrix} x_{o1} \\ x_{o2} \end{bmatrix} = \begin{bmatrix} 1 & -t_f/2 \\ 1 & t_f/2 \end{bmatrix} \begin{bmatrix} \zeta_f \\ \theta_f \end{bmatrix}$$

i.e.

$$x_{of} = A_{\mu f} \mu_f \quad \dots(4.45)$$

t_f is the front wheel track, ζ_f and θ_f are uncorrelated random functions and can be modelled as coloured noises resulting from the application of the first order shaping filter to the white noise signals w_1 and w_2 i.e.

$$\begin{bmatrix} \dot{\zeta}_f \\ \dot{\theta}_f \end{bmatrix} = -V \begin{bmatrix} d_1 & 0 \\ 0 & d_2 \end{bmatrix} \begin{bmatrix} \zeta_f \\ \theta_f \end{bmatrix} + V \begin{bmatrix} g_1 & 0 \\ 0 & g_2 \end{bmatrix} \begin{bmatrix} w_1 \\ w_2 \end{bmatrix} \quad \dots(4.46)$$

or

$$\dot{\mu}_f = F_{\mu f} \mu_f + B_{\mu f} v_f \quad \dots(4.47)$$

where d_1 , d_2 , g_1 and g_2 are the filter constants. The matrix W which appears in equation (4.5) is then of the form

$$W = q \begin{bmatrix} 1 & 0 \\ 0 & 1 \end{bmatrix}$$

where q is the road intensity. Using equations (4.45) and (4.47), the differential equation which describes the front road inputs may be written as:

$$\dot{x}_{of} = A_{\mu f} \dot{\mu}_f = A_{\mu f} F_{\mu f} A_{\mu f}^{-1} x_{of} + A_{\mu f} B_{\mu f} v_f = F_{\mu 1} x_{of} + B_{\mu 1} v_f \dots(4.48)$$

If a four wheel vehicle moves in a straight path with constant speed, it is reasonable to assume that the rear wheels have the same excitation as the front wheels except that it is delayed by the time interval $D=L/V$, where L is the vehicle wheelbase (m) and V is the vehicle speed (m/s). Hence, the same first order shaping filter approach can be used to include the cross correlation between the rear wheels and the general form of equation (4.48) for a vehicle with j axles may be written in the following form:

$$\dot{x}_o = F_\mu x_o + B_\mu w \quad \dots(4.49)$$

where F_μ and B_μ are diagonal matrices:

$$F_\mu = \begin{bmatrix} F_{\mu 1} & 0 & \dots & 0 \\ 0 & F_{\mu 2} & \dots & 0 \\ \cdot & \cdot & & \cdot \\ 0 & 0 & \dots & F_{\mu j} \end{bmatrix}, \quad B_\mu = \begin{bmatrix} B_{\mu 1} & 0 & \dots & 0 \\ 0 & B_{\mu 2} & \dots & 0 \\ \cdot & \cdot & & \cdot \\ 0 & 0 & \dots & B_{\mu j} \end{bmatrix}$$

Because equation (4.49) is in the same form as equation (4.4), the strategy discussed in section 4.2.1.1 to find the feedback gains will be also used here. Equations (4.6) to (4.20) will not be changed except that the matrices F_{w1} and I should be replaced by F_μ and B_μ respectively.

4.3.1.1.2 Time delay between the front and rear wheels.

The time delay available between the front and rear inputs appears to provide, in principle, an excellent opportunity to improve the rear axle actuator control. In practice, it is easy to use this sort of preview (wheelbase preview) in any actively suspended vehicle. This is true because a long preview length is available (i.e. wheelbase length) and all the required sensors are already available. No doubt, the

control law in this case will be more complicated than that obtained in the non-delay case. Two possible approaches to obtaining the control strategies have already been mentioned and the one discussed in this section is the less complicated one which uses the Pade approximation to represent the wheelbase time delay. Before going through the details of this technique, it must be mentioned that the part of equation (4.12) which was used to find the matrix G is no longer valid and another form which depends on the vehicle model must be used instead. For example, in the case of using the bounce and pitch half vehicle model, the matrix G is given by

$$G = R_c V \{ B_w B_w^T + b_{w2} b_{w1}^T P_p^T + P_p b_{w1} b_{w2}^T \} \quad \dots(4.50)$$

where $P_p = e^{\lambda_1 D}$, while b_{w1} and b_{w2} are sub-matrices in B_w in which:

$$B_w = [b_{w1} \quad | \quad b_{w2}] \quad \dots(4.51)$$

Hedrick and Firouztash [1974] provide further details of this. Because of this modification in the matrix G the gradient of the performance index will contain infinite series of the feedback gains, Fruhauf [1985]. Hence extending the Riccati controller algorithm to systems with time delay is not longer possible. Instead, the pure time delay between the front and rear inputs may be represented by an N^{th} order Pade approximation. The 2-axle 4-wheel vehicle model shown in Fig. 2.1 will be used to indicate this strategy. The transfer function of an N^{th} order Pade approximation is given in the frequency domain by:

$$\frac{v_3(s)}{v_1(s)} = \frac{v_4(s)}{v_2(s)} = e^{-Ds} = \frac{\alpha_0 - \alpha_1 s + \alpha_2 s^2 - \alpha_3 s^3 + \dots + \alpha_N s^N}{\alpha_0 + \alpha_1 s + \alpha_2 s^2 + \alpha_3 s^3 + \dots + \alpha_N s^N} \dots(4.52)$$

in which v_1 , v_2 , v_3 and v_4 are the front and rear white noise signals respectively and D is the time delay between the front and rear inputs. For the second order Pade approximation ($N=2$), the constants are $\alpha_0 = 12/D^2$, $\alpha_1 = 6/D$ and $\alpha_2 = 1$, while for the fourth order Pade approximation the constants are:

$$\alpha_0 = 1072/D^4, \quad \alpha_1 = 536/D^3, \quad \alpha_2 = 120/D^2, \quad \alpha_3 = 13.55/D, \quad \alpha_4 = 1$$

(see Athans et al [1966]). The above transfer function can be converted easily into state space representation. The results may be written as follows:

$$\dot{\eta}(t) = A_\eta \eta(t) + B_\eta v_f(t) \quad \dots(4.53)$$

with output:

$$v_r(t) = v_f(t - D) = C_\eta \eta(t) + v_f(t) \quad \dots(4.54)$$

where

$$v_f = \begin{bmatrix} v_1 \\ v_2 \end{bmatrix}, \quad v_r = \begin{bmatrix} v_3 \\ v_4 \end{bmatrix}, \quad \eta = \begin{bmatrix} \eta_n \\ \eta_o \end{bmatrix} \quad \dots(4.55)$$

and the matrices A_η , B_η and C_η are

$$A_\eta = \begin{bmatrix} A_{\eta 1} & 0 \\ 0 & A_{\eta 1} \end{bmatrix}, \quad B_\eta = \begin{bmatrix} B_{\eta 1} & 0 \\ 0 & B_{\eta 1} \end{bmatrix}, \quad C_\eta = \begin{bmatrix} C_{\eta 1} & 0 \\ 0 & C_{\eta 1} \end{bmatrix} \quad \dots(4.56)$$

These sub-matrices depend on the time delay D and the Pade approximation order. For example, in the second order approximation, these matrices may be written as follows:

$$A_{\eta 1} = \begin{bmatrix} 0 & 1 \\ -\alpha_0 & -\alpha_1 \end{bmatrix}, \quad B_{\eta 1} = \begin{bmatrix} -12/D \\ 72/D^2 \end{bmatrix}, \quad C_{\eta 1} = [1 \quad 0] \dots(4.57)$$

Alternatively, $B_{\eta 1}$ and $C_{\eta 1}$ may be written as

$$B_{\eta 1} = [0 \quad 1]^T, \quad C_{\eta 1} = [0 \quad -12/D] \quad \dots(4.58)$$

while for the fourth order approximation these matrices may be written as:

$$A_{\eta 1} = \begin{bmatrix} 0 & 1 & 0 & 0 \\ 0 & 0 & 1 & 0 \\ 0 & 0 & 0 & 1 \\ -a_0 & -a_1 & -a_2 & -a_3 \end{bmatrix}, \quad B_{\eta 1} = \begin{bmatrix} -2a_3 \\ 2a_3^2 \\ g_3 \\ g_4 \end{bmatrix}, \quad C_{\eta 1} = [1 \ 0 \ 0 \ 0]$$

$$g_3 = -2a_1 - 2a_3^3 + 2a_2a_3, \quad g_4 = 4a_1a_3 - 4a_2a_3^2 + 2a_3^4 \dots(4.59)$$

The matrices, $B_{\eta 1}$ and $C_{\eta 1}$ may also be written as

$$B_{\eta 1} = [0 \ 0 \ 0 \ 1]^T, \quad C_{\eta 1} = [0 \ -2a_1 \ 0 \ -2a_3] \dots(4.60)$$

The general form of equations (4.4) and (4.49) which describe the road input may be written as follows:

$$\dot{x}_o(t) = F_v x_o(t) + B_v w(t) \dots(4.61)$$

i.e. $F_v = F_{w1}$ and $B_v = I$ in the case of ignoring the cross correlation, while $F_v = F_{\mu}$ and $B_v = B_{\mu}$ in the case when this correlation is taken into account. Equation (4.61) may be re-written as:

$$\dot{x}_o(t) = F_v x_o(t) + b_1 v_f(t) + b_2 v_r(t) \dots(4.62)$$

where b_1 and b_2 are sub-matrices in the matrix B_v in which:

$$B_v = [b_1 \ | \ b_2] \dots(4.63)$$

Substituting equation (4.54) in equation (4.62) the results may be written as:

$$\dot{x}_o(t) = F_v x_o(t) + b_2 C_{\eta} \eta(t) + (b_1 + b_2) v_f(t) \dots(4.64)$$

It is however clear that the rear disturbances have disappeared from this equation and hence the problem can be treated in the same way as in the uncorrelated case. Combining equations (4.1), (4.64) and (4.53), the result may be written as:

$$\dot{x}_f(t) = A_f x_f(t) + B_f u(t) + B_b v_f(t) \dots(4.65)$$

where: $x_f = [x \ x_o \ \eta]^T$, $B_f = [B \ 0 \ 0]^T$, $B_b = [0 \ b_{wf} \ B_\eta]^T$

and

$$A_f = \begin{bmatrix} A & B_2 & 0 \\ 0 & F_v & b_c \\ 0 & 0 & A_\eta \end{bmatrix} \quad \dots(4.66)$$

Here $b_{wf} = b_1 + b_2$ and $b_c = b_2 C_\eta$. The control law is then related to x_f by:

$$u = -R^{-1} B_f^T P_f x_f = K_D x_f = [K_x \ K_{x_o} \ K_\eta] x_f \quad \dots(4.67)$$

where K_η is the additional part accounting for the time delay. The matrix P_f can be found as a solution of the algebraic Riccati equation:

$$P_f A_f + A_f^T P_f - P_f B_f R^{-1} B_f^T P_f + C_f^T Q C_f = 0 \quad (4.68)$$

where $C_f = [C_1 \ C_2 \ 0]$. Because the system considered here is not completely controllable, the same technique used in solving the Riccati equation as described in section 4.2.1.1 should be employed.

In the case of assuming two identical front white noise signals, equation (4.62) may be written as

$$\dot{x}_o(t) = F_v x_o(t) + (b_{f1} + b_{f2})v_1(t) + (b_{r1} + b_{r2})v_3(t) \quad \dots(4.69)$$

where

$$b_1 = [b_{f1} \ b_{f2}] , \quad b_2 = [b_{r1} \ b_{r2}] \quad \dots(4.70)$$

The problem formulation may be then simplified by setting

$$\eta = \eta_n = \eta_o , \quad A_\eta = A_{\eta 1} , \quad B_\eta = B_{\eta 1} , \quad C_\eta = C_{\eta 1} \quad \dots(4.71)$$

and

$$b_{wf} = b_{f1} + b_{f2} + b_{r1} + b_{r2} , \quad b_c = (b_{f1} + b_{f2})C_{\eta 1} \quad \dots(4.72)$$

4.3.1.2 Integrated white noise case.

In this section, attention is focussed only on those changes in the control law which occur as a result of assuming an integrated, as opposed to filtered, white noise input. It has been mentioned previously that it is easy to account for the cross correlation when the filtered white noise description is used. Here, this correlation is ignored and hence equation (4.24) will remain unchanged. This equation may be re-written as follows:

$$\dot{x}_s(t) = Ax_s(t) + Bu(t) + b_{s1}v_f(t) + b_{s2}v_r(t) \quad \dots(4.73)$$

where $B_{ws} = [b_{s1} \ b_{s2}]$. Substituting equation (4.54) in the previous equation, the result may be written as:

$$\dot{x}_s(t) = Ax_s(t) + Bu(t) + b_{s2}C_\eta\eta(t) + (b_{s1} + b_{s2})v_f(t) \quad \dots(4.74)$$

Combining equations (4.74) and (4.53) gives,

$$\begin{bmatrix} \dot{x}_s(t) \\ \dot{\eta}(t) \end{bmatrix} = \begin{bmatrix} A & b_{s2}C_\eta \\ 0 & A_\eta \end{bmatrix} \begin{bmatrix} x_s(t) \\ \eta(t) \end{bmatrix} + \begin{bmatrix} B \\ 0 \end{bmatrix} u(t) + \begin{bmatrix} b_{s1} + b_{s2} \\ B_\eta \end{bmatrix} v_f(t)$$

or

$$\dot{x}_{sf}(t) = A_{sf}x_{sf}(t) + B_{sf}u(t) + b_{sf}v_f(t) \quad \dots(4.75)$$

The control law is then:

$$u = -R^{-1}B_{sf}^T P_{sf} x_{sf} = K_{sf} x_{sf} \quad \dots(4.76)$$

The matrix P_{sf} should be found as a solution of:

$$P_{sf}A_{sf} + A_{sf}^T P_{sf} - P_{sf}B_{sf}R^{-1}B_{sf}^T P_{sf} + C_{sf}^T Q C_{sf} = 0 \quad \dots(4.77)$$

where $C_{sf} = [C_1 \ 0]$. The system considered here is also not controllable and hence the matrix P_{sf} should be solved as indicated in the previous section.

4.3.2 Limited state feedback available.

Consider first the filtered white noise case. The control law shown in equation (4.67) is based on having perfect measurement of the states x_f . However, in practice, some of these states (η) cannot be measured directly and some of them are difficult to measure (e.g. x_o). In the work presented here, a solution to this problem is obtained by using the concept of the limited state feedback control strategy. Having formulated the equation describing the road inputs as in equation (4.64), the gradient search technique can be used to derive control laws which do not depend on the states η or alternatively, any specified states. Hence the physical realisation of this system will be similar to that found in section 4.2.2.1 with the addition that the control law accounts for the cross correlation and/or the time delay which should improve the overall performance. Thus, a novel strategy for practical control laws for active systems on a full vehicle model is presented. Having combined the states x , x_o , and η in equation (4.65), the control law for the limited state feedback active system is then defined as explained in section 4.2.2.1:

$$u = K_H H x_f = K_H H [x \quad x_o \quad \eta]^T \quad \dots(4.78)$$

and steps (i) to (iv) are followed to find the gains K_H . Equations (4.30) to (4.34) are modified so that

$$\hat{A}_f X_f + X_f \hat{A}_f^T + B_b W B_b^T = 0 \quad \dots(4.79)$$

$$\hat{A}_f^T P + P \hat{A}_f + C_f^T Q C_f + H^T K_H^T R K_H H = 0 \quad \dots(4.80)$$

$$\hat{A}_f = A_f + B_f K_H H \quad \dots(4.81)$$

$$J = \text{trace}\{P(B_b W B_b^T)\} \quad \dots(4.82)$$

$$\partial J / \partial K_H = 2[RK_H H X_f H^T + B_f^T P X_f H^T] \quad \dots(4.83)$$

The Kalman filter algorithm discussed in section 4.2.2.2 may also be used to derive the control law of the limited state active systems with time delay. Based on Equation (4.65), equations (4.35) to (4.41) will not be changed except that x_a , \hat{x}_a , A_1 , B_1 , B_w and K will be replaced by x_f , \hat{x}_f , A_f , B_f , B_b and K_D respectively. Hence, the filter covariance matrix and the filter gains will be obtained from

$$A_f P_o + P_o A_f^T - P_o H^T V_a^{-1} H P_o + B_b W B_b^T = 0 \quad \dots(4.84)$$

$$K_k = P_o H^T V_a^{-1} \quad \dots(4.85)$$

If the road surface is described as integrated white noise, then equation (4.75) should be used instead of equation (4.65) and either of the previous methods, i.e. the gradient search technique or the Kalman filter algorithm, can be used as indicated above.

4.4 Computer software preparation.

In order to find the feedback gains which may be based on the filtered white noise description or the integrated white noise one, full or limited state feedback and which may account for the cross correlation and/or the time delay for variety of vehicle models, a general computer program called "ACTOPT" has been developed. Fig. 4.1 shows an outline flow diagram for this program indicating the major steps involved.

$$B = \begin{bmatrix} 0 & 0 & 0 & 0 \\ 0 & 0 & 0 & 0 \\ 0 & 0 & 0 & 0 \\ 0 & 0 & 0 & 0 \\ 0 & 0 & 0 & 0 \\ 0 & 0 & 0 & 0 \\ 0 & 0 & 0 & 0 \\ 0 & 0 & 0 & 0 \\ \frac{-1}{M_{wf}} & 0 & 0 & 0 \\ s_1 & s_2 & s_3 & s_4 \\ 0 & \frac{-1}{M_{wf}} & 0 & 0 \\ s_2 & s_1 & s_4 & s_3 \\ 0 & 0 & \frac{-1}{M_{wr}} & 0 \\ s_3 & s_4 & s_5 & s_6 \\ 0 & 0 & 0 & \frac{-1}{M_{wr}} \\ s_4 & s_3 & s_6 & s_5 \end{bmatrix}, \quad B_2 = \begin{bmatrix} 0 & 0 & 0 & 0 \\ 0 & 0 & 0 & 0 \\ 0 & 0 & 0 & 0 \\ 0 & 0 & 0 & 0 \\ 0 & 0 & 0 & 0 \\ 0 & 0 & 0 & 0 \\ 0 & 0 & 0 & 0 \\ 0 & 0 & 0 & 0 \\ \frac{K_t}{M_{wf}} & 0 & 0 & 0 \\ 0 & 0 & 0 & 0 \\ 0 & \frac{K_t}{M_{wf}} & 0 & 0 \\ 0 & 0 & 0 & 0 \\ 0 & 0 & \frac{K_t}{M_{wr}} & 0 \\ 0 & 0 & 0 & 0 \\ 0 & 0 & 0 & \frac{K_t}{M_{wr}} \\ 0 & 0 & 0 & 0 \end{bmatrix}$$

where

$$s_1 = \frac{\omega_a^2}{I_p^2} + \frac{t_s^2}{I_r^2} + \frac{1}{M_b}, \quad s_2 = \frac{\omega_a^2}{I_p^2} - \frac{t_s^2}{I_r^2} + \frac{1}{M_b}, \quad s_3 = \frac{-\omega_a \omega_b}{I_p^2} + \frac{t_s^2}{I_r^2} + \frac{1}{M_b}$$

$$s_4 = \frac{-\omega_a \omega_b}{I_p^2} - \frac{t_s^2}{I_r^2} + \frac{1}{M_b}, \quad s_5 = \frac{\omega_b^2}{I_p^2} + \frac{t_s^2}{I_r^2} + \frac{1}{M_b}, \quad s_6 = \frac{\omega_b^2}{I_p^2} - \frac{t_s^2}{I_r^2} + \frac{1}{M_b} \quad \dots(4.88)$$

Values for λ_0 and V will be taken equal to 0.01 cycle/m and 30 m/s respectively. The matrices I and F_{w1} of equation (4.4) are then

$$I = \begin{bmatrix} 1 & 0 & 0 & 0 \\ 0 & 1 & 0 & 0 \\ 0 & 0 & 1 & 0 \\ 0 & 0 & 0 & 1 \end{bmatrix}, \quad F_{w1} = \begin{bmatrix} F_w & 0 & 0 & 0 \\ 0 & F_w & 0 & 0 \\ 0 & 0 & F_w & 0 \\ 0 & 0 & 0 & F_w \end{bmatrix}, \quad F_w = -2\pi\lambda_0 V \quad \dots(4.89)$$

$$Q = \begin{bmatrix} q_1 & 0 & 0 & 0 & 0 & 0 & 0 & 0 & 0 & 0 & 0 \\ 0 & q_2 & 0 & 0 & 0 & 0 & 0 & 0 & 0 & 0 & 0 \\ 0 & 0 & q_3 & 0 & 0 & 0 & 0 & 0 & 0 & 0 & 0 \\ 0 & 0 & 0 & q_4 & 0 & 0 & 0 & 0 & 0 & 0 & 0 \\ 0 & 0 & 0 & 0 & q_5 & 0 & 0 & 0 & 0 & 0 & 0 \\ 0 & 0 & 0 & 0 & 0 & q_6 & 0 & 0 & 0 & 0 & 0 \\ 0 & 0 & 0 & 0 & 0 & 0 & q_7 & 0 & 0 & 0 & 0 \\ 0 & 0 & 0 & 0 & 0 & 0 & 0 & q_8 & 0 & 0 & 0 \\ 0 & 0 & 0 & 0 & 0 & 0 & 0 & 0 & q_9 & 0 & 0 \\ 0 & 0 & 0 & 0 & 0 & 0 & 0 & 0 & 0 & q_{10} & 0 \\ 0 & 0 & 0 & 0 & 0 & 0 & 0 & 0 & 0 & 0 & q_{11} \end{bmatrix}, \quad R = \begin{bmatrix} \rho_1 & 0 & 0 & 0 \\ 0 & \rho_2 & 0 & 0 \\ 0 & 0 & \rho_3 & 0 \\ 0 & 0 & 0 & \rho_4 \end{bmatrix}$$

and the output equation (4.7) may be written as:

$$y = \begin{bmatrix} sws_1 \\ sws_2 \\ sws_3 \\ sws_4 \\ DTD_1 \\ DTD_2 \\ DTD_3 \\ DTD_4 \\ \phi_f \\ \phi_r \\ \theta \end{bmatrix} = \begin{bmatrix} -1 & 1 & 0 & 0 & 0 & 0 & 0 & 0 & 0 & \dots & 0 \\ 0 & 0 & -1 & 1 & 0 & 0 & 0 & 0 & 0 & \dots & 0 \\ 0 & 0 & 0 & 0 & -1 & 1 & 0 & 0 & 0 & \dots & 0 \\ 0 & 0 & 0 & 0 & 0 & 0 & -1 & 1 & 0 & \dots & 0 \\ 1 & 0 & 0 & 0 & 0 & 0 & 0 & 0 & 0 & \dots & 0 \\ 0 & 0 & 1 & 0 & 0 & 0 & 0 & 0 & 0 & \dots & 0 \\ 0 & 0 & 0 & 0 & 1 & 0 & 0 & 0 & 0 & \dots & 0 \\ 0 & 0 & 0 & 0 & 0 & 0 & 1 & 0 & 0 & \dots & 0 \\ 0 & -\frac{1}{2t_s} & 0 & \frac{1}{2t_s} & 0 & 0 & 0 & 0 & 0 & \dots & 0 \\ 0 & 0 & 0 & 0 & 0 & \frac{-1}{2t_s} & 0 & \frac{1}{2t_s} & 0 & \dots & 0 \\ 0 & -\frac{1}{2L} & 0 & -\frac{1}{2L} & 0 & \frac{1}{2L} & 0 & \frac{1}{2L} & 0 & \dots & 0 \end{bmatrix} x + \begin{bmatrix} 0 & 0 & 0 & 0 \\ 0 & 0 & 0 & 0 \\ 0 & 0 & 0 & 0 \\ 0 & 0 & 0 & 0 \\ -1 & 0 & 0 & 0 \\ 0 & -1 & 0 & 0 \\ 0 & 0 & -1 & 0 \\ 0 & 0 & 0 & -1 \\ 0 & 0 & 0 & 0 \\ 0 & 0 & 0 & 0 \\ 0 & 0 & 0 & 0 \end{bmatrix} x_0$$

or

$$y = C_1 x + C_2 x_0$$

By choosing the weighting parameters q_1 to q_{11} and ρ_1 to ρ_4 in different ways, various control laws can be determined. In this example these parameters are chosen as

$$q_1 = q_2 = 0.9, \quad q_3 = q_4 = 1.1, \quad q_5 = q_6 = q_7 = q_8 = 12, \quad q_9 = q_{10} = 5, \quad q_{11} = 10^{-9}$$

and

$$\rho_1 = \rho_2 = \rho_3 = \rho_4 = 10^{-9}$$

The numerical solution of the Riccati equation (4.16) is obtained using the exponential method described in Kuo [1975].

The feedback gains K_x are then found as

$$\begin{bmatrix} 4797 & -3836 & 143 & 836 & 872 & -2166 & -986 & 2185 & 173 & -496 & 0 & -6 & -8 & -262 & 9 & 237 \\ 143 & 836 & 4797 & -3836 & -986 & 2185 & 872 & -2166 & 0 & -6 & 173 & -496 & 9 & 237 & -8 & -262 \\ 764 & -2105 & -864 & 2088 & 5100 & -4028 & 227 & 712 & -6 & -254 & 7 & 226 & 196 & -514 & 0 & -18 \\ -864 & 2088 & 764 & -2105 & 227 & 712 & 5100 & -4028 & 7 & 226 & -6 & -254 & 0 & -18 & 196 & -514 \end{bmatrix} \times 10$$

The feedback gains K_{x_0} can easily be obtained after solving the Lyapunov equation (4.17). The method described by Golub et al [1979] is used to solve this equation. The result is

$$K_{x_0} = \begin{bmatrix} -30650 & 6555 & -7732 & 8384 \\ 6555 & -30650 & 8384 & -7732 \\ -6768 & 7575 & -31300 & 6389 \\ 7575 & -6768 & 6389 & -31300 \end{bmatrix}$$

However, the matrix K_x will not be changed if the road surface is described as integrated white noise, while the matrix \hat{K}_0 should be obtained from

$$\hat{K}_0 = B_{ws} K_x$$

For the vehicle model considered here, the transformation matrix B_{ws} of equation (4.22) is defined as

$$\begin{bmatrix} -1 & -1 & 0 & 0 & 0 & 0 & 0 & 0 & 0 & 0 & 0 & 0 & 0 & 0 & 0 & 0 \\ 0 & 0 & -1 & -1 & 0 & 0 & 0 & 0 & 0 & 0 & 0 & 0 & 0 & 0 & 0 & 0 \\ 0 & 0 & 0 & 0 & -1 & -1 & 0 & 0 & 0 & 0 & 0 & 0 & 0 & 0 & 0 & 0 \\ 0 & 0 & 0 & 0 & 0 & 0 & -1 & -1 & 0 & 0 & 0 & 0 & 0 & 0 & 0 & 0 \end{bmatrix}^T$$

Hence the matrix \hat{K}_0 is given by

$$K_{x_0} = \begin{bmatrix} -9612 & -9784 & 12940 & -11994 \\ -9784 & -9612 & -11994 & 12940 \\ 13411 & -12243 & -10720 & -9389 \\ -12243 & 13411 & -9389 & -10720 \end{bmatrix}$$

Consider now the case that not all the states x_a can be measured and the gradient search method will be used to derive the control law. In this example, it is assumed that the

unmeasurable states are the road input displacements x_0 , and hence the matrix H in equation (4.29) is defined as

$$\begin{bmatrix} 1 & 0 & 0 & 0 & 0 & 0 & 0 & 0 & 0 & 0 & 0 & 0 & 0 & 0 & 0 & 0 & 0 & 0 & 0 \\ 0 & 1 & 0 & 0 & 0 & 0 & 0 & 0 & 0 & 0 & 0 & 0 & 0 & 0 & 0 & 0 & 0 & 0 & 0 \\ 0 & 0 & 1 & 0 & 0 & 0 & 0 & 0 & 0 & 0 & 0 & 0 & 0 & 0 & 0 & 0 & 0 & 0 & 0 \\ 0 & 0 & 0 & 1 & 0 & 0 & 0 & 0 & 0 & 0 & 0 & 0 & 0 & 0 & 0 & 0 & 0 & 0 & 0 \\ 0 & 0 & 0 & 0 & 1 & 0 & 0 & 0 & 0 & 0 & 0 & 0 & 0 & 0 & 0 & 0 & 0 & 0 & 0 \\ 0 & 0 & 0 & 0 & 0 & 1 & 0 & 0 & 0 & 0 & 0 & 0 & 0 & 0 & 0 & 0 & 0 & 0 & 0 \\ 0 & 0 & 0 & 0 & 0 & 0 & 1 & 0 & 0 & 0 & 0 & 0 & 0 & 0 & 0 & 0 & 0 & 0 & 0 \\ 0 & 0 & 0 & 0 & 0 & 0 & 0 & 1 & 0 & 0 & 0 & 0 & 0 & 0 & 0 & 0 & 0 & 0 & 0 \\ 0 & 0 & 0 & 0 & 0 & 0 & 0 & 0 & 1 & 0 & 0 & 0 & 0 & 0 & 0 & 0 & 0 & 0 & 0 \\ 0 & 0 & 0 & 0 & 0 & 0 & 0 & 0 & 0 & 1 & 0 & 0 & 0 & 0 & 0 & 0 & 0 & 0 & 0 \\ 0 & 0 & 0 & 0 & 0 & 0 & 0 & 0 & 0 & 0 & 1 & 0 & 0 & 0 & 0 & 0 & 0 & 0 & 0 \\ 0 & 0 & 0 & 0 & 0 & 0 & 0 & 0 & 0 & 0 & 0 & 1 & 0 & 0 & 0 & 0 & 0 & 0 & 0 \\ 0 & 0 & 0 & 0 & 0 & 0 & 0 & 0 & 0 & 0 & 0 & 0 & 1 & 0 & 0 & 0 & 0 & 0 & 0 \\ 0 & 0 & 0 & 0 & 0 & 0 & 0 & 0 & 0 & 0 & 0 & 0 & 0 & 1 & 0 & 0 & 0 & 0 & 0 \\ 0 & 0 & 0 & 0 & 0 & 0 & 0 & 0 & 0 & 0 & 0 & 0 & 0 & 0 & 1 & 0 & 0 & 0 & 0 \end{bmatrix}$$

The weighting parameters and the vehicle operating conditions used previously will not be changed. Employing the matrix K_x as an initial guess and using the matrix H to form equation \hat{A}_1 from (4.32) and following the procedure of section 4.2.2.1, The optimal solution K_H is found as

$$\begin{bmatrix} 2538 & -3014 & 383 & -791 & 378 & -825 & -464 & 835 & 123 & -401 & -2 & -127 & -2 & -158 & 3 & 132 \\ 383 & -791 & 2538 & -3014 & -464 & 835 & 378 & -825 & -2 & -126 & 123 & -402 & 3 & 131 & -2 & -157 \\ 318 & -763 & -392 & 753 & 2875 & -3141 & 468 & -796 & -2 & -147 & 2 & 119 & 146 & -418 & -3 & -126 \\ -392 & 753 & 318 & -763 & 468 & -796 & 2875 & -3141 & 2 & 119 & -2 & -148 & -3 & -127 & 146 & -418 \end{bmatrix} \times 10$$

4.5.2 Correlated road input case.

In this example the left and right tracks are assumed identical and the time delay between the front and rear inputs is considered, while the cross correlation case will be given in the next Chapter. Hence, the matrices F_v and B_v in the input equation (4.61) will be similar to F_{w1} and I respectively

as defined above and the matrices b_1 and b_2 in equation (4.70) will be

$$b_1 = \begin{bmatrix} 1 & 0 \\ 0 & 1 \\ 0 & 0 \\ 0 & 0 \end{bmatrix}, \quad b_2 = \begin{bmatrix} 0 & 0 \\ 0 & 0 \\ 1 & 0 \\ 0 & 1 \end{bmatrix}$$

The fourth order approximation is used here to represent the wheelbase time delay. The matrix $C_{\eta 1}$ in equation (4.59) is used to form b_c and the sub-matrices of b_1 and b_2 are used to find b_{wf} . Hence all the sub-matrices of A_f , B_f and B_b are known and the solution of the Riccati equation (4.68) is easily obtained as in the previous section. The feedback gains K_x and K_{x_0} represented above will remain unchanged while the time delay gain matrix K_η is found as

$$K_\eta = \begin{bmatrix} 0 & 0 & 0 & 0 \\ 0 & 0 & 0 & 0 \\ -1723 & -23 & 0 & 0 \\ -1723 & -23 & 0 & 0 \end{bmatrix}$$

Now consider the case in which only the measurements of the states x are available and the gradient search technique will be used to derive the control law. The same initial guess used in the uncorrelated case is employed here while the matrices $B_{\eta 1}$ and $C_{\eta 1}$ as given in equation (4.60) are used. This however, reduces the computing time necessary to reach to a satisfactory solution. The matrix H defined in equation (4.78) will be

$$\begin{bmatrix} 0 & 0 & 0 & 0 & 0 & 0 & 0 & 1 & -w_a & -t_s & -1 & 0 & 0 & 0 & 0 & 0 & 0 & 0 \\ 0 & 0 & 0 & 0 & 0 & 0 & 0 & 1 & -w_a & t_s & 0 & -1 & 0 & 0 & 0 & 0 & 0 & 0 \\ 0 & 0 & 0 & 0 & 0 & 0 & 0 & 1 & w_b & -t_s & 0 & 0 & -1 & 0 & 0 & 0 & 0 & 0 \\ 0 & 0 & 0 & 0 & 0 & 0 & 0 & 1 & w_b & t_s & 0 & 0 & 0 & -1 & 0 & 0 & 0 & 0 \end{bmatrix}$$

Standard deviations of the sensor random errors will be taken as 0.01 m/s . Using this value to form V_a from equation (4.36), the numerical solution of the filter error covariance matrix gives the following filter gains

$$\begin{bmatrix} 0 & 0 & 0 & 0 \\ 0 & 0 & 0 & 0 \\ 0 & 0 & 0 & 0 \\ 0 & 0 & 0 & 0 \\ 0 & 0 & 0 & 0 \\ 0 & 0 & 0 & 0 \\ 0 & 0 & 0 & 0 \\ 0 & 0 & 0 & 0 \\ 0 & 0 & 0 & 0 \\ 0 & 0 & 0 & 0 \\ -50.78 & 0 & 0 & 0 \\ 0 & -50.78 & 0 & 0 \\ 0 & 0 & -44.4 & 0 \\ 0 & 0 & 0 & -44.4 \\ -0.37 & 0 & 0 & 0 \\ 0 & -0.37 & 0 & 0 \\ 0 & 0 & -0.37 & 0 \\ 0 & 0 & 0 & -0.37 \end{bmatrix}$$

Consider now the case in which the wheelbase time delay is included in the control strategy. In this example, the 4th order Pade approximation is used to represent the wheelbase time delay and the matrices $A_{\eta 1}$ in (4.59) and $B_{\eta 1}$ and $C_{\eta 1}$ in equation (4.60) are chosen. Because the cross correlation is also ignored here and the left track is assumed identical to the right one, equations (4.70) to (4.72) are considered in formulating the matrices A_f , B_f and B_b of equation (4.65).

Again the measurements of the body - wheel relative velocities only are assumed available. Hence, the matrix V_a will remain unchanged, while the matrix H will be (4×22) . The first (4×18) elements will be similar to that defined in the uncorrelated case, while the rest of elements will be zero. Using these matrices to solve the Riccati equation (4.84), the filter gain obtained from equation (4.85) is

$$\begin{bmatrix} 0 & 0 & 0 & 0 \\ 0 & 0 & 0 & 0 \\ 0 & 0 & 0 & 0 \\ -0.02 & -0.02 & -0.15 & -0.15 \\ -0.02 & -0.02 & -0.15 & -0.15 \\ 0.15 & 0.15 & -0.02 & -0.02 \\ 0.15 & 0.15 & -0.02 & -0.02 \\ 0 & 0 & 0 & 0 \\ 0 & 0 & 0 & 0 \\ 0 & 0 & 0 & 0 \\ -33.81 & -33.81 & -0.18 & -0.18 \\ -33.81 & -33.81 & -0.18 & -0.18 \\ -0.18 & -0.18 & -10.97 & -10.97 \\ -0.18 & -0.18 & -10.97 & -10.97 \\ -0.35 & -0.35 & -0.16 & -0.16 \\ -0.35 & -0.35 & -0.16 & -0.16 \\ 0.16 & 0.16 & -0.07 & -0.07 \\ 0.16 & 0.16 & -0.07 & -0.07 \\ 0 & 0 & 0 & 0 \\ 0 & 0 & 0 & 0 \\ 0 & 0 & 0 & 0 \\ 0.14 & 0.14 & -0.05 & -0.05 \end{bmatrix}$$

4.6 Concluding remarks.

An outline of the application of linear optimal control theory to the design of the control laws for active suspension systems

has been given. Both common descriptions of the road surface, either as integrated white noise or filtered white noise, have been considered.

The mathematical details of deriving full and limited state feedback control laws were first reviewed for the case where the correlation between the road inputs is ignored. Modification to the problem formulation so that the control laws could account for the cross correlation and/or the wheelbase time delay was then given. The cross correlation term was presented by means of a first order shaping filter, while the time delay was represented by means of the Pade approximation. With this modification in the problem formulation, the linear control theory was shown to be still applicable to the active suspension problem.

Limited state feedback control laws for the correlated road input case were also discussed and a novel strategy based on the gradient search method for deriving practical control laws for a full vehicle was presented.

The outline flow diagram for the computer program used to generate control laws for different cases and variety of vehicle models has been shown. Finally, example solutions based on a three dimensional vehicle model for the uncorrelated and correlated cases have been given.

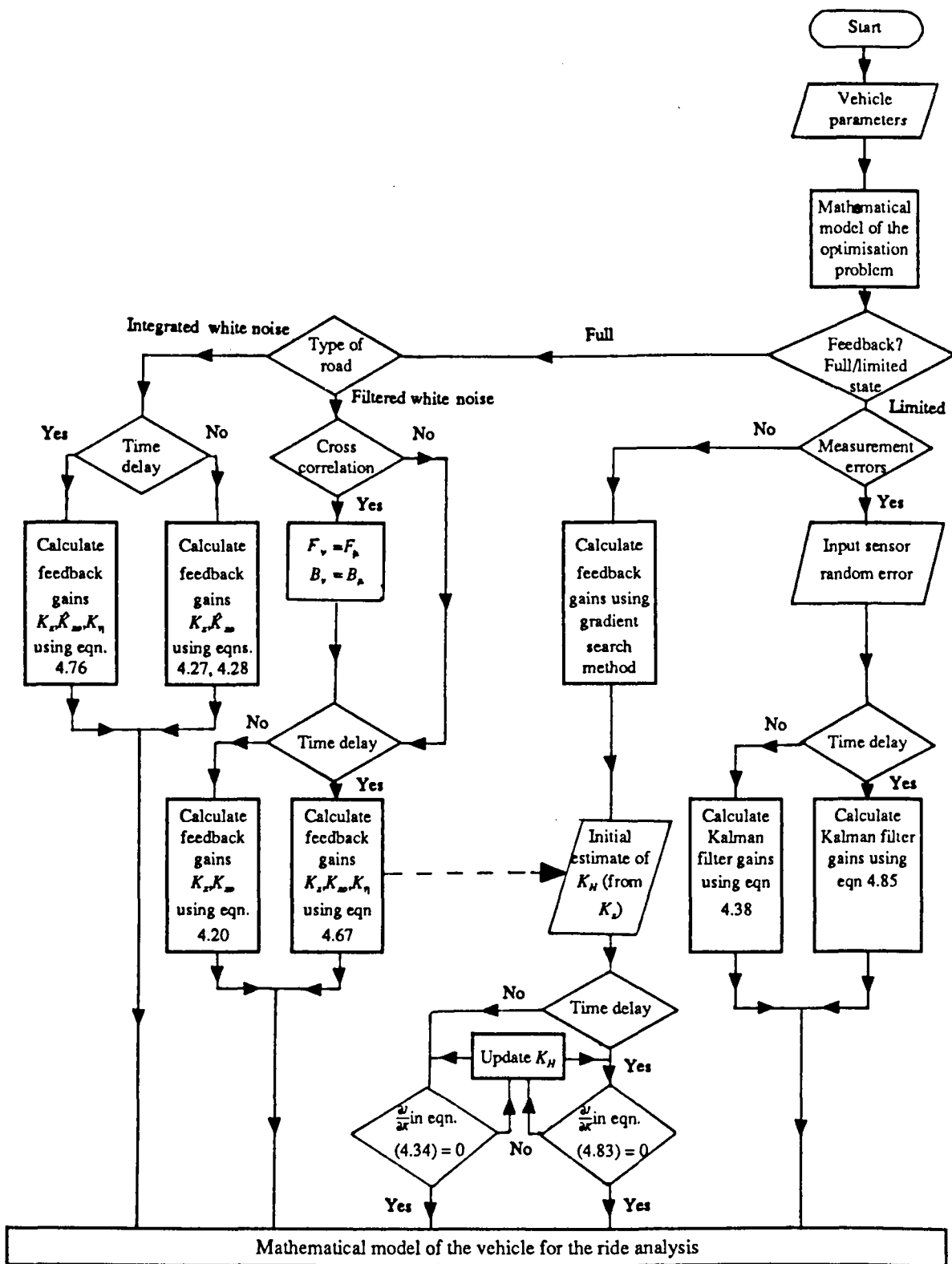


Fig. 4.1 Flow diagram of computer program "ACTOPT" for obtaining control laws.

CHAPTER 5

EFFECT OF MODELLING DETAILS ON THE PERFORMANCE OF THE ACTIVELY SUSPENDED VEHICLE

5.1 Introduction

In the previous Chapter, the formulation of different control laws for active suspension systems were discussed in detail for the case in which the road surface was described either as an integrated white noise or as a filtered white noise. In this Chapter, some of these control laws will be used to study:

- 1- the effect of including the cross correlation in deriving the control law,
- 2- the effect of time delay approximation and,
- 3- the effect of including the time delay on the performance of a decoupled bounce and pitch half vehicle model.

To date, the answer to the first point is not known. This cross correlation was considered in deriving the control law by Fruhauf et al [1985], but they did not indicate specifically its benefit on improving the performance.

The second problem arises from using the Pade approximation to represent the time delay in the control strategies. It is known that the use of higher orders in the Pade approximation reduces the possibility of having a solution far from the optimal one but this increases the system complexity. This

follows because the number of states η to be estimated is equal to the Pade order. Hence, it is a point of practical interest to find the minimum order of the Pade approximation which accurately represents the wheelbase time delay.

In the third problem, a decoupled bounce and pitch half vehicle model ($I_p = M_b \omega_a \omega_b$) is employed to compare directly the quarter car model (no time delay) with an equivalent version which includes the time delay.

In order to study these different points, the single ended vehicle model (bounce and roll) and the half vehicle model (bounce and pitch) shown in Figs. 5.1 and 5.2 respectively are used, each vehicle model having 4 d.o.f. For the vehicle model shown in Fig. 5.1, the sprung mass is treated as a rigid body with bounce and roll and two vertical motions of the front offside and nearside unsprung masses. In the vehicle model shown in Fig. 5.2, the vehicle is divided longitudinally by a vertical plane so that half values of M_b and I_p of those of the full car can be used. The front and rear unsprung masses, M_{wf} and M_{wr} , are assumed to move only vertically. The equations of motion for each vehicle model necessary for the ride calculations and the optimisation problems will be given in detail in the subsequent sections.

5.2 Effect of cross correlation.

In this section, the effect of including the cross correlation in deriving the control laws will be examined by using the simple bounce and roll vehicle model shown in Fig. 5.1. Table

5.1 summarises the vehicle parameters used to generate the results in this section. Because the distances from the c.g. to the front and rear axles (w_a and w_b) are nearly the same (see Table 3.1), values of sprung masses and roll moment of inertia are taken as half of those listed for the full vehicle in Table 3.1. The model is assumed to be only actively suspended. The equations of motion may be written in the form

$$\dot{x} = Ax + Bu + B_2x_o \quad \dots(5.1)$$

where

$$A = \begin{bmatrix} 0 & 0 & 0 & 0 & 1 & 0 & 0 & 0 \\ 0 & 0 & 0 & 0 & 0 & 1 & 0 & 0 \\ 0 & 0 & 0 & 0 & 0 & 0 & 1 & 0 \\ 0 & 0 & 0 & 0 & 0 & 0 & 0 & 1 \\ \frac{-K_t}{M_{wf}} & 0 & 0 & 0 & 0 & 0 & 0 & 0 \\ 0 & 0 & 0 & 0 & 0 & 0 & 0 & 0 \\ 0 & 0 & \frac{-K_t}{M_{wf}} & 0 & 0 & 0 & 0 & 0 \\ 0 & 0 & 0 & 0 & 0 & 0 & 0 & 0 \end{bmatrix}, \quad B = \begin{bmatrix} 0 & 0 \\ 0 & 0 \\ 0 & 0 \\ 0 & 0 \\ \frac{-1}{M_{wf}} & 0 \\ s_1 & s_2 \\ 0 & \frac{-1}{M_{wf}} \\ s_2 & s_1 \end{bmatrix}, \quad B_2 = \begin{bmatrix} 0 & 0 \\ 0 & 0 \\ 0 & 0 \\ 0 & 0 \\ \frac{K_t}{M_{wf}} & 0 \\ 0 & 0 \\ 0 & \frac{K_t}{M_{wf}} \\ 0 & 0 \end{bmatrix}$$

$$s_1 = \frac{1}{M_b} + \frac{t_s^2}{I_r}, \quad s_2 = \frac{1}{M_b} - \frac{t_s^2}{I_r}$$

In order to account for the cross correlation in deriving the control law, the road surface is described as filtered white noise. Based on equations (4.45) and (4.46), equation (4.48) may be written as

$$\begin{bmatrix} \dot{x}_{o1} \\ \dot{x}_{o2} \end{bmatrix} = -V \begin{bmatrix} \frac{d_1+d_2}{2} & \frac{d_1-d_2}{2} \\ \frac{d_1-d_2}{2} & \frac{d_1+d_2}{2} \end{bmatrix} \begin{bmatrix} x_{o1} \\ x_{o2} \end{bmatrix} + V \begin{bmatrix} g_1 & \frac{-g_2 t_w}{2} \\ g_1 & \frac{g_2 t_w}{2} \end{bmatrix} \begin{bmatrix} w_1 \\ w_2 \end{bmatrix}$$

i.e.

$$\dot{x}_{of} = F_{\mu 1} x_{of} + B_{\mu 1} u_f \quad \dots(5.2)$$

Given the above description of the road surface at the front axle, Rill [1983] showed that the power spectral densities for the left and right tracks are

$$S_r(\Omega) = S_l(\Omega) = S_o \frac{\Omega^2 + ((d_2^2 + \alpha d_1^2)/(1 + \alpha))}{\Omega^4 + (d_1^2 + d_2^2)\Omega^2 + d_1^2 d_2^2} \quad \dots(5.3)$$

with coherence function:

$$\gamma_c(\Omega) = \frac{(1 - \alpha)\Omega^2 + d_2^2 - \alpha d_1^2}{(1 + \alpha)\Omega^2 + d_2^2 + \alpha d_1^2} \quad \dots(5.4)$$

where Ω is the spatial frequency (rad/m),

$$\alpha = \left(\frac{t_f}{2} \frac{g_2}{g_1} \right)^2 \quad \dots(5.5)$$

$$S_o = \frac{V g_1^2 q (1 + \alpha)}{2\pi} \quad \dots(5.6)$$

The following values were found by Rill [1983] to produce a good match between road measurements and calculated spectral densities and the coherence function

$$S_o = 1.52 \times 10^{-5} \quad , \quad \alpha = 0.75 \quad , \quad d_1 = 0.3 m^{-1},$$

$$d_2 = 1.5 m^{-1} \quad , \quad g_1 = 1 \quad , \quad g_2 = 0.72 \quad \dots(5.7)$$

Two control laws will be considered. In the first one, where the cross correlation is considered, equation (5.2) is used to represent the road surface, while in the case where this correlation is ignored, the input equation is given by:

$$\dot{x}_{o1} = \dot{x}_{o2} = \dot{\zeta} = -V d_1 \zeta + V g_1 w_1 \quad \dots(5.8)$$

Having generated the feedback gains as described in section 4.2.1.1, and using the equation

$$u = Kx + K_{x_o} x_o \quad \dots(5.9)$$

equation (5.1) may be re-written as follows:

$$\dot{x} = (A + BK_x)x + (B_2 + BK_{x_0})x_0 \quad \dots(5.10)$$

This equation is of the form of equation (2.13), where $M_{x_{DD}}$ and M_{UD} are null matrices while,

$$M_{x_{DD}} = I \quad , \quad M_x = -(A + BK_x) \quad , \quad M_U = B_2 + BK_{x_0}$$

For both control strategies, the cross correlation effects are represented in the ride calculations in the correct way as described by equations (5.3) to (5.7)

Table 5.4 shows the r.m.s. values calculated for both control laws at different vehicle speeds. It is however, clear that the inclusion of the cross correlation in deriving the control laws does not affect the performance significantly. This conclusion is based on using Rill's method to represent the cross correlation and using filtered white noise to represent the road input.

5.3 Effect of time delay approximation.

5.3.1 Vehicle model and equations of motion.

In this section the bounce and pitch half vehicle model shown in Fig. 5.2 is considered. With reference to this figure, the equations of motion are

$$M_b \ddot{z}_b = F_1 + F_3 + u_1 + u_3 \quad \dots(5.11)$$

$$I_p \ddot{\theta} = -w_a F_1 + w_b F_3 - w_a u_1 + w_b u_3 \quad \dots(5.12)$$

$$M_{wf} \ddot{x}_1 = -F_1 + F_5 - u_1 \quad \dots(5.13)$$

$$M_{wr} \ddot{x}_5 = -F_3 + F_7 - u_3 \quad \dots(5.14)$$

or

$$\begin{bmatrix} M_b & 0 & 0 & 0 \\ 0 & I_p & 0 & 0 \\ 0 & 0 & M_{wf} & 0 \\ 0 & 0 & 0 & M_{wr} \end{bmatrix} \begin{bmatrix} \ddot{z}_b \\ \ddot{\theta} \\ \dot{x}_1 \\ \dot{x}_5 \end{bmatrix} = \begin{bmatrix} 1 & 1 & 0 & 0 \\ -w_a & w_b & 0 & 0 \\ -1 & 0 & 1 & 0 \\ 0 & -1 & 0 & 1 \end{bmatrix} \begin{bmatrix} F_1 \\ F_3 \\ F_5 \\ F_7 \end{bmatrix} + \begin{bmatrix} 1 & 1 \\ -w_a & w_b \\ -1 & 0 \\ 0 & -1 \end{bmatrix} \begin{bmatrix} u_1 \\ u_3 \end{bmatrix}$$

or

$$M_{XDD}\ddot{z} = M_f F_p + M_{f1} u \quad \dots(5.15)$$

By following the procedure described in section 2.2, the matrices M_{XD} , M_X and M_U are found for the passively suspended vehicle model as

$$M_{XD} = \begin{bmatrix} C_f + C_r & -w_a C_f + w_b C_r & -C_f & -C_r \\ -w_a C_f + w_b C_r & w_a^2 C_f + w_b^2 C_r & w_a C_f & -w_b C_r \\ -C_f & w_a C_f & C_f & 0 \\ -C_r & -w_b C_r & 0 & C_r \end{bmatrix},$$

$$M_X = \begin{bmatrix} K_f + K_r & -w_a K_f + w_b K_r & -K_f & -K_r \\ -w_a K_f + w_b K_r & w_a^2 K_f + w_b^2 K_r & w_a K_f & -w_b K_r \\ -K_f & w_a K_f & K_f + K_r & 0 \\ -K_r & -w_b K_r & 0 & K_r + K_t \end{bmatrix}, \quad M_U = \begin{bmatrix} 0 & 0 \\ 0 & 0 \\ K_t & 0 \\ 0 & K_t \end{bmatrix}$$

while the matrices A , B and B_2 necessary for obtaining the control laws are given by

$$A = \begin{bmatrix} 0 & 0 & 0 & 0 & 1 & 0 & 0 & 0 \\ 0 & 0 & 0 & 0 & 0 & 1 & 0 & 0 \\ 0 & 0 & 0 & 0 & 0 & 0 & 1 & 0 \\ 0 & 0 & 0 & 0 & 0 & 0 & 0 & 1 \\ \frac{-K_t}{M_{wf}} & 0 & 0 & 0 & 0 & 0 & 0 & 0 \\ 0 & 0 & 0 & 0 & 0 & 0 & 0 & 0 \\ 0 & 0 & \frac{-K_t}{M_{wr}} & 0 & 0 & 0 & 0 & 0 \\ 0 & 0 & 0 & 0 & 0 & 0 & 0 & 0 \end{bmatrix}, \quad B = \begin{bmatrix} 0 & 0 \\ 0 & 0 \\ 0 & 0 \\ 0 & 0 \\ \frac{-1}{M_{wf}} & 0 \\ s_1 & s_2 \\ 0 & \frac{-1}{M_{wr}} \\ s_2 & s_3 \end{bmatrix}, \quad B_2 = \begin{bmatrix} 0 & 0 \\ 0 & 0 \\ 0 & 0 \\ 0 & 0 \\ \frac{K_t}{M_{wf}} & 0 \\ 0 & 0 \\ 0 & \frac{K_t}{M_{wr}} \\ 0 & 0 \end{bmatrix}$$

where

$$s_1 = \frac{1}{M_b} + \frac{w_a^2}{I_p}, \quad s_2 = \frac{1}{M_b} - \frac{w_a w_b}{I_p}, \quad s_3 = \frac{1}{M_b} + \frac{w_b^2}{I_p}$$

The control law for this case is obtained when the road surface

is described as an integrated white noise. These matrices are used to derive control laws when the time delay is ignored as described in section 4.2.1.2 and to derive that which accounts for the time delay as discussed in section 4.3.1.2. Having the feedback gains available, it is easy to prepare the equations necessary for the ride analysis as discussed in the last section.

5.3.2 Identification of the time delay approximation by discrete optimal control theory.

In this section, the performance index results obtained based on the discrete optimal control theory by Louam et al [1988] will be used as a reference to identify the order of the Pade approximation necessary to approach the optimal solution. The vehicle parameters taken from Louam et al [1988] are as follows

$$M_b = 505.1 \text{ kg} , M_{wf} = 28.58 \text{ kg} , M_{wr} = 54.43 \text{ kg} , I_p = 651 \text{ kgm}^2 \\ K_t = 155.9 \text{ kN/m} , w_a = 1.0978 \text{ m} , w_b = 1.4676 \text{ m} \quad \dots(5.16)$$

This data will be used only in this section. The calculation of the performance index based on the optimal discrete theory is explained in detail in Louam et al, whereas for the Pade approximation case, the performance index may be obtained as follows;

1- Use the matrices A , B and B_2 defined in section 5.3.1 and the Pade approximation matrices A_η , B_η and C_η defined in section 4.3.1.1.2 to form A_{sf} , B_{sf} and b_{sf} as shown by equation (4.75).

2- Solve the Riccati equation (4.77) for P_{sf} .

3- Find the performance index from

$$J = \text{trace}\{P_{sf}(b_{sf}Wb_{sf}^T)\} \quad \dots(5.17)$$

A unit step input will be considered, hence the matrix W will be an $(8+N, 8+N)$ unit matrix, where N is the order of the Pade approximation.

Table 5.5 shows the performance index calculated by 2nd and 4th order Pade approximations and by the linear discrete theory. It can be seen from the Table that the 4th order Pade approximation accurately represents the wheelbase time delay giving results for the performance index which are close to those obtained from the discrete theory, while the 2nd order Pade approximation is not accurate enough for this vehicle (wheelbase = 2.565 m).

5.3.3 Identification of the time delay approximation by linear ride calculations.

It is possible to test the accuracy of the Pade approximation using the passively suspended half vehicle model. Two sets of calculations are performed; first using the standard method discussed in Chapter 2 in which the wheelbase time delay is represented by a pure time delay and second using various orders of Pade approximation to represent the wheelbase time delay. This is done for the vehicle data shown in Table 5.2 and the results are shown in Table 5.6. It can be seen from the table that complete agreement in the r.m.s. values of the vehicle responses at the rear suspension calculated based on

the pure time delay representation and those calculated based on the 4th order Pade approximation time delay representation occurs at 30 m/s . Agreement in the power spectral densities is shown in Figs. 5.3 and 5.4.

In general, this method represents an easy way to find out the accuracy of the time delay approximation. However, full agreement in the spectral density functions obtained from the standard and approximated methods is necessary to ensure that the Pade approximation order is enough to approach the optimality in deriving the control law. Particularly, the results show that for the vehicle dimensions shown in Table 5.2, the use of 4th order Pade approximation accurately represents the wheelbase time delay.

5.4 Decoupled vehicle model studies.

In ride calculations and in the optimisation problem, the bounce and pitch half vehicle model shown in Fig. 5.2 is decoupled, i.e. is equivalent to two quarter car models if

$$I_p = M_b \omega_a \omega_b \quad \dots(5.18)$$

In this section, it is intended to study the effect of including the time delay on deriving the control law on the performance of an actively suspended decoupled bounce and pitch half vehicle model. The road surface will be described as an integrated white noise to derive the control laws, while the road of $R_c = 3 \times 10^{-6}$, $\kappa = 2.5$ is assumed to be traversed at 30 m/s for the ride calculations. The vehicle parameters shown in Table 5.2 will be used except I_p which will be taken equal to 1546 kg.m^2 which satisfies equation (5.18). The r.m.s. values

of the body acceleration at the front and rear body connection points, front and rear dynamic tyre load and the front and rear suspension working space are shown in Table 5.7. The r.m.s. values of the body acceleration at the rear connection point are plotted against the rear dynamic tyre load in Fig. 5.5.

It can be seen from Table 5.7 and Fig. 5.5, that including the time delay in deriving the control law for this vehicle model dramatically improves body acceleration and the dynamic tyre load at the rear axle without any increase in the working space. It should be mentioned that if the time delay is considered in deriving the control laws the response at the rear axle will then depend on the Pade states η which in turn depend on the front input. On the other hand, if the time delay is ignored in deriving the control laws, the results obtained from the decoupled bounce and pitch half vehicle model will be identical to those obtained from two quarter car models which have the parameters listed in Table 5.3. Hence, it can be concluded that the use of quarter car models to derive the control laws of the active suspension system always results in sub-optimal control laws even for a decoupled bounce and pitch half vehicle model. The half vehicle control law takes advantage of the fact that information from the front wheels can essentially be used as preview to improve performance at the rear. It should be mentioned that the optimal control law uses extra information (time delay states η) which cannot be measured directly. In the next chapters, the effect of the time delay on the performance using various

control laws and methods for estimating or omitting the time delay states η will be given in detail based on the coupled 7 d.o.f. vehicle model.

5.5 Concluding remarks.

The effect of including the cross correlation in deriving the control law is examined by using a 4 d.o.f. bounce and roll single ended vehicle model together with the first order shaping filter introduced by Rill [1983]. It was shown that ignoring the cross correlation does not affect the performance level of the active suspension system.

Two methods were used to investigate the time delay approximation in the control law. First, for a half vehicle model, the performance index calculated using a 2nd and 4th order Pade approximation was compared with that calculated by Louam et al [1988] based on the discrete optimal control theory. Good agreement between the results obtained based on the 4th order Pade approximation and those obtained from the discrete theory was found for a range of vehicle speeds. Second, the Pade approximation was tested using the passively suspended vehicle. The half vehicle model response calculated using the pure time delay was compared with that obtained from representing the time delay by an N^{th} order Pade approximation. The results confirmed that the 4th order Pade approximation represented accurately the wheelbase time delay and hence this approximation can be confidently used in deriving the control laws.

The results from the decoupled half vehicle model showed that if the time delay is included in the derivation of the control law, dramatic improvements are obtained at the rear suspension compared with its quarter car equivalent version. It should be mentioned that the optimal control law (which accounts for the time delay) uses extra information (time delay states η) which cannot be measured directly. In the next Chapters, the effect of the time delay on the performance using various control laws and methods for estimating or omitting the time delay states η will be given in detail based on the coupled 7 d.o.f. vehicle model.

Table 5.1 Vehicle parameters used in the single end vehicle model (bounce and roll)

$$\begin{array}{lll}
 M_b = 855 \text{ kg} & M_{wf} = 57.5 \text{ kg} & t_s = 0.595 \text{ m} \\
 I_r = 600 \text{ kgm}^2 & K_t = 200 \text{ kN/m} & t_w = 1.54 \text{ m}
 \end{array}$$

Table 5.2 Vehicle parameters used in the half vehicle model (bounce and pitch)

$$\begin{array}{lll}
 M_b = 855 \text{ kg} & M_{wf} = 57.5 \text{ kg} & M_{wr} = 75 \text{ kg} \\
 I_p = 2500 \text{ kgm}^2 & K_t = 200 \text{ kN/m} & \omega_a = 1.335 \text{ m} \\
 w_b = 1.337 \text{ m} & &
 \end{array}$$

Table 5.3 Parameters of the front and rear quarter car models obtained from the decoupled bounce and pitch half vehicle model.

| | Front | Rear |
|----------|----------|----------|
| M_b | 425 kg | 430 kg |
| M_{wf} | 57.5 kg | 75 kg |
| K_t | 200 kN/m | 200 kN/m |

Table 5.4 Effect of including the cross correlation in deriving the control law on the performance of the active systems.

| speed m/s | Cross correlation | Root mean square values | | | | | |
|--------------|----------------------|----------------------------------|----------------------------------|---------------|---------------|------------------|------------------|
| | | \ddot{x}_1 m/s ² | \ddot{x}_2 m/s ² | $FDTL_1$ N | $FDTL_2$ N | sws_{f1} cm | sws_{f2} cm |
| 10 | Correlated | 0.74 | 0.74 | 635 | 635 | 0.6 | 0.6 |
| | Non-correlated | 0.77 | 0.77 | 636 | 636 | 0.6 | 0.6 |
| 20 | Correlated | 1.39 | 1.39 | 1206 | 1206 | 1.1 | 1.1 |
| | Non-correlated | 1.39 | 1.39 | 1226 | 1226 | 1.1 | 1.1 |
| 30 | Correlated | 2.00 | 2.00 | 1713 | 1713 | 1.4 | 1.4 |
| | Non-correlated | 2.05 | 2.05 | 1714 | 1714 | 1.4 | 1.4 |

Table 5.5 Comparison between the performance index calculated by the optimal discrete control theory which represents the time delay as a pure time delay and that calculated from the continuous control strategy which employs the Pade approximation to represent the time delay.

| Method | Speed m/s | | | | | |
|--|-----------|------|------|------|------|------|
| | 10 | 20 | 30 | 40 | 50 | 60 |
| Optimal discrete control theory * | 0.48 | 0.50 | 0.53 | ** | ** | ** |
| 4 th order Pade approximation | 0.50 | 0.51 | 0.53 | 0.59 | 0.62 | 0.63 |
| 2 nd order Pade approximation | 0.57 | 0.55 | 0.58 | 0.64 | 0.65 | 0.64 |

* The results are taken from Louam et al [1988]

** Results are not available.

Table 5.6 R.m.s. values of the body acceleration, dynamic tyre load and suspension working space at the rear suspension calculated for the passive system of $K_f = K_r = 24 \text{ kN/m}$ and $C_f = C_r = 24 \text{ kNs/m}$ when the road of $R_c = 3 \times 10^{-6}$ is traversed at 30 m/s.

| speed m/s | Time delay representation | Root mean square values | | |
|--------------|------------------------------|--------------------------------|-------------------------|-------------------------------------|
| | | \ddot{x}_6 m/s^2 | <i>RDTL</i> <i>N</i> | <i>sws_r</i> <i>cm</i> |
| 10 | Pure | 1.056 | 790 | 1.480 |
| | 4 th order | 1.070 | 793 | 1.478 |
| | 2 nd order | 1.02 | 795 | 1.490 |
| 20 | Pure | 1.781 | 1343 | 2.623 |
| | 4 th order | 1.783 | 1343 | 2.623 |
| | 2 nd order | 1.803 | 1353 | 2.623 |
| 30 | Pure | 2.401 | 1823 | 3.518 |
| | 4 th order | 2.401 | 1823 | 3.518 |
| | 2 nd order | 2.458 | 1825 | 3.517 |

Table 5.7 Effect of including the time delay in deriving the control law on the system performance of a decoupled bounce and pitch half vehicle model. These results were obtained when the road of $R_c = 3 \times 10^{-6}$ is traversed at 30 m/s.

| Control law | Weighting parameters | | | | | Root mean square values | | | | | |
|--------------------|--------------------------------|------------------|------------------|-----------------|-----------------|-------------------------|-------------------------|---------------|---------------|-----------------|-----------------|
| | ρ_1, ρ_2 u_1, u_2 | q_1 sws_f | q_2 sws_r | q_3 $FDTL$ | q_4 $RDTL$ | \ddot{x}_2 m/s^2 | \ddot{x}_6 m/s^2 | $FDTL$ N | $RDTL$ N | sws_f cm | sws_r cm |
| Without Time delay | 1×10^{-9} | 1.5 | 1.50 | 50 | 80 | 2.00 | 2.27 | 1214 | 1308 | 2.5 | 2.5 |
| | | 1.3 | 1.30 | 20 | 40 | 1.87 | 2.17 | 1340 | 1409 | 2.5 | 2.5 |
| | | 1.5 | 1.50 | 12 | 12 | 1.82 | 2.00 | 1419 | 1604 | 2.5 | 2.5 |
| With Time delay | 1×10^{-9} | 1.5 | 0.85 | 50 | 18 | 2.00 | 1.51 | 1214 | 808 | 2.5 | 2.5 |
| | | 1.3 | 0.70 | 20 | 12 | 1.87 | 1.45 | 1340 | 878 | 2.5 | 2.5 |
| | | 1.5 | 0.60 | 12 | 5. | 1.82 | 1.33 | 1419 | 1116 | 2.5 | 2.5 |

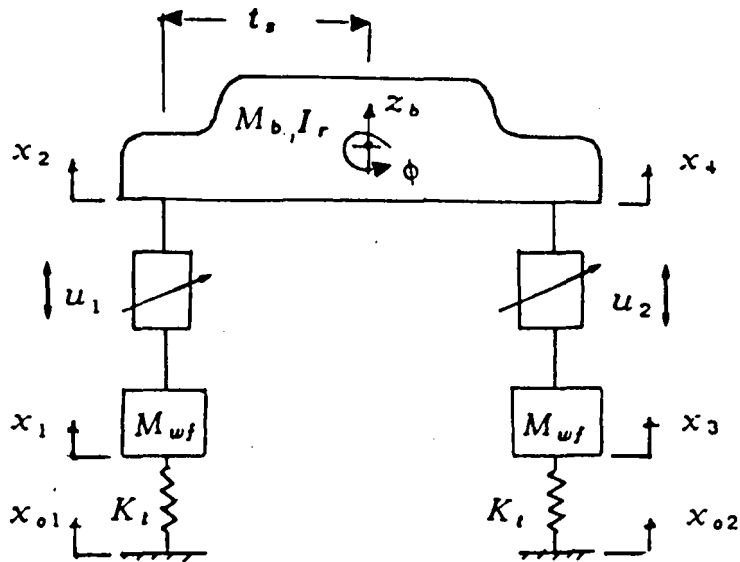


Fig. 5.1 Bounce and roll vehicle model

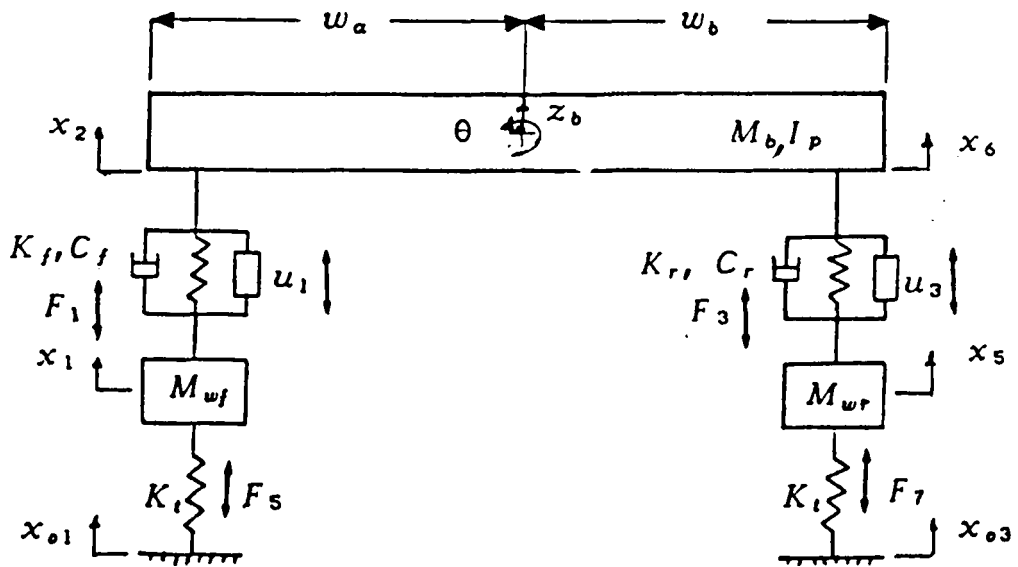


Fig. 5.2 Bounce and pitch half vehicle model

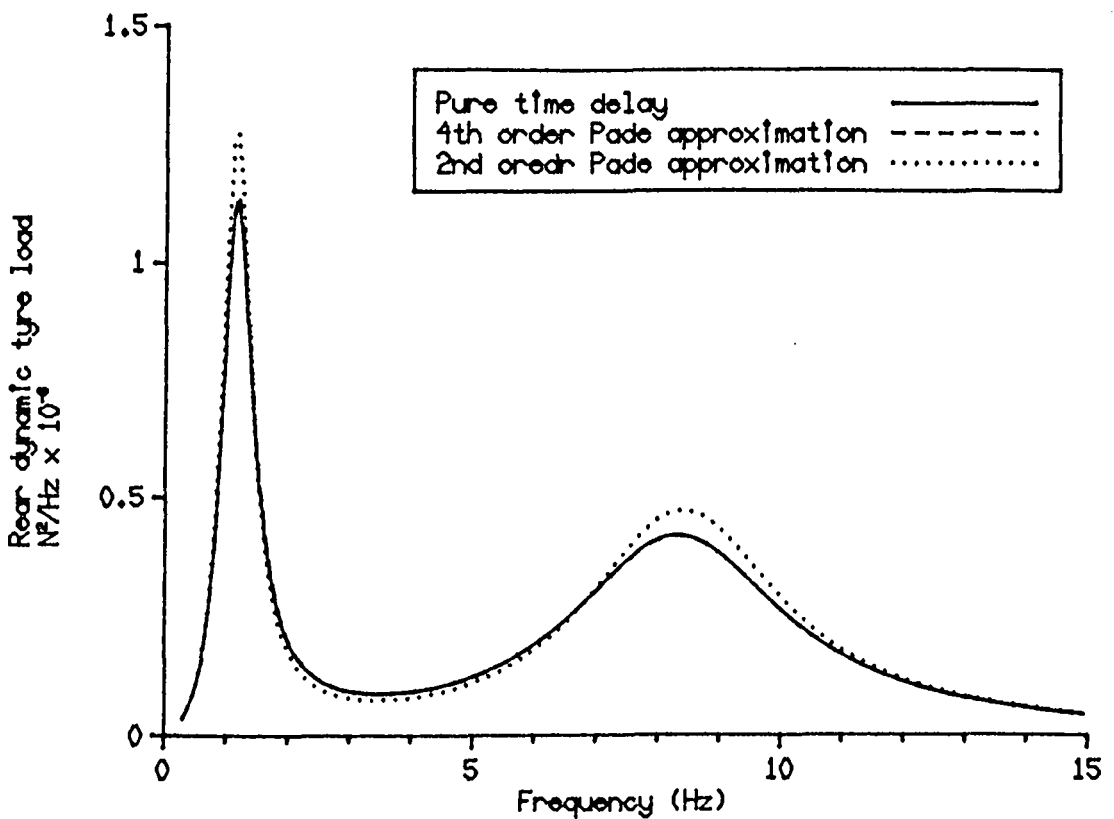
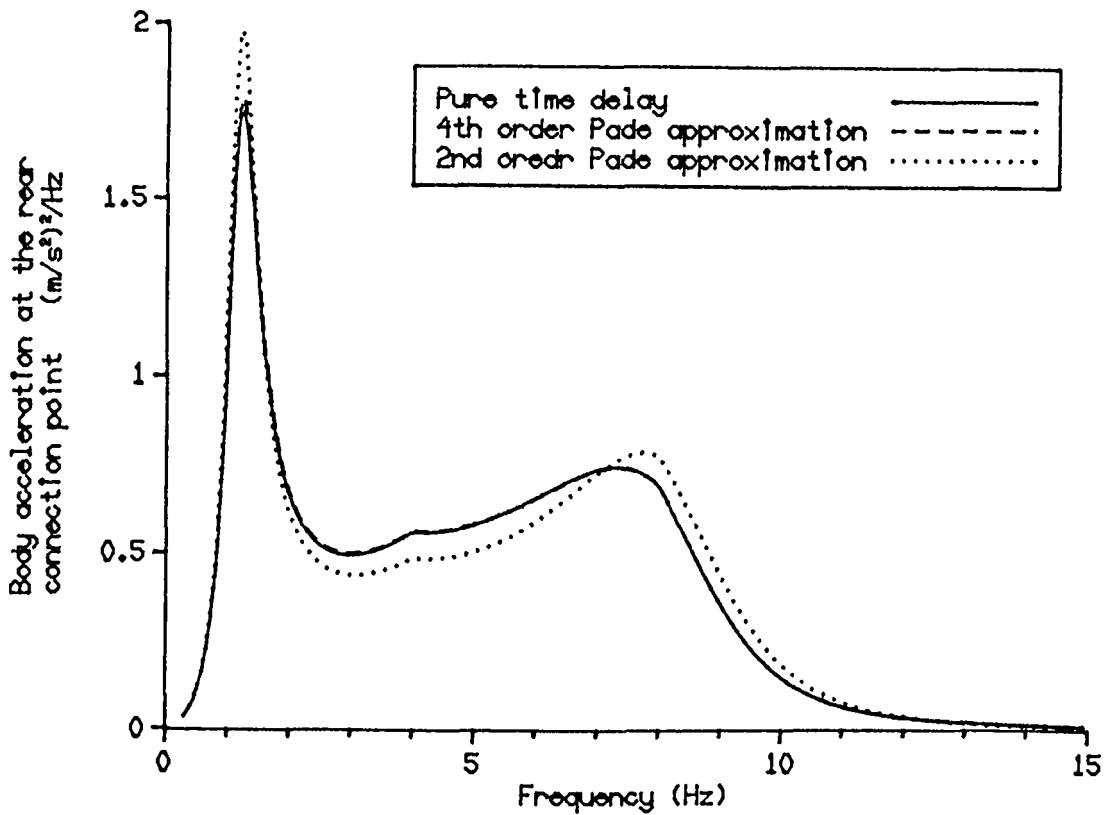


Fig. 5.3 Comparison between the power spectral densities calculated for a passive system when the wheelbase time delay is represented as a pure time delay and represented by 2nd and 4th order Pade approximations.

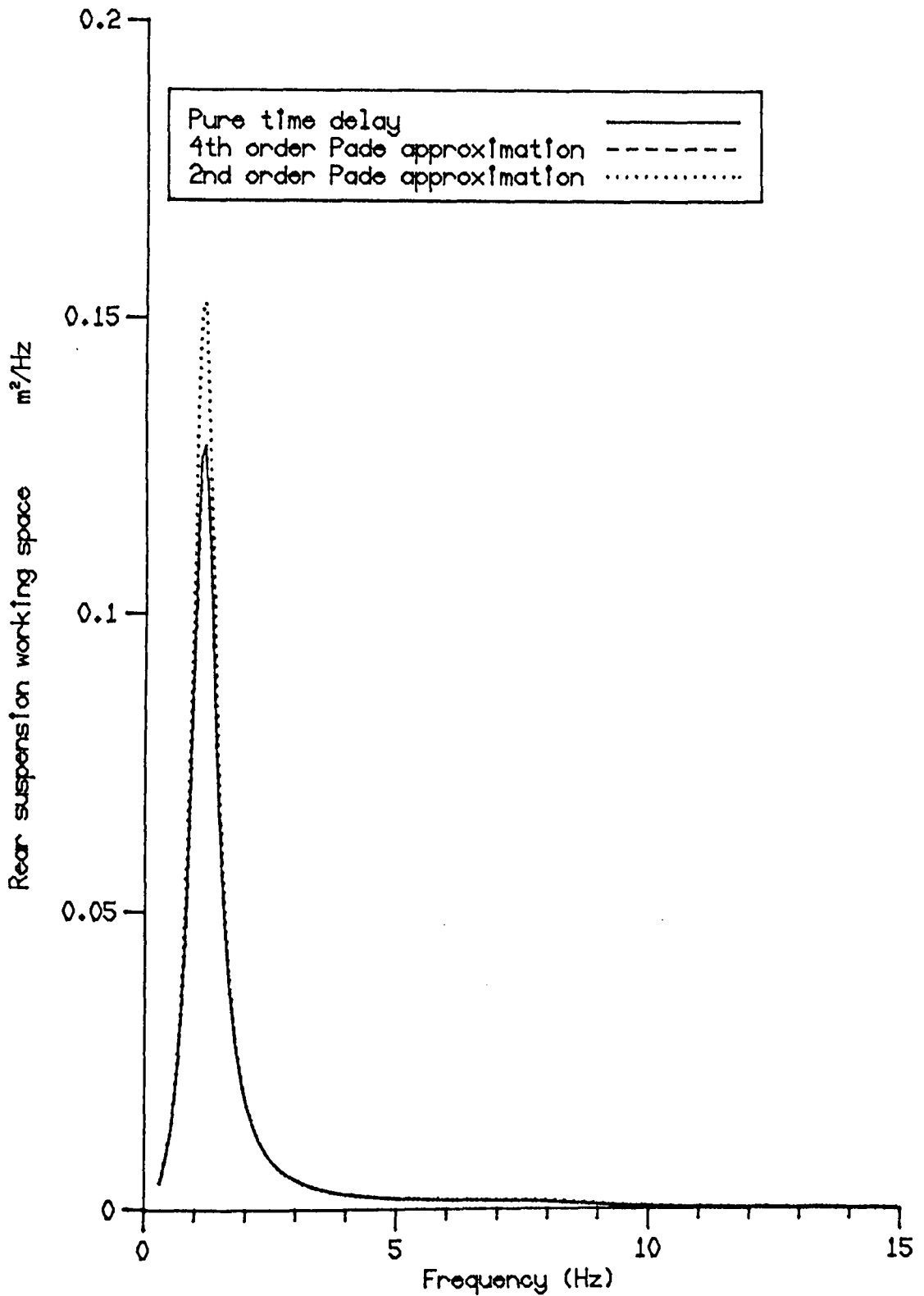


Fig. 5.4 Comparison between the power spectral densities calculated for a passive system when the wheelbase time delay is represented as a pure time delay and represented by 2nd and 4th order Pade approximations.

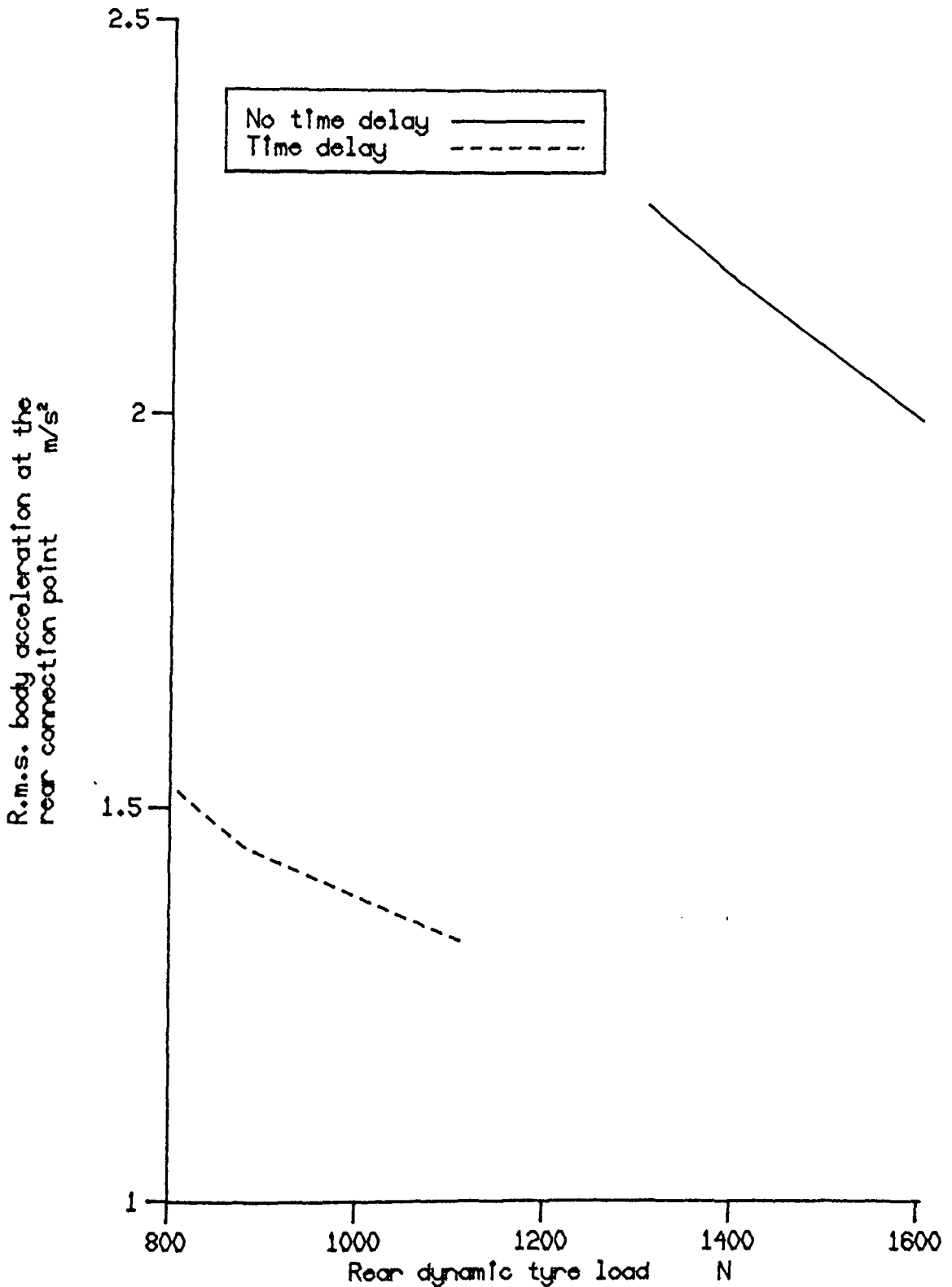


Fig. 5.5 The effect of including the time delay in deriving the control law of the active system on improving the rear suspension response for a decoupled vehicle model.

CHAPTER 6

FULL STATE FEEDBACK ACTIVE SUSPENSION SYSTEMS

6.1 Introduction

The possibility of modifying the design of the automotive suspension systems by using active controls is currently of great interest to the automotive industry. Most of the car manufacturers are involved in investigating the benefits which could be achieved from employing these systems. Active suspension systems are intelligent in the sense that they offer the potential of being adapted to the different vehicle operating conditions. The control strategies of the full state feedback active systems which were discussed in Chapter 4 and applied in Chapter 5 to two simple vehicle models can also be applied to the full vehicle model shown in Fig. 6.1. In general, various configurations of the full state feedback active systems may be considered. There are two reasons behind this:

- 1- The active suspension design formulation varies with the assumed description of the roadway disturbance, i.e. filtered white noise, or integrated white noise and whether cross correlation and/or wheelbase time delay will be considered or not.
- 2- Various types of feedback information are available. For example, an active system can be designed so that all the states at the c.g. position are measured. An alternative design could be based on measuring all the states at the connection points between body and suspension.

Based on these two points, six competing systems are selected to be compared with each other in terms of their ride performance. The classification of the systems *a* to *g* is presented in Table 6.1. In Chapter 5, the inclusion of the cross correlation in the control strategy was found not to be cost effective, hence this correlation is neglected in deriving the control laws of all the active systems considered here; instead two identical tracks are assumed available. Furthermore, it was found that the fourth order Pade approximation represents very accurately the wheelbase time delay. Hence, this approach is confidently used in deriving the control law of the systems *d*, *e* and *g*. Example solutions of finding the feedback gains were given in sections 4.5.1 and 4.5.2. Once these gains are calculated, the equations of motion of these linear systems can be derived in a straightforward manner, as will be described in the next section.

Throughout this chapter, the linear calculations are obtained in the same manner as described in Chapter 3. Again, the road surface is described by the power spectral density shown in equation 1.1. This description is employed in the analysis of all the active systems, both those which have control laws based on filtered white noise description and those which have control laws based on the white noise description (equations (4.2) and (4.3) respectively). Although the correlation between road inputs was ignored for the purpose of deriving control laws and the Pade approximation was used to present the wheelbase time delay in deriving control laws

of systems d , e and g , the cross correlation between left and right tracks and the effective time delay characteristic between front and rear wheels was correctly represented in the ride calculations. As in Chapter 3, all the results presented here are generated when the vehicle moves with constant forward speed and the linear calculations start at a cutoff wave number of $\lambda_0 = 0.01$ cycle/m.

It is possible now to consider the performance capabilities of these different full state feedback active systems, and indeed of suspension systems of the same type but with different weighting parameters. As in Chapter 3, the performance of any of these suspension systems is analysed in terms of r.m.s. values of the frequency weighted vertical, lateral and longitudinal seat accelerations (\ddot{z}_x , \ddot{y}_x and \ddot{x}_x), front and rear dynamic tyre loads ($FDTL$ and $RDTL$) and the fore/aft and the lateral dynamic tyre loads transfers ($FDTT$ and $LDTT$).

6.2 Equations of motion.

In this section, the development of the second order equations of motion of the active systems a to g is discussed. In deriving these equations, the vehicle is assumed to be only actively suspended i.e. the stiffness and damping coefficients K_f , K_r , C_f and C_r as well as the anti-roll bar stiffnesses K_{rf} and K_{rr} are taken equal to zero. With reference to Fig. 6.1, it is easy to show that

$$\begin{bmatrix} x_1 \\ x_2 \\ x_3 \\ x_4 \\ x_5 \\ x_6 \\ x_7 \\ x_8 \end{bmatrix} = \begin{bmatrix} 0 & 0 & 0 & 1 & 0 & 0 & 0 \\ 1 & -w_a & -t_s & 0 & 0 & 0 & 0 \\ 0 & 0 & 0 & 0 & 1 & 0 & 0 \\ 1 & -w_a & t_s & 0 & 0 & 0 & 0 \\ 0 & 0 & 0 & 0 & 0 & 1 & 0 \\ 1 & w_b & -t_s & 0 & 0 & 0 & 0 \\ 0 & 0 & 0 & 0 & 0 & 0 & 1 \\ 1 & w_b & t_s & 0 & 0 & 0 & 0 \end{bmatrix} \begin{bmatrix} z_b \\ \theta \\ \phi \\ x_1 \\ x_3 \\ x_5 \\ x_7 \end{bmatrix}$$

or

$$z_a = T_z z \quad \dots(6.1)$$

Consider now the active system α , the control force $u(t)$ may be expressed as

$$u = Kx + \hat{K}_o x_o = K_a T_z z + K_b T_z \dot{z} + \hat{K}_o x_o \quad \dots(6.2)$$

where $x = [z_a \ \dot{z}_a]^T$ and K_a and K_b are (nxm) sub matrices in K in which

$$K = [K_a \ | \ K_b]$$

Using equation (6.2) in equation (2.10), the matrices M_{xD} , M_x and M_U of equation (2.14) become

$$M_{xD} = M_f M_c M_f^T - M_{f1} K_b T_z \quad \dots(6.3)$$

$$M_x = M_f M_k M_f^T - M_{f1} K_a T_z \quad \dots(6.4)$$

$$M_U = -M_f M_k M_{DU} + M_{f1} \hat{K}_o \quad \dots(6.5)$$

while the matrix M_{UD} is a null matrix. It should be mentioned that the matrices M_{xDD} , M_f , M_{f1} , M_{DU} , M_k and M_c will remain unchanged as given in section 2.3 except that the elements K_{f1} , K_{r1} , K_{rf1} , K_{rr1} , C_f and C_r in the matrices M_k and M_c will be zero.

In the active system b , the matrices M_{XD} and M_X will be similar to those of system a , while in finding the matrix M_U , the matrix K_o should be used instead of \hat{K}_o .

Equations (6.3) to (6.6) may also be used to find M_{XD} , M_X and M_U of the active system c . In this case, the matrix T_z will be a unit matrix.

If the time delay between the front and rear inputs is included in deriving the control laws, the state vector z will then be

$$\begin{bmatrix} z \\ \eta \end{bmatrix} \quad \dots(6.6)$$

The matrices M_{XDD} , M_{XD} , M_X and M_U of the active system d are related to those of system a by

$$M_{XDD}^d = \begin{bmatrix} M_{XDD}^a & 0 \\ 0 & 0 \end{bmatrix}, \quad M_{XD}^d = \begin{bmatrix} M_{XD}^a & 0 \\ 0 & I \end{bmatrix}, \quad M_X^d = \begin{bmatrix} M_X^a & -M_{f1}^a K_\eta \\ 0 & -A_\eta \end{bmatrix}$$

$$M_U^d = \begin{bmatrix} M_U^a \\ 0 \end{bmatrix}, \quad M_{UD}^d = \begin{bmatrix} 0 & - & - \\ B_\eta & | & 0 \end{bmatrix}$$

where for example, M_{XDD}^a donates the matrix M_{XDD} for system a . The same relationship is valid between systems b and e and between systems c and g .

Because the outputs of interest (seat accelerations, dynamic tyre load, working space and the tyre load transfers) are considered as in the passive system, the non-zero elements of the output matrices T_{XDD} , T_{XD} , T_X and T_U of all the systems are similar to those given in section 2.6.

6.3 Results

The results presented here are related directly to studying (a) the effect of ground surface representation, (b) the effect of the various types of the feedback information, (c) the effect of the working space available and (d) the effect of including the wheelbase time delay in deriving the control laws. In order to study these problems, a set of results was calculated when a road of $R_c = 3 \times 10^{-6}$ and $\kappa = 2.5$ was traversed at 30 m/s. Because the system performance depends strongly on the working space available, four design values of the working space r.m.s. values equal to 2, 2.5, 3 and 3.5 cm were considered to be consumed at this vehicle speed. Furthermore, for each particular value of the working space, each suspension type was represented in the various systems by changing the performance index weighting parameters. However, the generation of the results in this way enabled the following features to be studied: firstly, problems (a) to (c) for different design possibilities (working space available is considered as a design parameter), secondly a comparison between the active systems at equal usage of the working space and finally the effect of the working space itself on the system performance. Results for the active suspension *a* are shown in Figs. 6.2 to 6.4. In these figures, the r.m.s. of the ISO weighted vertical, lateral and longitudinal seat accelerations, rear dynamic tyre load, fore/aft and the lateral dynamic tyre load transfers are plotted against the front dynamic tyre load. Results for active systems *b*, *d* and *e* are shown in Figs. 6.5 to 6.7, 6.8

to 6.10 and 6.11 to 6.13 respectively. The results are also summarised in Tables 6.2 to 6.5 for working space r.m.s. values of 2 ,2.5, 3 and 3.5 cm respectively. Having generating these baseline results, it is easy now to use them in studying the sub-problems (a) to (d) as it will be indicated in the next sections.

6.4 Discussion of results.

6.4.1 Effect of ground surface representation.

It is known that the power spectral density form (1.1) describes more accurately the road surface than either the filtered white noise form (4.2) or the integrated white noise form (4.3). Hence, the best control law should be the one which is based on equation (1.1). A control strategy based on this road description has yet to be found, and the question arises: which is more realistic, the use of the filtered white noise description or the integrated white noise one?. Thompson [1976] reported that the filtered white noise form improves slightly the performance when compared with the integrated white noise form. However, this finding is not always true, as will be proved later. In this section, the effect of the way in which the ground is represented can be investigated by comparing systems a and b (no time delay) or by comparing d and e (time delay included). The comparison between a and b is summarised in Table 6.6 and Figs. 6.14 to 6.16 while that for d and e is summarised in Table 6.7 and Figs. 6.17 to 6.19. It can be seen from Table 6.6 that the active system b exhibits a

significant advantage over system a in conditions where the working space is most limited. The improvements achieved from system $b[1]$ at 2 cm working space appear in Figs. 6.14 to 6.16 as a reduction of the peaks related to the body and wheel resonances when compared with system $a[1]$. Moving towards the other end of the working space range, particularly at 3.5 cm there is not much difference between the two systems. Using Table 6.7, it can be seen that the above finding is also correct for system e when compared with system d . In Fig. 6.17 to 6.19, the higher peaks of the ISO weighted seat accelerations and the dynamic tyre load are for the active system d . These peaks are responsible for the high r.m.s. values in Table 6.2 (system $d[1]$). The active system e significantly reduces these peaks but with a slight increase in the peaks of the fore/aft and the lateral dynamic tyre load transfer at the wheel resonance (see Fig. 6.19). However, the dramatic reduction achieved in the lateral seat acceleration from systems b and e when compared with systems a and d respectively is not very useful here. This is because the r.m.s. values in the latter two systems are not high in the first place. Nevertheless it can be said that in other operating conditions where it will be necessary to control the roll motion, the active systems b and e will be able to do so without excessive variation in the lateral load transfer.

The next problem is to discuss the reasons behind these improvements. It has been mentioned in Chapter 4 that the only differences between the control law of the active

systems a and b in one hand and those of d and e in the other hand are the feedback gains K_o . Hence the different methods of calculating these gains are behind these improvements. In systems b and e , the calculation of these gains depends on the gains K_x and the cutoff wave number λ_o , while in systems a and d , the calculation of K_o depends only on the feedback gains K_x . Hence, introducing the cutoff wave number in finding K_o for the case in which high weighting is placed on the working space (small value of available sws) is the prime reason behind these improvements. This conclusion is confirmed as follows. The performance capabilities of systems a and b is compared as the cutoff wave number in the power spectral densities (1.1) and (4.2) is varied. In this comparison, the r.m.s values of the working space, fore/aft and the lateral dynamic load transfer are kept equal in the two systems. Therefore, it is then possible to compare these systems only in terms of the seat accelerations and the dynamic tyre loads. Figs 6.20 and 6.21 show this comparison when the working space available is most restricted i.e. $sws = 2.15$ cm at $\lambda_o = 0.01$ cycle/m, while Figs. 6.22 and 6.23 show that obtained when a large working space is assumed available i.e. $sws = 3.5$ cm at $\lambda_o = 0.01$ cycle/m. It can be seen from Figs 6.20 and 6.21, that as the value of λ_o approaches zero the gap between the systems a and b reduces and even at 0.001 cycle/m the active system a reduces slightly the longitudinal acceleration without increasing the other performance categories. It can also be seen that the seat acceleration and the dynamic tyre load of the active system a are not sensitive to the

variation of λ_o , while those of the active system b are significantly reduced as λ_o is increased. On the other hand, the selection of the weighting parameters for which the working space becomes large (see Figs. 6.22 and 6.23) reduces strongly the effect of considering λ_o in finding K_o in system b and hence the performance of this system becomes very close to system a .

The practical limitations arising from describing the road surface either as a filtered white noise or as an integrated white noise will be discussed later.

6.4.2 Effect of various types of feedback information

Barak and Sachs [1986], Malek and Hedrick [1986] and Barak and Hrovat [1988] prefer to use the feedback of the absolute displacements and velocities at the body c.g. as done here in system c rather than those at the body connection points as done for system b . Because the state variables at the c.g. position are related linearly to those at the body connection points, the performance of the active systems b and e should be identical to those of the systems c and g respectively. This fact is confirmed clearly in Tables 6.8 and 6.9. However, in practice, the measurement of these absolute displacements and velocities is possible but not easy. Wilson et al [1987] suggested a method for measuring the states at the body connection points and the wheels by using a body mounted accelerometer and relative displacement transducers between body and wheel at each corner. On the other hand, it is more expensive to use gyroscopes to measure angles θ and ψ and

their rates at the c.g. position. Hence, in general the choice of which state feedback information to use is simply a matter of practical convenience and performance of the system is not affected.

6.4.3 The effect of the working space available.

The effect of the working space available on the performance of the active systems a , b , d and e is shown in Figs 6.30 and 6.31. These results were obtained as follows. For each active suspension type, the systems of interest which consume 2.5, 3 and 3.5 cm working space are selected and then the percentage improvements in terms of the seat acceleration, dynamic tyre load and the fore/aft dynamic tyre load achieved from each system when compared with that selected for 2 cm working space is calculated. It can be seen from these figures that significant improvements in the performance of all the suspension systems can be achieved if the working space r.m.s. values are increased up to 3 cm, while from this particular operating condition (speed 30 m/s and $R_c = 3 \times 10^{-6}$), there is no further gain in increasing the working space from 3 cm to 3.5 cm. This 3.5 cm working space will be useful in other working conditions where the factor $R_c V^{1.5}$ is higher.

6.4.4 The effect of the wheelbase time delay.

Because the control law of the active systems d and e are identical to the systems a and b respectively except that in the former systems the wheelbase time delay is considered, it is possible to study the effect of including this time

delay by comparing the performance of system d with system a and that of system e with system b . These comparisons can be made by using the results generated above. For each value of the working space standard deviation, the active system of interest is selected from the active suspension a and compared with that selected from the active suspension d . Table 6.10 summarises the percentage reduction in the seat accelerations and the dynamic tyre load achieved from system d when compared with system a . However, this selection is made carefully so that for any value of the working space standard deviation the active system d reduces one or more of the performance categories without any increase in the rest. The same sequence is repeated in the comparison between the systems b and e and the percentage improvements achieved from system e are shown in Table 6.11. Furthermore, the spectral densities of the seat accelerations and the rear dynamic tyre load, fore/aft and lateral dynamic tyre load transfer for the active systems $a[1]$ and $d[1]$ are shown in Figs. 6.24 to 6.26, while those of the active systems $b[1]$ and $e[1]$ are shown in Figs. 6.27 to 6.29 (see Table 6.2 for the r.m.s. values of these systems).

It can be seen from Tables 6.10 and 6.11 that the inclusion of the wheelbase time delay in deriving the control law reduces dramatically the r.m.s. values of the seat accelerations and the rear dynamic tyre load. These improvements are achievable for any value of the working space. Furthermore, the great reductions obtained in the r.m.s values of the rear dynamic tyre load of systems d and e (40% - 50%) also result in dramatic reductions in the body resonance peaks in Figs 6.25 and 6.28

when compared with those of systems *a* and *b*, while the peaks appearing in the latter two systems at the wheel resonance completely disappear in systems *d* and *e*. With these great improvements in the rear dynamic tyre load, the active systems *d* and *e* still provide significant reductions in the peaks of the vertical and longitudinal seat accelerations (see Figs 6.24 and 6.27 respectively). Furthermore, these systems reduce the peaks of the fore/aft dynamic tyre load appearing at 2 Hz in Figs. 6.26 and 6.29 respectively but with a slight increase in the peaks at 10 Hz for the lateral dynamic tyre load transfer. However, the improvements obtained from including the time delay in deriving the control law can be redistributed so that higher improvements in the seat accelerations could be available at the expense of reducing the improvements achieved in the rear dynamic tyre load. In general, this finding also shows how the use of a preview sensor looking ahead could improve the performance. However, a preview distance equal to the wheelbase length may not be available in practice. The practical distance would be 0.6 m (e.g. for a sensor mounted on the front bumper), and hence the improvements achieved at the front wheels would probably be less than those obtained above for the rear wheels. Also, most of the available strategies are difficult to realise in practice because of the large amount of information which must be calculated on-line within a short period of time. Practical ways of introducing control laws with both types of preview (wheelbase preview and the looking ahead preview) have yet to be found.

6.4.5 Discussion of some of the practical limitations of the full state feedback active systems.

The performance of these full state feedback active systems discussed above may be achieved if (a) perfect measurements of all the state variables including those related to the road input displacements are possible, (b) it is practical to carry out all the calculations relating to the idea that the control law at any corner is a function of the state variables measured at all the four corners and (c) perfect estimations of the time delay states η in systems *d*, *e* and *g* which cannot be measured directly are available. Focussing attention on the first problem, the most practical limitation is the need to measure the body and wheel position relative to the road in systems *a* and *d* and to measure the road profile height in systems *b*, *c*, *e* and *g*. This difficulty is due to the fact that most of the possible transducers are either too expensive or do not work reliably on all the types of the road surface, e.g. the ultrasonic distance measuring transducers and the ultrasonic ranging transducers respectively. Methods for measuring the absolute displacements and velocities of the states in systems *b*, *c*, *e* and *g* were discussed in section 6.3.2.

The active systems considered above are designed so that the control force at any corner is a function of the state variables measured at all the four corners and the body c.g. Hence in order to achieve the general form of the suspension forces $u = Kx$, the force demand signals generated in the microprocessor depend on a lot of data. To indicate this

point, consider the active system b . With reference to section 4.5.1, the control force u_1 may be written in the form:

$$u_1 = h_1 x_1 + h_2 \dot{x}_2 + h_3 x_3 + h_4 x_4 + h_5 x_5 + h_6 x_6 + h_7 x_7 + h_8 x_8 + h_9 \dot{x}_1 + h_{10} \dot{x}_2 + h_{11} \dot{x}_3 + h_{12} \dot{x}_4 + h_{13} \dot{x}_5 + h_{14} \dot{x}_6 + h_{15} \dot{x}_7 + h_{16} \dot{x}_8 + h_{17} x_{o1} + h_{18} x_{o2} + h_{19} x_{o3} + h_{20} x_{o4}$$

The forces u_2 , u_3 and u_4 are of a similar form to u_1 but the feedback coefficients h_1 to h_{20} will be replaced with j_1 to j_{20} , k_1 to k_{20} and l_1 to l_{20} respectively. However, this large number of the feedback gains would require a lot of computer processing which may lead to delays in the microprocessor due to the calculations necessary. In principle, it seems unlikely that the rear wheel information is significant for front control forces. The importance of this information can be investigated by using a sub-optimal control law in which the front control forces do not depend on any of the information measured at the rear wheels. In this particular example the front control force u_1 will be:

$$u_1 = h_1 x_1 + h_2 \dot{x}_2 + h_3 x_3 + h_4 x_4 + h_9 \dot{x}_1 + h_{10} \dot{x}_2 + h_{11} \dot{x}_3 + h_{12} \dot{x}_4 + h_{17} x_{o1} + h_{18} x_{o2}$$

The question which arises now is how much performance will be lost due to using a sub-optimal control law?. To examine this point, the performance of the active systems $a[1]$, $b[1]$, $d[1]$ and $e[1]$ appearing in Table 6.2 are recalculated using the sub-optimal control forces related to each system. The new performance capabilities are compared with those presented above for the optimal case. Table 6.12 summarises the results of this comparison. In this Table, the percentage increases in the performance parameters due to employing the sub-optimal control forces are given. It can be seen from the Table that using the sub-optimal front control forces does not cause any

deterioration in performance except for an increase in the lateral seat acceleration of 18% for system *a*, 23% for system *b*, 7% for system *d* and 15% for system *e*. However, this increase is not very significant since the r.m.s values of the lateral seat acceleration are small and as mentioned above, become smaller as the working space increases.

The third problem which arises in systems *d*, *e* and *g* from introducing new states (η) that cannot be measured directly is the most complicated one. In principle, these states may be calculated on line as follows. Consider for example the active system *d*, in which

$$\dot{\eta} = A_{\eta}\eta + B_{\eta}\dot{x}_{o1}$$

which has the solution:

$$\eta_{k+1} = P_p \eta_k + Q_q \dot{x}_{o1k}$$

where $P_p = e^{A_{\eta}T}$ and $Q_q = (P_p - I)A_{\eta}^{-1}B_{\eta}$ are constant matrices for a constant vehicle speed. Having the road input information \dot{x}_{o1} known at any time (*t*), then one can use the computed value of $\eta(t)$ as the initial condition to the system and generate the solution at small, discrete steps as time progresses. It is clear that this method requires a very fast microprocessor to carry out the calculations in a short time at high vehicle speed. Furthermore, it requires an accurate knowledge of the road profile velocity. This latter requirement takes us again to the first problem. In the next Chapter, a more realisable

approach using the concept of the limited state feedback active system in which the ground input information and the desired states η can be omitted from the control law is given.

6.5 Active system adaptation.

Previous comparative results have not considered the possibility of using the active suspension system as adaptive ones. However, the active systems each provide different potential types of adaptation. A system could be adaptive to the vehicle speed or to the road quality or to both of them. For example, the control strategy used to develop the control laws for the systems *b*, *c*, *d*, *e* and *g* depends on the vehicle speed so that an optimal system for one particular speed is not optimal for other speeds and hence a part of the feedback gains should be changed as the vehicle speed changes. This means that these systems should be adaptive at least for the vehicle speed. However, they could also be adaptive for the road quality. Having the measurements of the speed and the road information available, it is a simple matter to make the active system adaptive, by selecting suitable feedback gains for each speed-ground combination from those calculated off line and stored in the microprocessor controller. The perfect selection of these gains should provide the possibility of consuming all the working space available so that further improvements in the seat accelerations and/or the dynamic tyre load could be achieved in this way.

The purpose of this section is to discuss the effect of the system adaptation on the system performance. In addition to the speed of 30 m/s considered above, results have been generated for these systems at 10 and 20 m/s. For each speed, the active system b is designed so as to consume all the available working space (2.5 cm standard deviation is assumed available). System a which does not depend on the vehicle speed is represented by two versions of the same basic system, aa and au . In system aa , the feedback gains are changed so that at any operating conditions the 2.5 cm working space will be fully consumed, while system au is assumed to be non-adaptive system so that constant set of gains is used. The results shown in Table 6.14 were obtained as follows. Firstly, system $a[4]$ in Table 6.3 is selected to represent the active system au . The performance of this system is recalculated at 10 and 20 m/s and shown in Table 6.13. Secondly, results for systems aa and b are generated at 10 and 20 m/s. For each vehicle speed, the best performing system within the 2.5 cm working space is selected and represented in Table 6.13. Table 6.14 summarises the percentage improvements achieved from these adaptive systems when compared with fixed parameter active system au . It can be seen from Table 6.14 that a significant improvement in seat accelerations can be achieved from the adaptive active systems aa and b at 10 and 20 m/s. In general, these comparisons showed that the suspension adaptation is a powerful feature behind the overall performance improvements available from active suspension systems over a typical spectrum of operating conditions.

6.6 Concluding remarks

The performance analyses of all the full state feedback active systems considered above have shown that:

1- The active systems *b* and *e* exhibited significant advantages over systems *a* and *d* respectively in conditions where the working space was most limited. This advantage appeared as a considerable reduction in the vertical and longitudinal seat accelerations (around 7% and 10% respectively for the case of 2.5 cm working space, $R_c = 3 \times 10^{-6}$ and $V = 30$ m/s) and as a dramatic reduction in the lateral seat acceleration (around 42% for 2 and 2.5 cm working space). A detailed analysis to find out the reasons which are behind these improvements was introduced and the results showed that the description of the road surface as a filtered white noise in deriving the control law of the systems *b* and *e* was responsible for these improvements. On the other hand, if the working space available is large (3.5 cm when $R_c = 3 \times 10^{-6}$ is traversed at 30 m/s), the performance of the active systems *a* and *d* was found to be close to those of systems *b* and *e* respectively.

2- The performance capabilities of the active systems *b* and *e* were found to be identical to the active systems *c* and *g* respectively. Hence the feedback of the absolute displacement and velocity of the body bounce, pitch and roll instead of those of the body connection points has no influence on the system performance. In practice, it is likely that measurement of the absolute displacements and velocities at the connection points is more attractive than the measurements based at the vehicle c.g.

3- Increasing the design value of the available working space improved all the performance categories without any increase in the lateral dynamic tyre load transfer. However, this finding is different from that obtained for the passive suspension systems where the r.m.s. values of the lateral seat acceleration and/or the dynamic tyre load transfer (according to the spring stiffness) were found to increase as the working space increased.

4- Including the wheelbase time delay in deriving the control law was found to improve dramatically the performance of the active systems. It was shown that it is possible to reduce the r.m.s. value of the rear dynamic tyre load by 45% with considerable reductions in the vertical and longitudinal accelerations (around 14% and 20% respectively for 3 cm working space). Based on these results, the possibility of using the preview looking ahead should be examined since the implications are that further improvements may be available.

5- The practical limitations of realising the control laws of these systems in practice were discussed. A practical method was suggested to overcome the problems arising from the need to collect information at the rear wheels to derive the front control forces. In this, the optimal control law was replaced with a sub-optimal one which does not depend on this information. This sub-optimal control law causes only a slight increase in the lateral seat acceleration in the case where the working space is most limited. Furthermore, the most practical problem arising in systems *d*, *e* and *g* from introducing new states which cannot be measured directly was discussed. It was shown that these states can be calculated

on-line providing road input information is available accurately and that sufficient processing power is available.

6- Results obtained at 10 and 20 m/s showed that significant improvements in the seat acceleration could be achieved from the adaptive systems b and aa when compared with the fixed parameter active system au . Furthermore, these comparisons showed that the suspension adaptation is a dominant feature behind the overall performance improvements available with controlled suspensions.

Table 6.1 Full state feedback active suspension systems studied.

| Suspension type | State vector | Control strategy |
|-----------------|--|---|
| <i>a</i> | $[x_i - x_{oj} , \dot{x}_i]^T$ $i = 1, 2, 3, \dots, 8$ $j = 1, 1, 2, 2, 3, 3, 4, 4$ | Integrated white noise case |
| <i>b</i> | $[x_i , \dot{x}_i , x_{ok}]^T$ $i = 1, 2, 3, \dots, 8$ $k = 1, 2, 3, 4$ | Filtered white noise case (states at body/suspension connection points) |
| <i>c</i> | $[z_b, \theta, \phi, x_m, \dot{z}_b, \dot{\theta}, \dot{\phi}, \dot{x}_m, x_{ok}]^T$ $k = 1, 2, 3, 4$ $m = 1, 3, 5, 7$ | Filtered white noise case (states at c.g. position) |
| <i>d</i> | $[x_i - x_{oj} , \dot{x}_i , \eta_k]^T$ $j = 1, 1, 2, 2, 3, 3, 4, 4$ $k = 1, 2, 3, 4$ | Integrated white noise case with time delay |
| <i>e</i> | $[x_i , \dot{x}_i , x_{ok} , \eta_k]^T$ $i = 1, 2, 3, \dots, 8$ $k = 1, 2, 3, 4$ | Filtered white noise case with time delay (states at body/suspension connection points) |
| <i>g</i> | $[z_b, \theta, \phi, x_m, \dot{z}_b, \dot{\theta}, \dot{\phi}, \dot{x}_m, x_{ok}, \eta_k]^T$ $m = 1, 3, 5, 7$ $k = 1, 2, 3, 4$ | Filtered white noise case with time delay (states at c.g. position) |

Table 6.2 Performance properties of the active systems a , b , d and e calculated for 2 cm r.m.s. working space.

| Suspension type | System No. | Root mean square values | | | | | | |
|-----------------|------------|-------------------------|-------------------------|-------------------------|---------------|---------------|--------|--------|
| | | \ddot{z}_x m/s^2 | \ddot{y}_x m/s^2 | \ddot{x}_x m/s^2 | $FDTL$ N | $RDTL$ N | $FDTT$ | $LDTT$ |
| a | 1 | 1.69 | 0.62 | 0.64 | 1355 | 1445 | 0.209 | 0.139 |
| | 2 | 1.59 | 0.62 | 0.59 | 1606 | 1796 | 0.224 | 0.204 |
| | 3 | 1.57 | 0.61 | 0.58 | 1630 | 1815 | 0.222 | 0.210 |
| b | 1 | 1.57 | 0.43 | 0.56 | 1277 | 1354 | 0.194 | 0.136 |
| | 2 | 1.54 | 0.40 | 0.55 | 1340 | 1410 | 0.197 | 0.151 |
| | 3 | 1.47 | 0.35 | 0.53 | 1510 | 1719 | 0.214 | 0.202 |
| d | 1 | 1.45 | 0.63 | 0.45 | 1349 | 958 | 0.165 | 0.157 |
| | 2 | 1.39 | 0.61 | 0.44 | 1588 | 1087 | 0.179 | 0.201 |
| | 3 | 1.37 | 0.61 | 0.43 | 1623 | 1193 | 0.182 | 0.214 |
| e | 1 | 1.34 | 0.38 | 0.41 | 1316 | 828 | 0.163 | 0.159 |
| | 2 | 1.27 | 0.32 | 0.37 | 1511 | 1094 | 0.175 | 0.212 |
| | 3 | 1.25 | 0.31 | 0.36 | 1572 | 1245 | 0.181 | 0.230 |

Table 6.3 Performance properties of the active systems *a*, *b*, *d* and *e* calculated for 2.5 cm r.m.s. working space.

| Suspension type | System No. | Root mean square values | | | | | | |
|--------------------|---------------|--|--|--|-------------------------|-------------------------|-------------|-------------|
| | | \ddot{z}_x <i>m/s²</i> | \ddot{y}_x <i>m/s²</i> | \ddot{x}_x <i>m/s²</i> | <i>FDTL</i> <i>N</i> | <i>RDTL</i> <i>N</i> | <i>FDTT</i> | <i>LDTT</i> |
| <i>a</i> | 1 | 1.43 | 0.45 | 0.45 | 1234 | 1280 | 0.172 | 0.142 |
| | 2 | 1.39 | 0.45 | 0.43 | 1335 | 1391 | 0.178 | 0.164 |
| | 3 | 1.32 | 0.44 | 0.42 | 1350 | 1542 | 0.188 | 0.176 |
| | 4 | 1.28 | 0.45 | 0.41 | 1471 | 1673 | 0.193 | 0.201 |
| | 5 | 1.25 | 0.46 | 0.40 | 1709 | 1890 | 0.196 | 0.247 |
| <i>b</i> | 1 | 1.38 | 0.31 | 0.42 | 1239 | 1254 | 0.169 | 0.149 |
| | 2 | 1.2 | 0.26 | 0.36 | 1439 | 1635 | 0.190 | 0.209 |
| | 3 | 1.19 | 0.25 | 0.35 | 1546 | 1715 | 0.191 | 0.229 |
| | 4 | 1.14 | 0.23 | 0.35 | 1800 | 1960 | 0.196 | 0.279 |
| <i>d</i> | 1 | 1.31 | 0.45 | 0.36 | 1231 | 668 | 0.154 | 0.145 |
| | 2 | 1.22 | 0.44 | 0.33 | 1331 | 810 | 0.164 | 0.174 |
| | 3 | 1.18 | 0.44 | 0.31 | 1462 | 929 | 0.172 | 0.200 |
| | 4 | 1.13 | 0.44 | 0.3 | 1596 | 1245 | 0.183 | 0.237 |
| | 5 | 1.13 | 0.45 | 0.3 | 1693 | 1270 | 0.185 | 0.251 |
| <i>e</i> | 1 | 1.22 | 0.3 | 0.33 | 1222 | 703 | 0.156 | 0.164 |
| | 2 | 1.11 | 0.26 | 0.28 | 1425 | 922 | 0.171 | 0.211 |
| | 3 | 1.03 | 0.25 | 0.25 | 1648 | 1278 | 0.185 | 0.261 |

Table 6.4 Performance properties of the active systems α , b , d and e calculated for 3 cm r.m.s. working space.

| Suspension type | System No. | Root mean square values | | | | | | |
|-----------------|------------|-------------------------|-------------------------|-------------------------|---------------|---------------|--------|--------|
| | | \ddot{z}_x m/s^2 | \ddot{y}_x m/s^2 | \ddot{x}_x m/s^2 | $FDTL$ N | $RDTL$ N | $FDTT$ | $LDTT$ |
| α | 1 | 1.36 | 0.39 | 0.41 | 1211 | 1249 | 0.167 | 0.143 |
| | 2 | 1.28 | 0.37 | 0.36 | 1323 | 1406 | 0.178 | 0.170 |
| | 3 | 1.15 | 0.32 | 0.34 | 1433 | 1627 | 0.189 | 0.201 |
| | 4 | 1.10 | 0.33 | 0.29 | 1574 | 1786 | 0.194 | 0.229 |
| | 5 | 1.07 | 0.33 | 0.28 | 1678 | 1887 | 0.196 | 0.249 |
| b | 1 | 1.36 | 0.31 | 0.41 | 1236 | 1252 | 0.168 | 0.151 |
| | 2 | 1.28 | 0.29 | 0.38 | 1307 | 1409 | 0.177 | 0.175 |
| | 3 | 1.15 | 0.25 | 0.31 | 1428 | 1622 | 0.188 | 0.210 |
| | 4 | 1.02 | 0.23 | 0.25 | 1698 | 1885 | 0.198 | 0.261 |
| d | 1 | 1.25 | 0.38 | 0.34 | 1209 | 580 | 0.153 | 0.148 |
| | 2 | 1.10 | 0.33 | 0.25 | 1430 | 834 | 0.172 | 0.200 |
| | 3 | 1.01 | 0.32 | 0.22 | 1672 | 1201 | 0.187 | 0.254 |
| e | 1 | 1.17 | 0.29 | 0.33 | 1238 | 675 | 0.155 | 0.171 |
| | 2 | 1.08 | 0.25 | 0.27 | 1408 | 826 | 0.167 | 0.209 |
| | 3 | 0.96 | 0.22 | 0.20 | 1668 | 1197 | 0.187 | 0.264 |

Table 6.5 Performance properties of the active systems a , b , d and e calculated for 3.5 cm r.m.s. working space.

| Suspension type | System No. | Root mean square values | | | | | | |
|-----------------|------------|-------------------------|-------------------------|-------------------------|---------------|---------------|--------|--------|
| | | \ddot{z}_x m/s^2 | \ddot{y}_x m/s^2 | \ddot{x}_x m/s^2 | $FDTL$ N | $RDTL$ N | $FDTT$ | $LDTT$ |
| a | 1 | 1.21 | 0.34 | 0.34 | 1340 | 1486 | 0.182 | 0.179 |
| | 2 | 1.14 | 0.31 | 0.30 | 1434 | 1596 | 0.188 | 0.200 |
| | 3 | 0.98 | 0.26 | 0.22 | 1754 | 1972 | 0.202 | 0.265 |
| b | 1 | 1.22 | 0.30 | 0.35 | 1345 | 1488 | 0.181 | 0.185 |
| | 2 | 1.14 | 0.26 | 0.31 | 1423 | 1616 | 0.188 | 0.208 |
| | 3 | 1.08 | 0.26 | 0.27 | 1558 | 1722 | 0.192 | 0.231 |
| d | 1 | 1.17 | 0.35 | 0.33 | 1206 | 641 | 0.154 | 0.159 |
| | 2 | 1.09 | 0.30 | 0.26 | 1416 | 771 | 0.169 | 0.198 |
| | 3 | 0.96 | 0.27 | 0.18 | 1753 | 1152 | 0.190 | 0.265 |
| e | 1 | 1.11 | 0.27 | 0.31 | 1342 | 739 | 0.161 | 0.195 |
| | 2 | 1.08 | 0.26 | 0.28 | 1416 | 769 | 0.165 | 0.208 |
| | 3 | 0.94 | 0.25 | 0.19 | 1772 | 1112 | 0.188 | 0.267 |

Table 6.6 Percentage reduction in r.m.s. values for system *b* compared with system *a*.

| <i>sws</i> cm | System No. | Percentage reduction in r.m.s. values. | | | | | | |
|------------------|-------------------|--|-------------|--------------|-------------|-------------|-------------|-------------|
| | | \ddot{z}_x | \dot{y}_x | \ddot{x}_x | <i>FDTL</i> | <i>RDTL</i> | <i>FDTT</i> | <i>LDTT</i> |
| 2.0 | $\alpha[2], b[3]$ | 7 | 43 | 10 | 6 | 4 | 4 | 1 |
| 2.5 | $\alpha[4], b[2]$ | 6 | 42 | 12 | 2 | 2 | 2 | -4 |
| 3.0 | $\alpha[3], b[3]$ | 0 | 22 | 0 | 0 | 0 | 1 | -4 |
| 3.5 | $\alpha[2], b[2]$ | 0 | 17 | -2 | 1 | -1 | 0 | -4 |

Table 6.7 Percentage reduction in r.m.s. values for system *e* compared with system *d*.

| <i>sws</i> cm | System No. | Percentage reduction in r.m.s. values. | | | | | | |
|------------------|---------------|--|-------------|--------------|-------------|-------------|-------------|-------------|
| | | \ddot{z}_x | \dot{y}_x | \ddot{x}_x | <i>FDTL</i> | <i>RDTL</i> | <i>FDTT</i> | <i>LDTT</i> |
| 2.0 | $d[2], e[2]$ | 9 | 48 | 15 | 5 | 0 | 0 | -5 |
| 2.5 | $d[3], e[2]$ | 7 | 40 | 10 | 3 | 0 | 0 | -5 |
| 3.0 | $d[2], e[2]$ | 2 | 24 | -6 | 0 | 0 | 3 | -5 |
| 3.5 | $d[2], e[2]$ | 0 | 15 | -9 | 0 | 0 | 2 | -5 |

Table 6.8 Performance properties of the active systems $b[2]$ and c calculated for 2.5 cm r.m.s. working space.

| Suspension type | Root mean square values | | | | | | |
|--------------------|-------------------------|-------------------------|-------------------------|---------------|---------------|--------|--------|
| | \ddot{z}_x m/s^2 | \ddot{y}_x m/s^2 | \ddot{x}_x m/s^2 | $FDTL$ N | $RDTL$ N | $FDTT$ | $LDTT$ |
| b | 1.2 | 0.26 | 0.36 | 1439 | 1635 | 0.19 | 0.209 |
| c | 1.2 | 0.25 | 0.36 | 1441 | 1638 | 0.19 | 0.210 |

Table 6.9 Performance properties of the active systems $e[2]$ and g calculated for 2.5 cm r.m.s. working space.

| Suspension type | Root mean square values | | | | | | |
|--------------------|-------------------------|-------------------------|-------------------------|---------------|---------------|--------|--------|
| | \ddot{z}_x m/s^2 | \ddot{y}_x m/s^2 | \ddot{x}_x m/s^2 | $FDTL$ N | $RDTL$ N | $FDTT$ | $LDTT$ |
| e | 1.11 | 0.26 | 0.28 | 1425 | 922 | 0.171 | 0.211 |
| g | 1.11 | 0.26 | 0.27 | 1423 | 927 | 0.17 | 0.210 |

Table 6.10 Percentage reduction in r.m.s. values resulting from including the time delay i.e. system d compared with system a .

| <i>sws</i> cm | System No. | Percentage reduction in r.m.s. values. | | | | | | |
|------------------|---------------|--|--------------|--------------|-------------|-------------|-------------|-------------|
| | | \ddot{z}_x | \ddot{y}_x | \ddot{x}_x | <i>FDTL</i> | <i>RDTL</i> | <i>FDTT</i> | <i>LDTT</i> |
| 2.0 | $d[2],a[2]$ | 13 | 2 | 26 | 0 | 39 | 14 | -1 |
| 2.5 | $d[2],a[2]$ | 12 | 2 | 24 | 0 | 42 | 8 | -6 |
| 3.0 | $d[1],a[1]$ | 8 | 3 | 17 | 0 | 54 | 8 | -3 |
| 3.5 | $d[2],a[2]$ | 5 | 4 | 14 | 0 | 52 | 10 | -1 |

Table 6.11 Percentage reduction in r.m.s. values resulting from including the time delay i.e. system e compared with system b .

| <i>sws</i> cm | System No. | Percentage reduction in r.m.s. values. | | | | | | |
|------------------|---------------|--|--------------|--------------|-------------|-------------|-------------|-------------|
| | | \ddot{z}_x | \ddot{y}_x | \ddot{x}_x | <i>FDTL</i> | <i>RDTL</i> | <i>FDTT</i> | <i>LDTT</i> |
| 2.0 | $e[1],b[2]$ | 13 | 7 | 25 | 0 | 41 | 17 | -5 |
| 2.5 | $e[1],b[1]$ | 12 | 4 | 22 | 0 | 44 | 8 | -9 |
| 3.0 | $e[1],b[1]$ | 14 | 5 | 20 | 0 | 46 | 8 | -12 |
| 3.5 | $e[1],b[1]$ | 10 | 11 | 12 | 0 | 50 | 11 | -5 |

Table 6.12 Effect of using sub-optimal control laws on the performance of the active systems *a*, *b*, *d*, and *e* at 2 cm r.m.s. working space.

| Suspension type | Optimality case | Root mean square values | | | | | | |
|--------------------|--------------------|--|---------------------------------------|--|-------------------------|-------------------------|-------------|-------------|
| | | \ddot{z}_x <i>m/s²</i> | \dot{y}_x <i>m/s²</i> | \ddot{x}_x <i>m/s²</i> | <i>FDTL</i> <i>N</i> | <i>RDTL</i> <i>N</i> | <i>FDTT</i> | <i>LDTT</i> |
| <i>a</i> | optimal | 1.69 | 0.62 | 0.64 | 1355 | 1445 | 0.209 | 0.139 |
| | sub-optimal | 1.71 | 0.76 | 0.62 | 1337 | 1452 | 0.207 | 0.142 |
| <i>b</i> | optimal | 1.57 | 0.43 | 0.56 | 1277 | 1354 | 0.194 | 0.136 |
| | sub-optimal | 1.60 | 0.56 | 0.55 | 1255 | 1359 | 0.192 | 0.138 |
| <i>d</i> | optimal | 1.45 | 0.63 | 0.45 | 1349 | 958 | 0.165 | 0.157 |
| | sub-optimal | 1.46 | 0.68 | 0.45 | 1348 | 973 | 0.165 | 0.162 |
| <i>e</i> | optimal | 1.34 | 0.38 | 0.41 | 1316 | 828 | 0.163 | 0.159 |
| | sub-optimal | 1.35 | 0.45 | 0.41 | 1300 | 847 | 0.162 | 0.161 |

Table 6.13 R.m.s. values of the active systems au , aa and b at 10 and 20 m/s.

| Suspension type | Speed m/s | Root mean square values | | | | | | |
|-----------------|-----------|----------------------------------|----------------------------------|----------------------------------|-----------|-----------|-------|-------|
| | | \ddot{z}_x m/s ² | \ddot{y}_x m/s ² | \ddot{x}_x m/s ² | FDTL N | RDTL N | FDTT | LDTT |
| au | 10 | 0.52 | 0.23 | 0.24 | 640 | 722 | 0.095 | 0.084 |
| | 20 | 0.91 | 0.36 | 0.36 | 1079 | 1232 | 0.166 | 0.128 |
| aa | 10 | 0.46 | 0.17 | 0.16 | 637 | 723 | 0.091 | 0.086 |
| | 20 | 0.80 | 0.26 | 0.25 | 1071 | 1218 | 0.162 | 0.132 |
| b | 10 | 0.47 | 0.15 | 0.16 | 637 | 724 | 0.090 | 0.090 |
| | 20 | 0.80 | 0.20 | 0.25 | 1078 | 1223 | 0.159 | 0.143 |

Table 6.14 Percentage reduction in the r.m.s. values for systems *aa* and *b* when compared with system *au* at 10 and 20 m/s.

| Suspension type | Speed m/s | Percentage reduction in the r.m.s. values. | | | | | | |
|--------------------|--------------|---|--------------|--------------|-------------|-------------|-------------|-------------|
| | | \ddot{z}_x | \ddot{y}_x | \ddot{x}_x | <i>FDTL</i> | <i>RDTL</i> | <i>FDTT</i> | <i>LDTT</i> |
| <i>aa</i> | 10 | 11 | 24 | 36 | 0 | 0 | 4 | -3 |
| | 20 | 12 | 29 | 32 | 0 | 0 | 2 | -3 |
| <i>b</i> | 10 | 10 | 33 | 33 | 0 | 0 | 5 | -8 |
| | 20 | 11 | 44 | 31 | 0 | 0 | 4 | -10 |

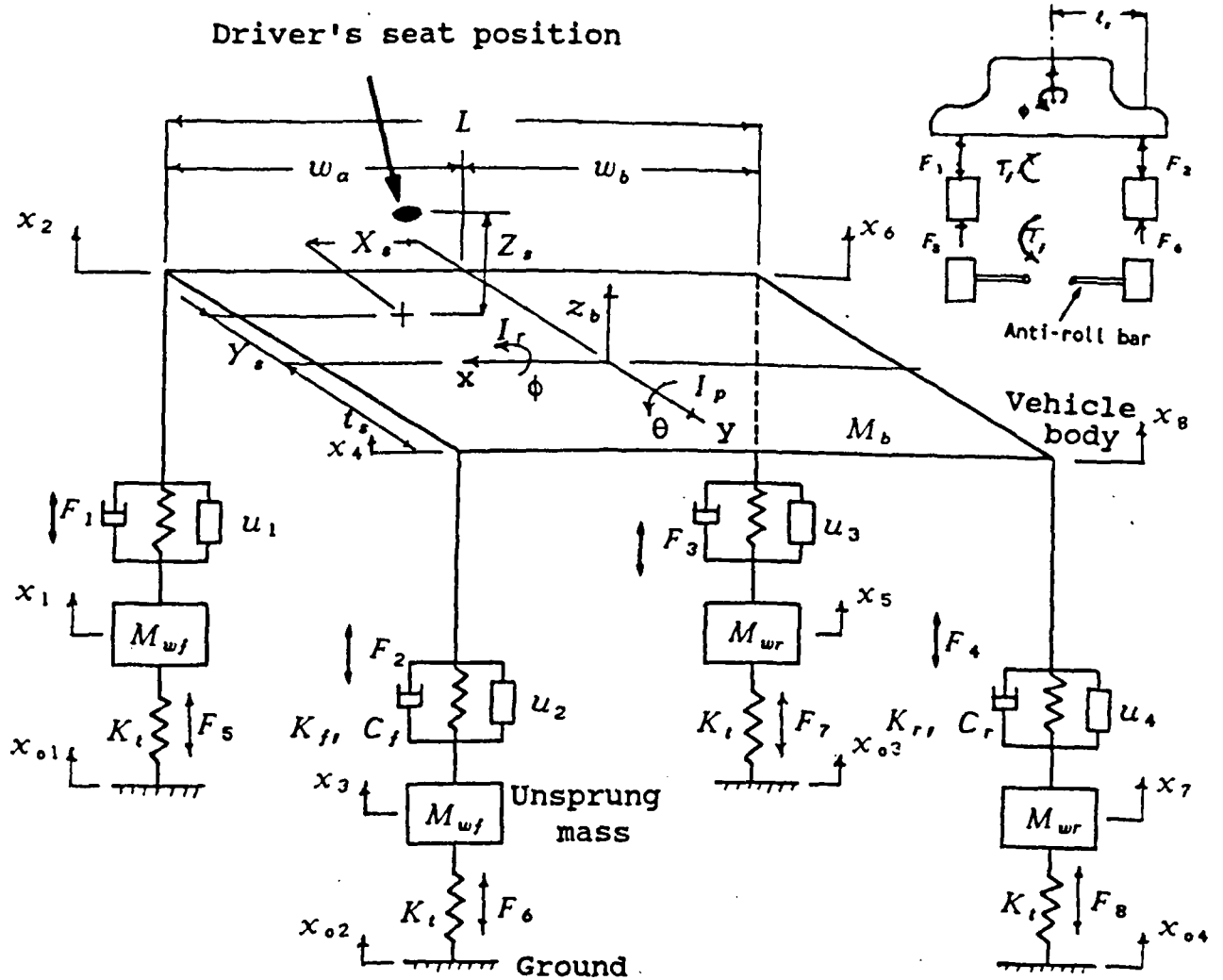


Fig 6.1 Vehicle model

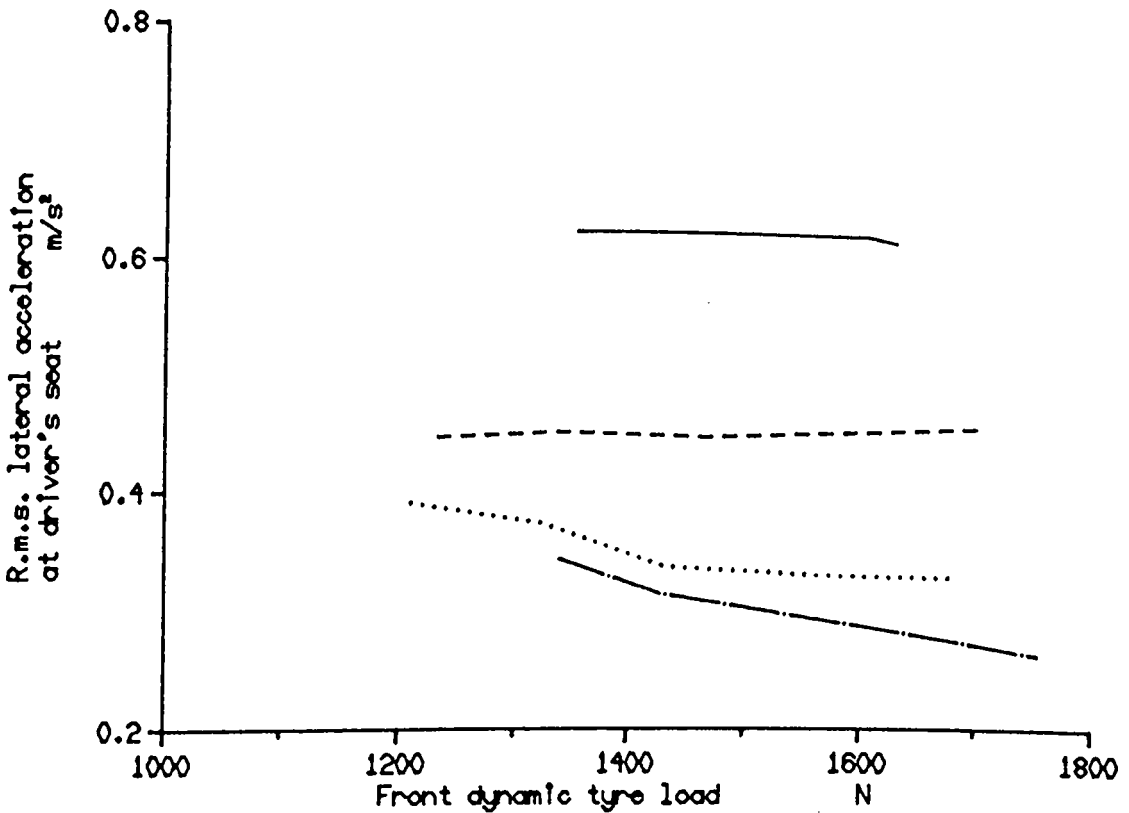
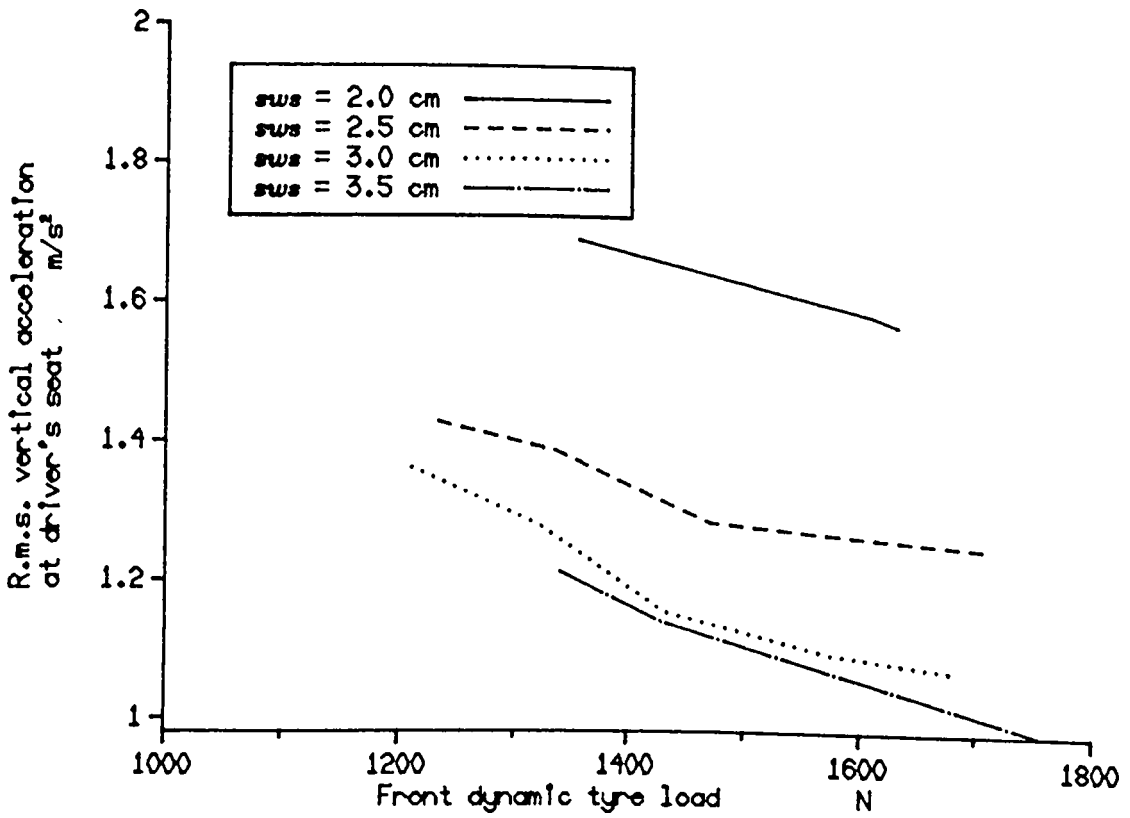


Fig. 6.2 Vertical and lateral acceleration r.m.s. results for active system a for various values of suspension working space (sws).

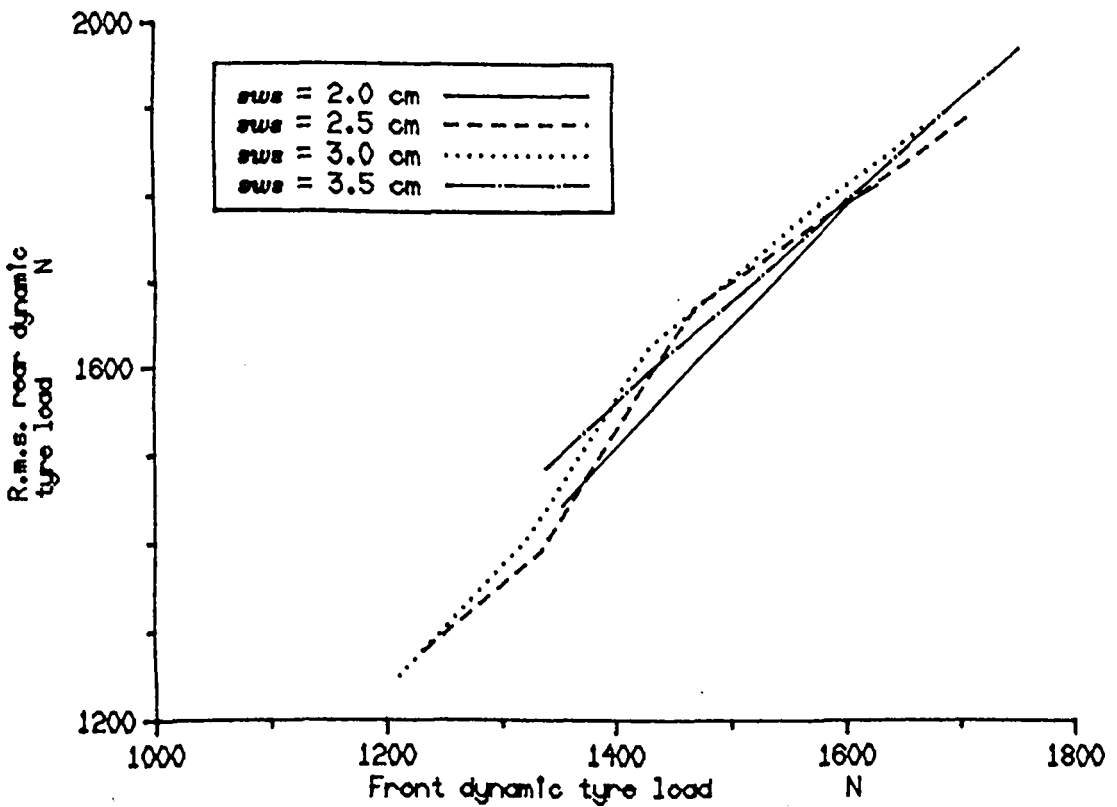
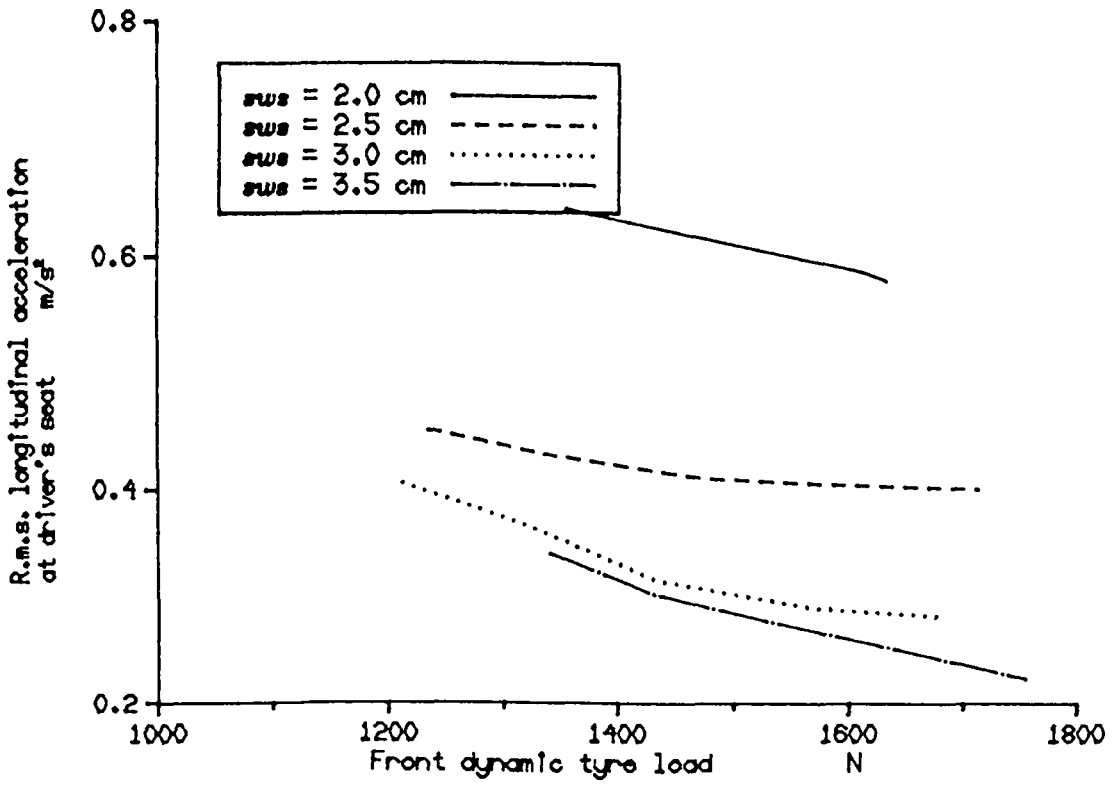


Fig. 6.3 Longitudinal acceleration and rear dynamic tyre load results for active system a for various values of suspension working space (sWS).

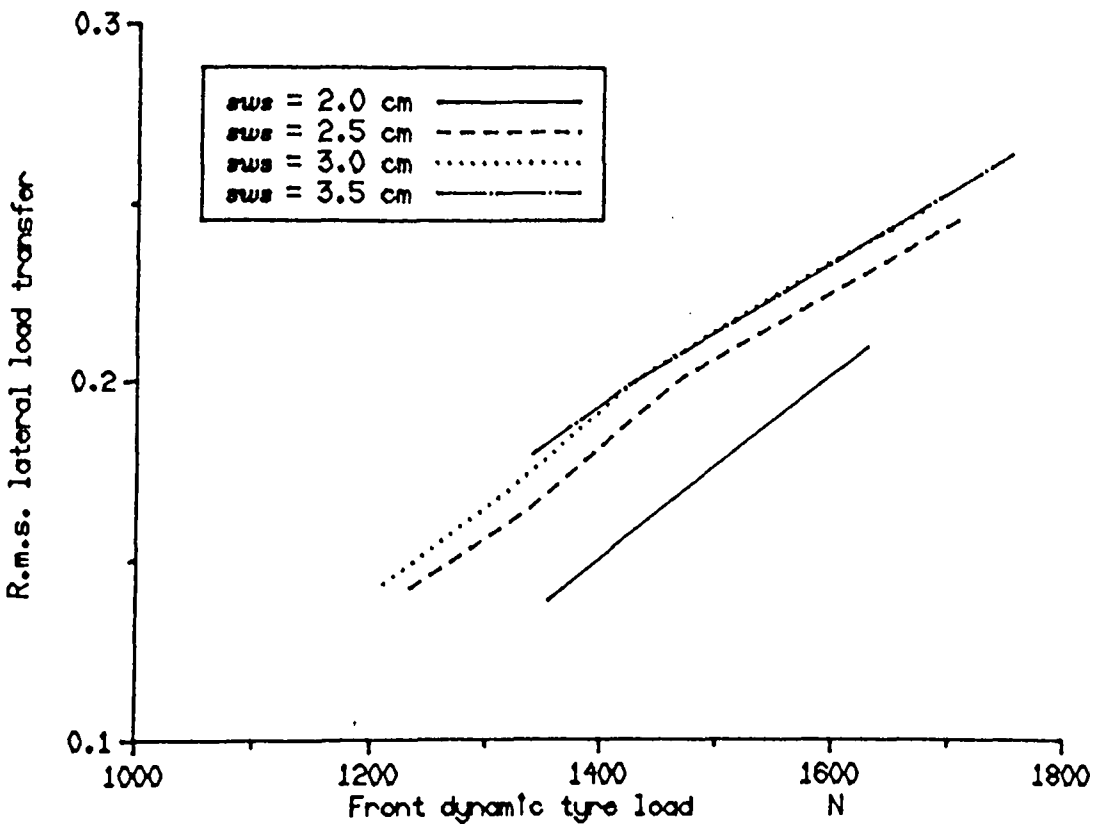
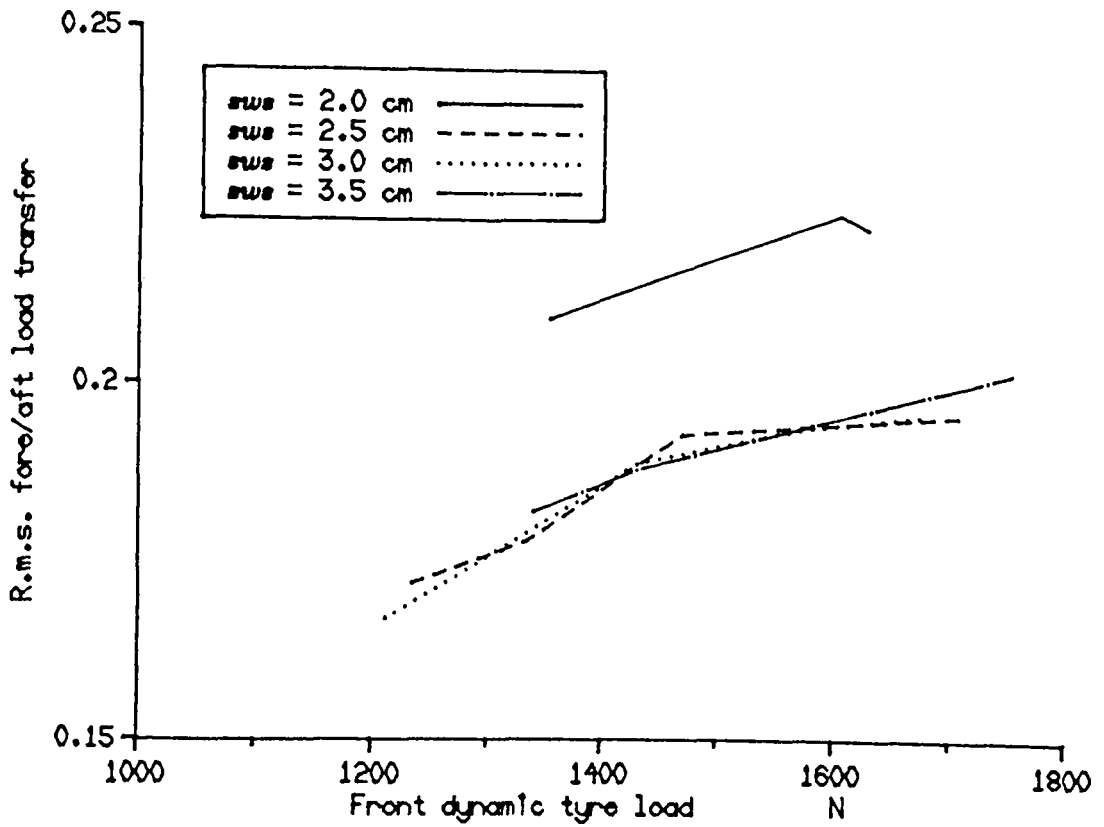


Fig. 6.4 Fore/aft and lateral dynamic tyre load transfer results for active system α for various values of suspension working space (sws).

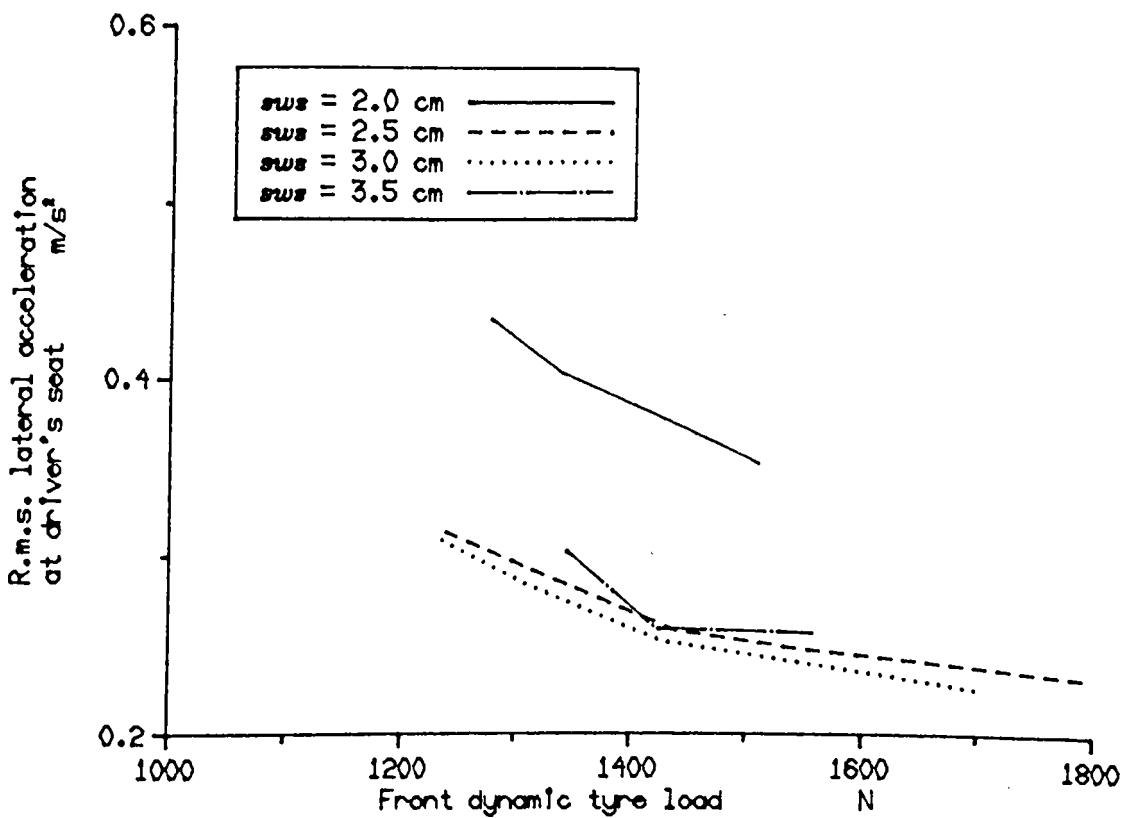
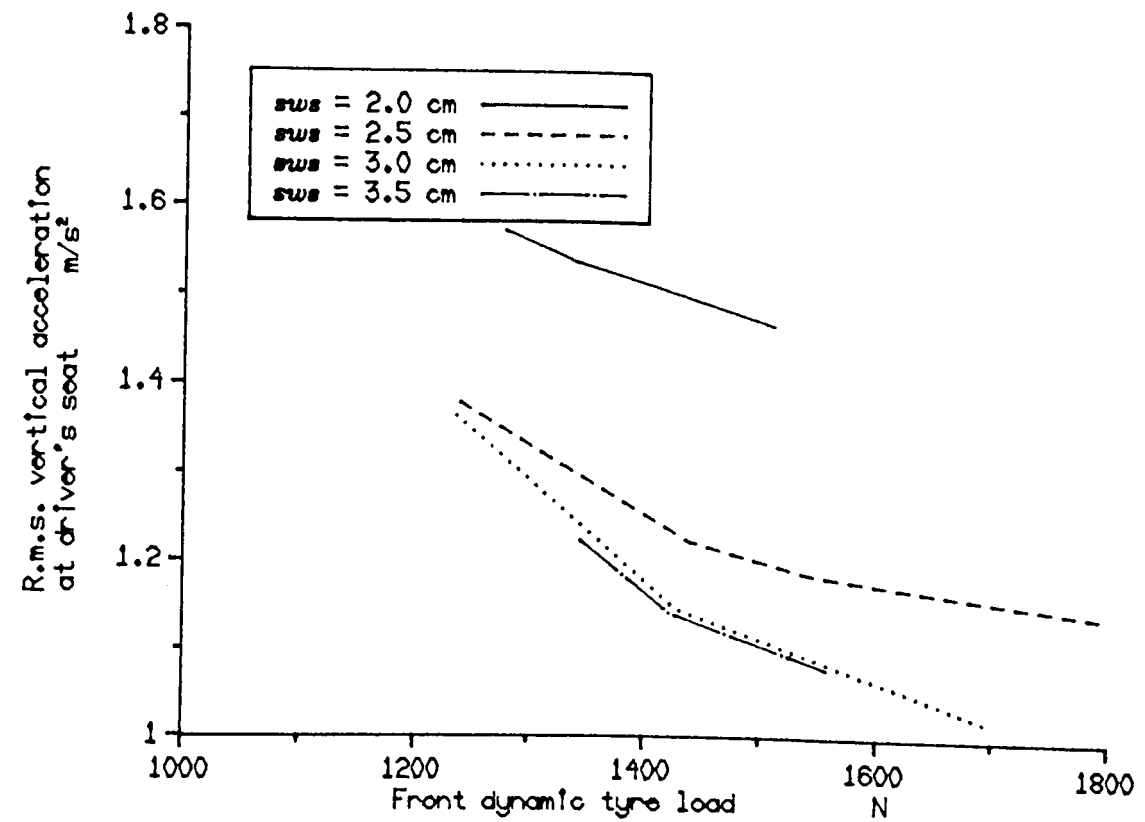


Fig. 6.5 Vertical and lateral acceleration r.m.s. results for active system b for various values of suspension working space (sWS).

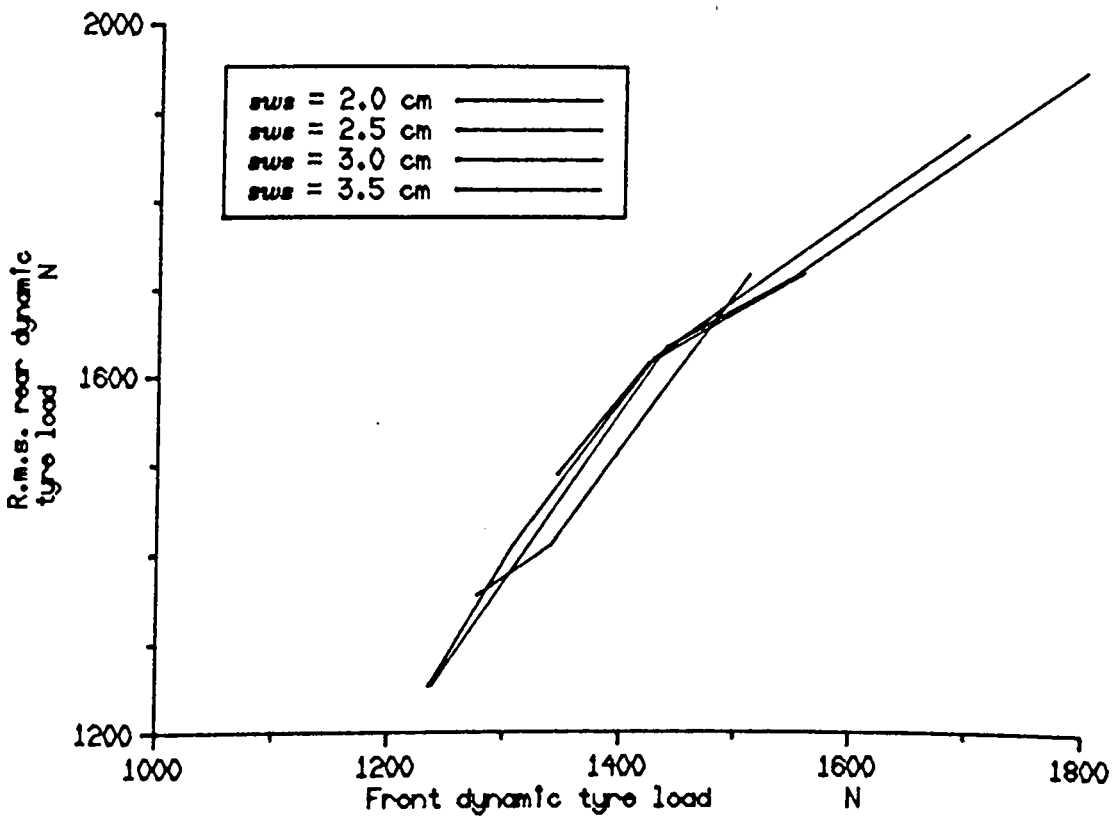
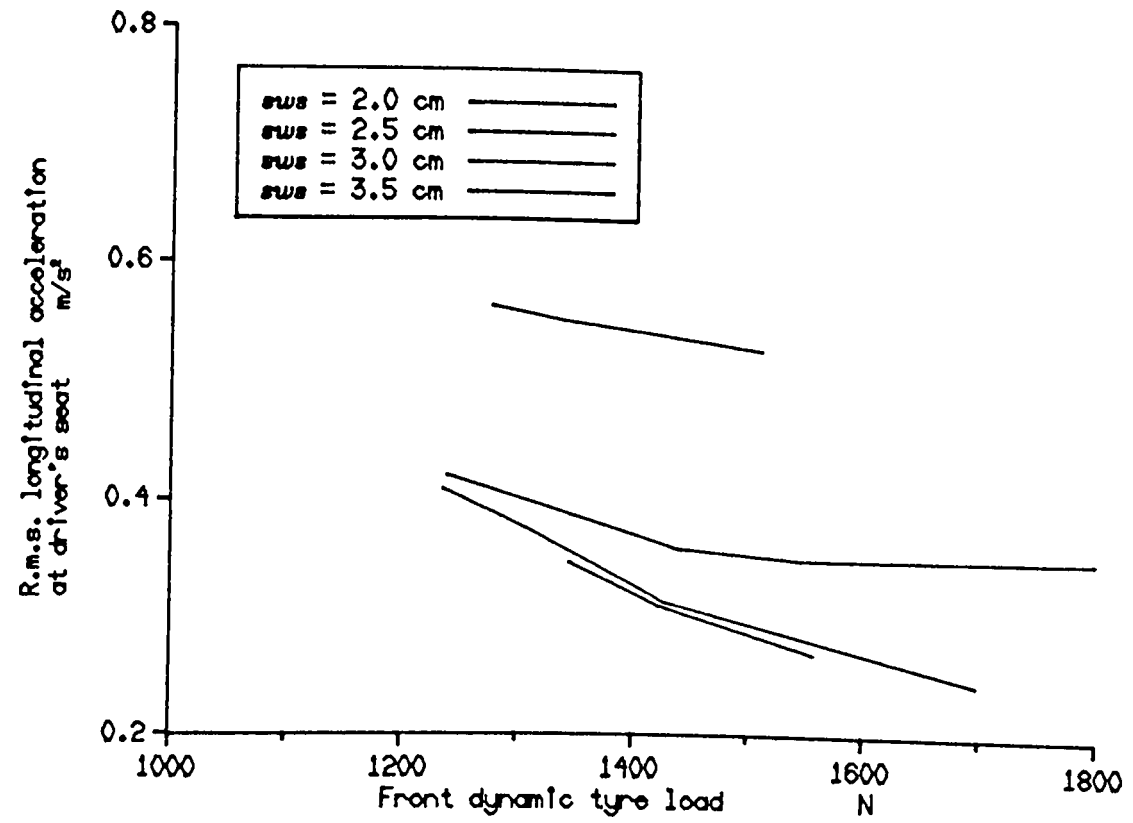


Fig. 6.6 Longitudinal acceleration and rear dynamic tyre load results for active system b for various values of suspension working space (sws).

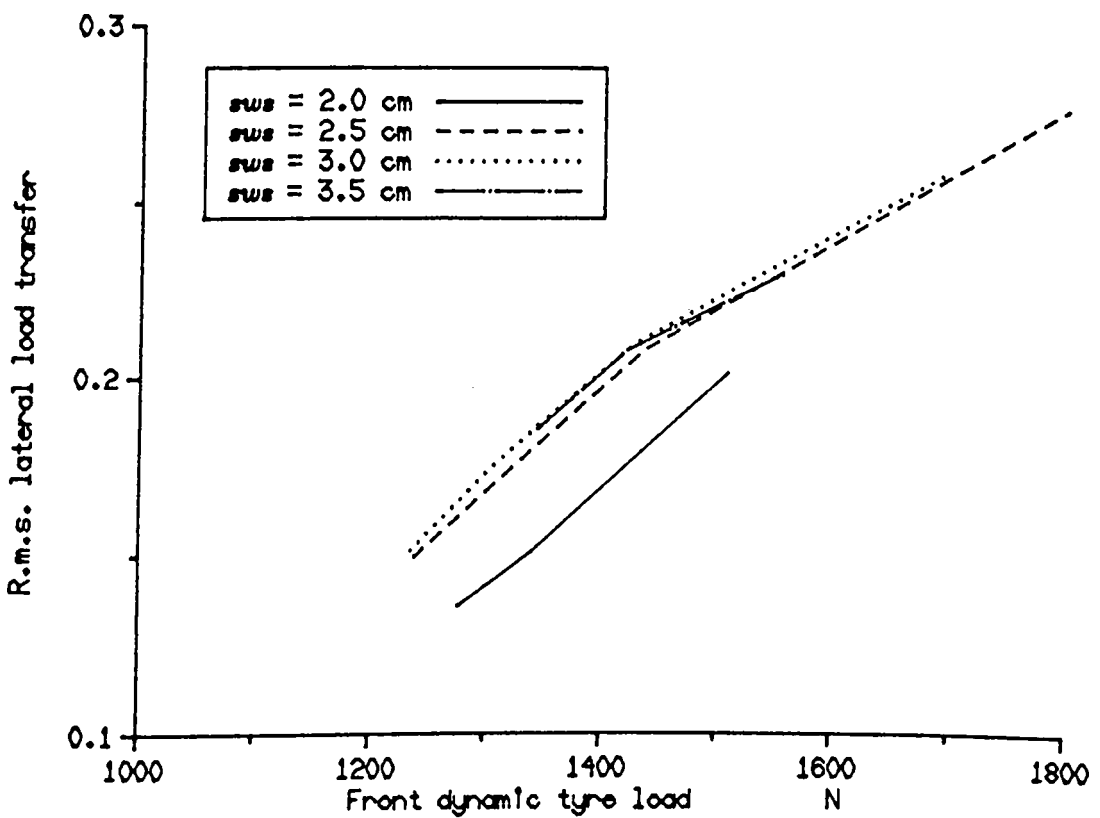
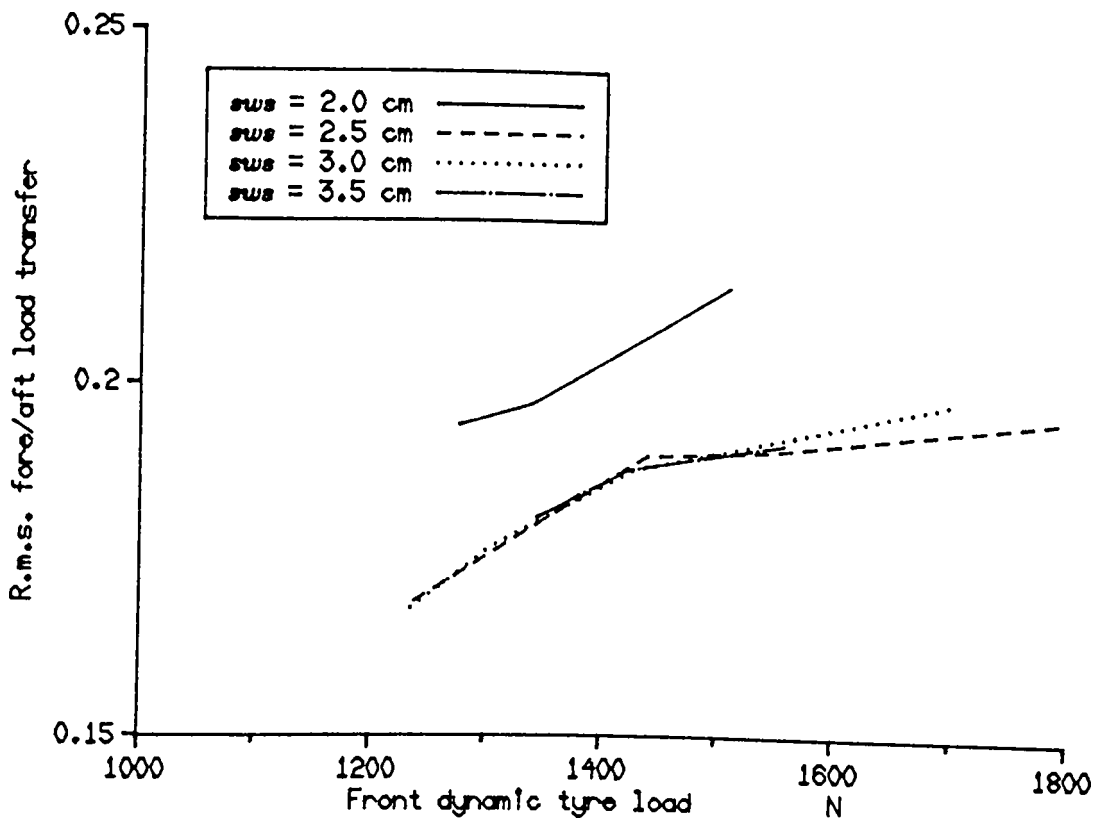


Fig. 6.7 Fore/aft and lateral dynamic tyre load transfer results for active system δ for various values of suspension working space (sws).

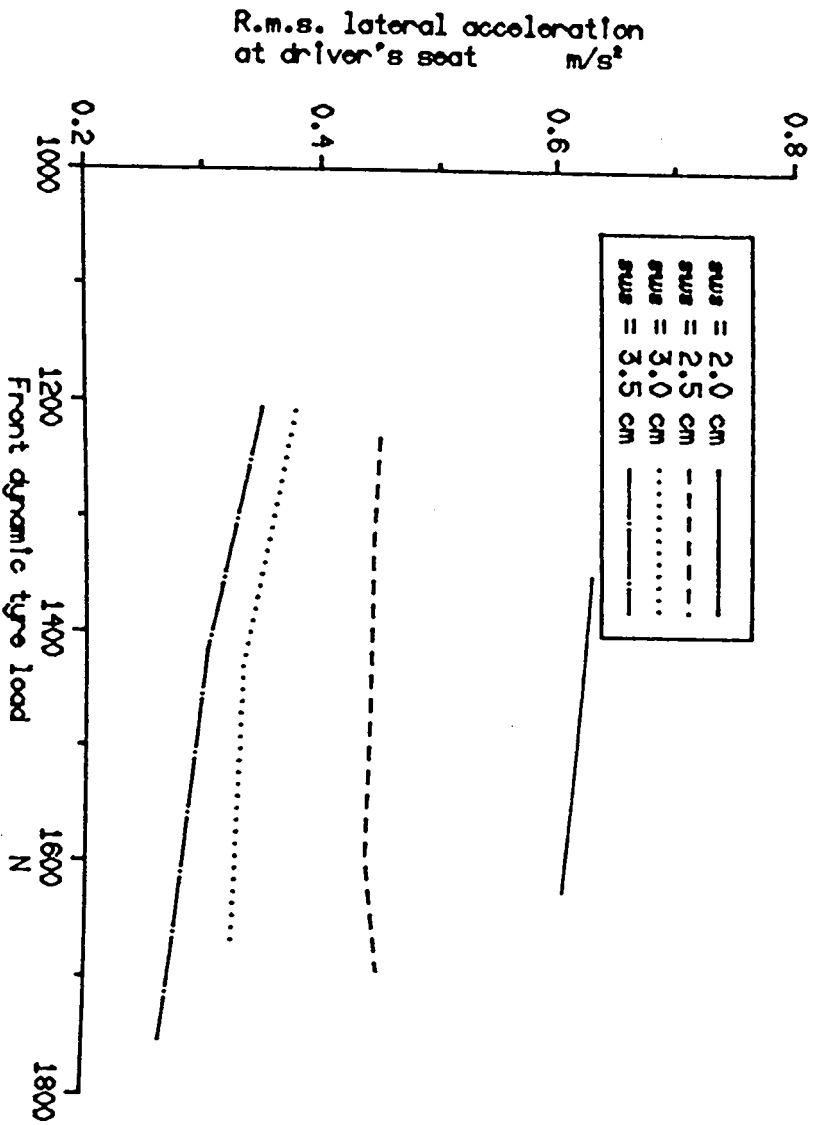
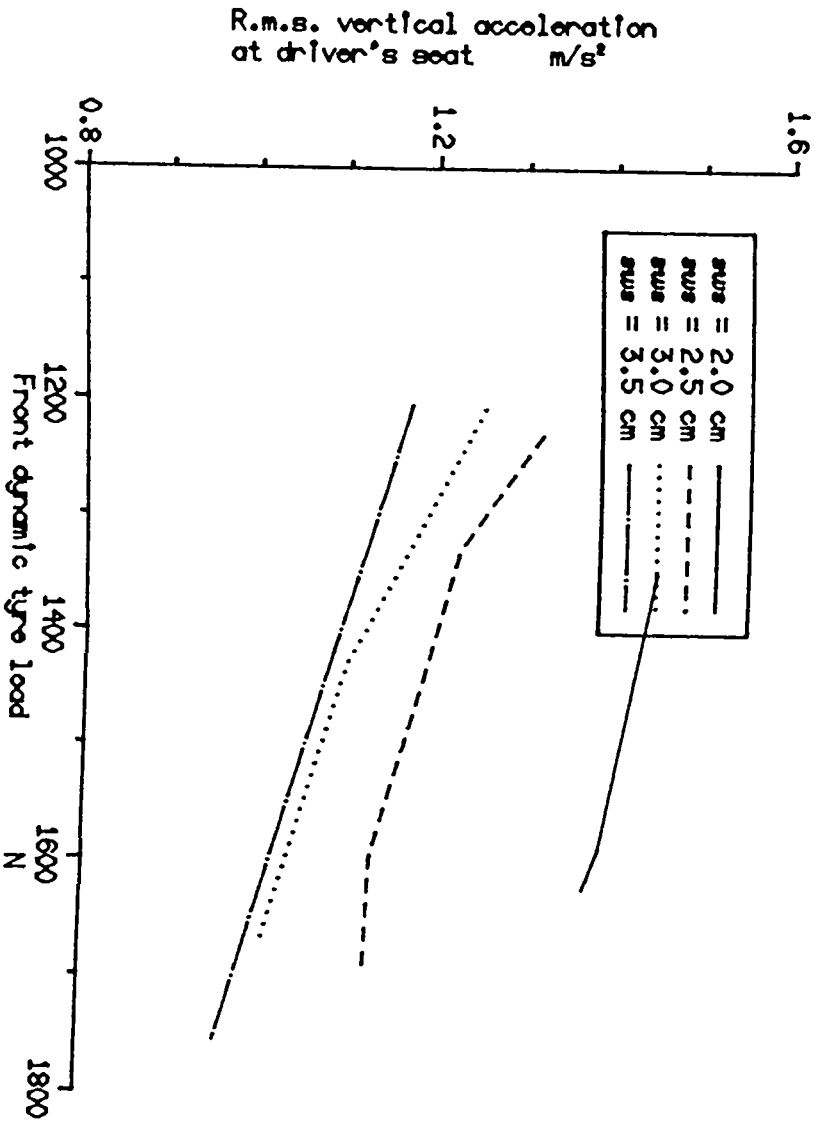


Fig. 6.8 Vertical and lateral acceleration r.m.s. results for active system & for various values of suspension working space (s.w.s.).

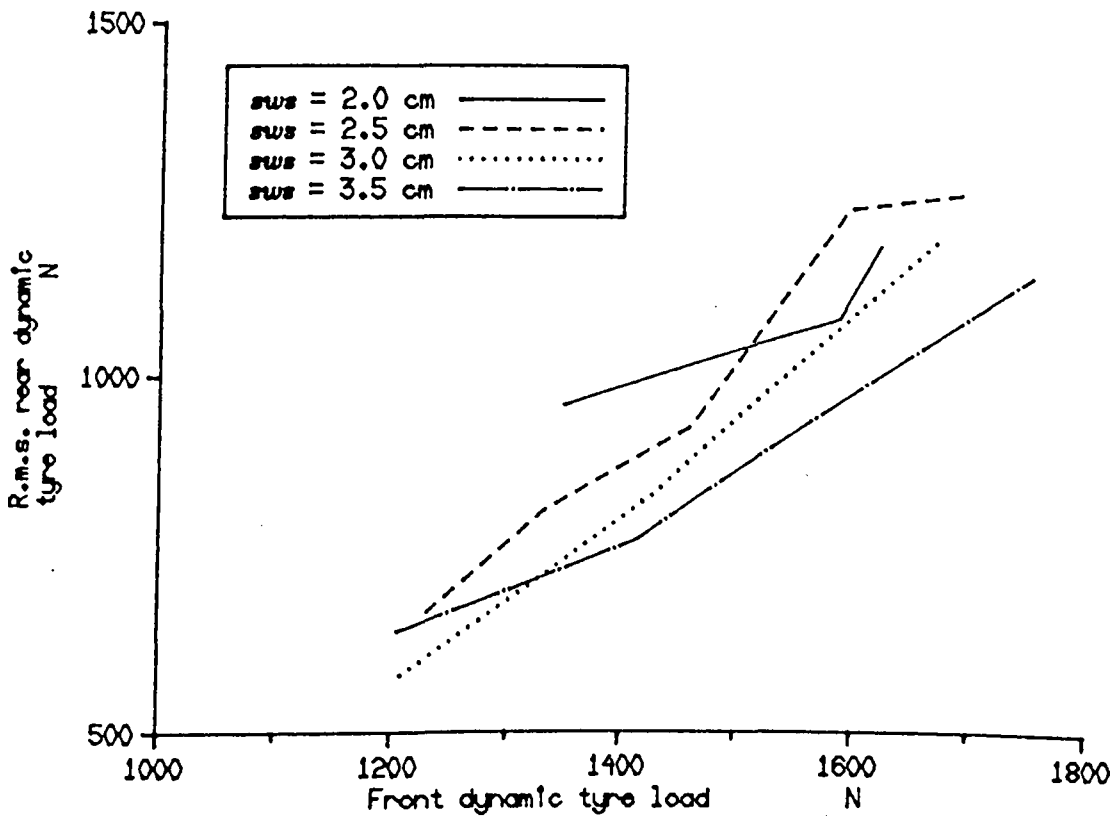
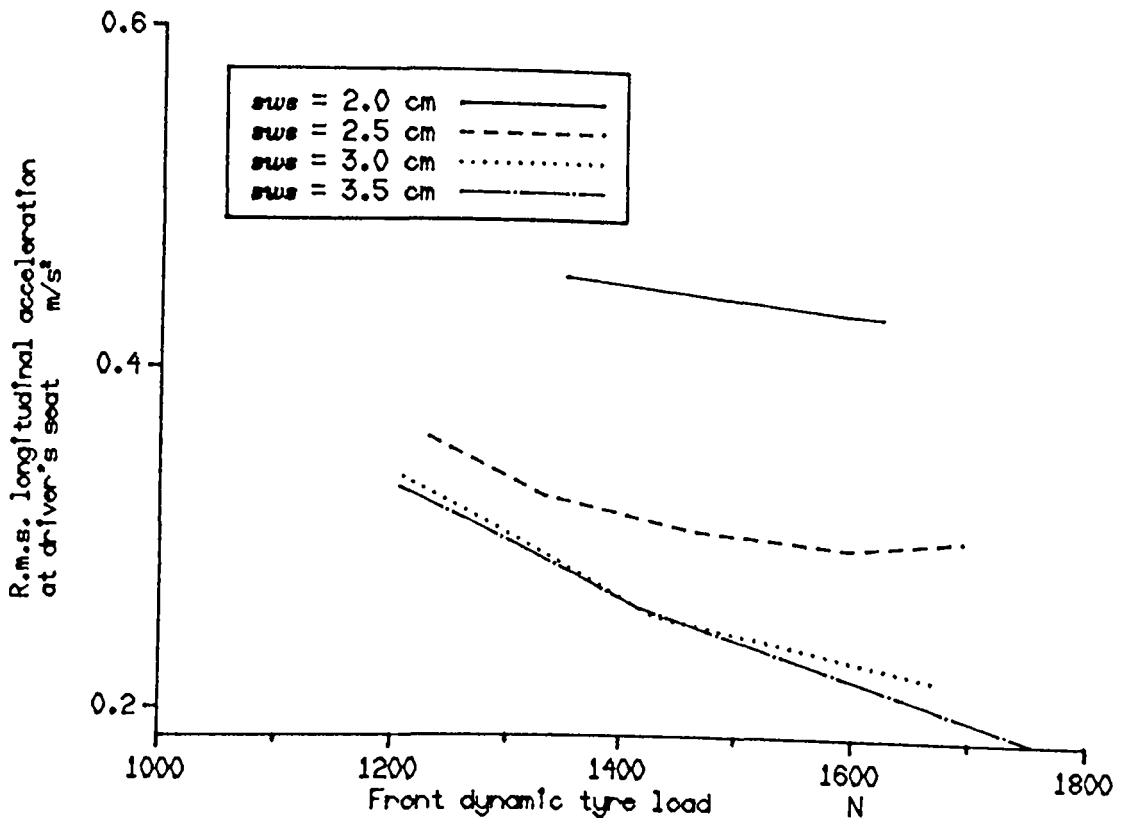


Fig. 6.9 Longitudinal acceleration and rear dynamic tyre load results for active system *d* for various values of suspension working space (*sws*).

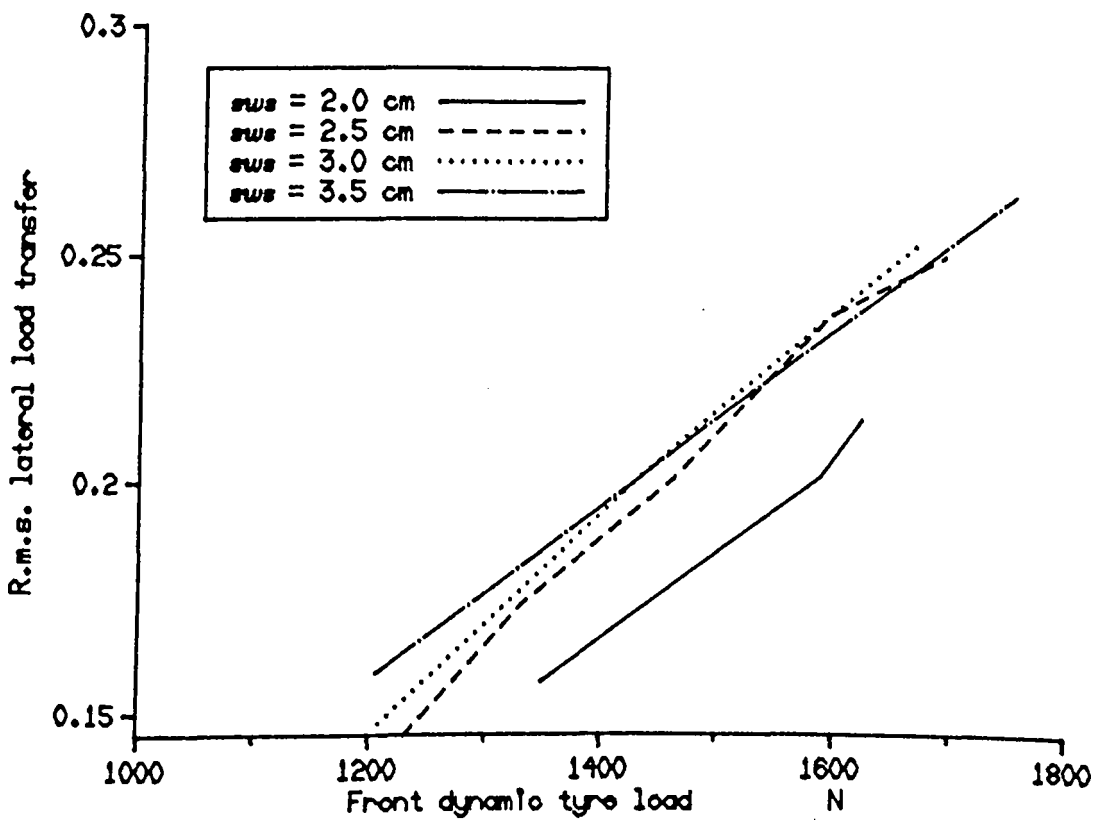
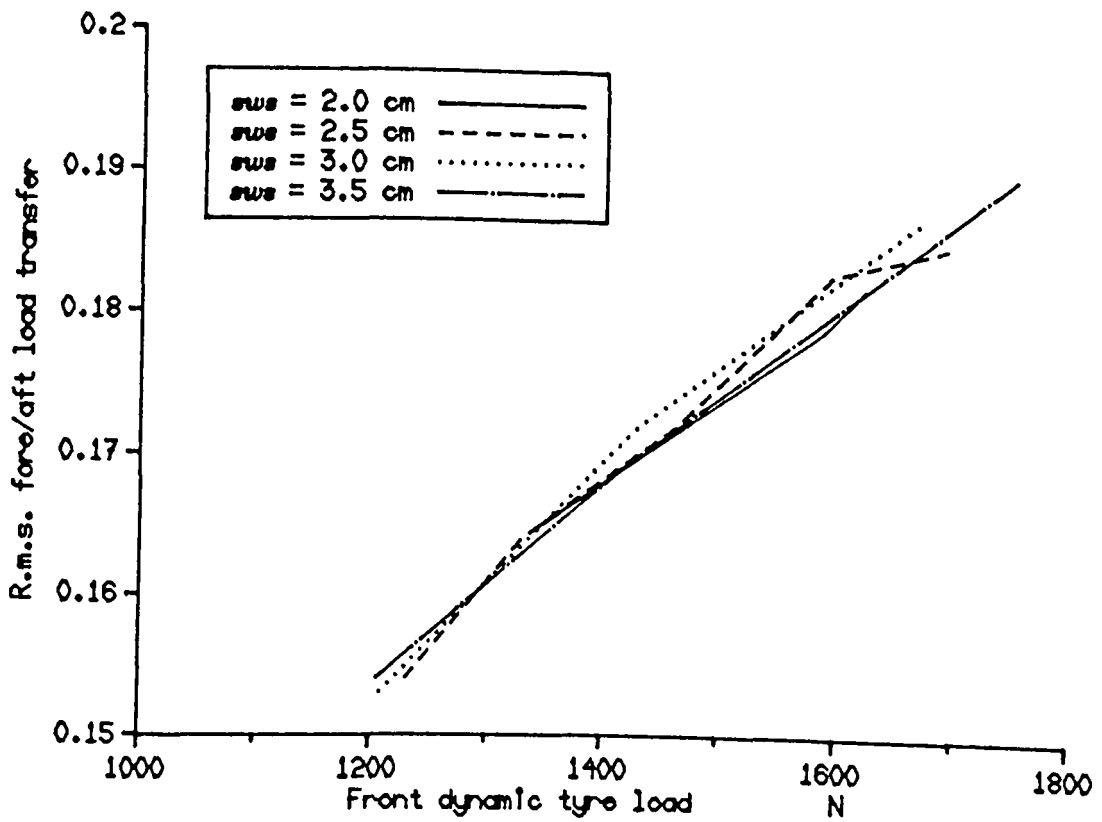


Fig. 6.10 Fore/aft and lateral dynamic tyre load transfer results for active system & for various values of suspension working space (sws).

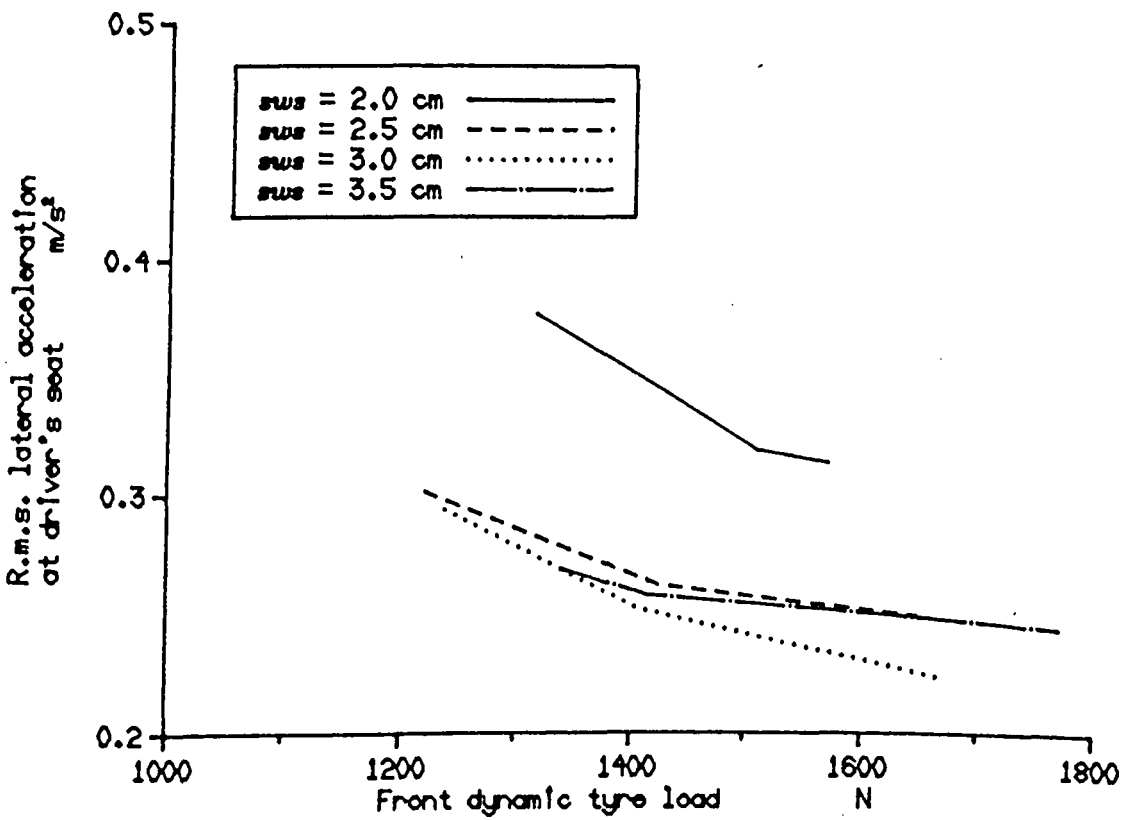
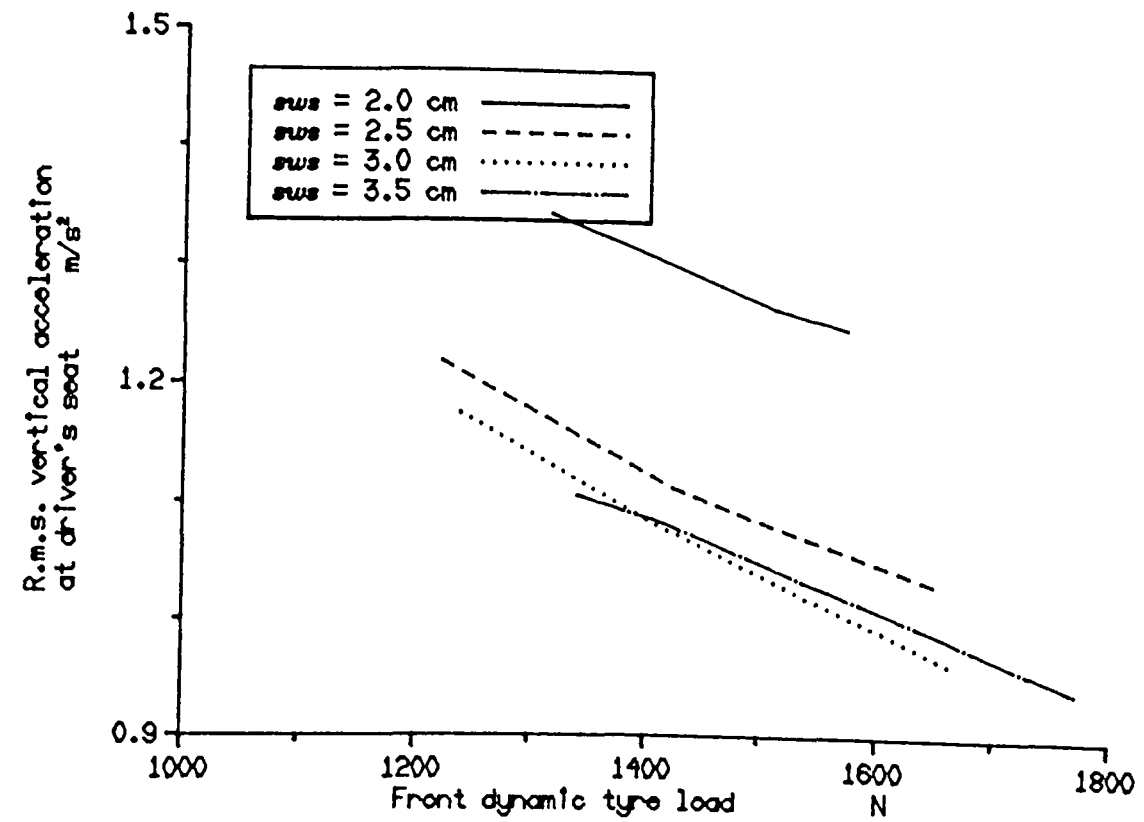


Fig. 6.11 Vertical and lateral acceleration r.m.s. results for active system for various values of suspension working space (sWS).

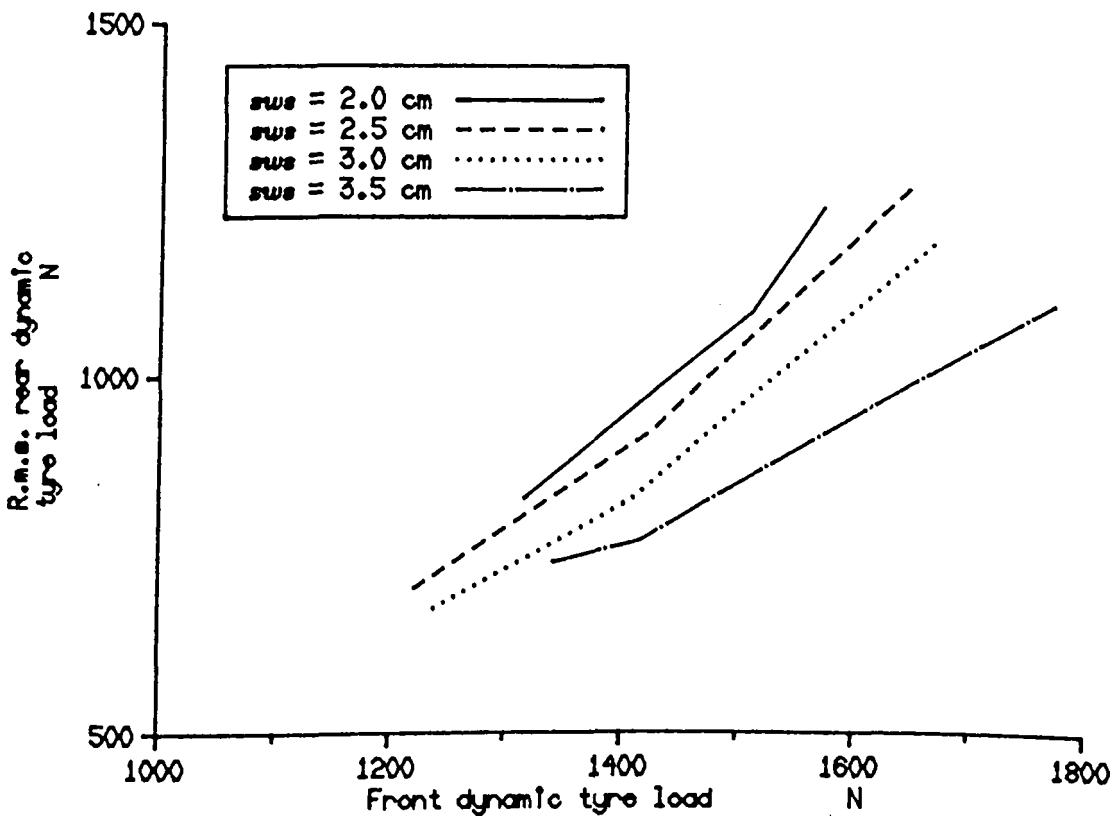
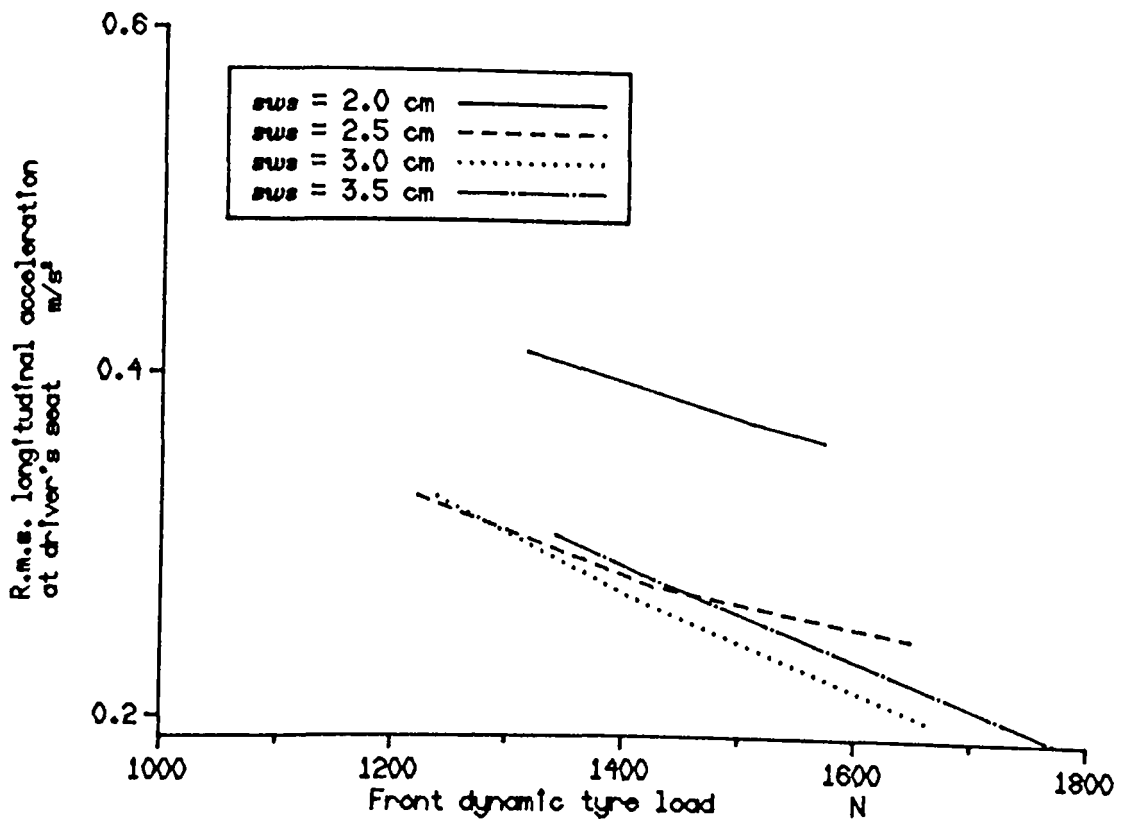


Fig. 6.12 Longitudinal acceleration and rear dynamic tyre load results for active system for various values of suspension working space (sws).

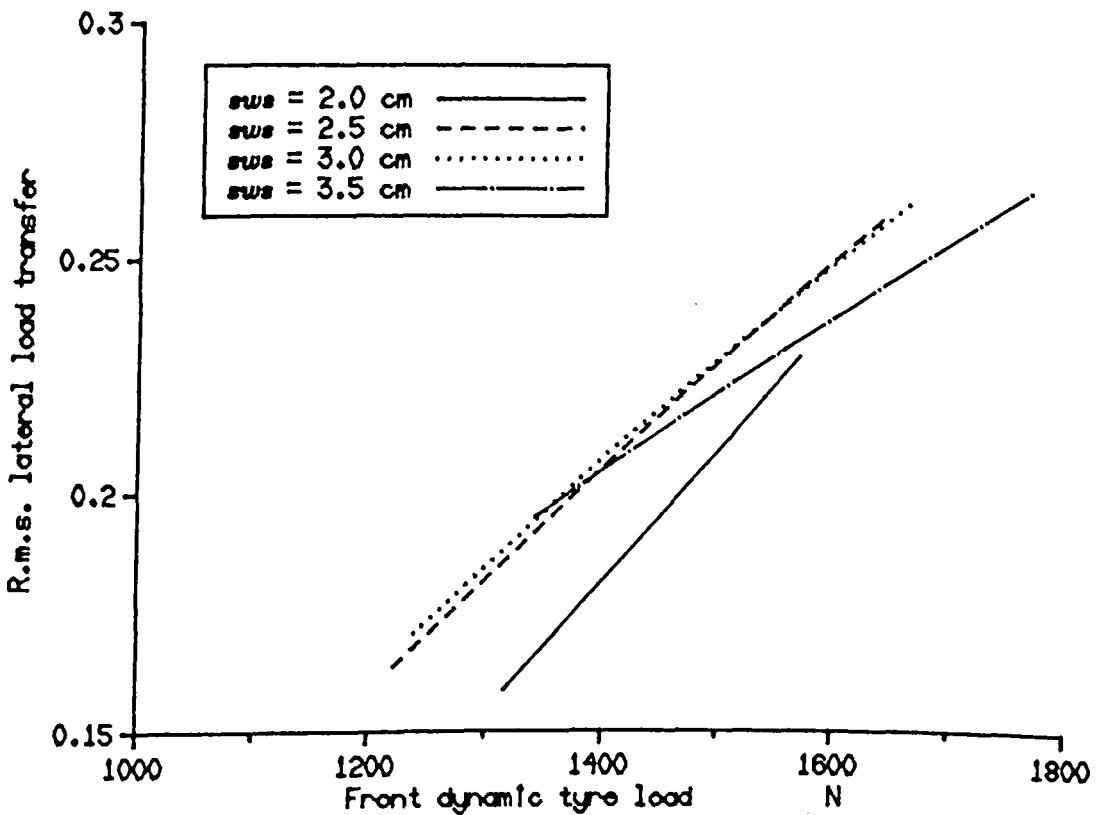
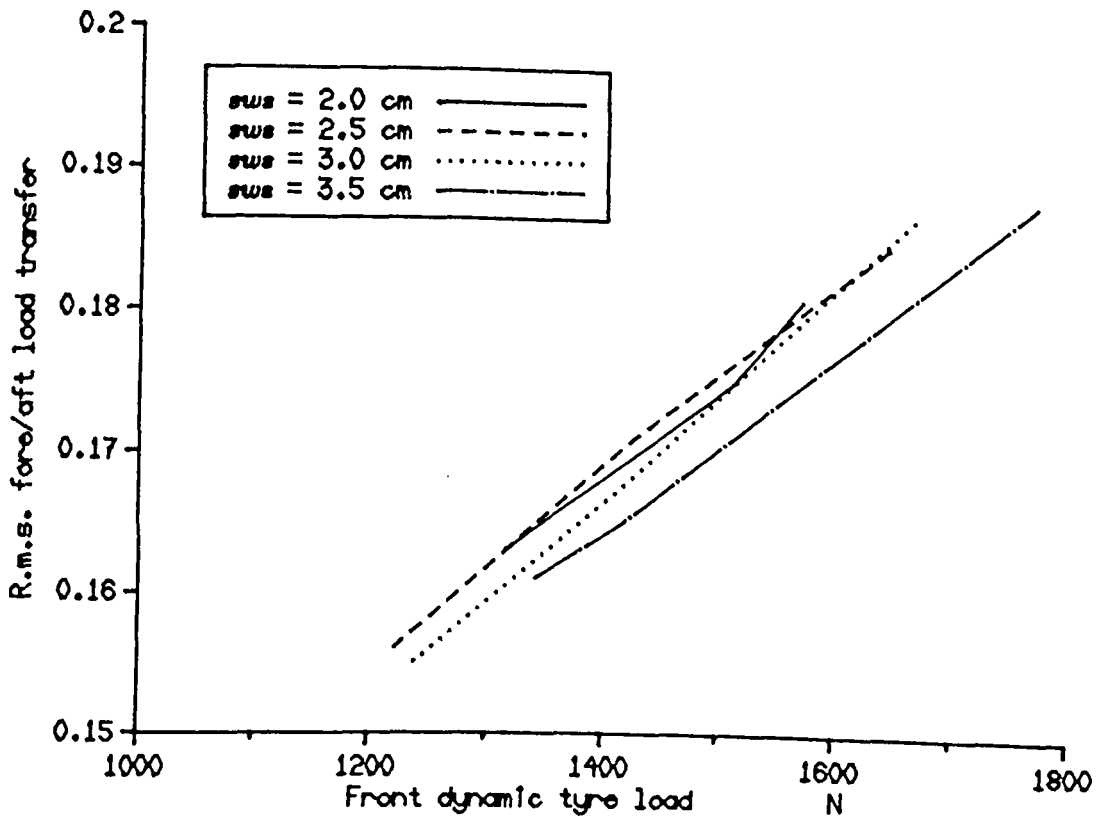


Fig. 6.13 Fore/aft and lateral dynamic tyre load transfer results for active system ϵ for various values of suspension working space (sws).

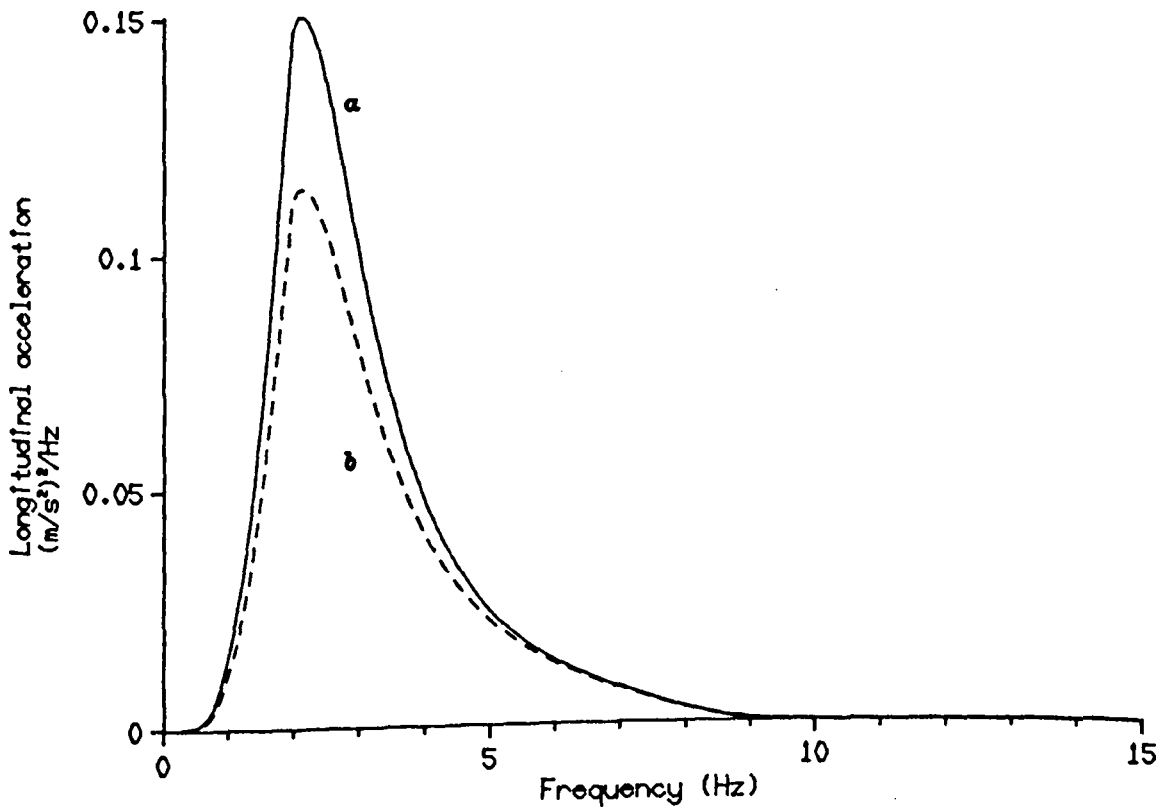
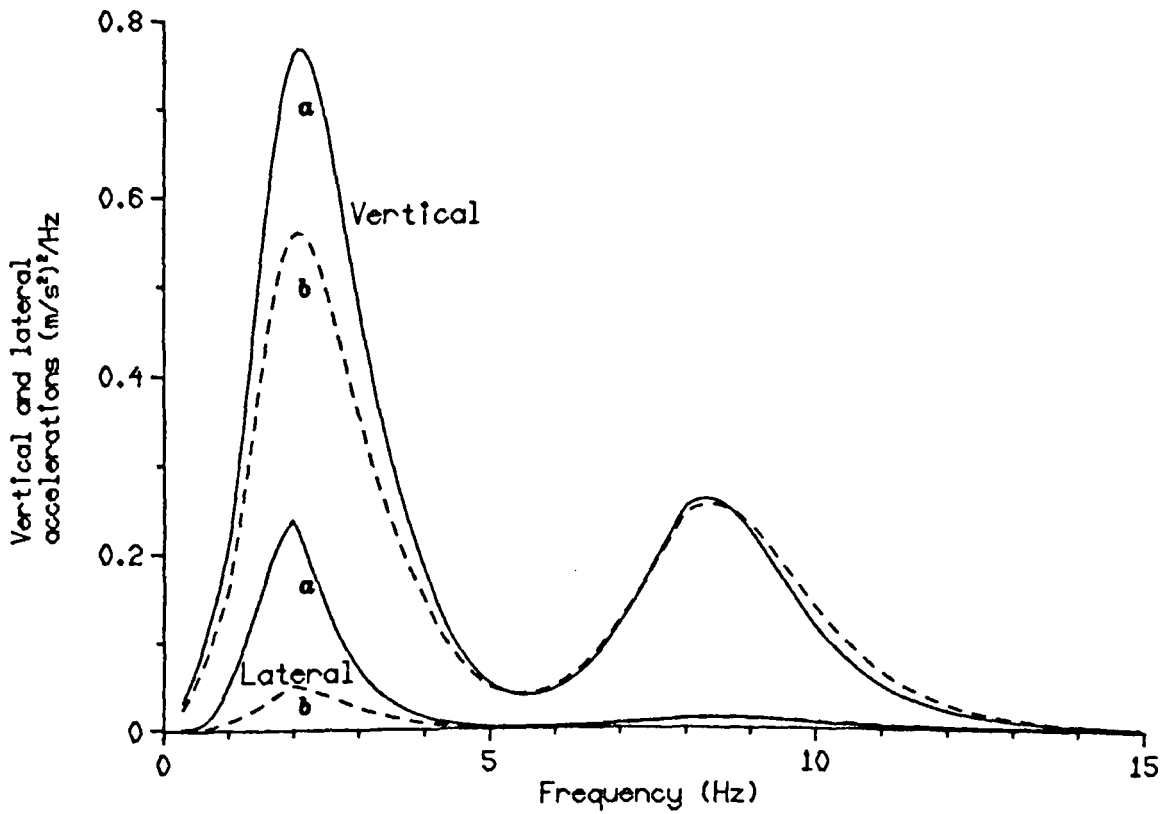


Fig. 6.14 Spectral densities of the I.S.O. weighted seat accelerations for active systems a [1] and b [1] for a suspension working space of 2 cm.

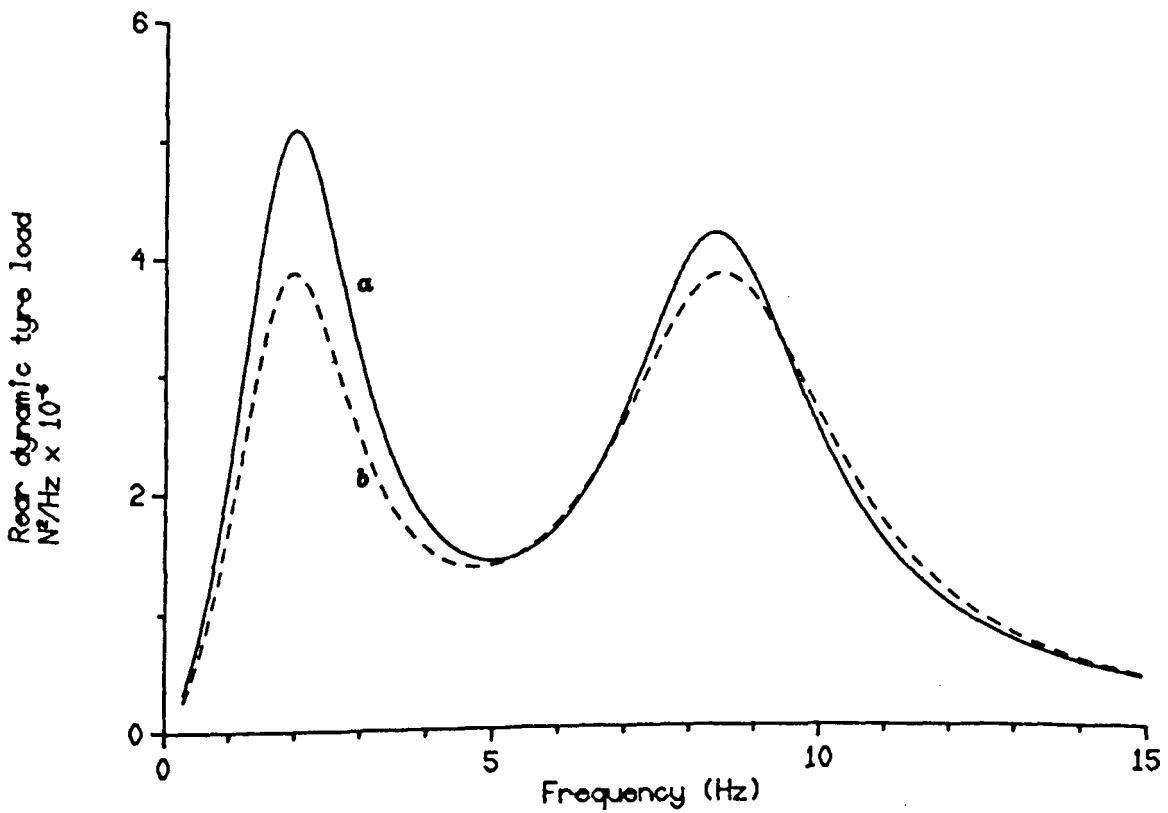
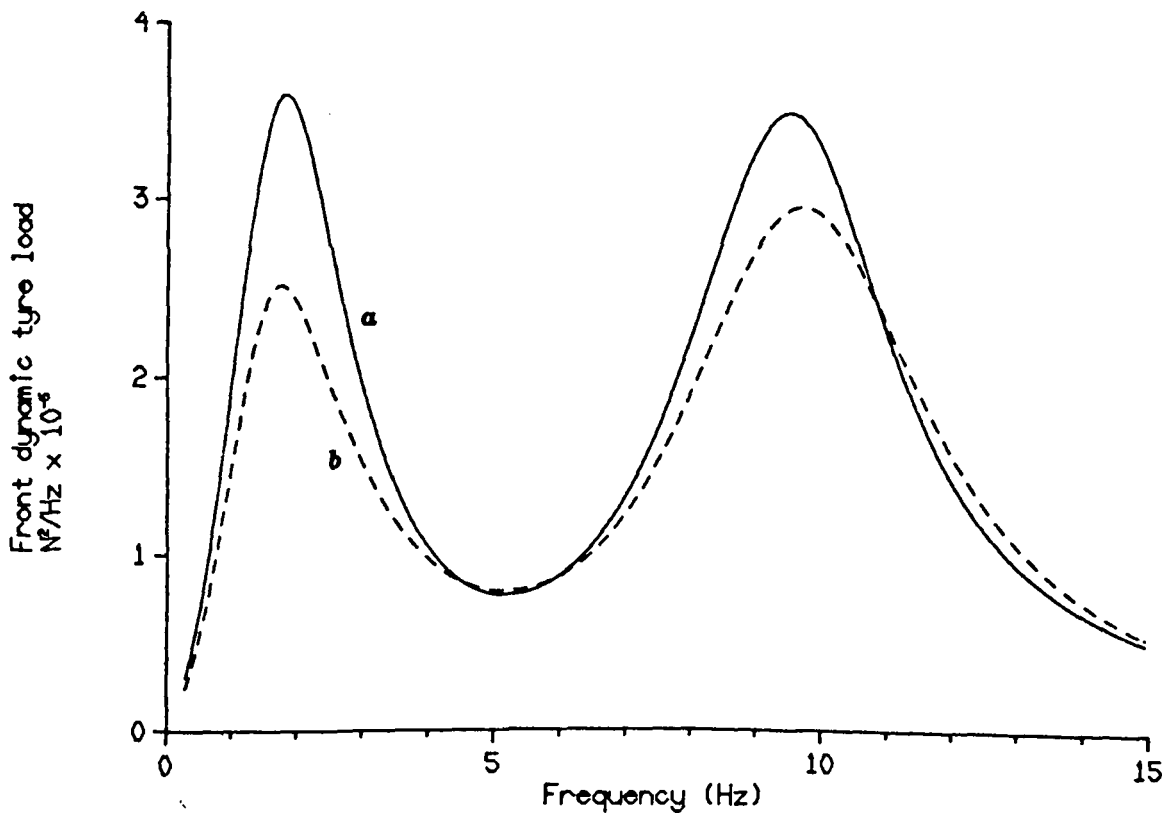


Fig. 6.15 Spectral densities of the front and rear dynamic tyre load for active systems a [1] and b [1] for a suspension working space of 2 cm.

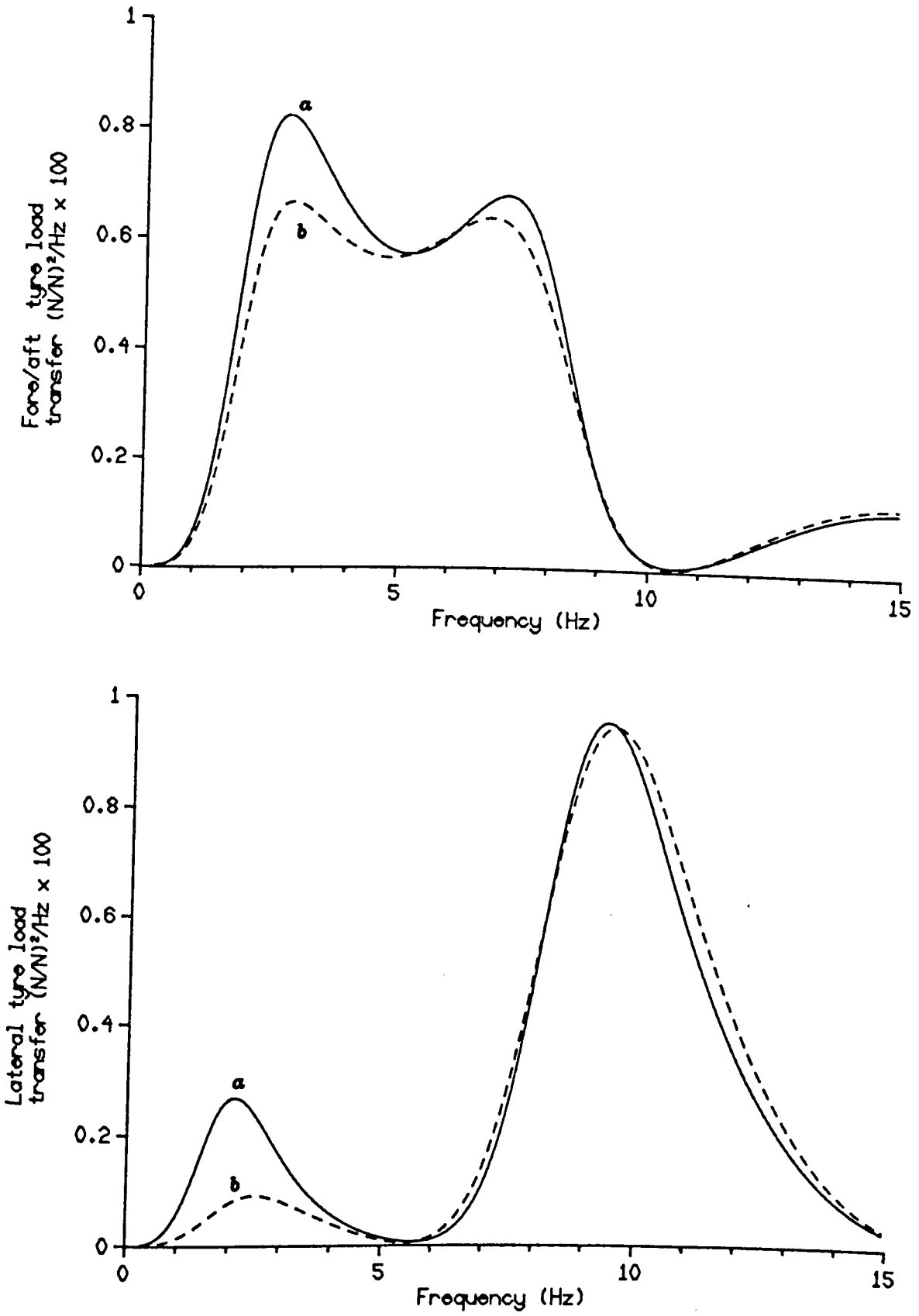


Fig. 6.16 Spectral densities of the fore/aft and lateral dynamic tyre load transfer for active systems a [1] and b [1] for a suspension working space of 2 cm.

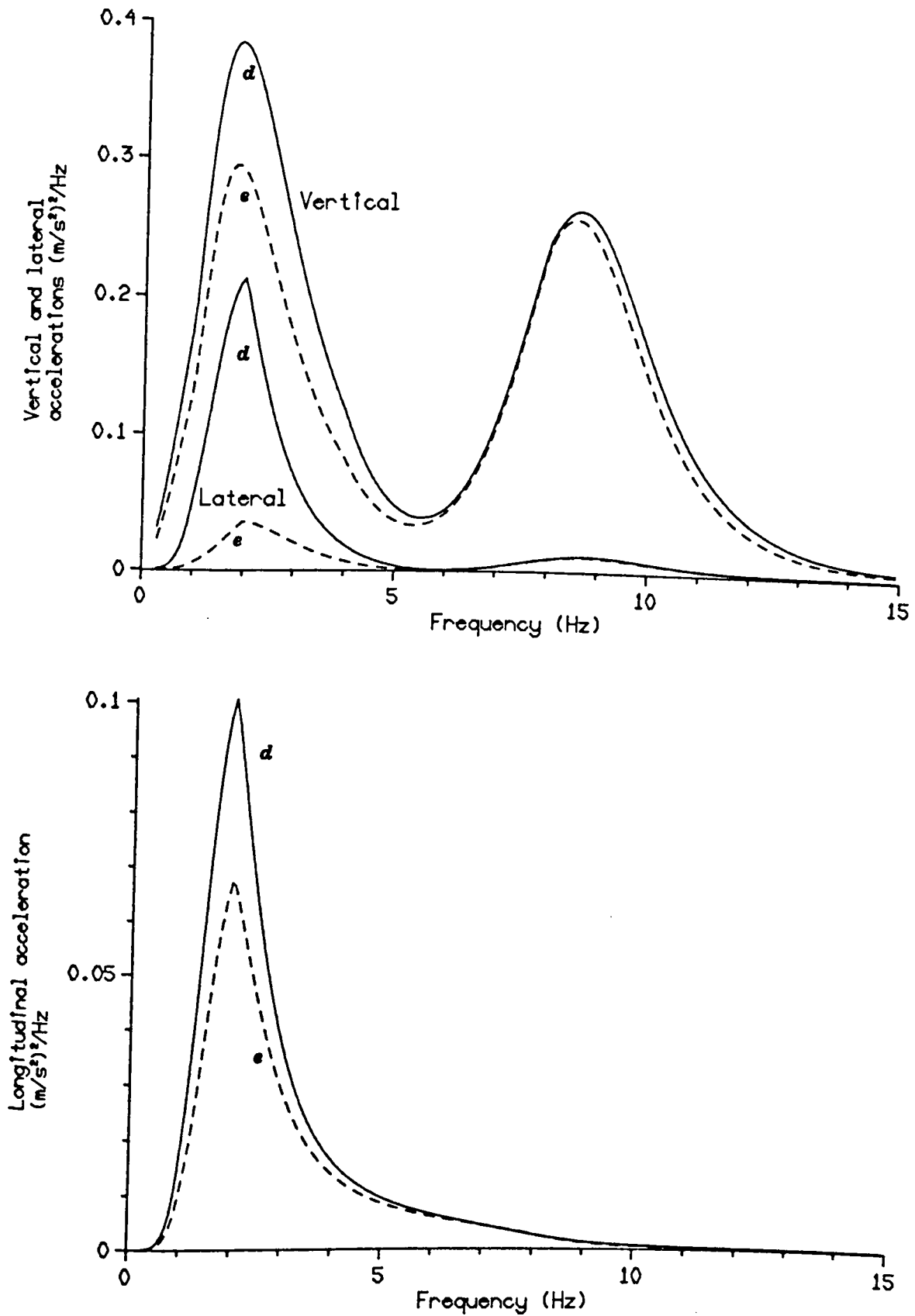


Fig. 6.17 Spectral densities of the I.S.O. weighted seat accelerations for active systems *d* [1] and *e* [1] for a suspension working space of 2 cm.

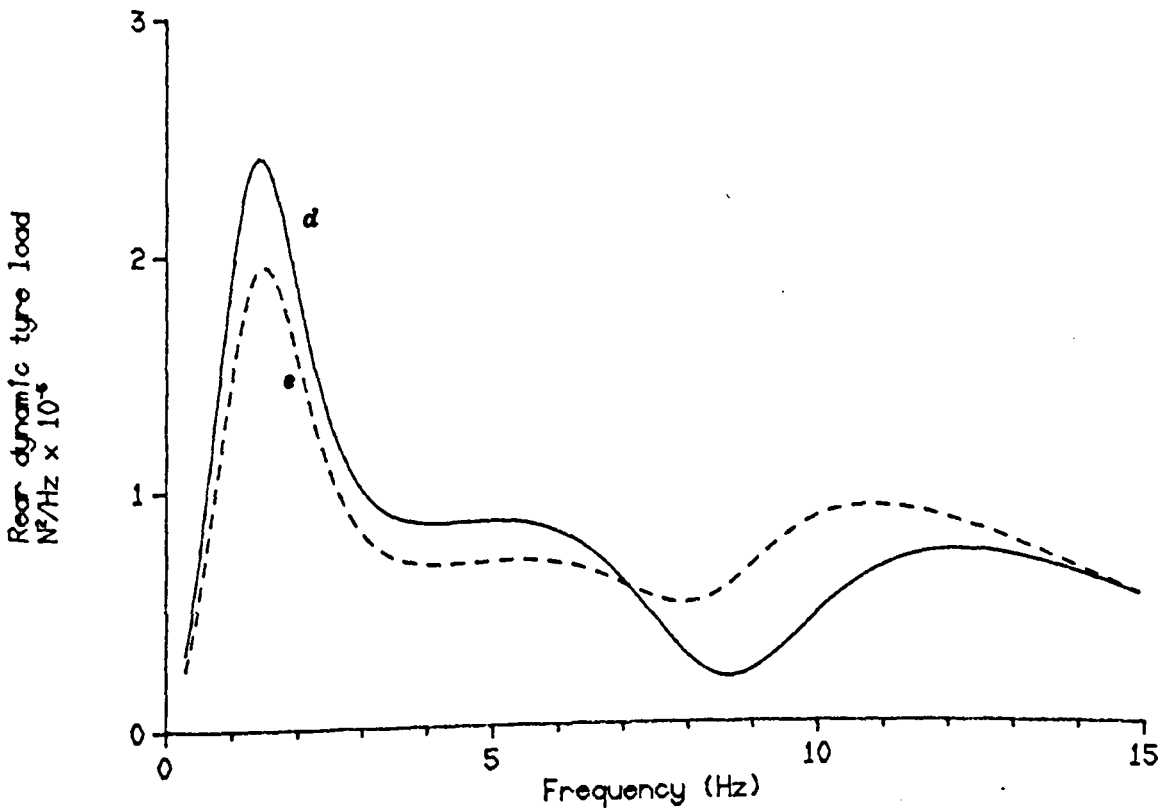
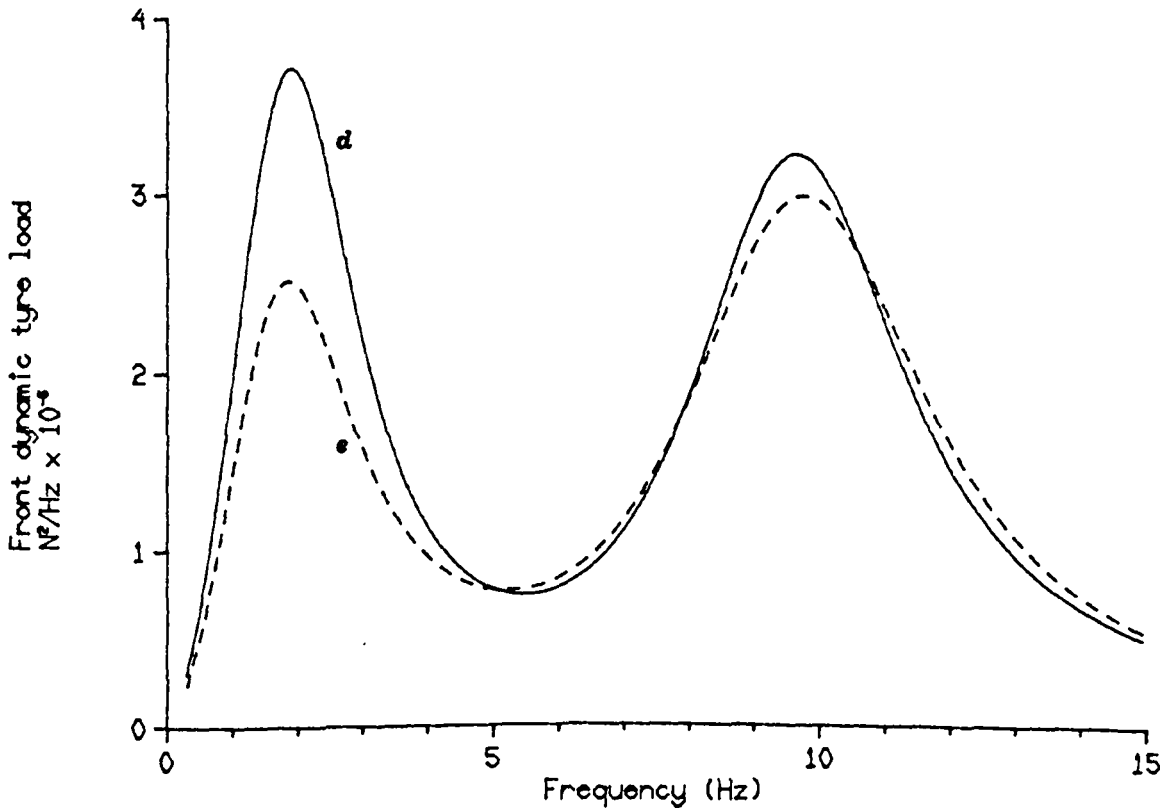


Fig. 6.18 Spectral densities of the front and rear dynamic tyre load for active systems a [1] and \bullet [1] for a suspension working space of 2 cm.

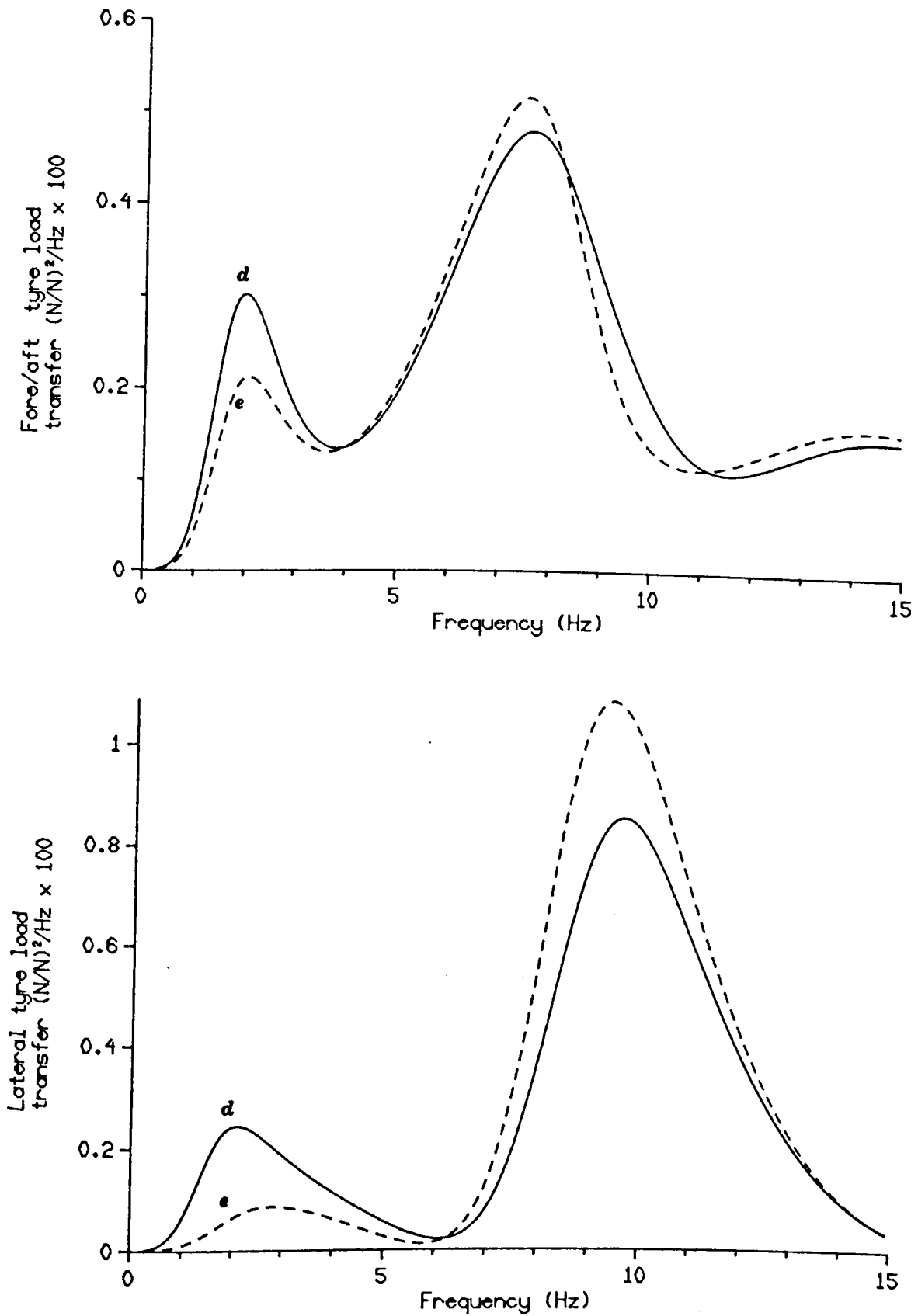


Fig. 6.19 Spectral densities of the fore/aft and lateral dynamic tyre load transfer for active systems *a* [1] and *e* [1] for a suspension working space of 2 cm.

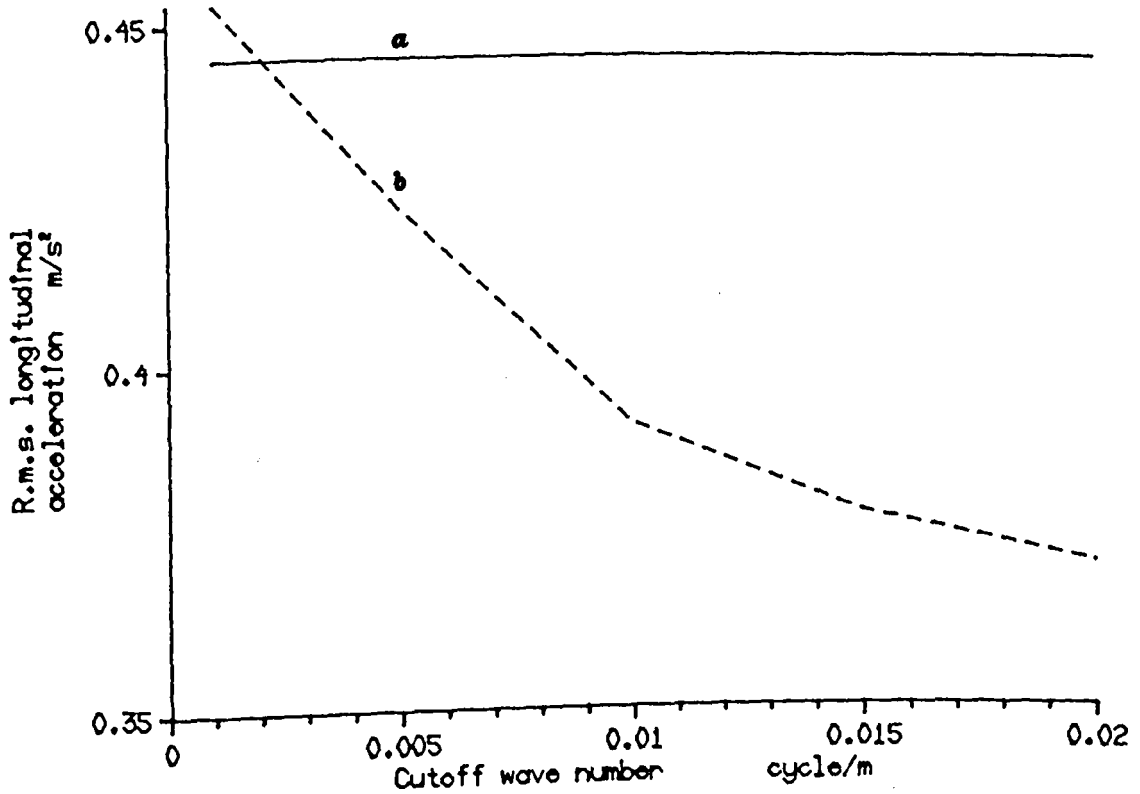
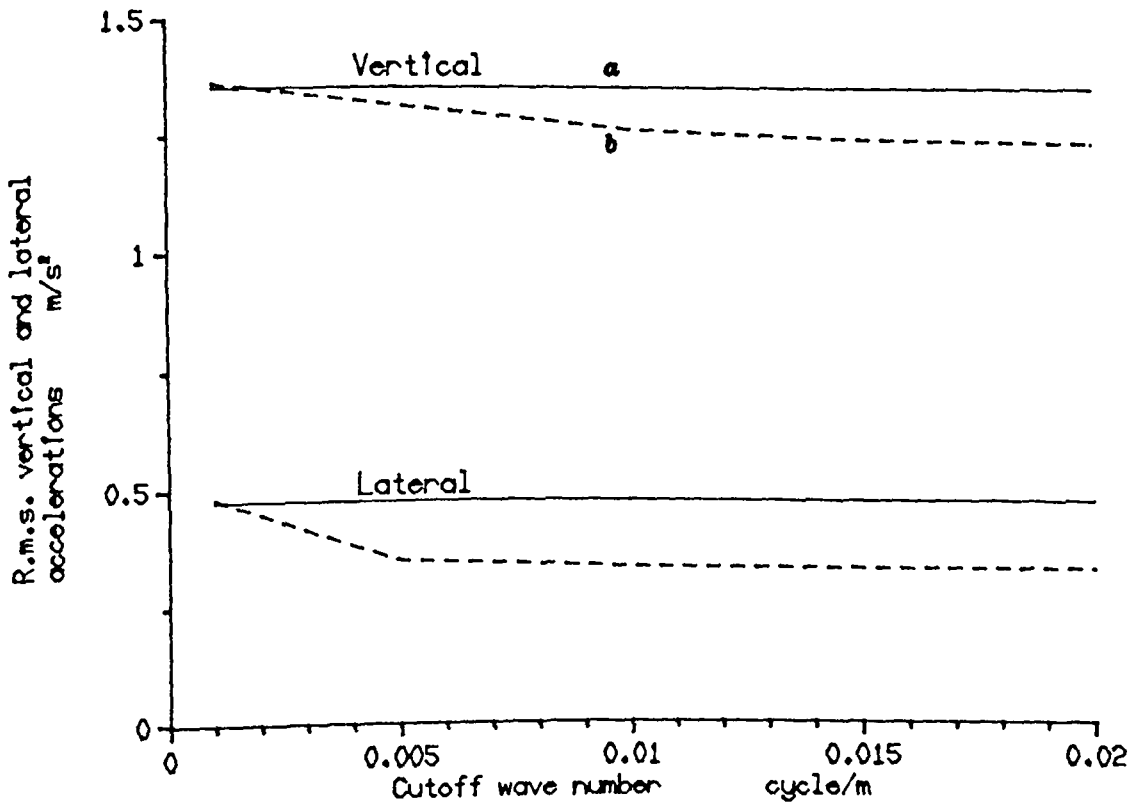


Fig. 6.20 Comparison at equal sws of seat accelerations for systems *a* and *b* as the cutoff wave number is varied. the comparison is always made at equal values of r.m.s. sws, ranging from 2.7 cm at $\lambda = 0.001$ cycle/m to 2.2 cm at $\lambda = 0.02$ cycle/m.

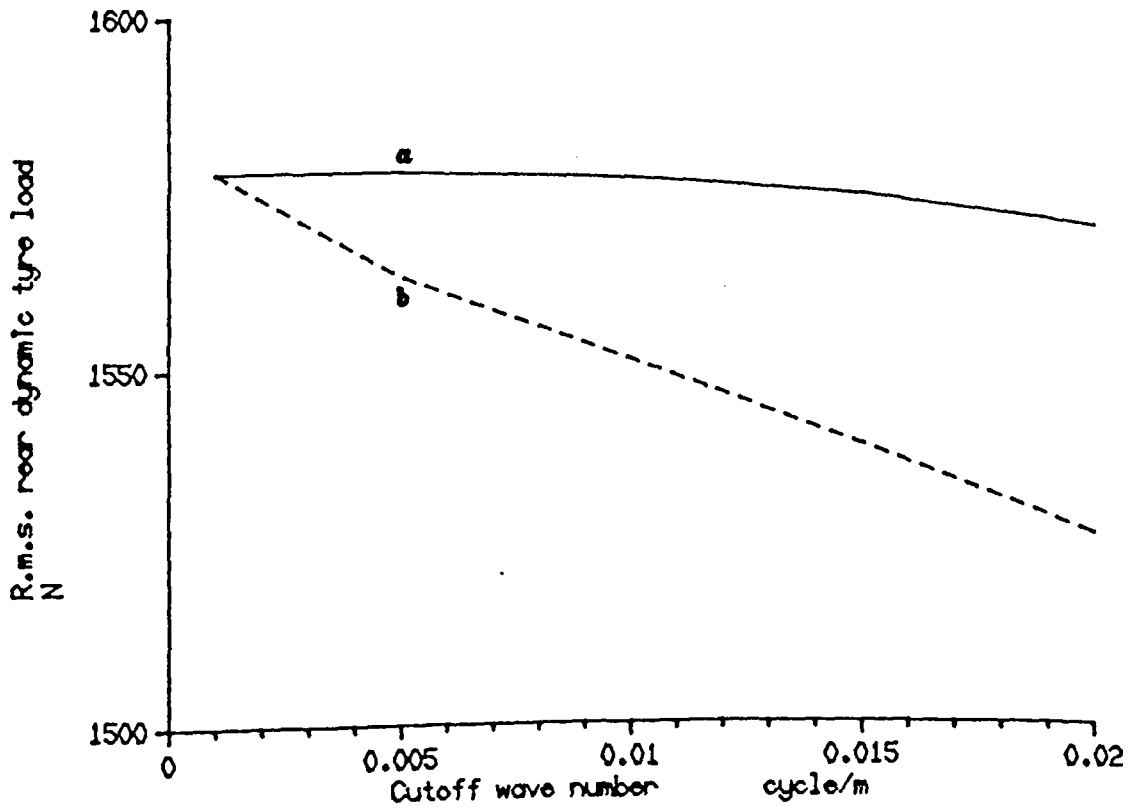
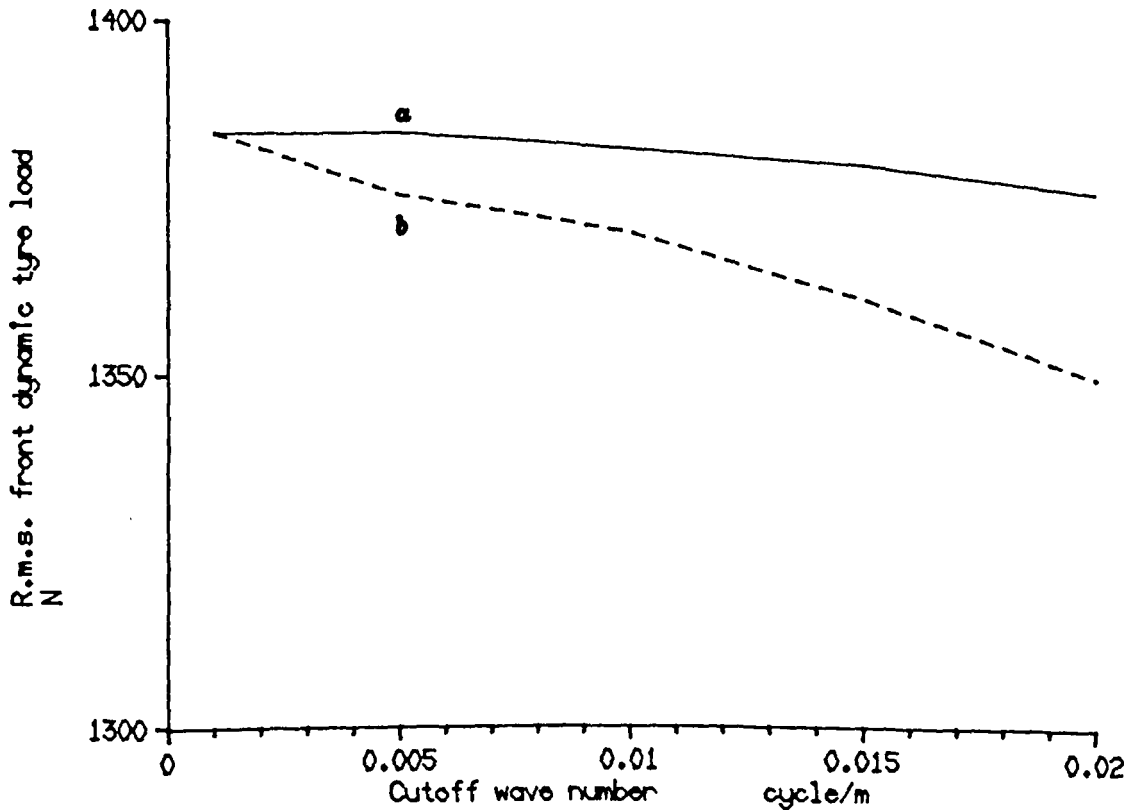


Fig. 6.21 Comparison at equal sws of dynamic tyre load for systems a and b as the cutoff wave number is varied. the comparison is always made at equal values of r.m.s. sws, ranging from 2.7 cm at $\lambda = 0.001$ cycle/m to 2.2 cm at $\lambda = 0.02$ cycle/m.

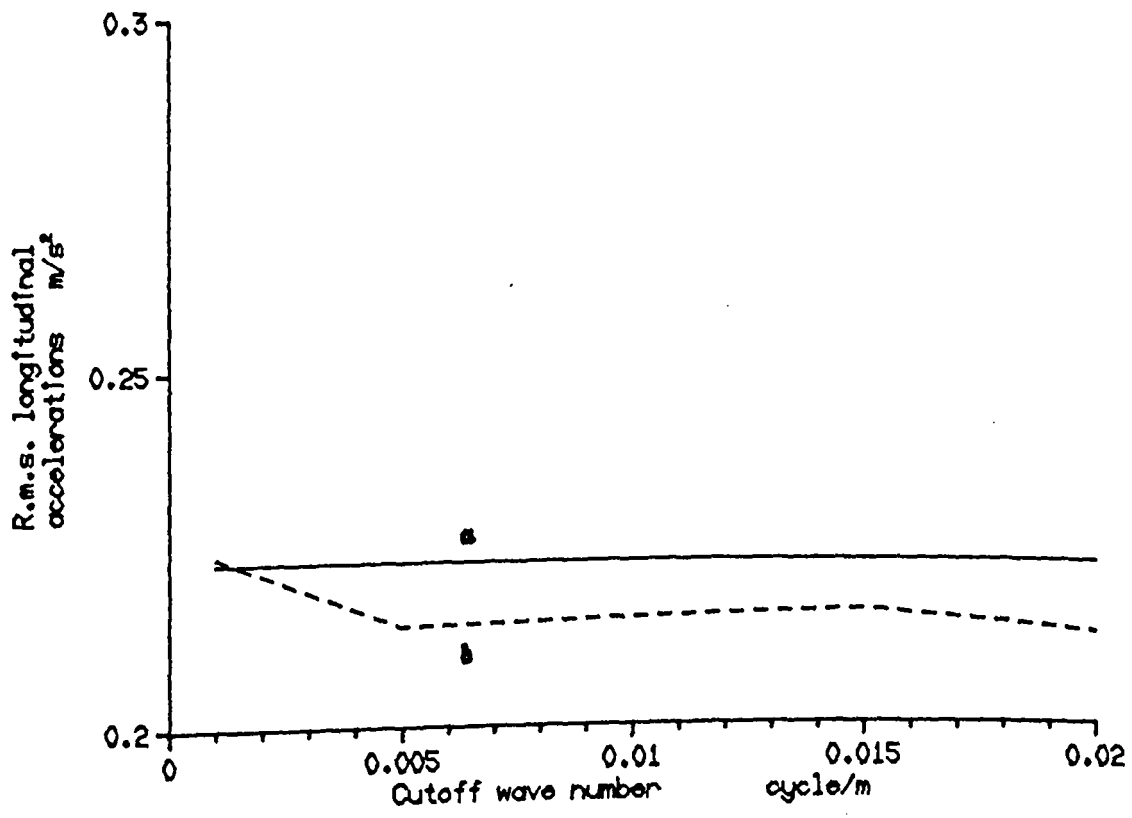
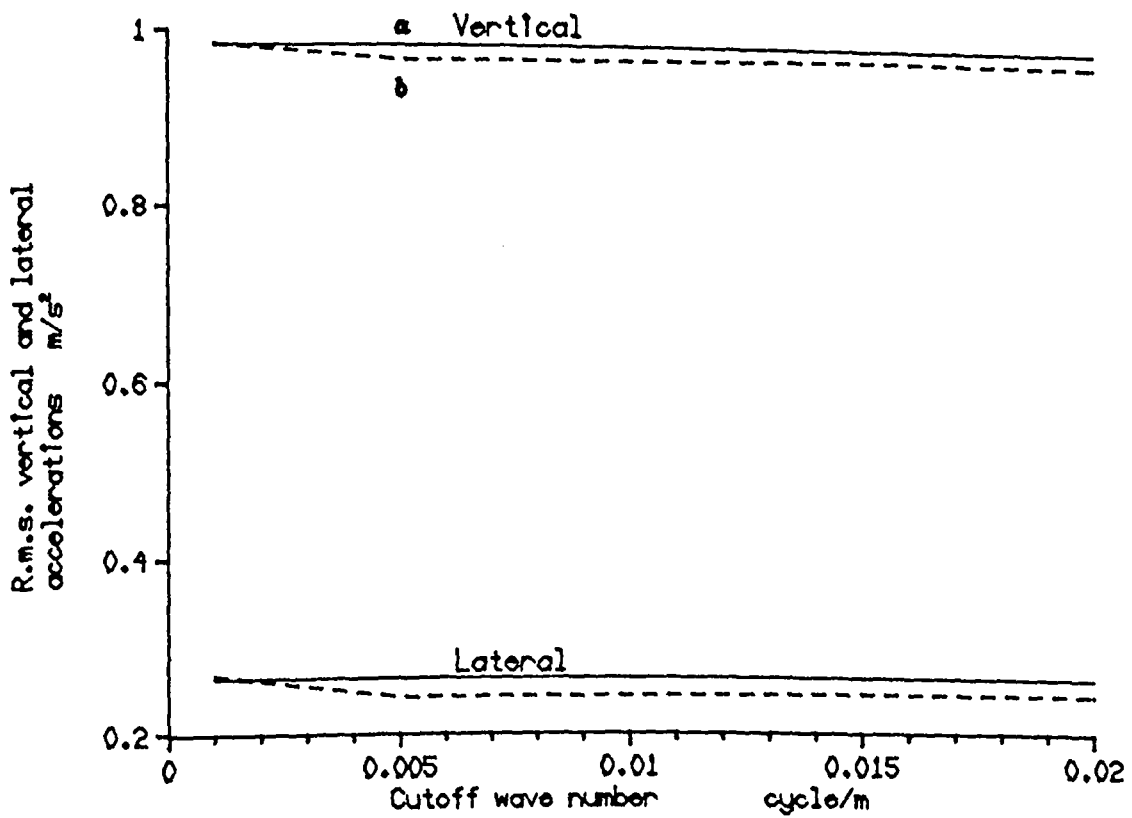


Fig. 6.22 Comparison at equal sws of seat accelerations for systems a and b as the cutoff wave number is varied. the comparison is always made at equal values of r.m.s. sws, ranging from 4.3 cm at $\lambda = 0.001$ cycle/m to 2.8 cm at $\lambda = 0.02$ cycle/m.

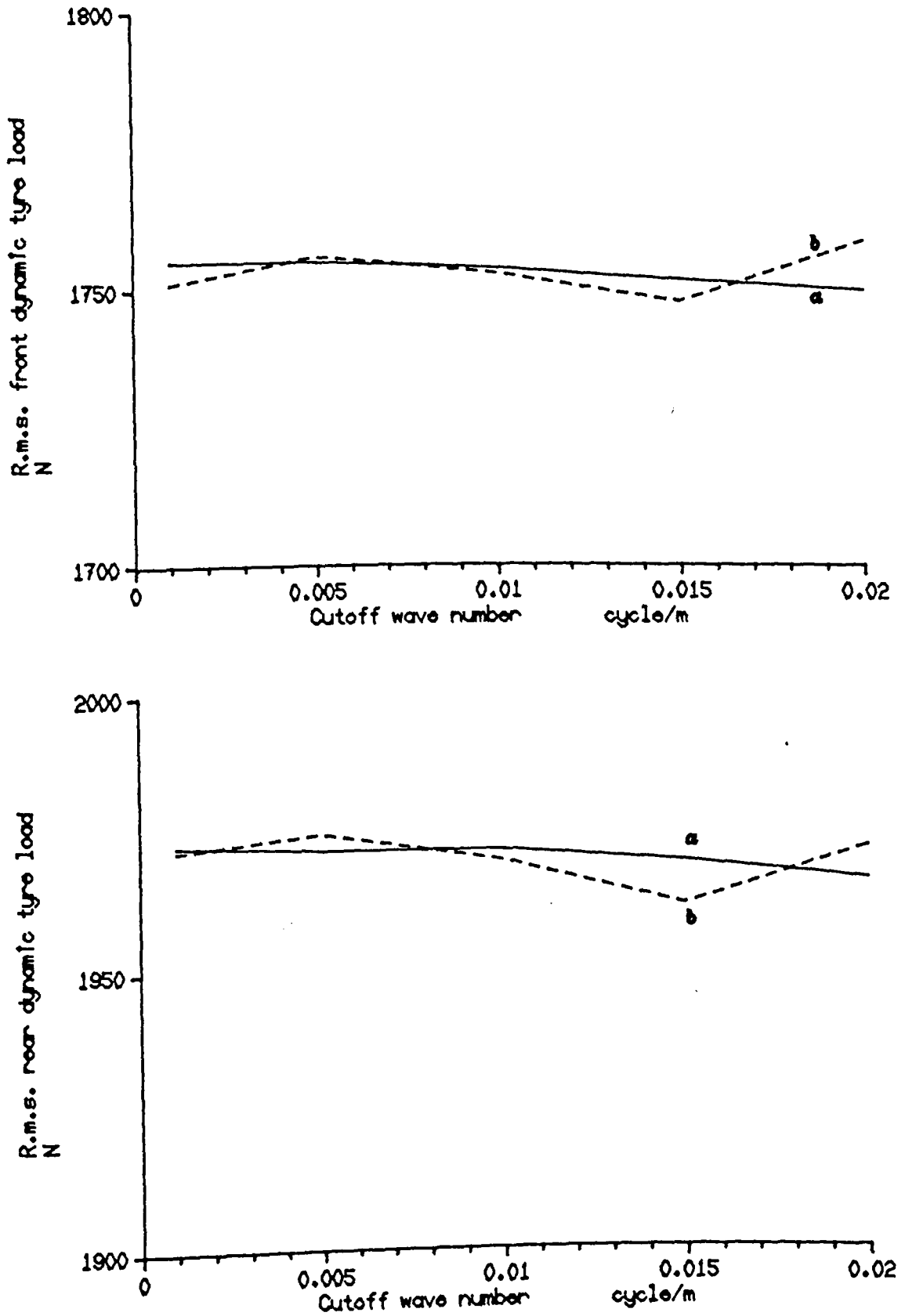


Fig. 6.23 Comparison at equal sws of dynamic tyre load for systems a and b as the cutoff wave number is varied. the comparison is always made at equal values of r.m.s. sws, ranging from 4.3 cm at $\lambda = 0.001$ cycle/m to 2.8 cm at $\lambda = 0.02$ cycle/m.

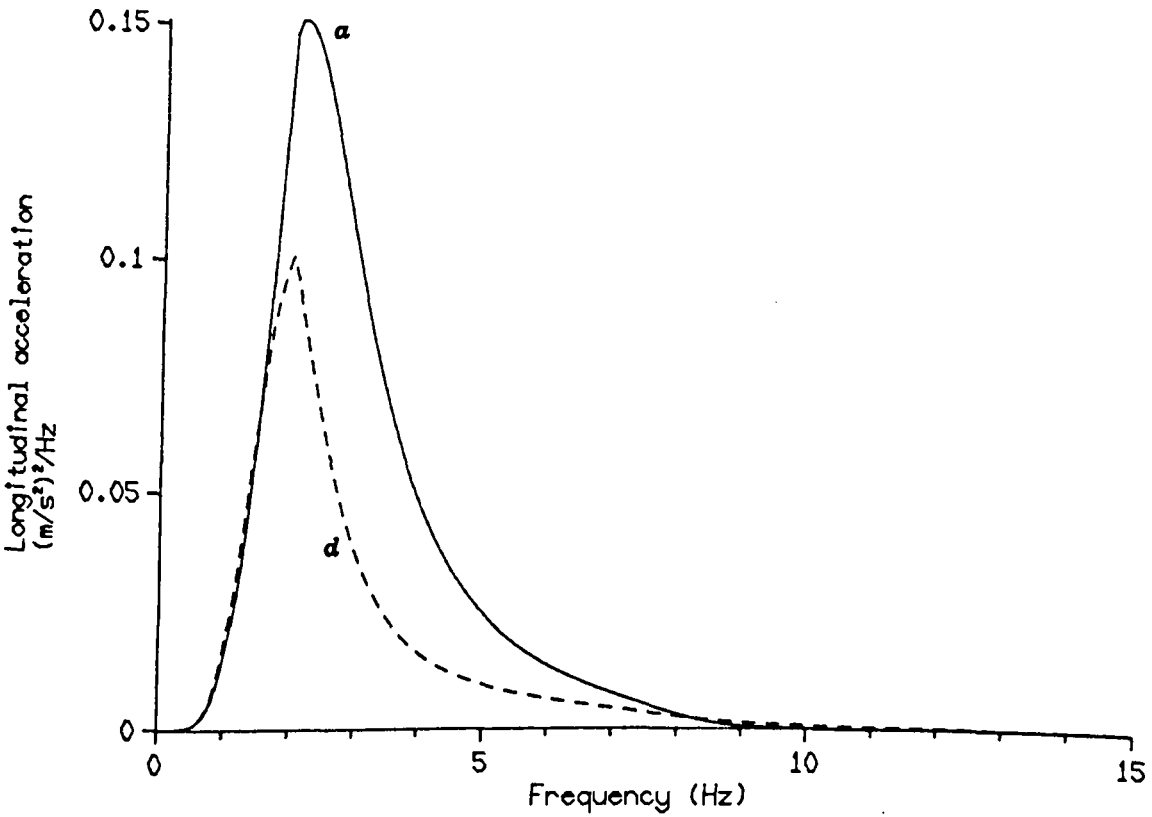
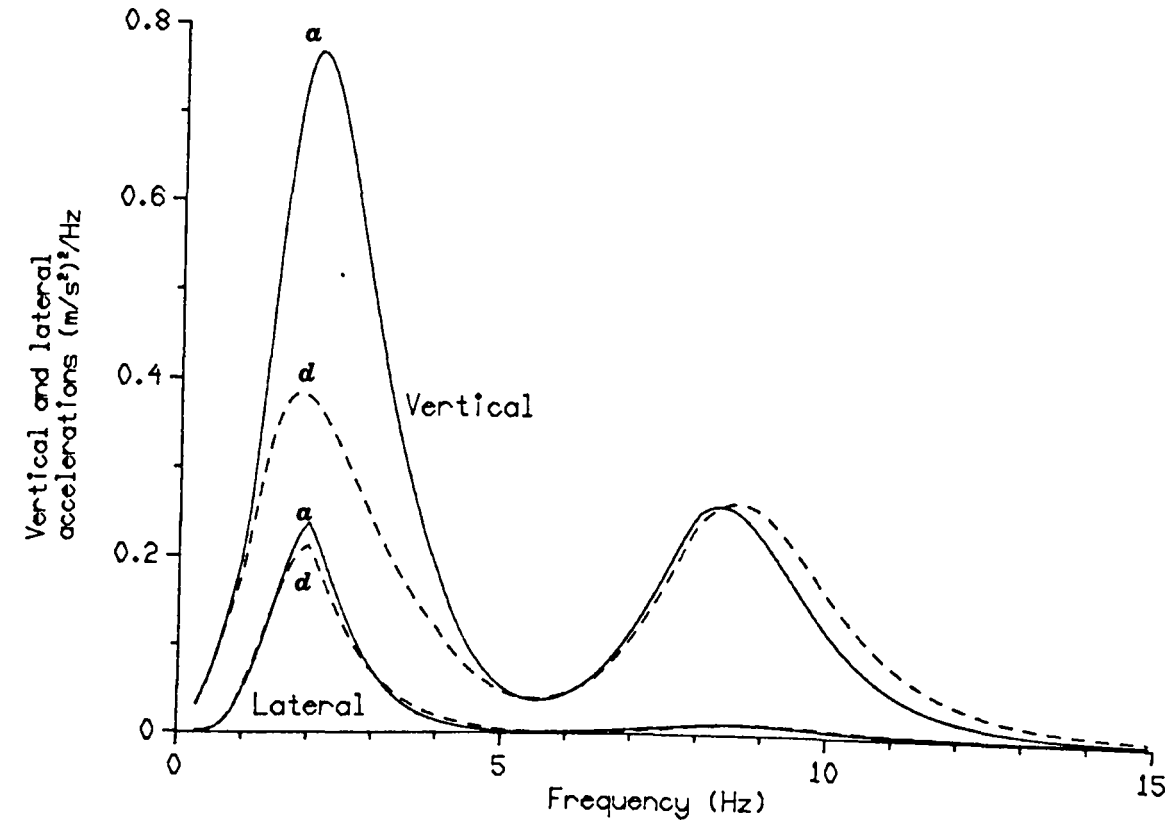


Fig. 6.24 Spectral densities of the I.S.O. weighted seat accelerations for active systems *a* [1] and *d* [1] for a suspension working space of 2 cm.

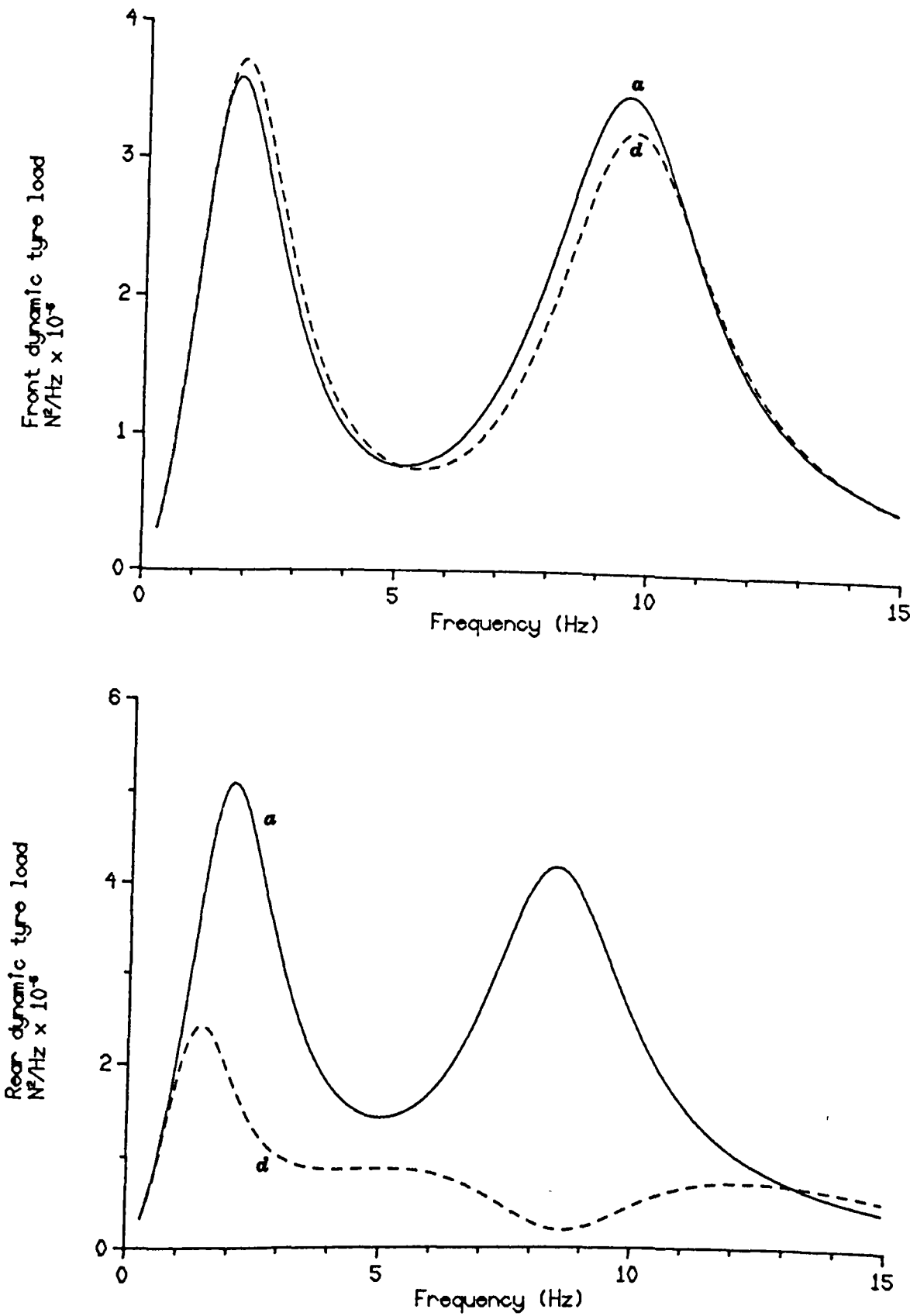


Fig. 6.25 Spectral densities of the front and rear dynamic tyre load for active systems *a* [1] and *d* [1] for a suspension working space of 2 cm.

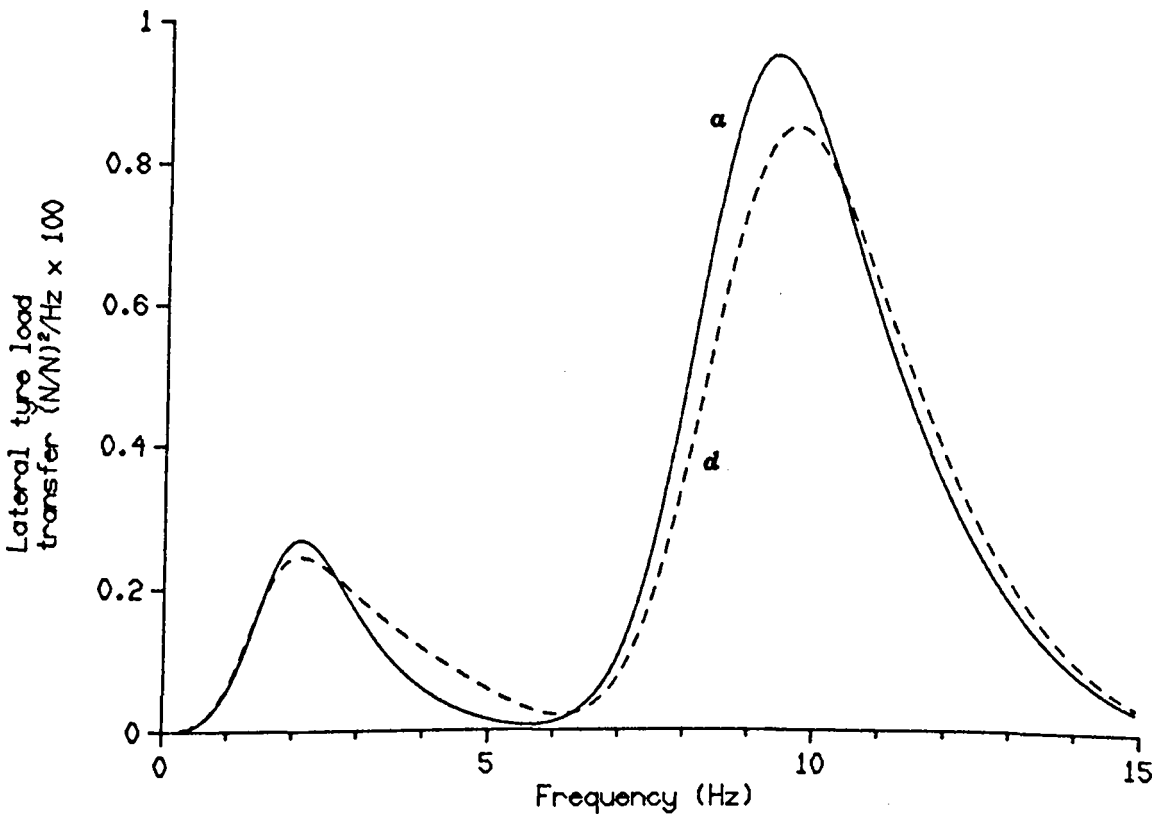
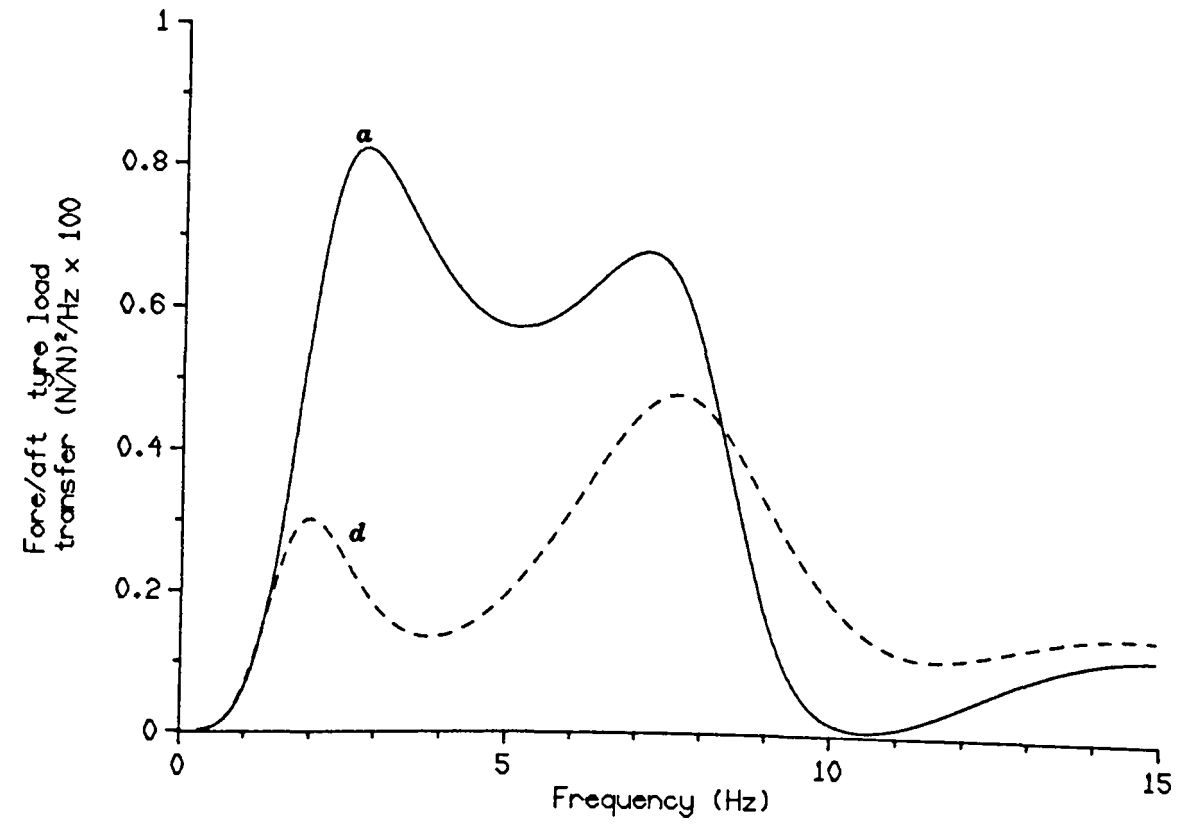


Fig. 6.26 Spectral densities of the fore/aft and lateral dynamic tyre load transfer for active systems *a* [1] and *d* [1] for a suspension working space of 2 cm.

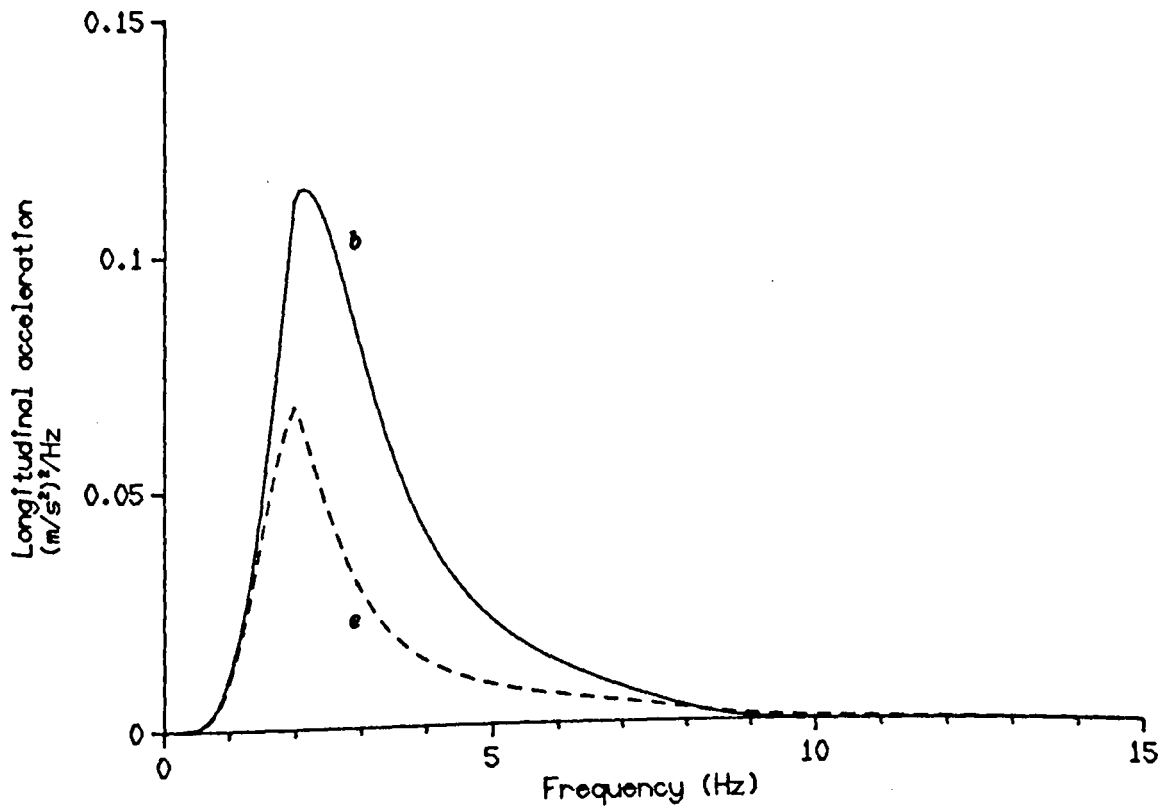
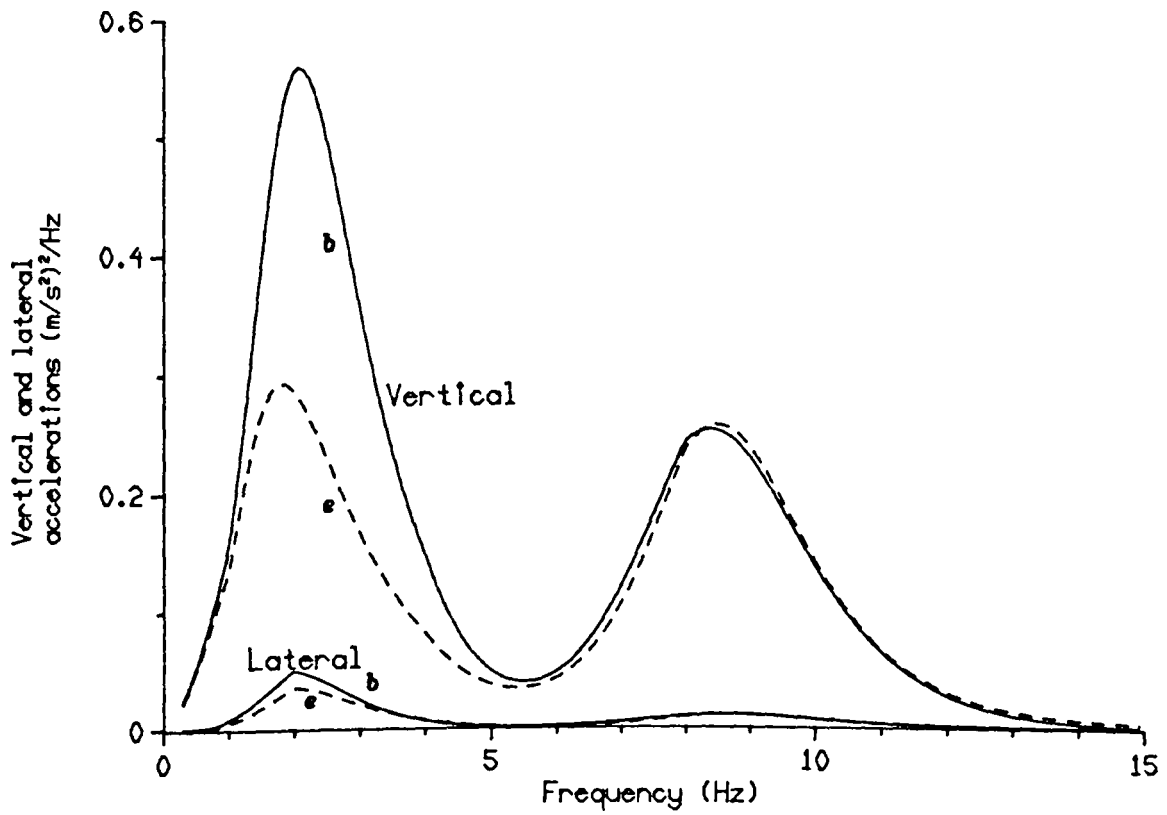


Fig. 6.27 Spectral densities of the I.S.O. weighted seat accelerations for active systems *b* [1] and *e* [1] for a suspension working space of 2 cm.

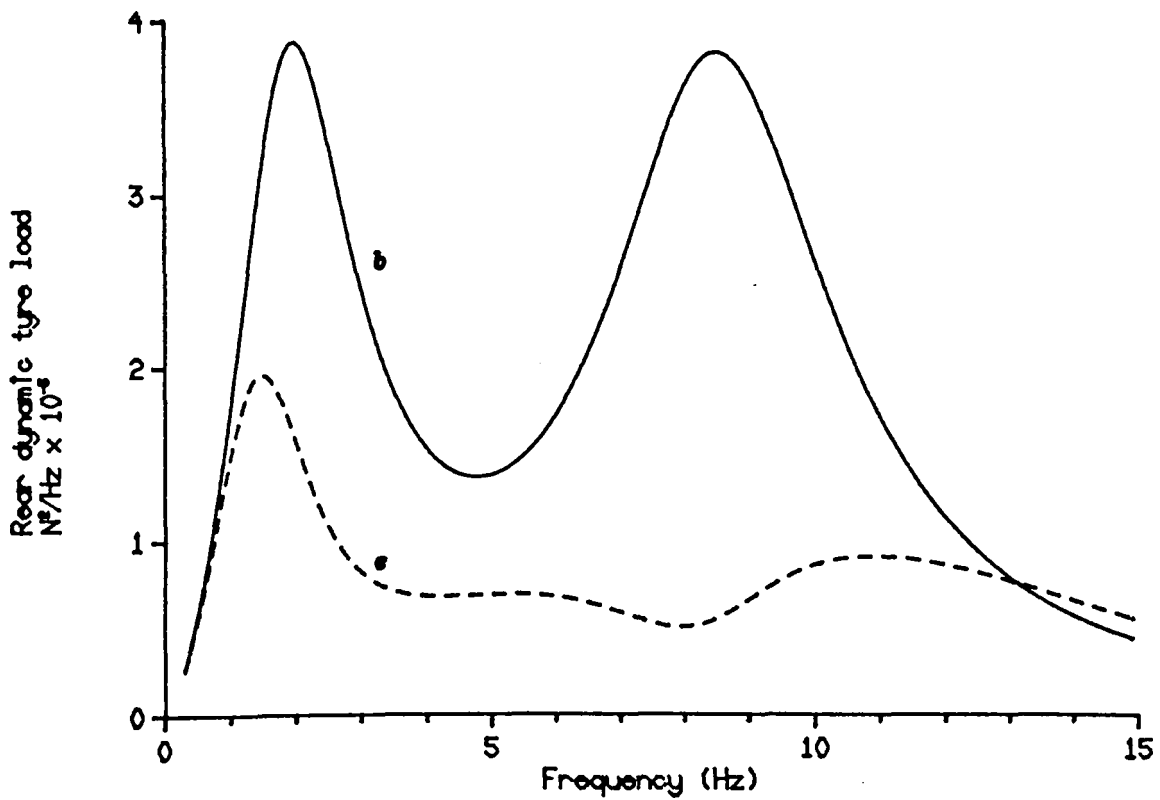
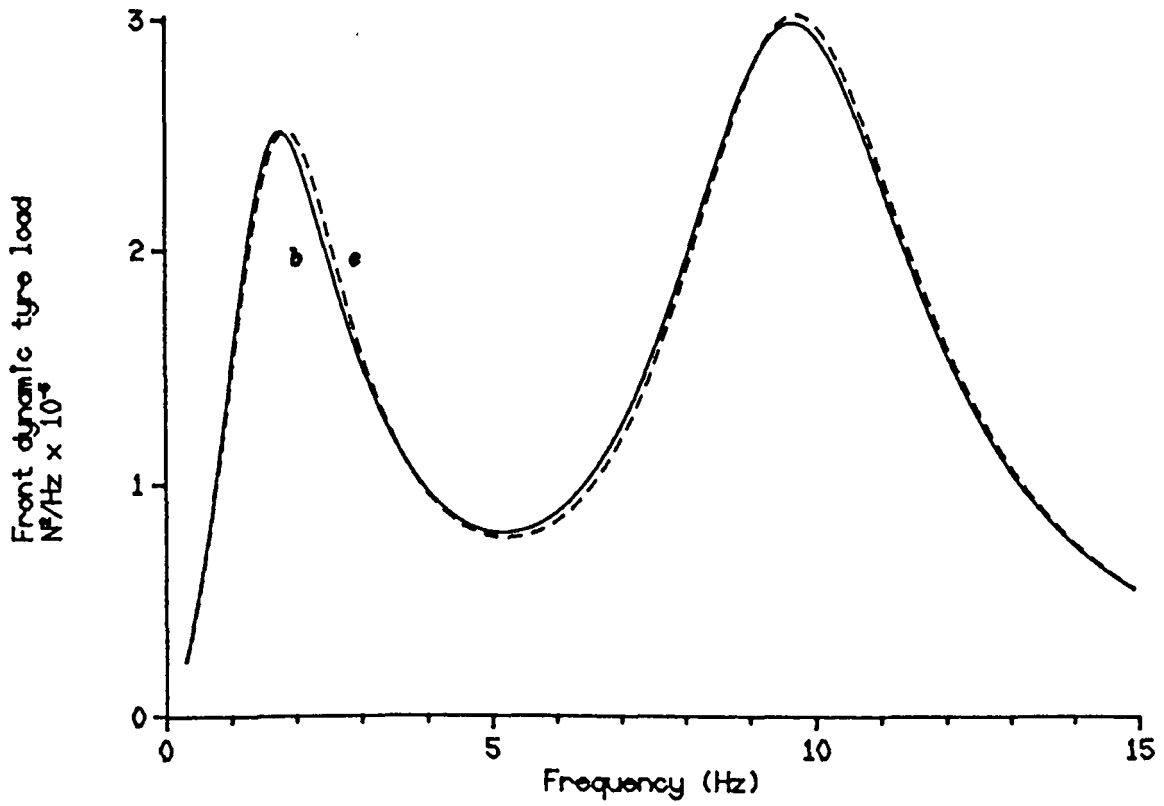


Fig. 6.28 Spectral densities of the front and rear dynamic tyre load for active systems b [1] and e [1] for a suspension working space of 2 cm.

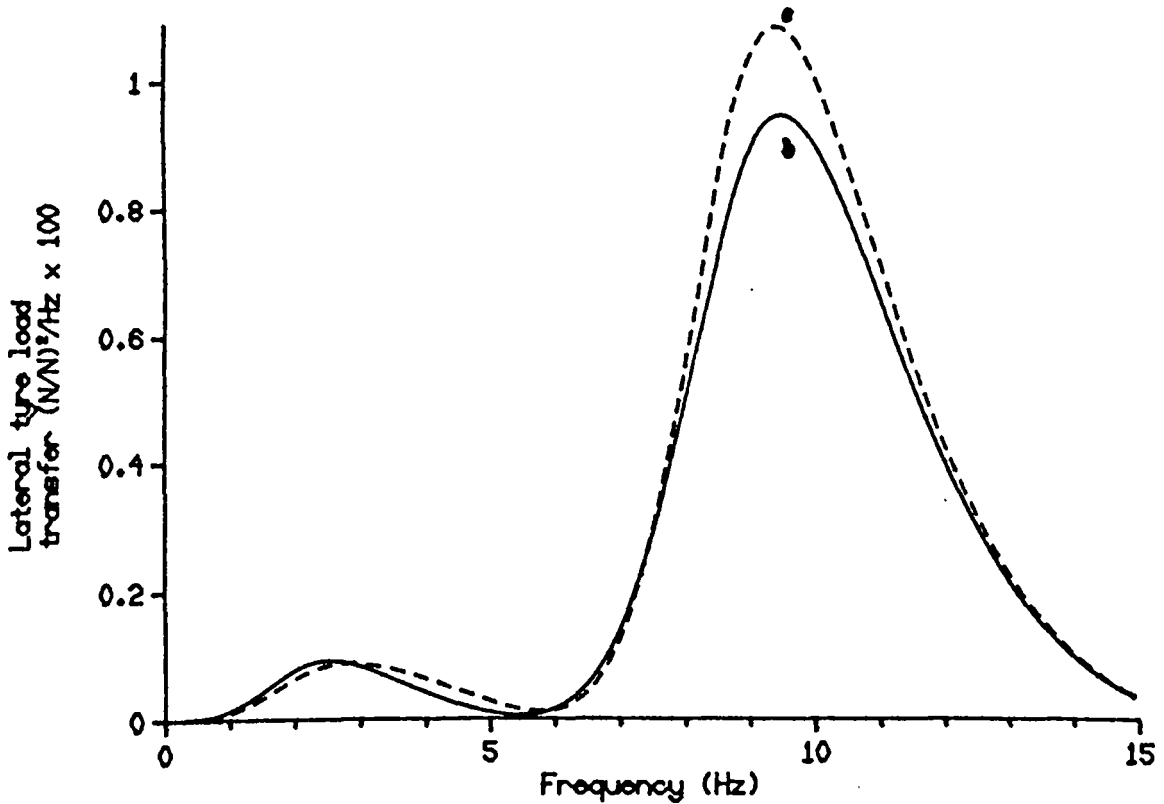
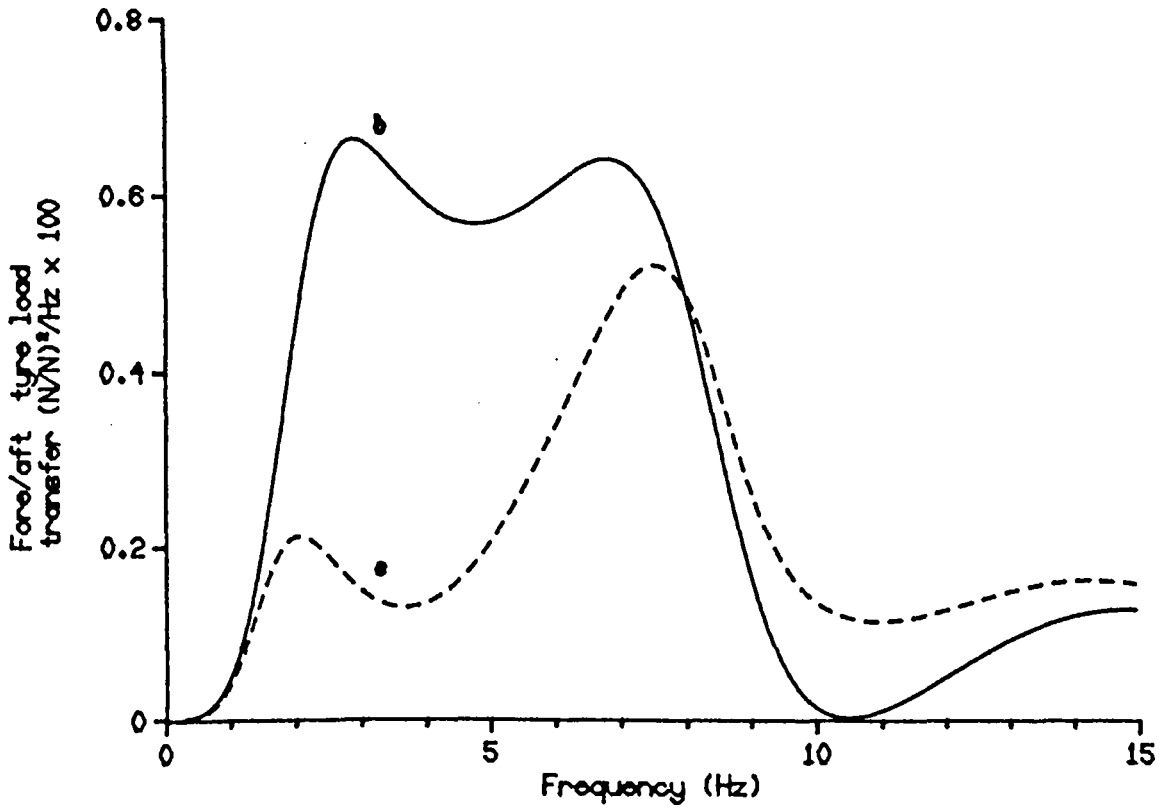


Fig. 6.29 Spectral densities of the fore/aft and lateral dynamic tyre load transfer for active systems b [1] and • [1] for a suspension working space of 2 cm.

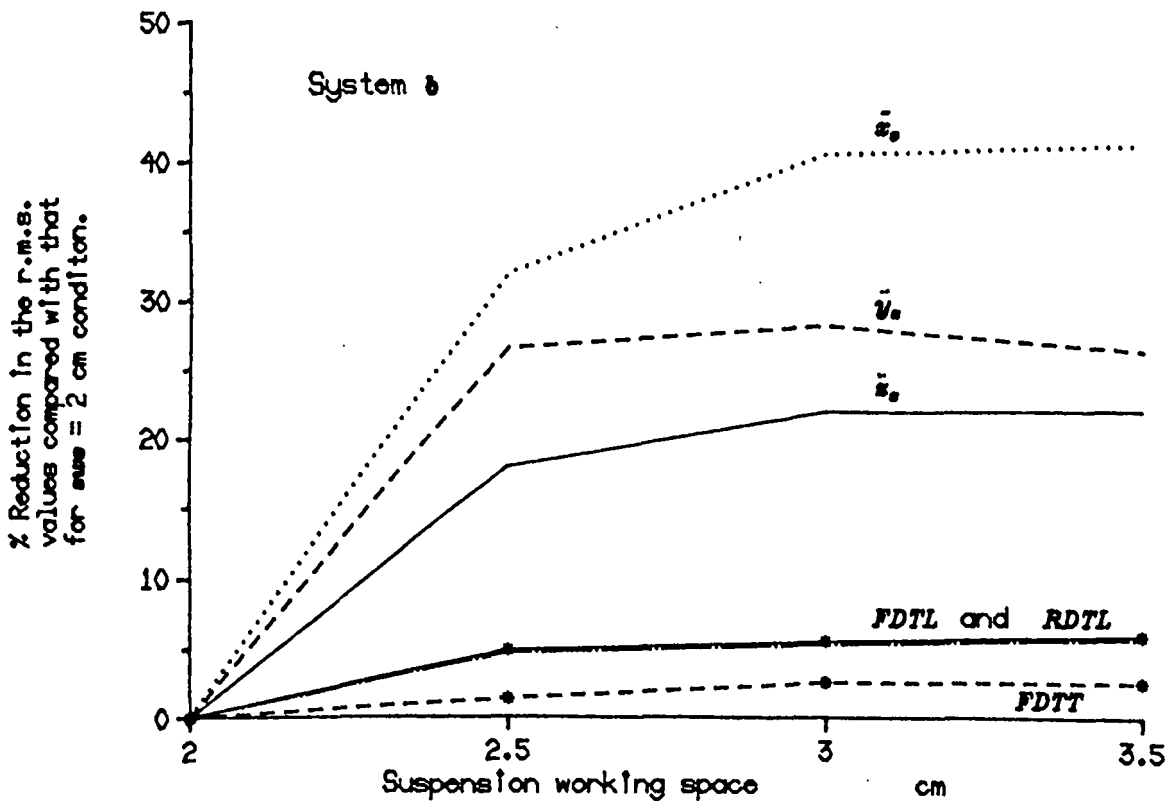
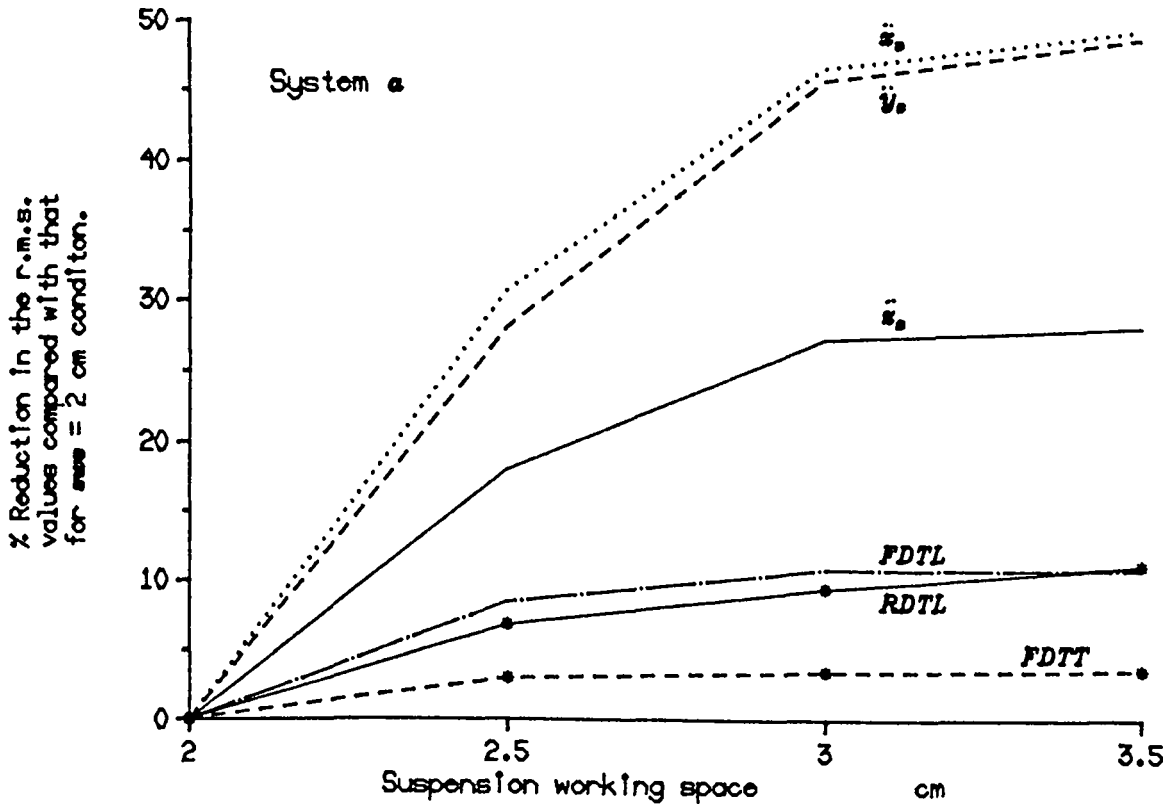


Fig. 6.30 Effect of increasing the working space on improving the performance of the active systems a and b.

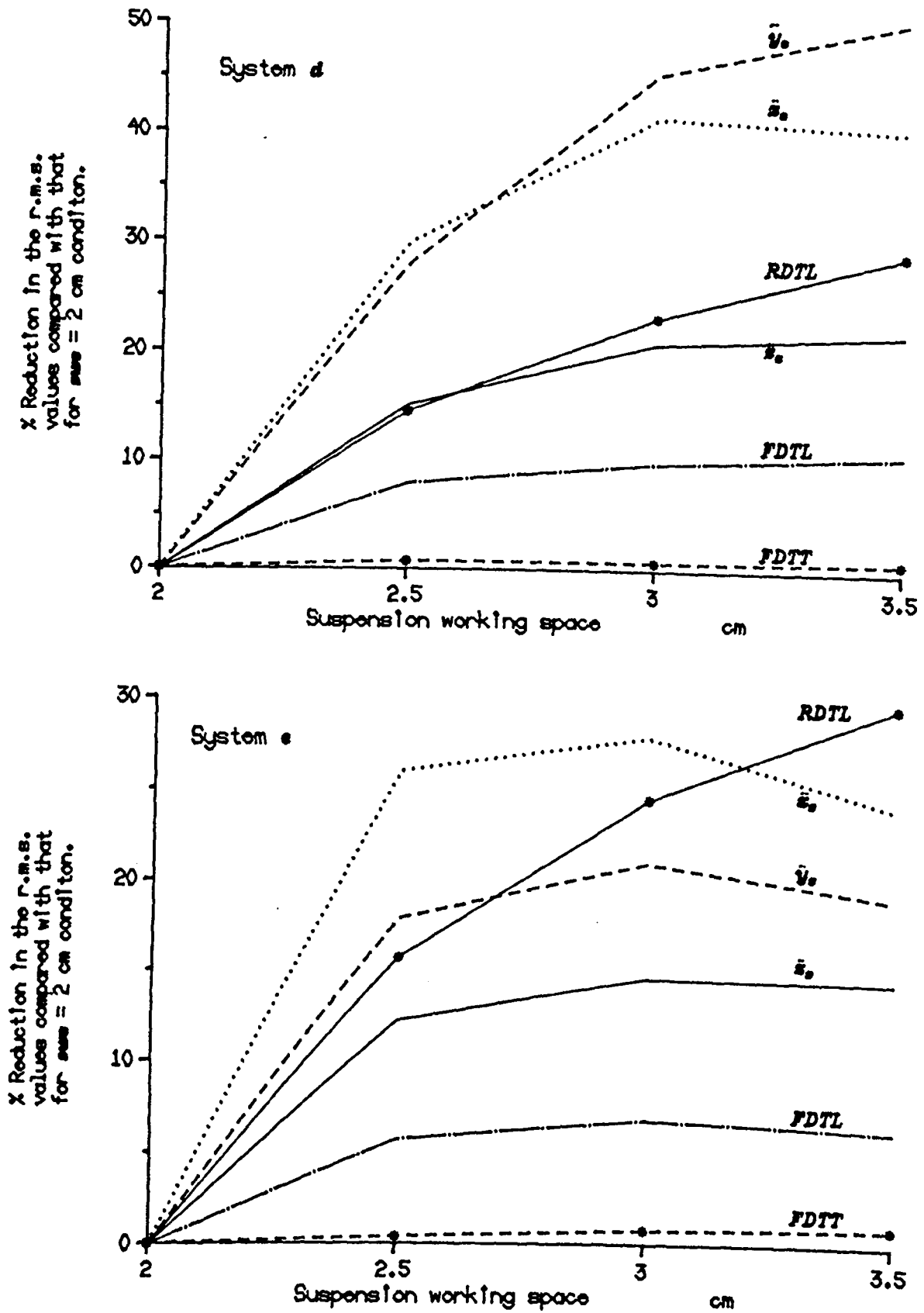


Fig. 6.31 Effect of increasing the working space on improving the performance of the active systems d and e.

CHAPTER 7

LIMITED STATE FEEDBACK ACTIVE SUSPENSION SYSTEMS

7.1 Introduction

In the last chapter, it was shown how the full state feedback active systems perform well and how their performance can be improved further by including the wheelbase time delay in deriving the control laws. However, the major problems of these systems are the high cost and complexity. In general, this complexity is increased as the performance of the full state feedback systems is improved. For example, in Chapter 6, it was shown that the best performing full state active system (e) may be realised if the following conditions are met.

1- Perfect measurements of all the states at the wheels and the body connections points are available as well as the road input displacements.

2- A very fast microprocessor is available which can carry out the calculations necessary to evaluate the time delay states within a very short time.

3- Because the feedback gains are related to the road inputs and the time delay states depend on the vehicle speed, this means that this system should be adaptive at least to the vehicle speed.

On the other hand, the lowest performance level was obtained with the active system α . This system may be realised in practice providing accurate body and wheel mounted sensors are available. Although this requirement is not easy to meet,

it is less complicated than the requirements necessary to realise system e which involves more calculations. The question now is how we can reduce the practical limitations of a full state feedback active system e.g. system e without great losses in its performance level ?. The solution of this problem may be obtained by employing limited state feedback active systems. In these systems, the ground input information and time delay states as well as any other states which are difficult to measure in practice may be omitted from the control laws. However, most of the work to date on these systems has been applied to the quarter car model and has been concerned in particular with omitting the road information from the control law. In Chapter 4, it was shown how the re-formulation of the optimisation problem allows the Kalman filter algorithm and the gradient search technique to be used to derive control laws which account for the wheelbase time delay. In this Chapter, the performance capabilities of active systems which employ these limited state feedback control laws will be examined. The classification of the systems is presented in Table 7.1. It can be seen from the table that the effect of the wheelbase time delay can be studied by comparing systems L_a and L_b , L_c and L_e , L_d and L_f . Furthermore, because in the systems L_c , L_d , L_e and L_f , noisy measurements are assumed, there is also an opportunity to study the effect of the measurement errors on the system performance. Before going into the details of these problems in sections 7.4 and 7.5, the equations of motion of all these systems are given in section 7.2.

Throughout this Chapter, the linear calculations are obtained in the frequency range 0.3-15 Hz. A road specified by $R_c = 3 \times 10^{-6}$ is assumed to be traversed at 30 m/s. For the non-linear analysis, the accuracy of the calculations in the time domain is first checked in section 7.3 by using a linear passive system and various profile inputs with different numbers of points. The profile of interest which gives the highest calculation accuracy level is then used confidently to generate the results of the system L_c , L_d , L_o and L_f discussed in section 7.5.

7.2 Equations of motion.

In this section, the equations of motion for all the active systems considered are given. Consider first systems L_a and L_b . In these systems, the gradient search method is used to derive the control laws. These control laws may be written as

$$u = K_x x \quad \dots(7.1)$$

where

$$x = [x_1 \quad x_2 \quad \dots \quad x_8 \quad \dot{x}_1 \quad \dot{x}_2 \quad \dots \quad \dot{x}_8]^T \quad \dots(7.2)$$

(see Fig. 6.1). It is clear that in the two systems the road height information is not required in deriving the control law. Furthermore, the Pade approximation states η are omitted from the control law of system L_b . Therefore, the equations of motion of these systems are identical to the full state feedback active system a (see equations 6.3 to 6.5) except.

for the matrix M_U . In equation (6.5), because the matrix K_o is a null matrix, the term $M_{f_1}K_o$ is also a null matrix. Hence, the matrix M_U is identical to that used in the passive system.

Consider now the active systems L_c and L_a . In these systems, the Kalman filter algorithm is used to derive the control laws. Because noisy measurements are assumed, the derivation of the equations of motion is a more complicated issue compared with the previous case. The following strategy is used in deriving these equations of motion. Using equations (4.6), (4.37) and (4.40), the estimation error, the differential equation and the control law may be re-written as

$$\dot{e}_r = (A_1 - K_k H)e_r + B_w w - K_k v_a \quad \dots(7.3)$$

$$u = Kx_a - Ke_r, \quad K = [K_x \mid K_o] \quad \dots(7.4)$$

Hence equation 4.1 may be written as

$$\dot{x} = (A + BK_x)x + (B_2 + BK_o)x_o - BK_e r \quad \dots(7.5)$$

Combining equations (7.5) and (7.3) and using u as defined above, the result may be written as

$$\begin{bmatrix} \dot{x} \\ \dot{e}_r \end{bmatrix} = \begin{bmatrix} A + BK_x & -BK \\ 0 & A_1 - K_k H \end{bmatrix} \begin{bmatrix} x \\ e_r \end{bmatrix} + \begin{bmatrix} B_2 + BK_o \\ 0 \end{bmatrix} x_o + \begin{bmatrix} 0 \\ B_w \end{bmatrix} \dot{x}_o + \begin{bmatrix} 0 \\ -K_k \end{bmatrix} v_a$$

Once the filter gains K_k are obtained as explained in section 4.2.2.2 and by using the feedback gains K_x and K_o generated for the full state feedback case (see section 4.2.1.1), it is possible to generate the time history of the output of interest as explained in section 2.5. Having these time histories available, it is possible to process them into the frequency domain using an FFT algorithm, to apply the ISO

weighting functions to the acceleration outputs and to obtain the r.m.s. values of all the outputs in the frequency range (0.3 - 15) Hz as required.

The equations of motion of the systems L_o and L_f may be obtained in a similar manner to that explained above. Equations (7.3) to (7.5) will remain unchanged except that A_1 , B_w and K should be replaced by A_f , B_b and K_D respectively. These matrices are defined in equations (4.66) and (4.67). The final result for the equations of motion may be then written as

$$\begin{bmatrix} \dot{x} \\ \dot{\eta} \\ \dot{e}_r \end{bmatrix} = \begin{bmatrix} A+BK_x & BK_\eta & -BK_D \\ 0 & A_\eta & 0 \\ 0 & 0 & A_f - K_k H \end{bmatrix} \begin{bmatrix} x \\ \eta \\ e_r \end{bmatrix} + \begin{bmatrix} B_2+BK_o \\ 0 \\ 0 \end{bmatrix} x_o + \begin{bmatrix} 0 \\ B_\eta | 0 \\ B_b | 0 \end{bmatrix} \dot{x}_o \\ + \begin{bmatrix} 0 \\ 0 \\ -K_k \end{bmatrix} v_a \quad \dots(7.6)$$

As in Chapters 3 and 6, the performance of any of these active systems is analysed in terms of r.m.s. values of the vertical, lateral and longitudinal seat accelerations, front and rear dynamic tyre load and fore/aft and lateral dynamic tyre load transfer. The non-zero elements of the output matrices T_{XDD} , T_{XD} , T_X and T_U of all the systems are similar to those given in section 2.6 for the passive system.

7.3 Accuracy of the calculations in the time domain.

It has been indicated above that the systems L_c , L_d , L_o and L_f are non-linear. Thus it is necessary to evaluate the performance of these systems in the time domain. In the next Chapter the performance of some of these systems will be

compared with those obtained for the linear passive and active systems. The accuracy of this comparison depends on the accuracy of the calculations in the time domain which in turn depends on the accuracy of the ground input profile representation and the method used to find the time histories of the states x . The accuracy of the road profile representation increases as the number of points defined for a certain track length is increased. In this section the number of points necessary to be used in the road input profiles so that the non-linear calculations agree with those obtained linearly in the frequency domain is evaluated as follows. Firstly, four profiles are generated from the input spectral density (1.1) for $R_c = 3 \times 10^{-6}$ and $n = 2.5$. Each of these profiles is 100 m long and contains two correlated tracks as explained in section 2.2. In profile No. 1, each of the two tracks employed consists of 1024 points, while in profiles No. 2, 3 and 4 the number of points is increased to 2048 points, 8192 points and 16384 points respectively. Secondly, the second order equations of the linear passive system are transformed into first order form as explained in section 2.3. Thirdly, the performance of a linear passive system is calculated in the time domain when each profile is traversed at 30 m/s. This system has front and rear springs with stiffness equal to $K_f = K_r = 24.2 \text{ kN/m}$ and damping ratios of 0.5. The anti-roll bar is not considered in this calculation. Two different ways are used to evaluate the time histories of the outputs of interest, i.e. seat acceleration, dynamic tyre load and the suspension working space. The first way is based on the method which is explained in section 2.5 and translated into

the Fortran program explained in section 2.7 , while in the second way, the program VDAS developed by Horton [1988] is used. Fourthly, the time history of the outputs from the time domain are processed in the frequency domain to give the r.m.s. values in the frequency range (0.3 - 15 Hz). These values are compared with those obtained from the linear calculations in the frequency domain. The results are collected and presented in Tables 7.2 to 7.4 and the following conclusions may be drawn

1- Good agreement is obtained between the program explained in section 2.8 and the program VDAS. Minor differences between the outputs from the two programs appear when the profile No. 3 is used (8192 points). However the program explained in section 2.8 is slightly more accurate at this condition.

2- The accuracy of the solution obtained from profile No. 1 (1024 points) is not too far from that obtained for profile No. 3 (8192 points) when compared with the frequency domain results which appear in Table 7.2, while in order to achieve accurate outputs close to the results of Table 7.2, profile No. 4 (16384 points) must be used. In the following sections, all the non-linear calculations were obtained using profile No. 4.

7.4 Effect of the wheelbase time delay.

In the last Chapter, the inclusion of the time delay in deriving the control law was shown to improve dramatically the performance of the active systems. For example, it was shown that including the time delay improves the vertical

seat acceleration and the rear dynamic tyre load by 11% and 40% respectively. However, as has been explained in the last Chapter and in section 7.1, these improvements are associated with increased hardware complexity and expense. In this section there is a more realistic scheme to study the effect of the wheelbase time delay by comparing the performance of system L_b with system L_a . These systems require exactly the same hardware. The only difference between them is the feedback gain values. The results for 2.5 cm r.m.s. working space are shown in Figs. 7.1 to 7.3. It is clear that the system L_b provides significant improvements in the performance when compared with L_a . For example, the active system L_b [3] improves the vertical and longitudinal accelerations, front and the rear dynamic tyre load, fore/aft and the lateral tyre load transfer by 10%, 8%, 12%, 6%, 13% and 11% respectively at the expense of increasing the lateral seat acceleration by 6% when compared with system L_a [2].

7.5 The effect of measurement errors.

It is known that the measurements of the state variables in practice would be noisy and thus the performance of the active systems would suffer. The main objectives of this part are to examine the effect of the measurement errors on (a) the performance of the systems L_c , L_d , L_e and L_f , (b) on the improvements achieved from including the wheelbase time delay and (c) on the number of the measurements available. In order to study these problems, a set of results was calculated for each active system when the profile No. 4 [100 m long and

16384 points] is traversed at 30 m/s. The suspension working space with 2.5 cm r.m.s. value is assumed to be consumed at this speed. The results appearing in Figs. 7.7 to 7.17 and Table 7.5 are obtained as follows. First, the r.m.s. values of the ISO weighted vertical, lateral and longitudinal seat accelerations, front and rear dynamic tyre load and the fore/aft and the lateral dynamic tyre load transfer are calculated for the active system L , and shown in Figs. 7.4 to 7.6. In these calculation, four values of sensor random error (SRE) assuming a normal distribution with standard deviations equal to 1×10^{-3} , 1.49×10^{-3} , 3.16×10^{-3} and 4.08×10^{-3} with units of either m or m/s. Secondly, graphs similar to those of system L , are generated for the systems L_c , L_d and L_f . Finally, for each suspension type, the systems of interest are selected and used to develop Figs. 7.7 to 7.17. Table 7.5 summarises the r.m.s. values shown in Figs. 7.7 to 7.14. Comments arising from these figures and Table 7.5 are as follows.

1- As the measurement errors increase, the suspension performance deteriorates as would be expected (see Figs. 7.7 to 7.14). For example, for system L_c (Figs. 7.7 and 7.8), as the sensor random error increases from 0.001 to 0.00408, the vertical, lateral and longitudinal accelerations increases by 8%, 21% and 16% respectively, while in systems L_d , these accelerations are increased by 11%, 23% and 21% respectively. At the same time, this increase in the sensor random error causes an increase of the r.m.s. values of the vertical and lateral seat accelerations, rear dynamic tyre load and fore/aft tyre load transfer of system L , by 7%, 15%, 13% and 4%

respectively, while for system L_f , these r.m.s. values are increased by 6%, 18%, 16% and 5% respectively.

2- For sensor random error of 4.08×10^{-3} (most noisy measurements considered), there is not much difference between the performance level of systems L_d and L_f (which require only the measurements of wheel - body relative velocities) and those of systems L_c and L_e respectively although the latter two systems require the measurements of wheel-body relative displacements and velocities and the wheel- ground relative displacements. Hence, these active systems are more sensitive to the measurement errors than the number of the states measured. However, in other working conditions where the sensor random error is increased further, the use of systems L_c and L_e instead of systems L_d and L_f would be useful. The most important practical problem implied in systems L_c and L_e is the need to measure the wheel displacements relative to the ground $DTD_i, i=1,2,3,4$. This problem can be overcome in principle by the following strategy. The four wheel mounted sensors are replaced by four accelerometers to measure the vertical acceleration of the body connection points and another four to measure the acceleration of the unsprung masses. Using the example of Chapter 4 (section 4.5.1) and Fig. 6.1, it can then be shown that

$$\begin{bmatrix} \ddot{x}_2 \\ \ddot{x}_4 \\ \ddot{x}_6 \\ \ddot{x}_8 \end{bmatrix} = \begin{bmatrix} s_1 & s_2 & s_3 & s_4 \\ s_2 & s_1 & s_4 & s_3 \\ s_3 & s_4 & s_5 & s_6 \\ s_4 & s_3 & s_6 & s_5 \end{bmatrix} \begin{bmatrix} u_1 \\ u_2 \\ u_3 \\ u_4 \end{bmatrix}, \quad \dots(7.7)$$

$$s_1 = \frac{w_a^2}{I_p^2} + \frac{t_s^2}{I_r^2} + \frac{1}{M_b} , \quad s_2 = \frac{w_a^2}{I_p^2} - \frac{t_s^2}{I_r^2} + \frac{1}{M_b} , \quad s_3 = \frac{-w_a w_b}{I_p^2} + \frac{t_s^2}{I_r^2} + \frac{1}{M_b}$$

$$s_4 = \frac{-w_a w_b}{I_p^2} - \frac{t_s^2}{I_r^2} + \frac{1}{M_b} , \quad s_5 = \frac{w_b^2}{I_p^2} + \frac{t_s^2}{I_r^2} + \frac{1}{M_b} , \quad s_6 = \frac{w_b^2}{I_p^2} - \frac{t_s^2}{I_r^2} + \frac{1}{M_b}$$

and

$$\begin{bmatrix} M_{wf} & 0 & 0 & 0 \\ 0 & M_{wf} & 0 & 0 \\ 0 & 0 & M_{wr} & 0 \\ 0 & 0 & 0 & M_{wf} \end{bmatrix} \begin{bmatrix} \ddot{x}_1 \\ \ddot{x}_3 \\ \ddot{x}_5 \\ \ddot{x}_7 \end{bmatrix} = \begin{bmatrix} -K_t & 0 & 0 & 0 \\ 0 & -K_t & 0 & 0 \\ 0 & 0 & -K_t & 0 \\ 0 & 0 & 0 & -K_t \end{bmatrix} \begin{bmatrix} DTD_1 \\ DTD_2 \\ DTD_3 \\ DTD_4 \end{bmatrix} - \begin{bmatrix} u_1 \\ u_2 \\ u_3 \\ u_4 \end{bmatrix},$$

$$DTD_i = x_j - x_{oi} , \quad i = 1, 2, 3, 4 , \quad j = 1, 3, 5, 7 \quad \dots(7.8)$$

or

$$\ddot{x}_b = Z_1 u , \quad Z_2 \ddot{x}_w = Z_3 DTD - u$$

hence,

$$DTD = Z_3^{-1} Z_2 \ddot{x}_w + Z_3^{-1} Z_1^{-1} \ddot{x}_b \quad \dots(7.9)$$

In this study the tyre stiffness is assumed to be the same for all four tyres. Hence, the inverse of the Z_3 matrix is simply

$$Z_3^{-1} = -\frac{1}{K_t} I \quad \dots(7.10)$$

The matrix Z_1 which contains system parameters and dimensions may be inverted in a symbolic form using an algebraic manipulation package, for example 'Reduce' [1985]. Then by storing Z_1^{-1} and Z_2 in the system software and having measurements of \ddot{x}_b and \ddot{x}_w available, equation (7.9) can be used to give a direct estimation of the DTD vector.

3- The final point to be studied in this section is the effect of the inclusion of the time delay in deriving the control law in the case of noisy measurements. This point can be studied by comparing the performance of the active system L .

with L_c or that of L_f with L_d . Here, only the latter case is considered. It can be seen from Figs. 7.15 to 7.17 how the time delay reduces dramatically the r.m.s. values of system L_f when compared with system L_d . For example, the r.m.s. values of the vertical, lateral and longitudinal seat accelerations, rear dynamic tyre load and the fore/aft and the lateral dynamic tyre load transfer are reduced by 5%, 9%, 18%, 55%, 14% and 5% respectively when system $L_f[1]$ is compared with system $L_d[1]$. On the other hand, the comparison between systems $L_f[4]$ and $L_d[4]$ in Table 7.5 ($SRE = 4.08 \times 10^{-3}$), shows that considering the time delay in the former system reduces the r.m.s values of the vertical, lateral and longitudinal seat accelerations, rear dynamic tyre load and the fore/aft and the lateral dynamic tyre load transfer by 7%, 7%, 35%, 44%, 10% and 4% respectively. It is however clear, that the improvements levels are still retained even if the SRE is increased from 0.001 to 0.00408. Hence, it can be concluded that under this operating condition, the measurement errors have no significant effect on the improvements achieved from incorporating the wheelbase time delay in the derivation of the control laws.

In practice, to achieve the performance level of any of these systems which either account for the time delay or which ignore it, there are two main requirements. It is necessary firstly, to estimate perfectly the sensors random error and use it to select or calculate (based on the vehicle speed and road roughness condition) the filter gains stored in the vehicle computer and secondly, to update the optimum estimates of the non-measurable states at small, discrete steps as time

progresses. However the first requirement is the most difficult one. A perfect knowledge of the sensors random error is not possible in practice and hence in general the calculations of the filter gains will be based on estimated values of measurement noise. Good practice as explained by Sharp and Wilson [1989] is to repeat the calculations for different estimates so that results obtained are not unreasonably specific and restricted.

7.6 Concluding remarks.

The accuracy of the time domain calculations was examined by comparing the r.m.s values of a linear passive system calculated in the frequency domain with those calculated based on the non-linear calculations scheme explained in section 2.5. The results were also checked using a variable-order variable-step Adams method in program VDAS, Horton [1988]. The following comments are drawn:

1- Good agreement between the two programs was found although small differences occurred when the profile No. 3 was used (8192 points). However the program explained in section 2.8 was found to be more accurate in this condition.

2- The accuracy as the solution obtained from profile No. 1 (1024 points) was not too far from that obtained for profile No. 3 (8192 points) when compared with the linear results obtained in the frequency domain, but in order to achieve the best agreement profile No. 4 (16384 points) must be used.

The novel application of the gradient search technique in deriving the control law of the active system incorporating the effect of the time delay showed the following:

- 1- It is possible to generate control laws which account for the wheelbase time delay without the need to estimate the time delay states η (using the Kalman filter algorithm) or to calculate them on line. Furthermore, the road input information is omitted from these control laws. The results therefore represent the most practical control law available in the literature which accounts for the wheelbase time delay.
- 2- The comparison of the performance of the active system L_b which uses this control law with system L_a which differs only in that the time delay is ignored, showed that the former system reduces the vertical and longitudinal accelerations, front and the rear dynamic tyre load, fore/aft and the lateral tyre load transfer by 10%, 8%, 12%, 6%, 13% and 11% respectively at the expense of increasing the lateral seat acceleration by 6%.

The analysis of the performance capabilities of the active systems which have control strategies based on the Kalman filter algorithm showed the following:

- 1- As the measurement error increased, the suspension performance deteriorated. For example, in system L_c , as sensor random error increased from 0.001 to 0.00408, the vertical, lateral and longitudinal accelerations increased by 8%, 21% and 16% respectively.
- 2- In the case where the measurement error is minimised, there was no difference between the performance level of systems

L_d and L_f (which require only the measurements of wheel - body relative velocities) and those of systems L_c and L_e , respectively although the latter two systems require the measurements of wheel-body relative displacements and velocities and the wheel-ground relative displacements. In general, the results showed that these active systems are more sensitive to the measurement errors than the number of the states to be measured.

3- A practical method to overcome the problems arising from the need to measure the wheel-ground relative displacements in system L_c and L_e has been proposed. In this method, the measurement system is modified to allow these relative displacements to be estimated after measuring the vertical acceleration of the body and wheel connection points.

4- The effect of including the wheelbase time delay in deriving the control laws for the case of noisy measurements was obtained by comparing the performance of system L_f with L_d . The results showed that the inclusion of the time delay substantially improves the performance of the system L_f . This improvement was not affected significantly as the sensor random error increased.

Table 7.1 Limited state feedback active suspension systems studied.

| System | Full state feedback State vector | Measurements | Control strategy |
|--------|--|--|---------------------------------|
| L_a | $[x_i, \dot{x}_i, x_{ok}]^T$ $i = 1, 2, \dots, 8$ $k = 1, 2, 3, 4$ | Perfect measurements of all states at body and suspension connection points x_i, \dot{x}_i | Gradient search |
| L_b | $[x_i, \dot{x}_i, x_{ok}, \eta_k]^T$ $i = 1, 2, \dots, 8$ $k = 1, 2, 3, 4$ | As in L_a | Gradient search with time delay |
| L_c | $[z_b, \theta, \phi, x_j, \dot{z}_b, \dot{\theta}, \dot{\phi}, \dot{x}_j, x_{ok}]^T$ $j = 1, 3, 5, 7$ $k = 1, 2, 3, 4$ | Noisy measurements of all wheel to ground displacements, body to wheel displacements and velocities $x_j - x_{ok}, \dot{x}_j - \dot{x}_{j,1}$ | Kalman filter |
| L_d | As in L_c | Noisy measurements of body/wheel velocities $\dot{x}_j - \dot{x}_{j,1}$ | Kalman filter |
| L_e | $[z_b, \theta, \phi, x_j, \dot{z}_b, \dot{\theta}, \dot{\phi}, \dot{x}_j, x_{ok}, \eta_k]^T$ $j = 1, 3, 5, 7$ $k = 1, 2, 3, 4$ | As in L_c | Kalman filter with time delay |
| L_f | As in L_e | As in L_d | Kalman filter with time delay |

Table 7.2 R.m.s values of the seat accelerations, front and rear dynamic tyre load and the front and rear working space calculated in the frequency domain for the passive system of $K_f = 24.2 \text{ kN/m}$ and $DR = 0.5$.

| Root mean square values calculated when the road of $R_c = 3 \times 10^{-6}$ was traversed at 30 m/s. | | | | | | |
|---|-------------------------|-------------------------|---------------|---------------|-----------------|-----------------|
| \ddot{z}_x m/s^2 | \ddot{y}_x m/s^2 | \ddot{x}_x m/s^2 | $FDTL$ N | $RDTL$ N | sws_f cm | sws_r cm |
| 1.64 | 0.63 | 0.63 | 1518 | 1710 | 2.27 | 2.46 |

Table 7.3 R.m.s. values calculated for the passive system of $K_f = 24.2 \text{ kN/m}$ and $DR = 0.5$, by applying FFT on the time histories of the seat accelerations, dynamic tyre load and suspension working space. These results were obtained using the program explained in section 2.7.

| Profile No. | No. of points | Root mean square values calculated in the frequency range (0.3-15) Hz. | | | | | | |
|--------------------|----------------------|---|-------------------------|-------------------------|---------------|---------------|-----------------|-----------------|
| | | \ddot{z}_x m/s^2 | \ddot{y}_x m/s^2 | \ddot{x}_x m/s^2 | $FDTL$ N | $RDTL$ N | sws_f cm | sws_r cm |
| 1 | 1024 | 1.64 | 0.68 | 0.64 | 1574 | 1719 | 2.43 | 2.41 |
| 2 | 2048 | 1.66 | 0.72 | 0.60 | 1534 | 1712 | 2.18 | 2.34 |
| 3 | 8192 | 1.69 | 0.62 | 0.61 | 1527 | 1710 | 2.21 | 2.37 |
| 4 | 16384 | 1.63 | 0.63 | 0.64 | 1521 | 1707 | 2.29 | 2.44 |

Table 7.4 R.m.s. values calculated for the passive system of $K_f = 24.2 \text{ kN/m}$ and $DR = 0.5$, by applying FFT on the time histories of the seat accelerations, dynamic tyre load and suspension working space. These results were obtained using the program VDAS, Horton [1988].

| Profile No. | No. of points | Root mean square values calculated in the frequency range (0.3-15) Hz. | | | | | | |
|----------------|------------------|---|-------------------------|-------------------------|---------------|---------------|-----------------|-----------------|
| | | \ddot{z}_x m/s^2 | \ddot{y}_x m/s^2 | \ddot{x}_x m/s^2 | $FDTL$ N | $RDTL$ N | sws_f cm | sws_r cm |
| 1 | 1024 | 1.65 | 0.68 | 0.65 | 1569 | 1716 | 2.43 | 2.39 |
| 2 | 2048 | 1.66 | 0.71 | 0.59 | 1509 | 1691 | 2.13 | 2.29 |
| 3 * | 8192 | 1.68 | 0.64 | 0.63 | 1527 | 1713 | 2.13 | 2.32 |

* The maximum No. of points in program VDAS is 8192 points.

Table 7.5 Effect of the measurement errors on the performance of the active system L_c , L_d , L_o and L_f . The r.m.s. values are calculated when profile No. 4 (16384 points) was traversed at 30 m/s.

| Active system | SRE | Root mean square values | | | | | | |
|---------------|-----------------------|----------------------------------|----------------------------------|----------------------------------|-----------|-----------|-------|-------|
| | | \ddot{z}_x m/s ² | \ddot{y}_x m/s ² | \ddot{x}_x m/s ² | FDTL N | RDTL N | FDTT | LDTT |
| L_c | 1×10^{-3} | 1.21 | 0.30 | 0.36 | 1407 | 1598 | 0.193 | 0.200 |
| | 1.49×10^{-3} | 1.22 | 0.30 | 0.37 | 1416 | 1598 | 0.192 | 0.200 |
| | 3.16×10^{-3} | 1.26 | 0.32 | 0.38 | 1416 | 1596 | 0.190 | 0.199 |
| | 4.08×10^{-3} | 1.32 | 0.38 | 0.43 | 1421 | 1623 | 0.190 | 0.200 |
| L_d | 1×10^{-3} | 1.21 | 0.29 | 0.36 | 1407 | 1595 | 0.195 | 0.200 |
| | 1.49×10^{-3} | 1.22 | 0.30 | 0.35 | 1403 | 1592 | 0.194 | 0.200 |
| | 3.16×10^{-3} | 1.26 | 0.34 | 0.38 | 1427 | 1600 | 0.192 | 0.201 |
| | 4.08×10^{-3} | 1.36 | 0.38 | 0.45 | 1423 | 1606 | 0.199 | 0.193 |
| L_o | 1×10^{-3} | 1.17 | 0.30 | 0.31 | 1402 | 777 | 0.171 | 0.191 |
| | 1.49×10^{-3} | 1.18 | 0.30 | 0.30 | 1407 | 780 | 0.172 | 0.192 |
| | 3.16×10^{-3} | 1.24 | 0.31 | 0.30 | 1409 | 805 | 0.174 | 0.188 |
| | 4.08×10^{-3} | 1.27 | 0.35 | 0.29 | 1417 | 891 | 0.177 | 0.188 |
| L_f | 1×10^{-3} | 1.18 | 0.29 | 0.31 | 1406 | 766 | 0.171 | 0.192 |
| | 1.49×10^{-3} | 1.18 | 0.28 | 0.31 | 1410 | 777 | 0.172 | 0.194 |
| | 3.16×10^{-3} | 1.26 | 0.28 | 0.30 | 1427 | 845 | 0.176 | 0.189 |
| | 4.08×10^{-3} | 1.26 | 0.36 | 0.29 | 1423 | 906 | 0.180 | 0.185 |

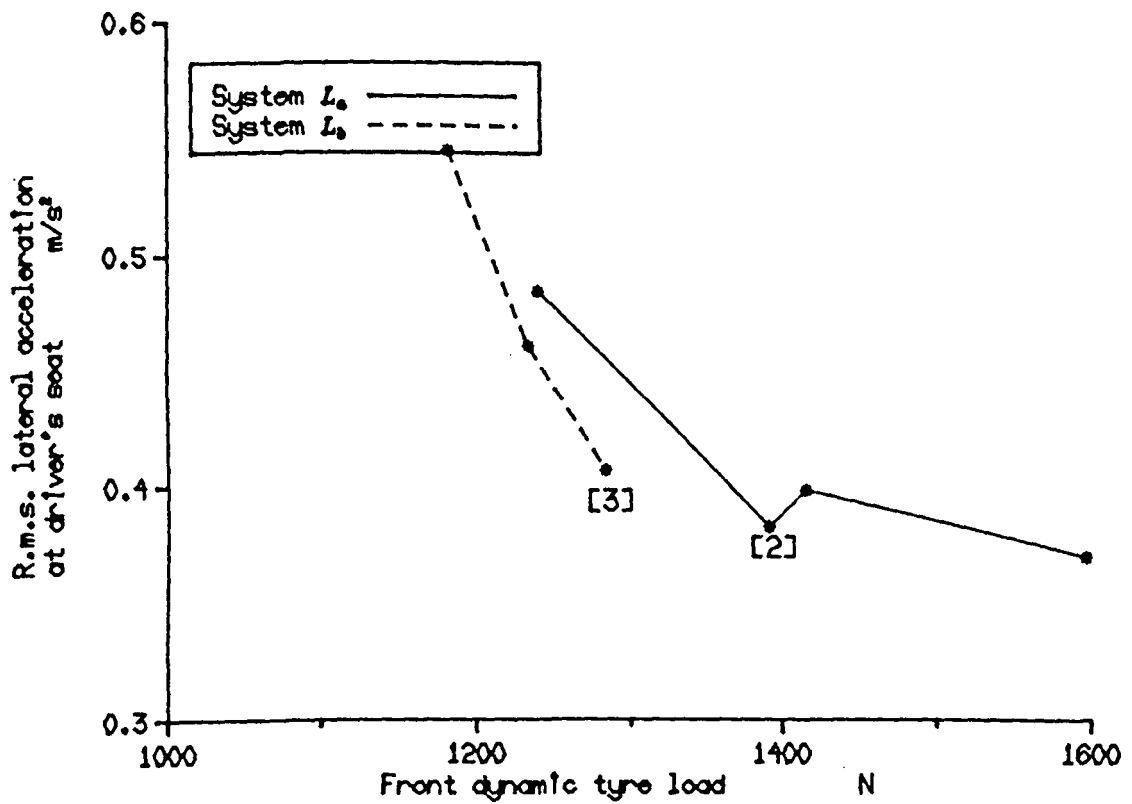
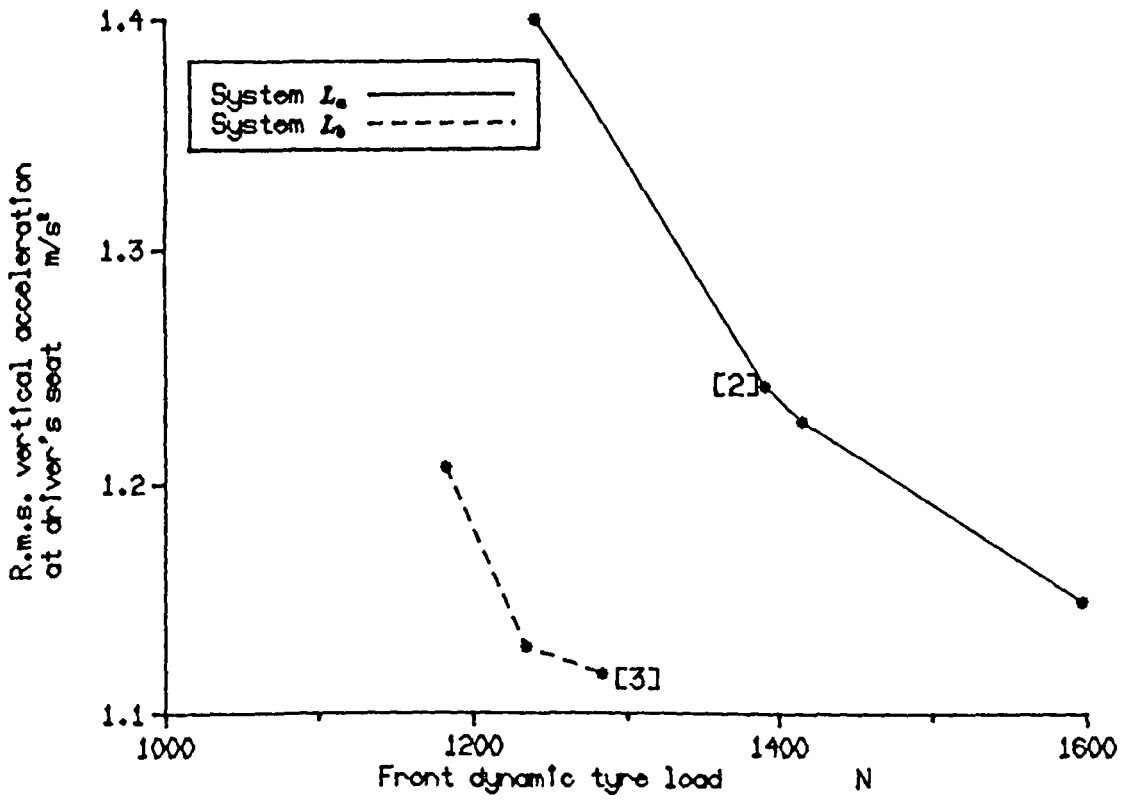


Fig. 7.1 R.m.s. values of the vertical and lateral accelerations of the systems L_0 and L_3 at a suspension working space usage of 2.5 cm r.m.s.

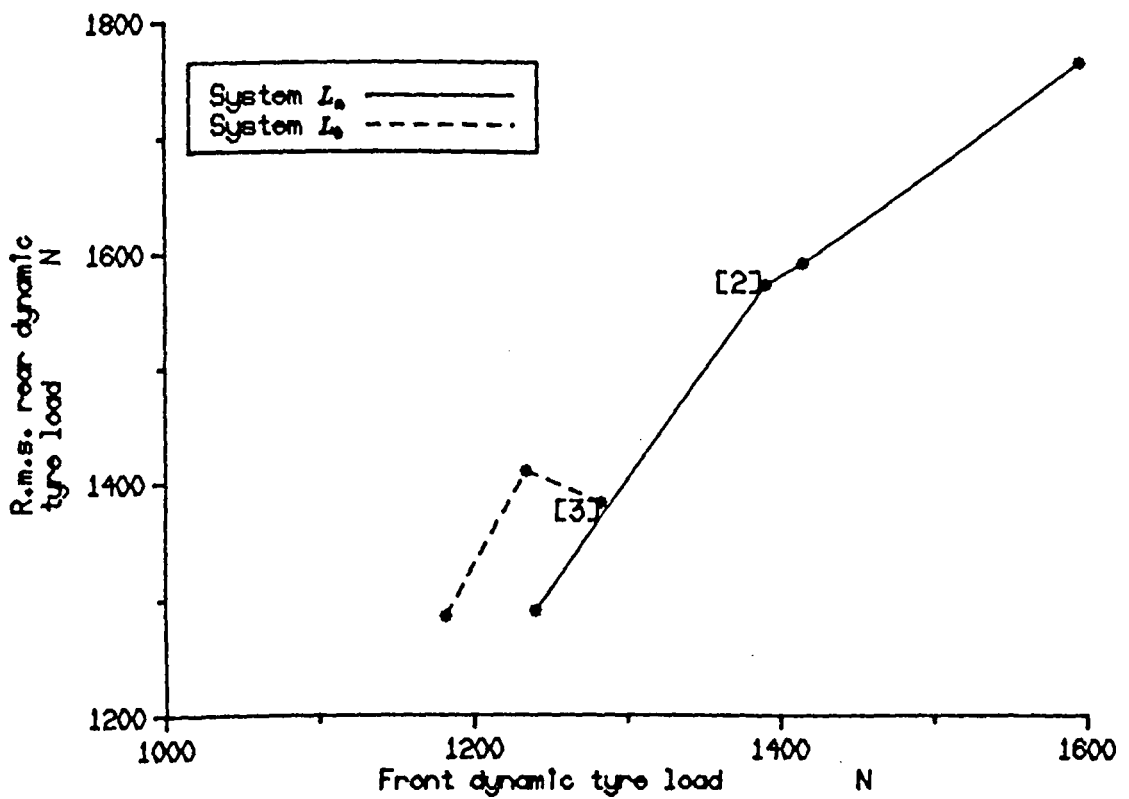
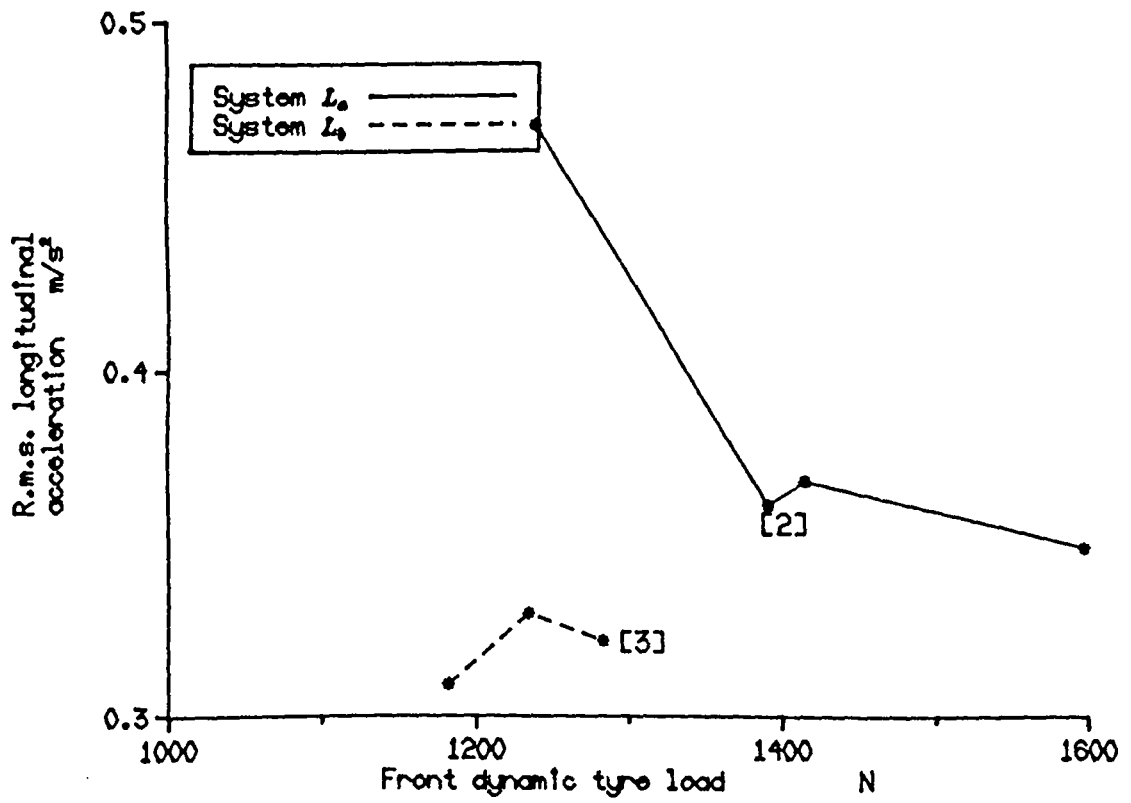


Fig. 7.2 R.m.s. values of the longitudinal acceleration and the rear dynamic tyre load of the systems L_a and L_e at a suspension working space usage of 2.5 cm r.m.s.

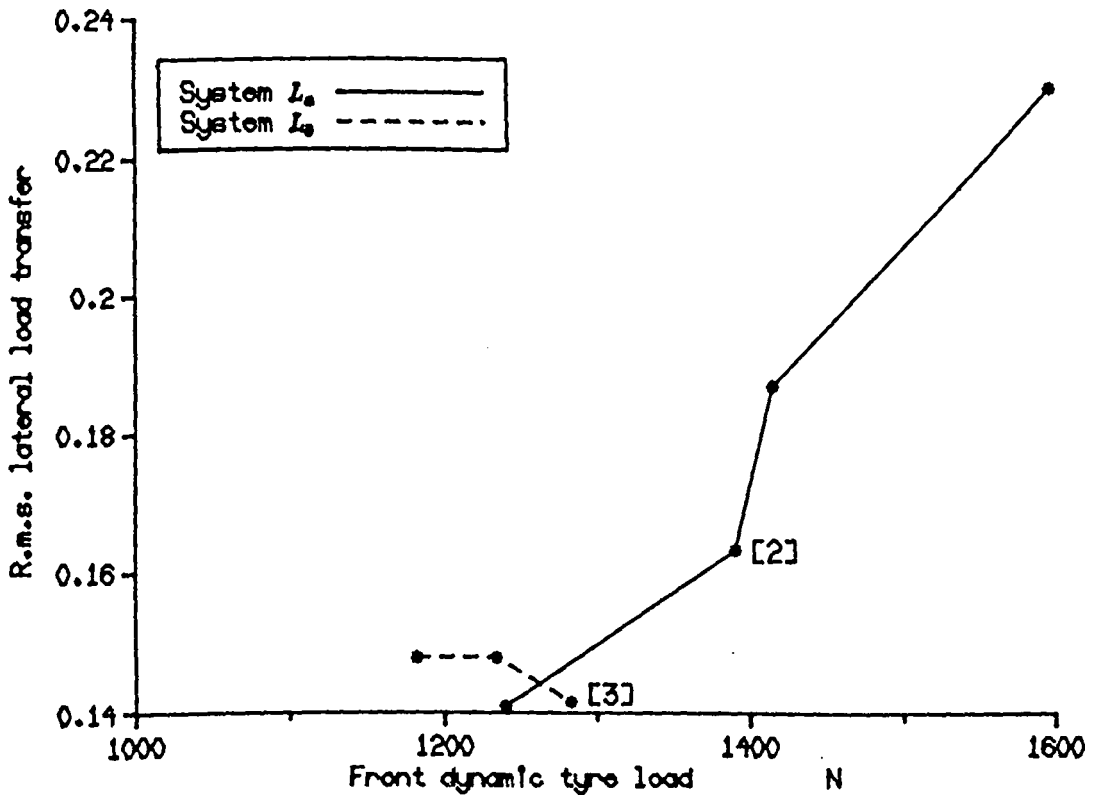
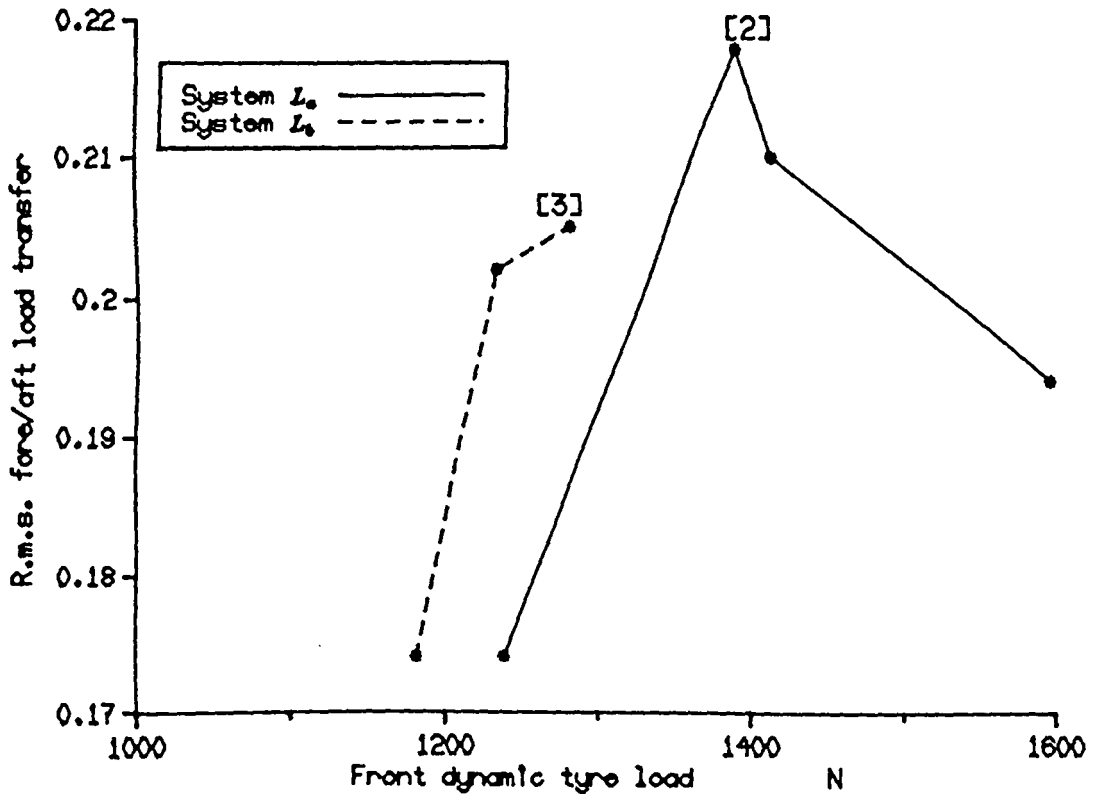


Fig. 7.3 R.m.s. values of the fore/aft and lateral tyre load transfer of the systems L_1 and L_2 at a suspension working space usage of 2.5 cm r.m.s.

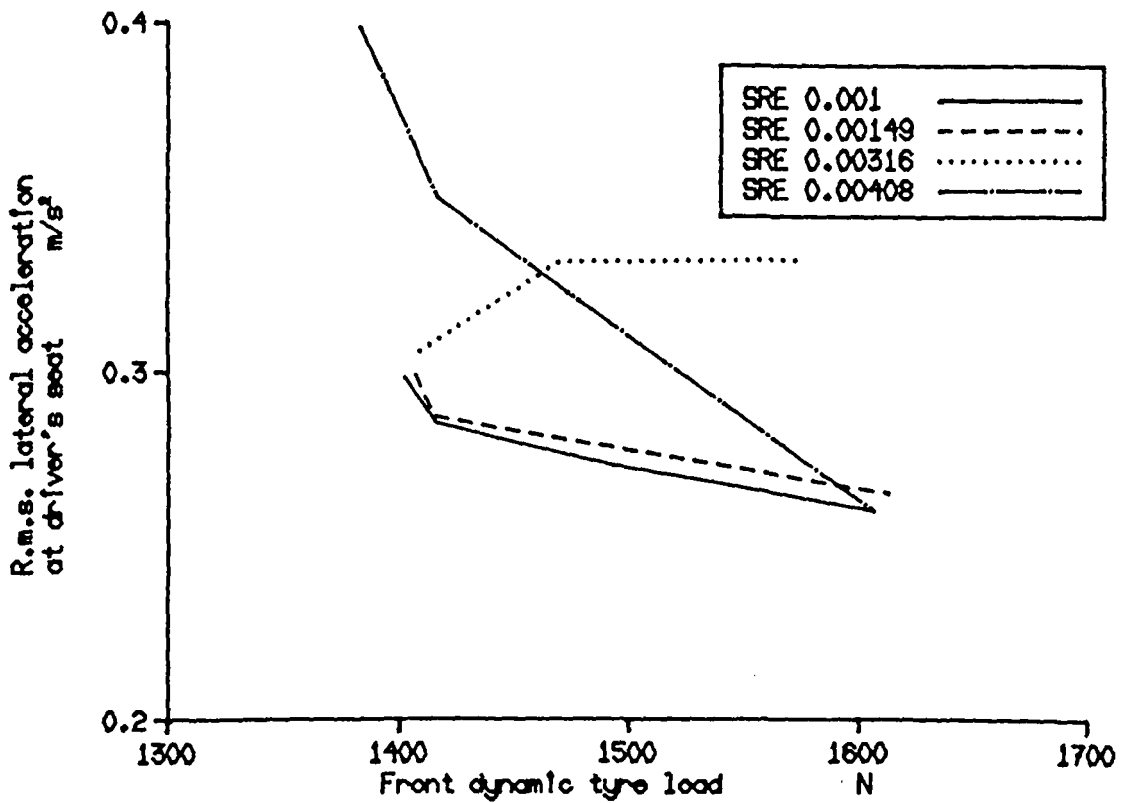
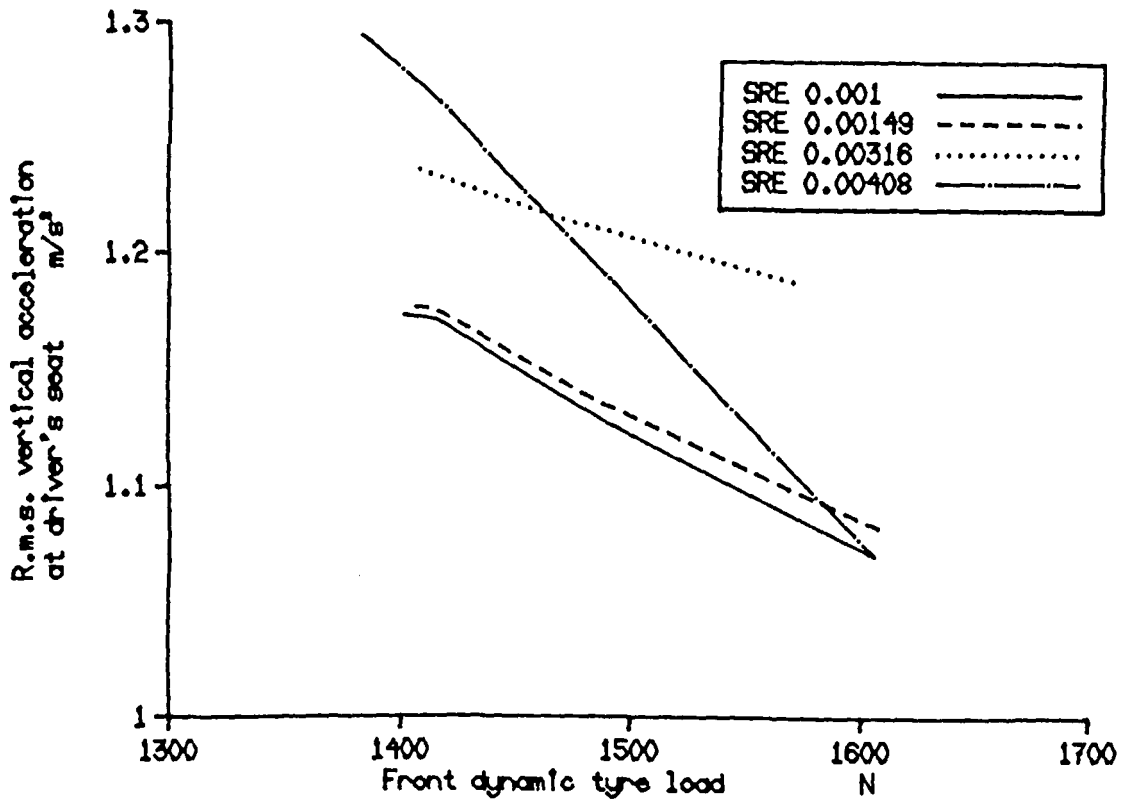


Fig. 7.4 R.m.s. values of the vertical and lateral accelerations of the system Z_0 , calculated for different values of the sensor random error (SRE) and for 2.5 cm working space.

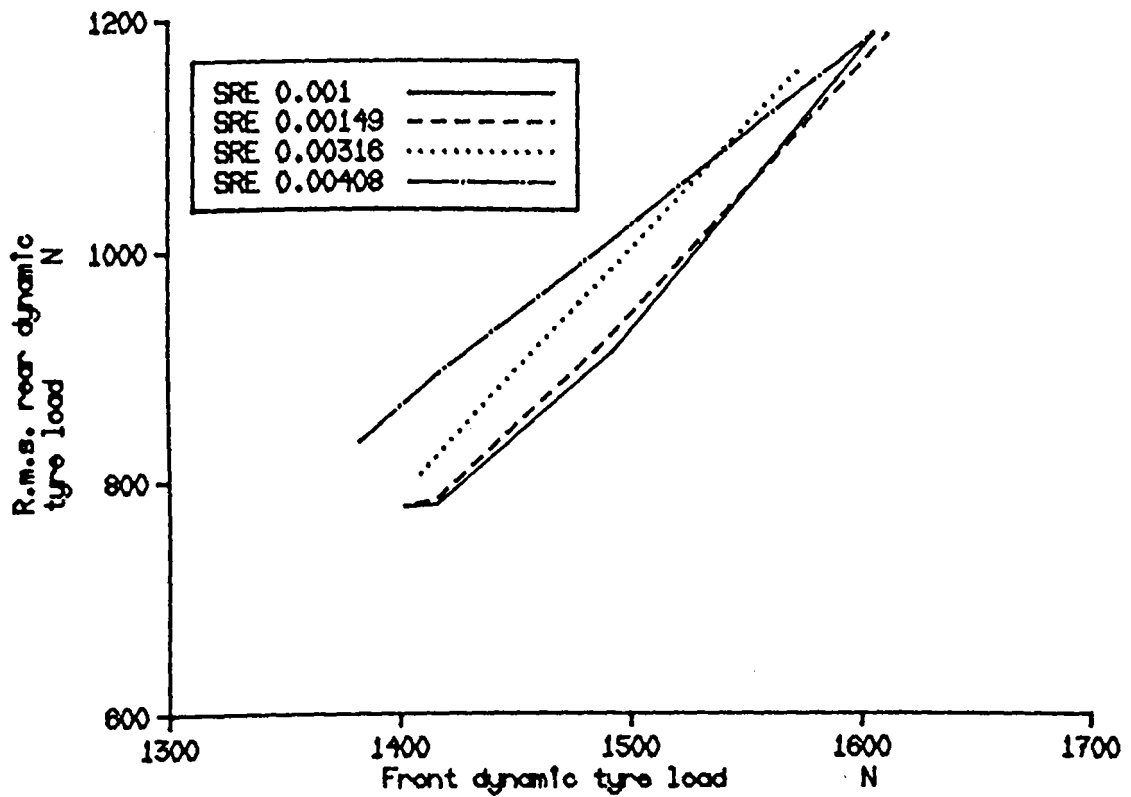
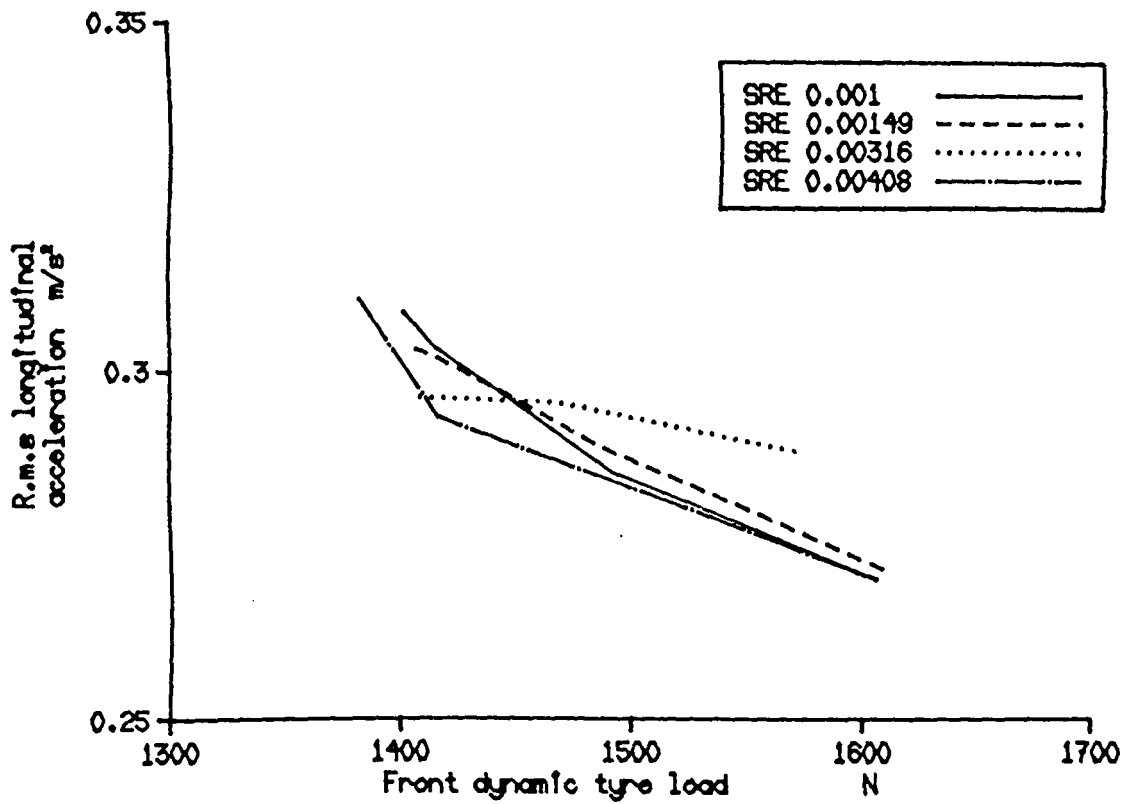


Fig. 7.5 R.m.s. values of the longitudinal acceleration and the rear dynamic tyre load of the system L_0 , calculated for different values of the sensor random error (SRE) and for 2.5 cm working space.

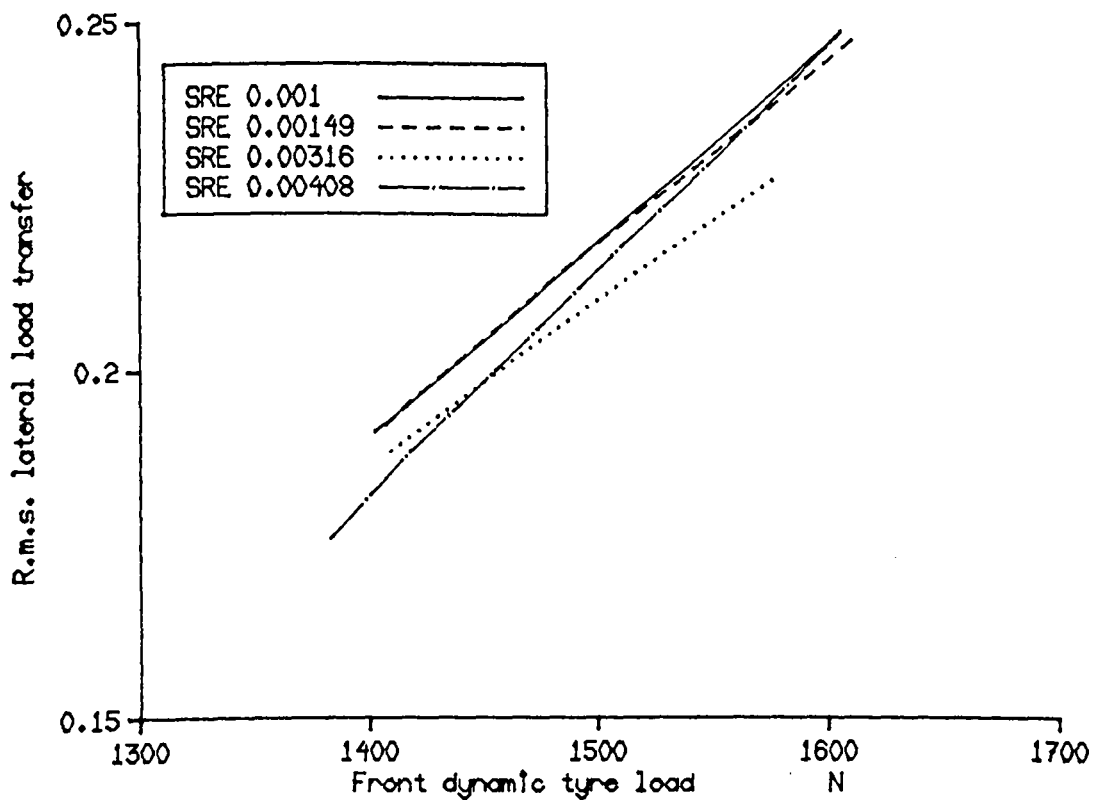
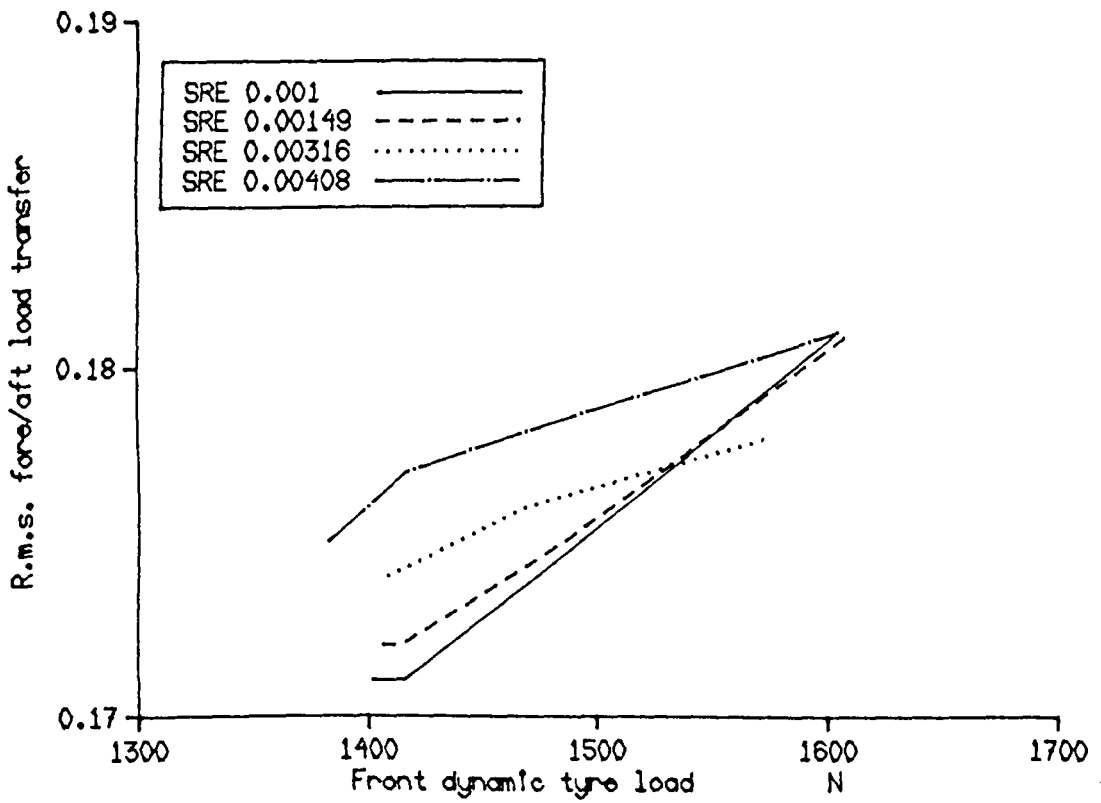


Fig. 7.6 R.m.s. values of the fore/aft and lateral tyre load transfer of the systems L_0 calculated for different values of the sensor random error (SRE) and for 2.5 cm working space.

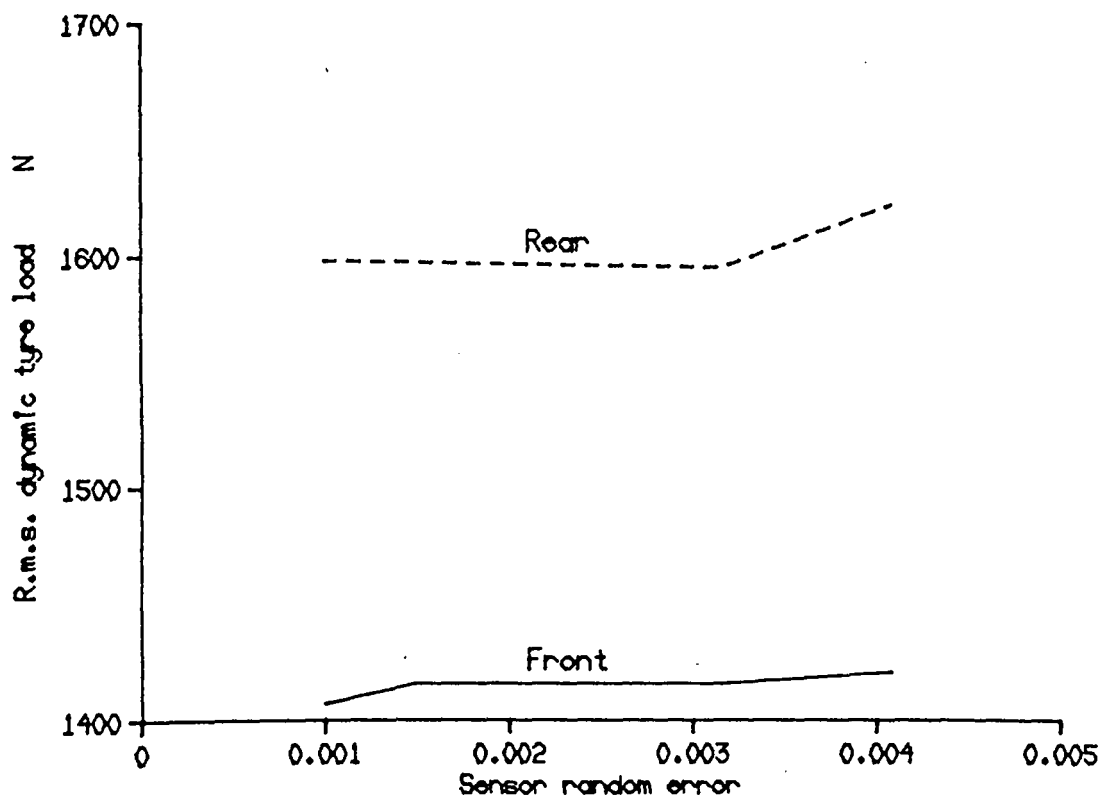
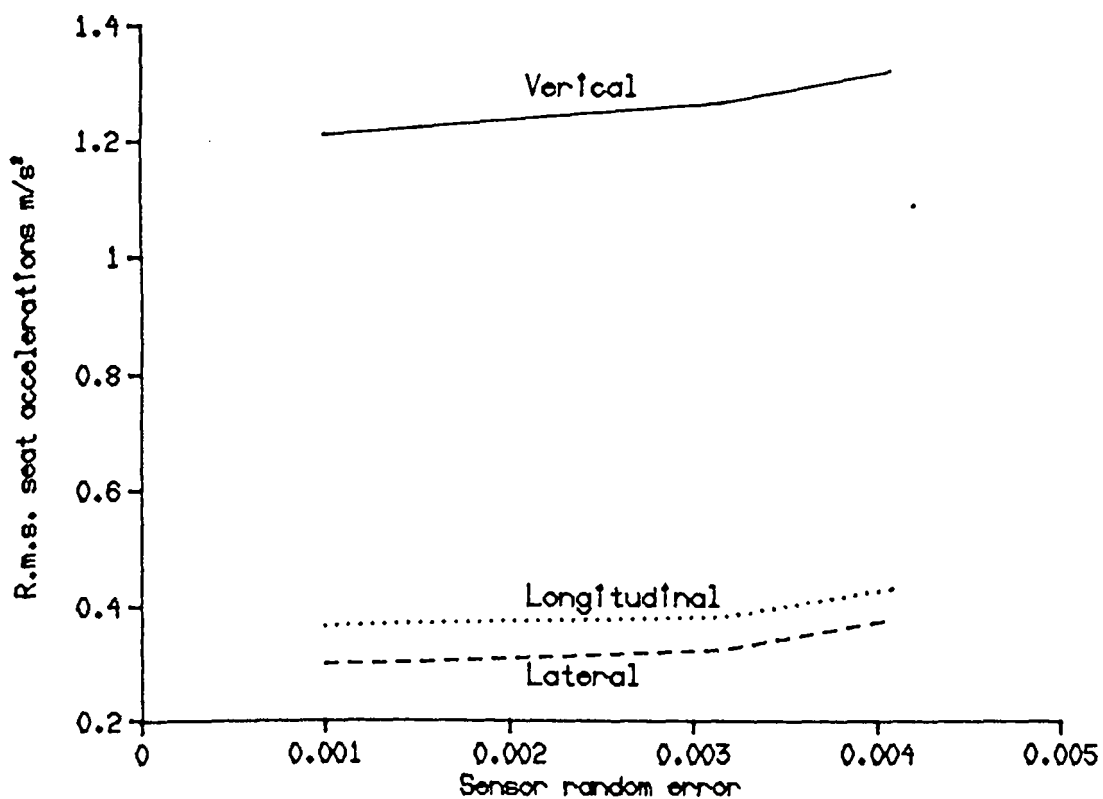


Fig. 7.7 The effect of the measurement errors on the performance of the active system L_a . The r.m.s. values were calculated when the profile No. 4 was traversed at 30 m/s and for 2.5 r.m.s. cm working space.

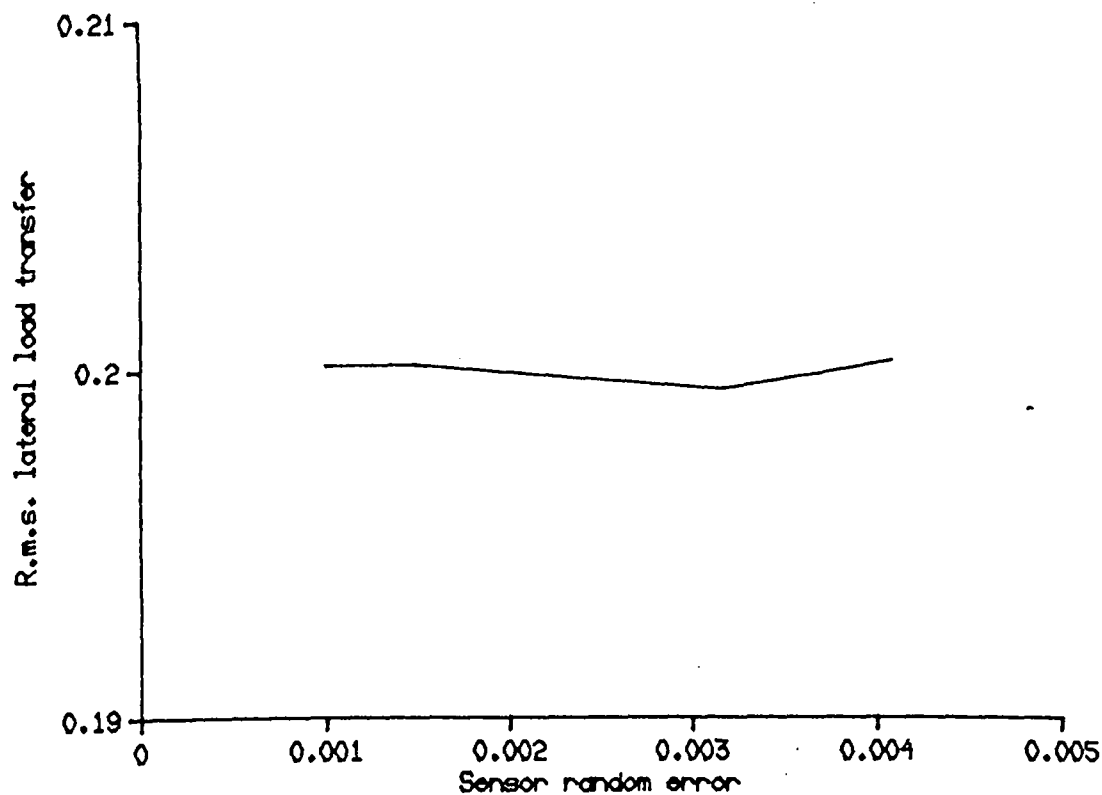
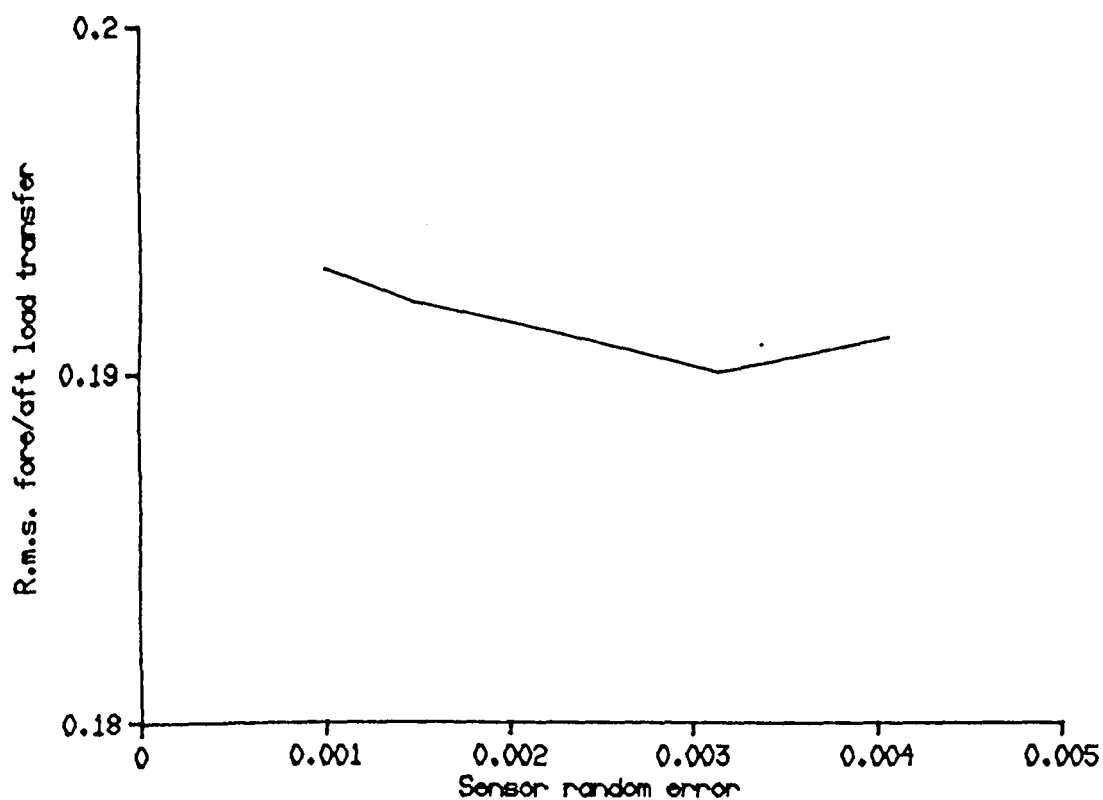


Fig. 7.8 The effect of the measurement errors on the performance of the active system L_0 . The r.m.s. values were calculated when the profile No. 4 was traversed at 30 m/s and for 2.5 r.m.s. cm working space.

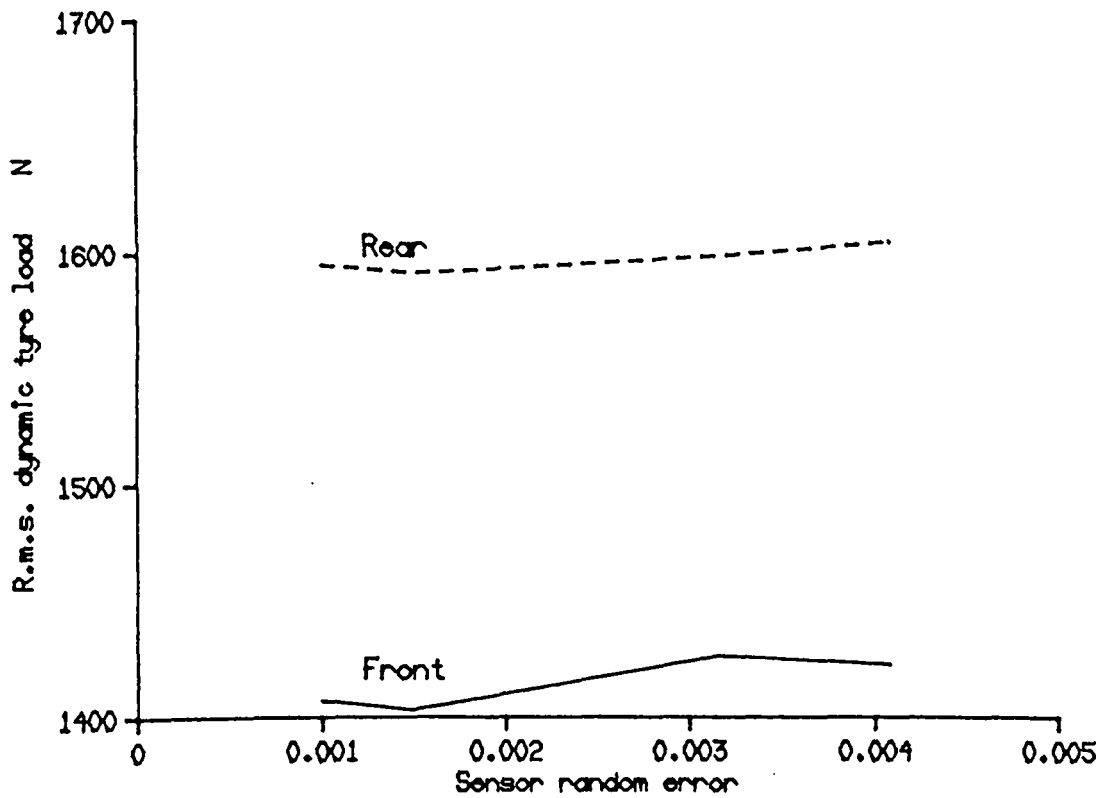
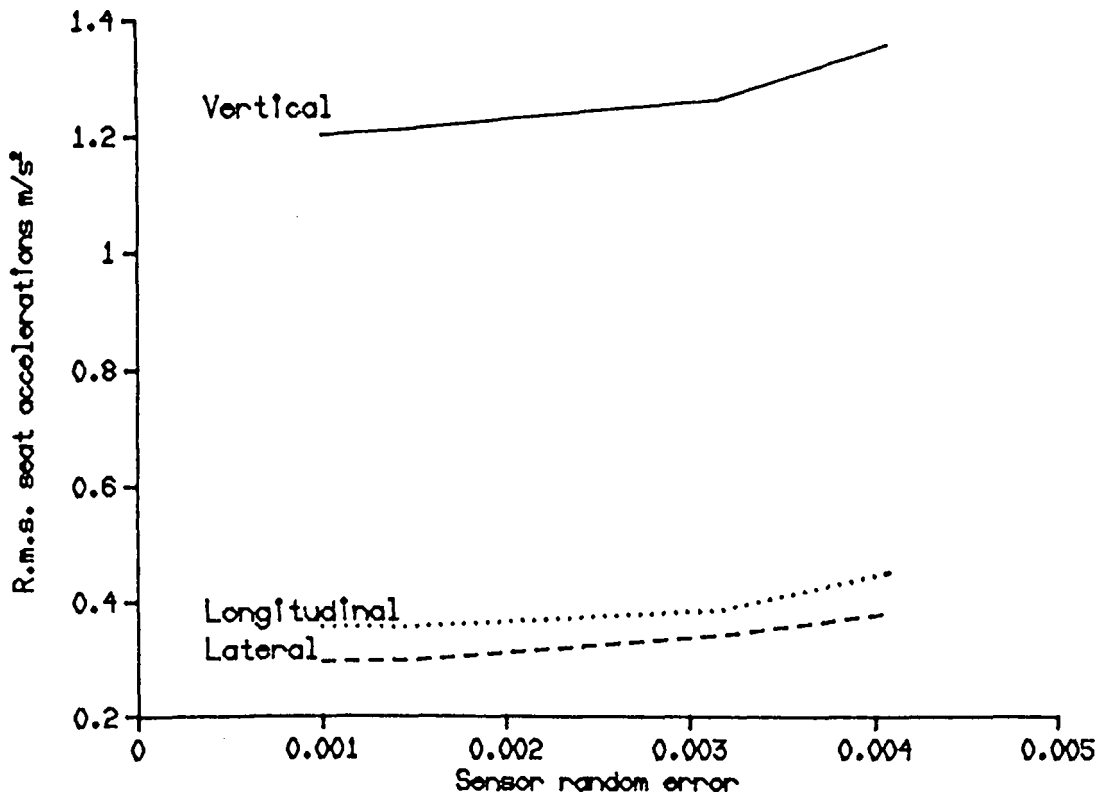


Fig. 7.9 The effect of the measurement errors on the performance of the active system L_4 . The r.m.s. values were calculated when the profile No. 4 was traversed at 30 m/s and for 2.5 r.m.s. cm working space.

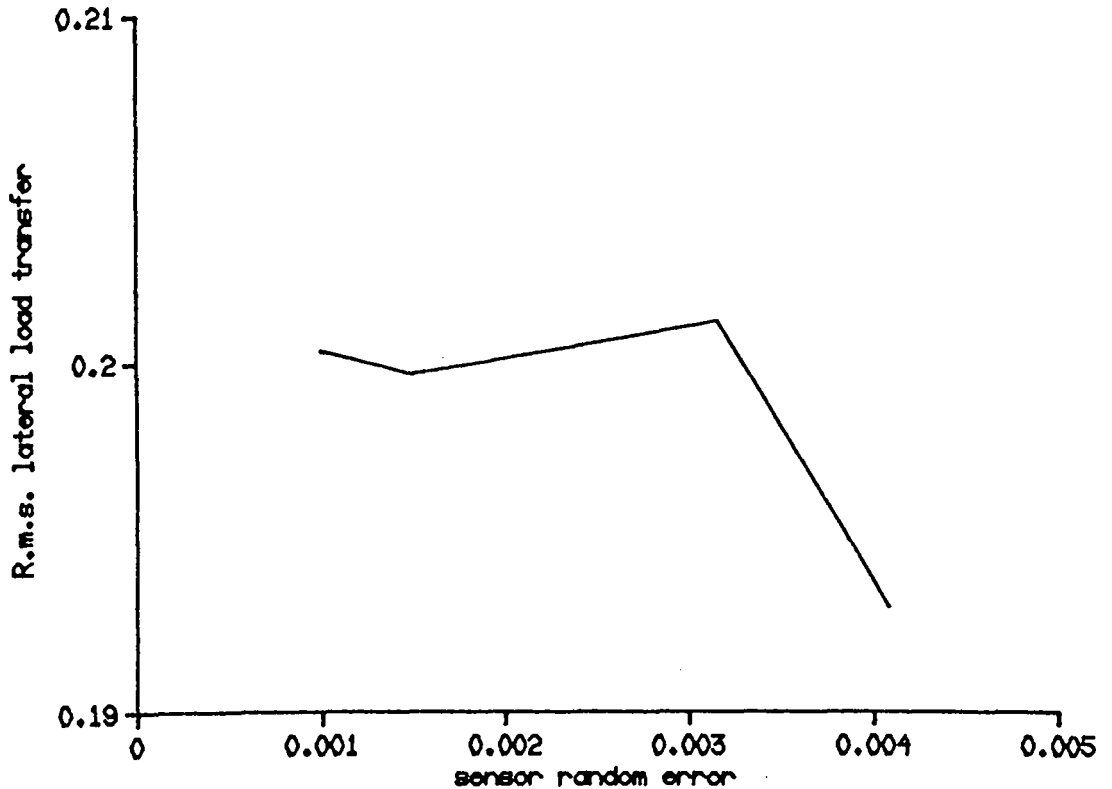
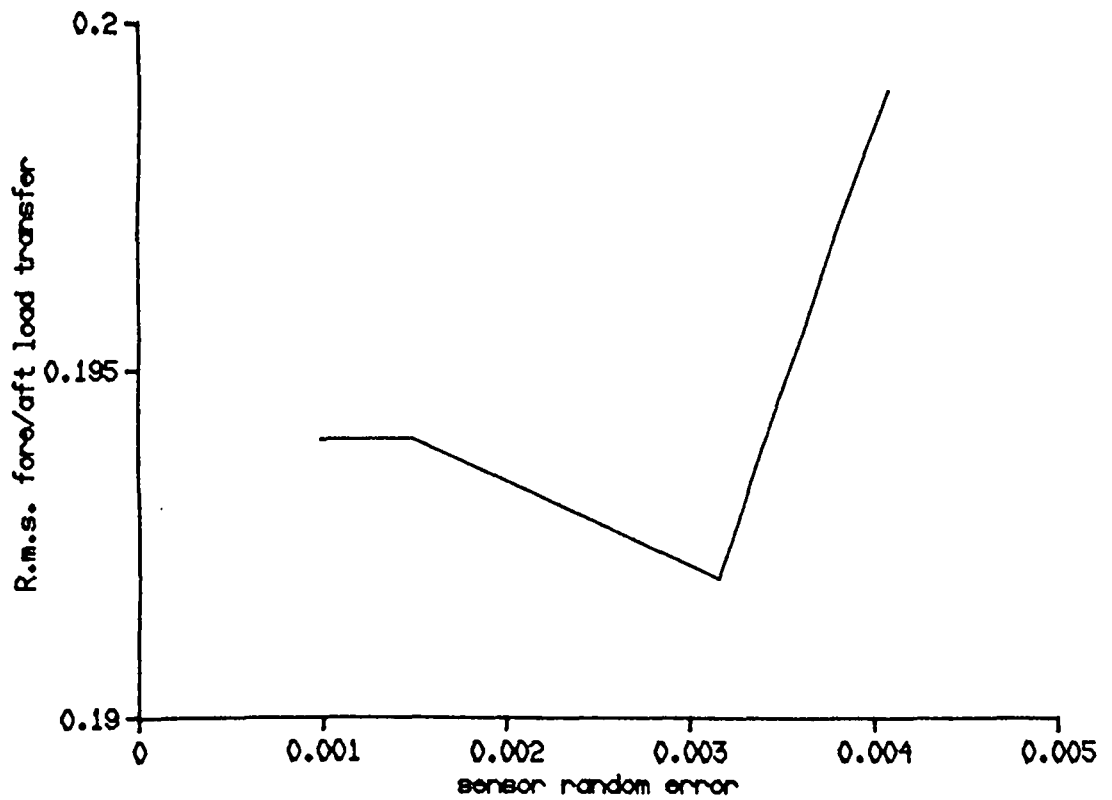


Fig. 7.10 The effect of the measurement errors on the performance of the active system L_4 . The r.m.s. values were calculated when the profile No. 4 was traversed at 30 m/s and for 2.5 r.m.s. cm working space.

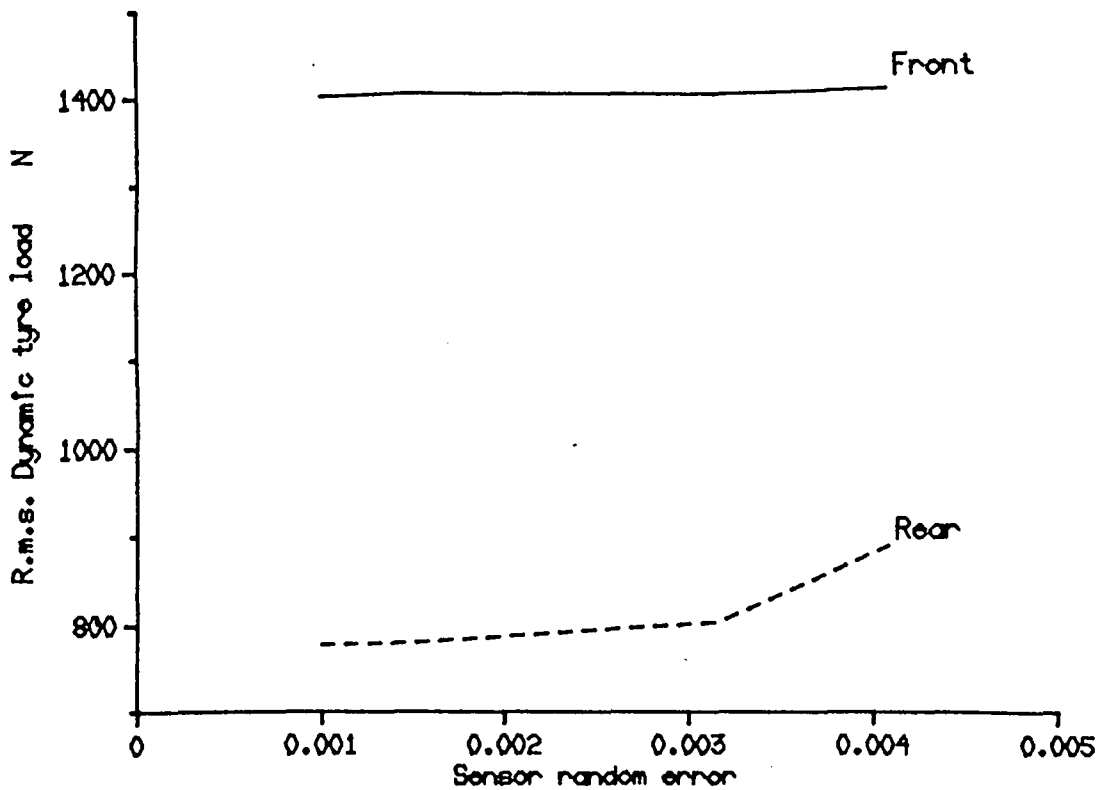
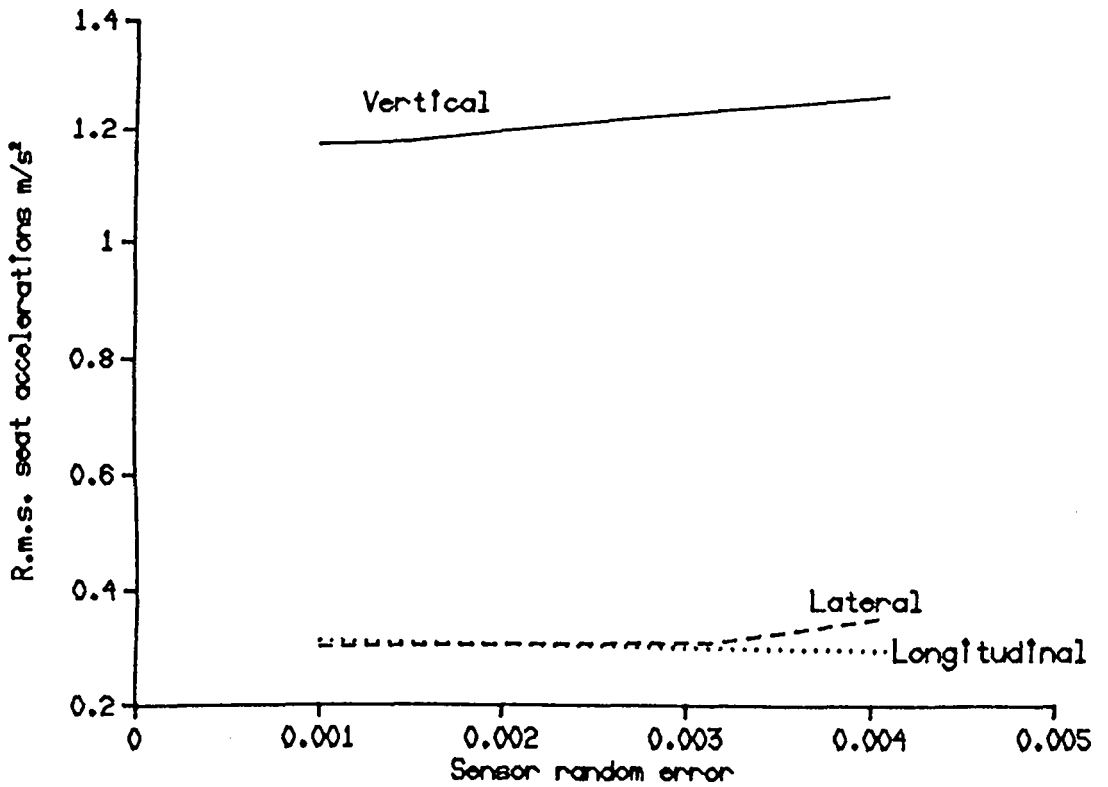


Fig. 7.11 The effect of the measurement errors on the performance of the active system L_s . The r.m.s. values were calculated when the profile No. 4 was traversed at 30 m/s and for 2.5 r.m.s. cm working space.

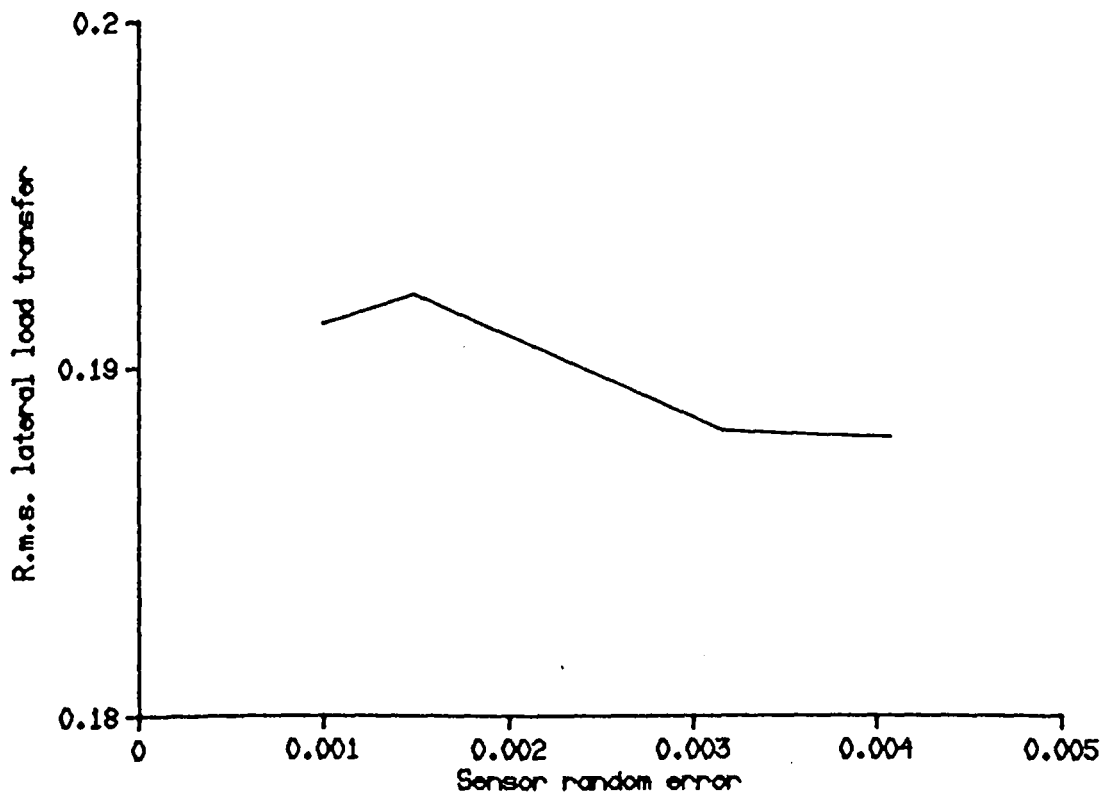
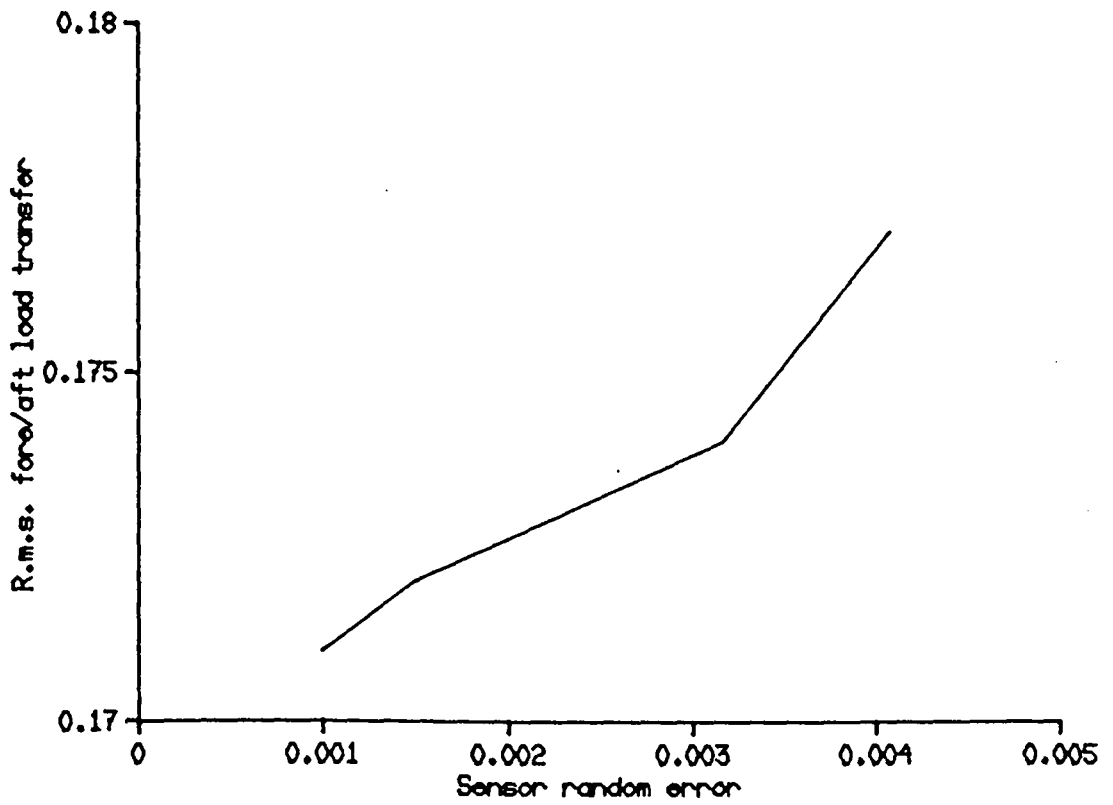


Fig. 7.12 The effect of the measurement errors on the performance of the active system L_0 . The r.m.s. values were calculated when the profile No. 4 was traversed at 30 m/s and for 2.5 r.m.s. cm working space.

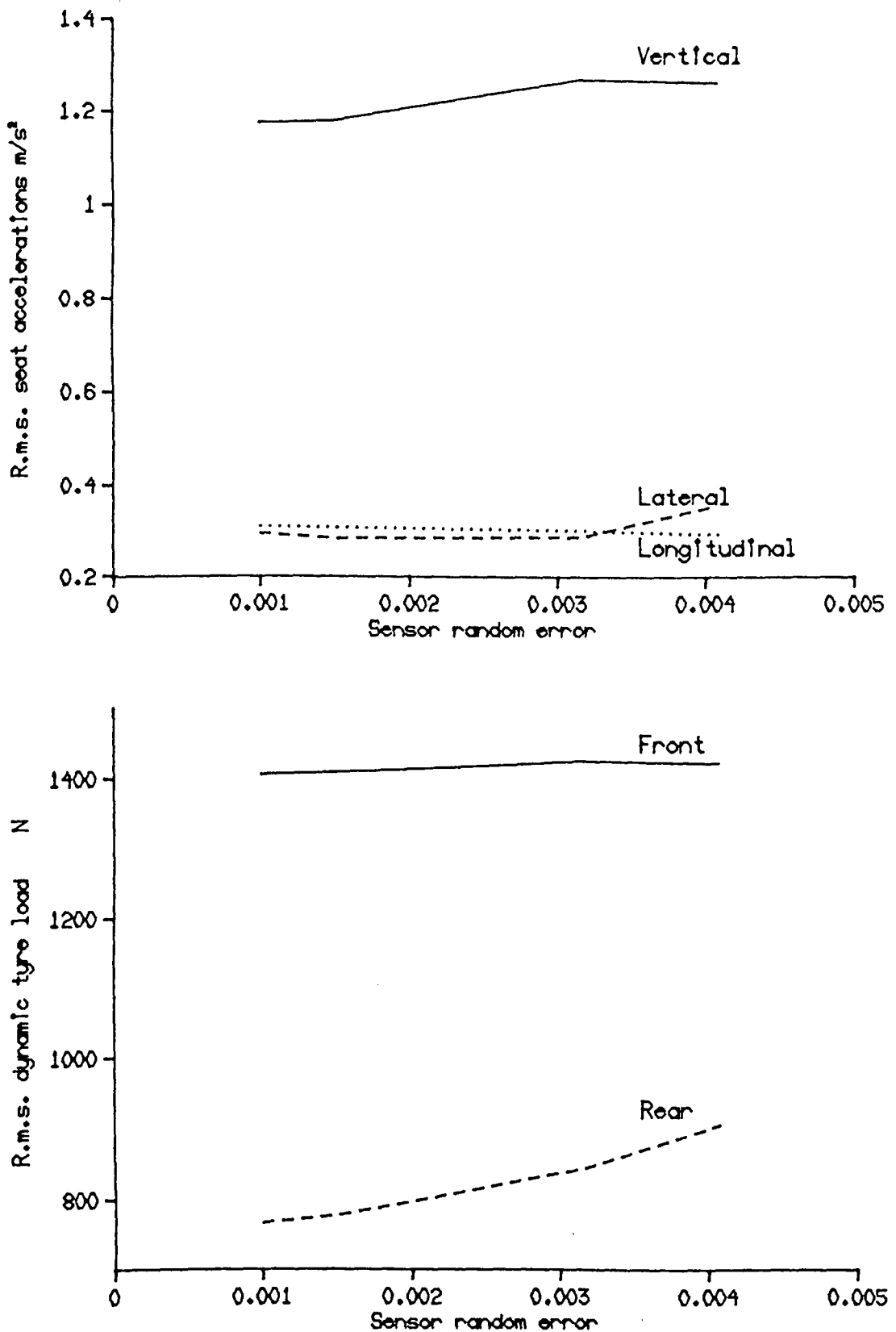


Fig. 7.13 The effect of the measurement errors on the performance of the active system L_p . The r.m.s. values were calculated when the profile No. 4 was traversed at 30 m/s and for 2.5 r.m.s. cm working space.

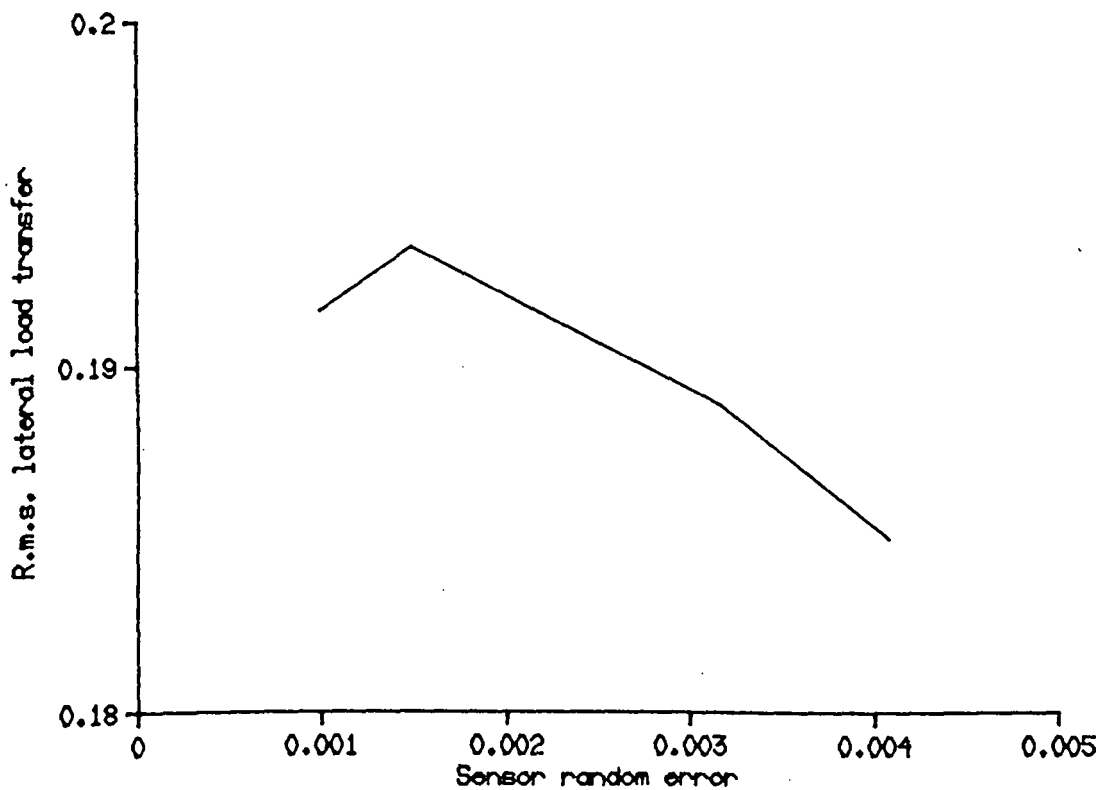
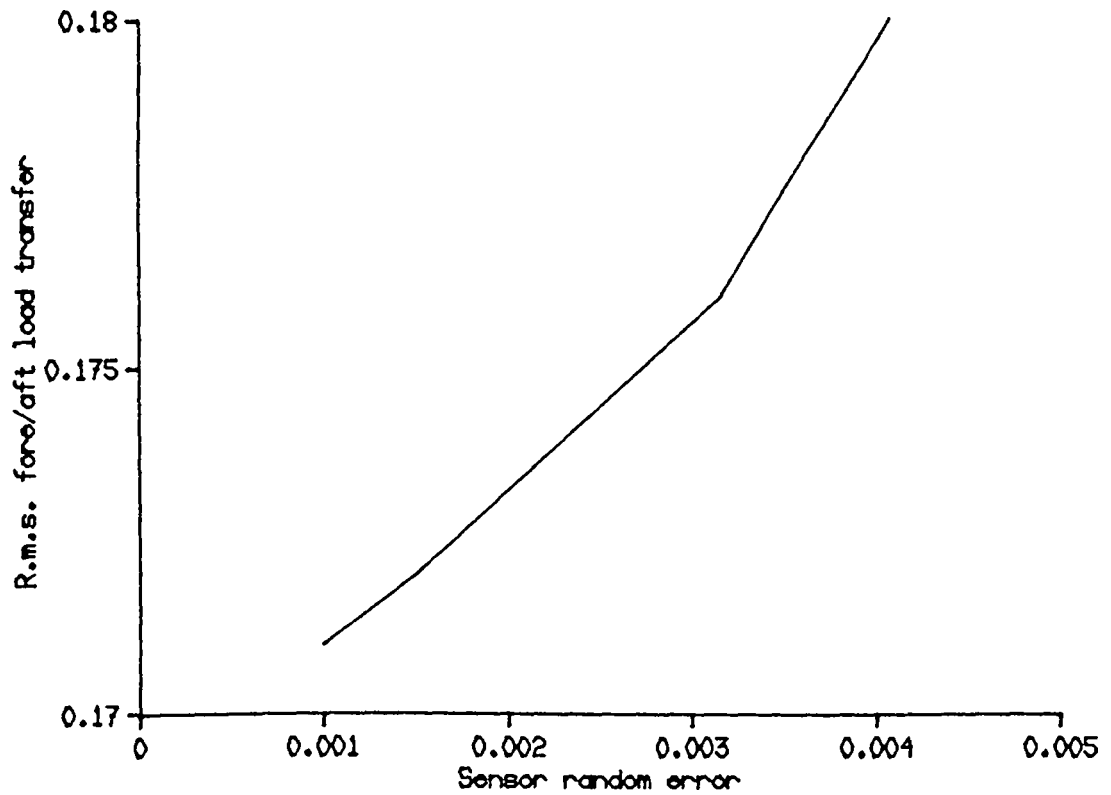


Fig. 7.14 The effect of the measurement errors on the performance of the active system L_p . The r.m.s. values were calculated when the profile No. 4 was traversed at 30 m/s and for 2.5 r.m.s. cm working space.

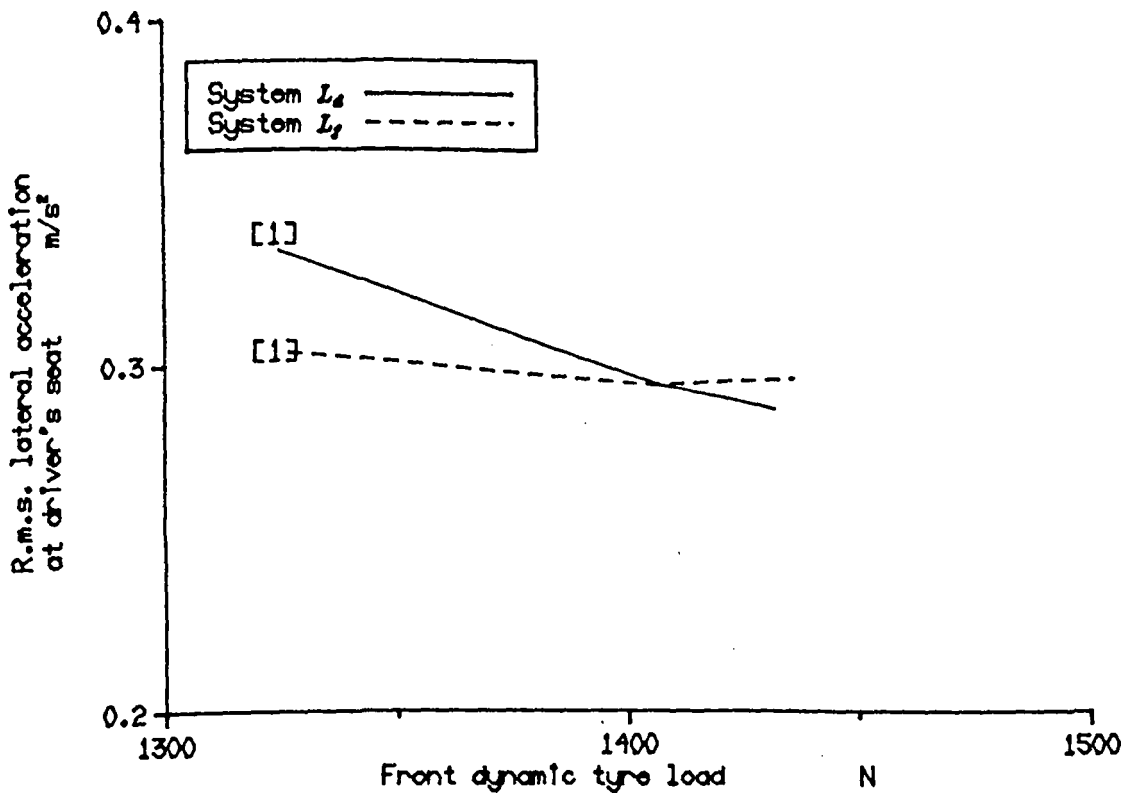
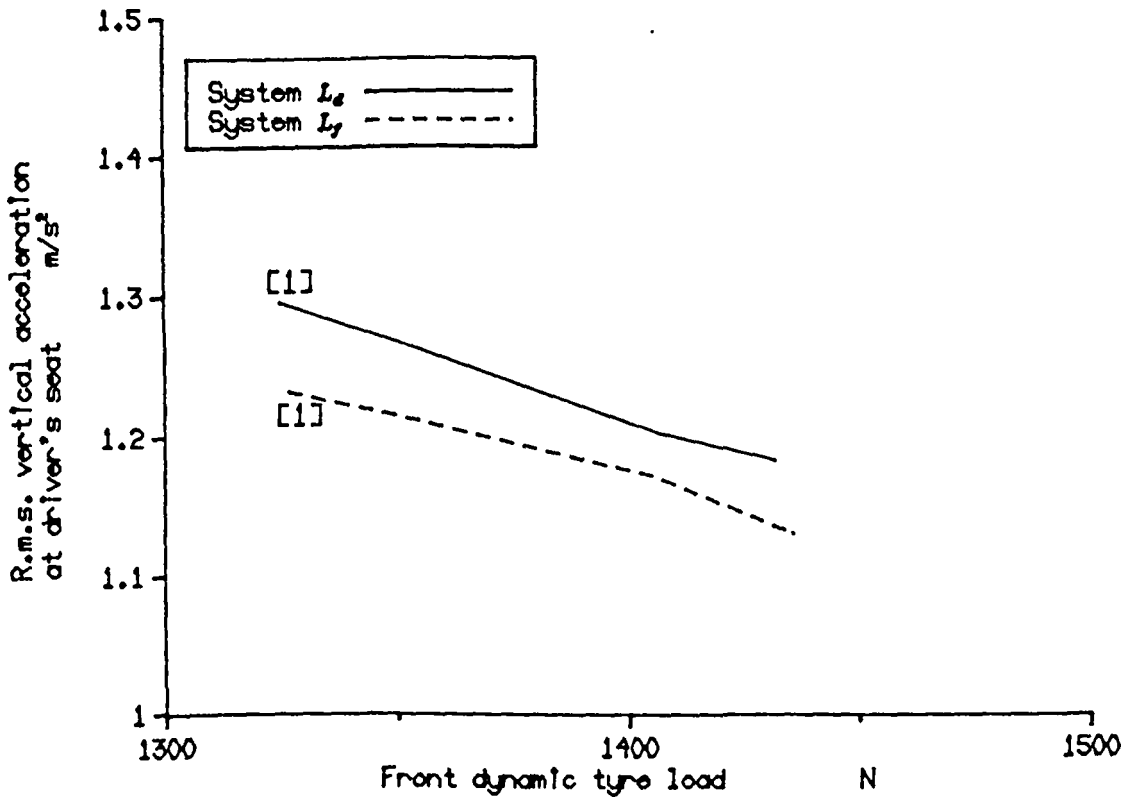


Fig. 7.15 Comparison of the performance of system L_f (which includes the effect of the wheelbase time delay) and L_e (which ignores this effect) for SRE = 0.001.

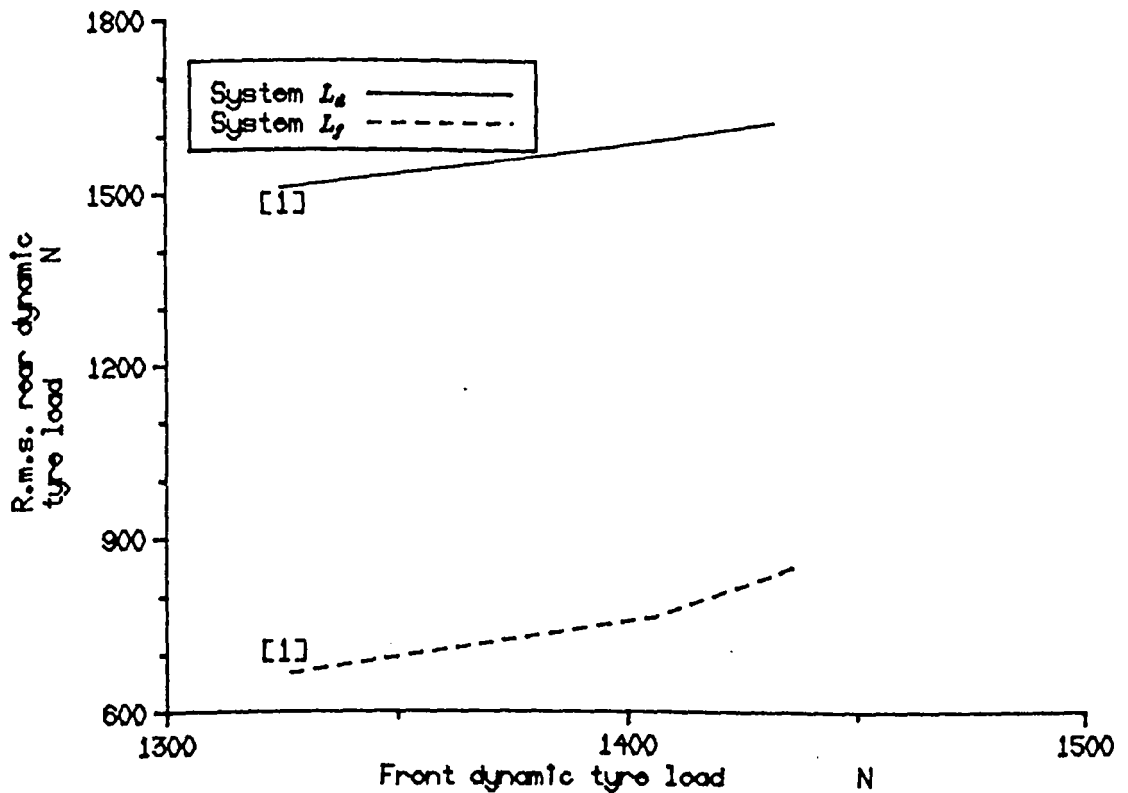
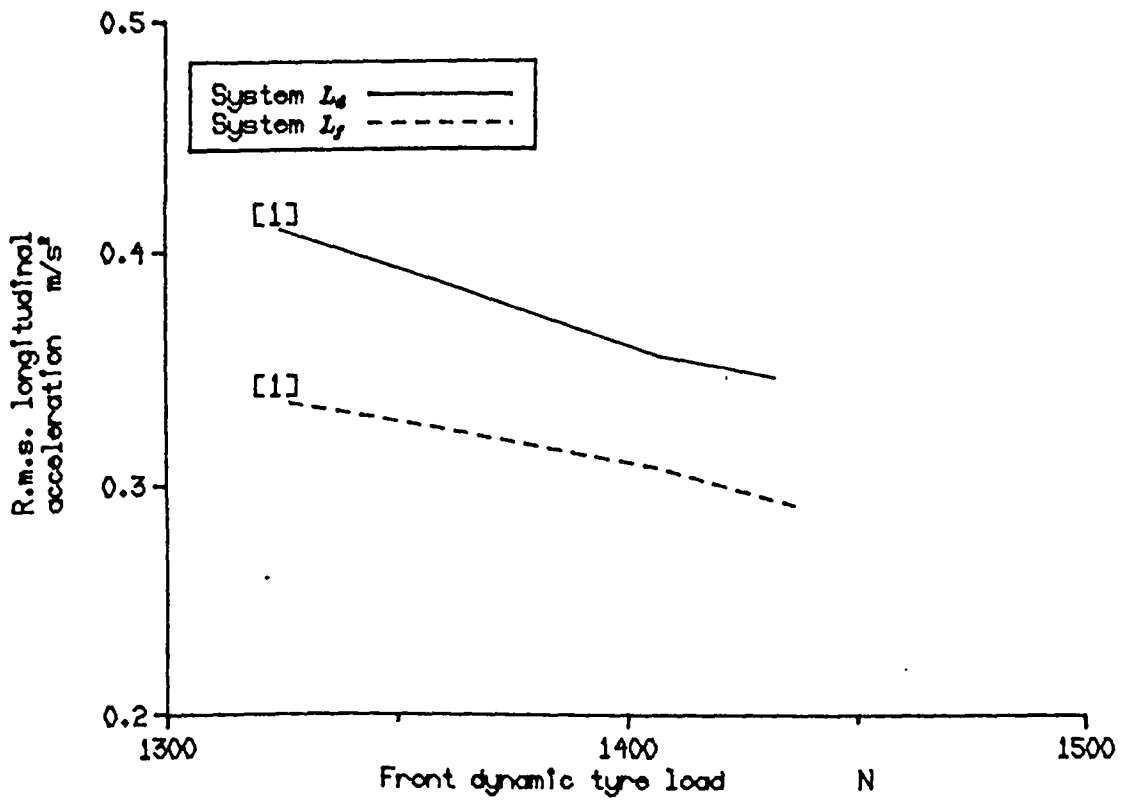


Fig. 7.16 Comparison of the performance of system L_7 (which includes the effect of the wheelbase time delay) and L_6 (which ignores this effect) for SRE = 0.001.

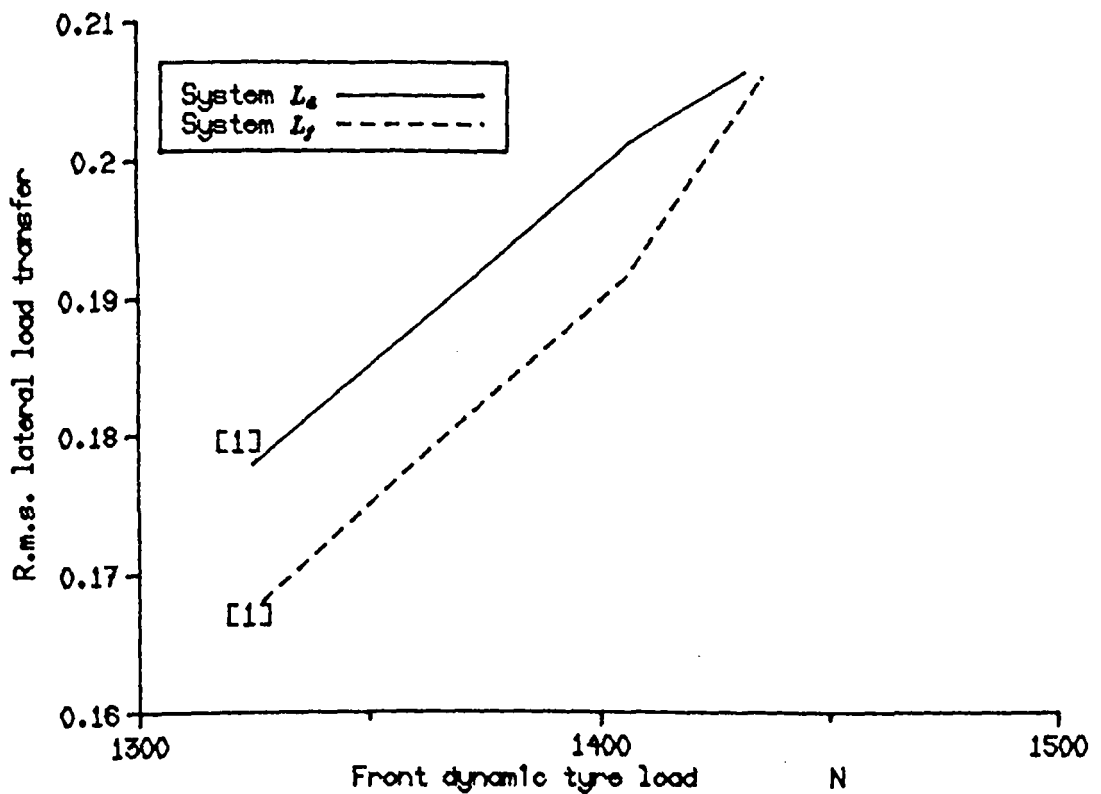
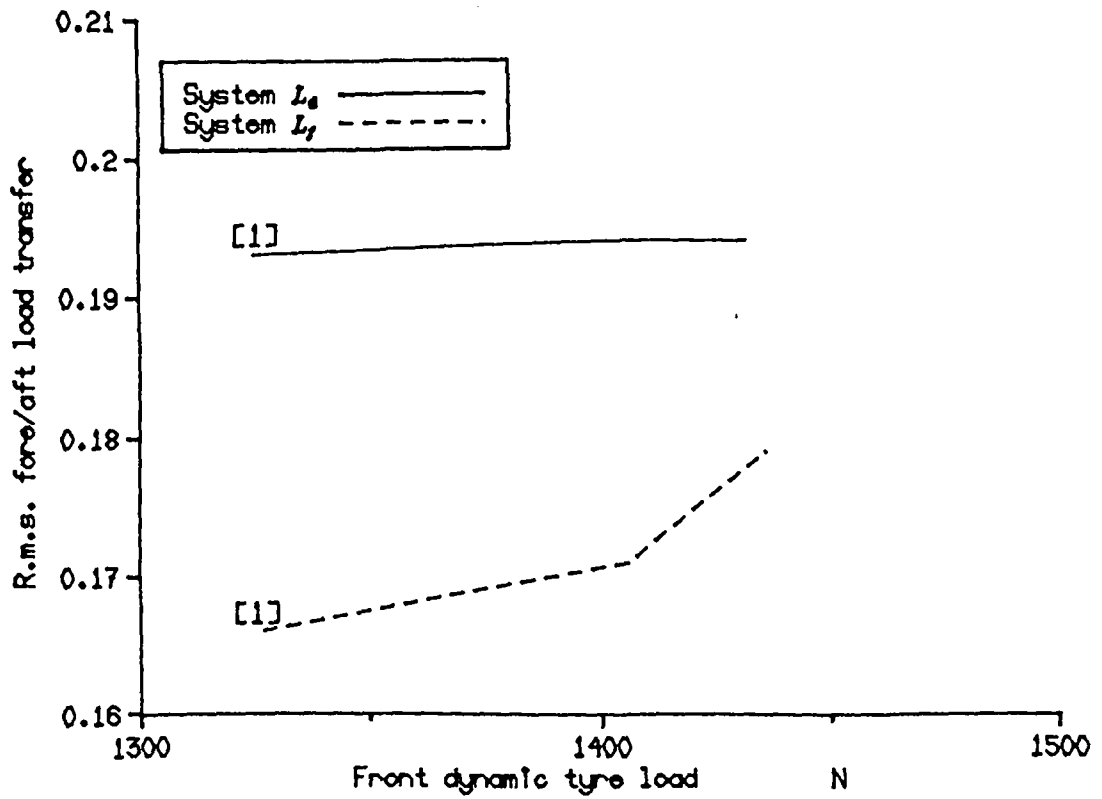


Fig. 7.17 Comparison of the performance of system L_f (which includes the effect of the wheelbase time delay) and L_s (which ignores this effect) for SRE = 0.001.

CHAPTER 8

PERFORMANCE COMPARISON OF PROPOSED SYSTEMS

8.1 Introduction

In Chapter 6 and Chapter 7, various control strategies have been applied to a 7 d.o.f. actively suspended vehicle model to study the ride behaviour of the active suspension systems. In this Chapter, it is intended to study the benefits which could be achieved from these systems when compared with the passive suspension systems. This study is important, particularly because of the confusion arising from previous attempts to compare relative performances of active and passive systems using a three dimensional vehicle model. This confusion may be interpreted as follows. In Barak and Sachs [1985] and Barak and Hrovat [1988], the active system was found to reduce r.m.s. seat acceleration by 87% when compared with the passive one, but their comparison was not revealing since the active system involved more than twice the working space and dynamic tyre load of those for the passive system. In a fair comparison based on an equal usage of working space, Chalasani [1986 b] found that the active system reduces the vertical acceleration by 15% when compared with a well designed passive system. However, in both Barak and Sachs and in Chalasani, the wheelbase time delay is ignored and perfect measurement of all the states including the road input displacement was assumed. The result of Fruhauf et al [1985] are different from either of the above authors. They showed that the active system without including the time delay offers reductions in the r.m.s.

values of the seat acceleration and the dynamic tyre load by 50% and 8% respectively although details of working space usage were not quoted. If the wheelbase time delay is included, these improvements become 75% and 16% respectively. Hence, it can be concluded that even on the basis of theoretical investigations it is still not clear how much the performance of well designed passive systems differs from the optimal active systems. The first important purpose on this Chapter is to attempt to clarify this comparison.

The next problem is to discuss the basis under which a comparison between the active and passive suspension systems may be made. As in Chapters 3 and 6, two techniques will be used i.e. comparison at equal usage of working space and comparison at different vehicle operating conditions. Because of the ability of the active systems to be adaptive to different speeds and road qualities, the comparison between these systems and the passive system at equal usage of working space is a justifiable comparison if the passive system employed is adaptive. On the other hand, if a fixed parameter passive system is employed, a more equitable basis for performance comparison is by considering different vehicle operating conditions, in which the active systems and the adaptive passive system are always able to consume all the available working space while it is impossible for the fixed parameter passive system to do so.

In addition to the comparison between the active systems and the passive systems, it is intended also to clarify the losses in the performance of the active systems due to employing

limited state feedback control strategies. Furthermore, it is also important to know the difference between the proposed strategies i.e. the Kalman filter algorithm and the gradient search technique from the point of view of both system performance and practical realisation.

8.2 Comparison of the performance at equal usage of working space.

8.2.1 Overall performance comparison.

In this section, the performances of some of the active systems discussed in Chapter 6 and Chapter 7 are compared with those obtained for the passive system in Chapter 3 when the road $R_c = 3 \times 10^{-6}$, $\kappa = 2.5$ is traversed at 30 m/s. Table 8.1 shows the active systems which are selected. In each suspension type, the system performance has been computed in terms of the r.m.s. values of the seat accelerations, dynamic tyre load and fore/aft and lateral tyre load transfer. Figs. 8.1 to 8.6 show these r.m.s. values for 2.5 cm r.m.s. working space, while Figs. 8.7 to 8.12 show the r.m.s. values of the passive system and the active systems a , b and e at 3 cm r.m.s. working space. It can be seen from the figures that the active system e (full state feedback with time delay) exhibits the best overall performance. For example, the active system $e[2]$ in Figs 8.1 to 8.6 improves the vertical, lateral and longitudinal seat accelerations, rear dynamic tyre load and the fore/aft tyre load transfer by 25, 63, 49, 45 and 30 percent respectively but at the expense of increasing the lateral tyre load transfer by 22 percent when compared with the best passive system (No.

6). To avoid the increase associated with system $e[2]$ in the r.m.s. value of the lateral tyre load transfer, system $e[1]$ may be used instead. This system improves the vertical, lateral and longitudinal seat accelerations, front and rear dynamic tyre load and the fore/aft tyre load transfer by 18, 58, 39, 17, 58 and 36 percent respectively without any increase in the r.m.s. value of the lateral dynamic tyre load transfer when compared with the passive system No. 6. In Figs 8.7 to 8.12, comparing active system $e[1]$ with the passive system No. 5, the percentage improvements become 12, 58, 22, 14, 59, 29 and 6 percent respectively. Hence, increasing the amount of the design working space reduces the improvements achieved from the active systems when compared with the passive systems. This conclusion is also correct for other active systems but the reduction in the improvements achieved in the r.m.s. values is different from one system to another. It is also worth noting the following points. Firstly, the dramatic improvements achieved in the longitudinal and lateral accelerations pointed out above are not of great practical significance because the r.m.s. values of these accelerations are not high. Secondly, the fitting of the suspension system e to any real vehicle is difficult and expensive (see sections 6.4.5 and 7.1 for more details).

8.2.2 Effect of ground description/control strategy.

The full state feedback active system α has the lowest performance of the active systems (see Figs 8.1 to 8.12 and Tables 8.2 and 8.3). The control law of this system is based

on the integrated white noise road surface description and does not consider the wheelbase time delay. For example, system $a[2]$ in Figs 8.1 to 8.6 improves the vertical, lateral and longitudinal accelerations, front and rear dynamic tyre load and the fore/aft tyre load transfer only by 7, 37, 20, 9, 17 and 27 percent respectively when compared with the passive system No. 6. It is also clear that even the limited state feedback system L_a (filtered white noise case without time delay) is much better than system a with performance approaching that of the full state feedback active system b . This however, supports the conclusion that the use of a realistic description of the road surface results directly in a performance improvement even when a limited state feedback control strategy is used. Together with this relatively low performance level, active system a requires measurements among other things (see Table 7.1) of the body and wheel positions relative to the road surface which is not easy to realise in practice. Therefore, in general, fitting systems a and b or even system L_a to a practical vehicle is not worthwhile. On the other hand, system L_b is attractive. It includes the wheelbase time delay and only requires measurements of the absolute displacements and velocities of the body and wheel connection points and it improves performance when compared with the best passive system or even with the active systems a , L_a or b . For example, system $L_b[3]$ offers 25, 43, 40, 12, 17, 16 and 14 percent reductions in the r.m.s. values of the vertical, lateral and longitudinal seat accelerations, front and rear dynamic tyre load and the fore/aft and the lateral tyre load transfer respectively when compared with passive

system No. 6. Overall, therefore the results in this section provide a better understanding of the problem than hitherto. It is shown for the first time that using the gradient search method in deriving the control law for a system with time delay offers an active system which reduces the practical limitations and improves the system performance compared with previously proposed active systems.

8.2.3 Effect of full/limited state feedback.

In this section it is intended to examine the losses in the performance due to employing limited state feedback control strategies. This will be studied by first comparing the limited state feedback active system L_b with the full state feedback system e . However it is not easy to use Figs 8.1 to 8.6 to compare directly these two systems. Instead, the results shown in Table 8.2 can be used. It can be seen that the only drawback with the limited state version is a deterioration in rear dynamic tyre load. On the other hand, system L_b has the obvious practical advantages of not requiring any measurements of the road inputs or any on-line calculations of the time delay states η .

The limited state feedback active system L_b requires the least number of measurements (only the body to wheel relative velocities are required). Although measurement errors are included in this system ($SRE = 0.001$), it performs very closely to the full state feedback active system e (see Figs 8.1 to 8.6). But in contrast with the limited state feedback system

L_b , L_f requires two additional functions: firstly, it is necessary to estimate the sensors random error and use it to select (based on the vehicle speed and road roughness combination) the filter gains stored in the vehicle computer and secondly, it is necessary to update the optimum estimates of the non-measurable states at small, discrete steps as time progresses. Although these requirements can in principle be realised in practice (see section 7.5), active system L_b still looks less complicated from a practical viewpoint.

8.3 Effect of adaptation.

In this part, the results presented in sections 3.5 and 6.5 are collected and re-plotted in Figs 8.13 to 8.19. The summary of these results is as follows. In addition to the speed used previously of 30 m/s, the 2.5 cm r.m.s. working space is assumed to be fully consumed at 10 and 20 m/s conditions by the adaptive active systems a and b as well as the adaptive passive system, while it is impossible for the fixed parameter passive system ($f_n \approx 1.2$ Hz) and the active system au to do so. It should be mentioned that the system au has the same control law as system a at 30 m/s but the possibility of changing the feedback gains at other speeds is assumed to be unavailable. It can be seen from Figs 8.16 to 8.19 that the r.m.s. values of the dynamic tyre load, fore/aft tyre and lateral load transfer of the active systems a , b and au are close to those of the fixed parameter passive system. Hence, the improvements achieved from the former systems when compared with that fixed parameter passive system can be summarised

conveniently in terms of the seat accelerations. These improvements are calculated and shown in Table 8.3. Comments arising from Fig. 8.13 to 8.15 and Table 8.3 are as follows.

1- The fixed parameter passive system is the poorest system from the ride comfort point of view when compared with any other suspension system.

2- For the 10 and 20 m/s, the fixed parameter active system *au* (worst performing active system) performs only slightly better than the adaptive passive system. If the adaptive active systems *a* and *b* are employed, further improvements in the seat accelerations can be achieved. However, the control laws of these two systems do not account for the wheelbase time delay, and so as shown previously even further improvements are available if the time delay is included in the control law formulation.

3- These results as well as those discussed in Chapter 3 and Chapter 6 show that the suspension adaptation is a powerful feature behind the overall performance improvements. Also, as outlined before, adaptation is much easier to arrange for any active system than it is for passive systems.

8.4 Concluding remarks.

The performance analyses of all the systems considered at 30 m/s show that:

1- The full state feedback active system *e* was found to give the best overall performance.

2- The active systems shows a greater percentage improvement as the available working space is reduced.

3- In the various methods used to obtain the control laws, some assume that the ground is represented as an integrated white noise input and some as filtered white noise. The results in Chapter 6 indicated that the latter is preferable. This finding is confirmed in this Chapter as shown for example by the superiority of system L_a (filtered white noise but limited state feedback) over system a (integrated white noise and full state feedback).

4- The new results generated from the limited state feedback active system L_b (which includes the time delay and only requires measurements of the body and wheel absolute displacements and velocities) showed that performance approaching that of the full state feedback active system e could be obtained. From a practical viewpoint, it is preferable to previously proposed systems, represented here for example as system a and b .

5- For the limited state feedback active system L_f , which only requires measurements of the wheel-body relative velocities, it was found that this system also performs very closely to the full state feedback active system e . In contrast with the limited state feedback system L_b , the system L_f has two additional requirements: firstly, it is necessary to estimate the sensor's random error and use it to select (based on the vehicle speed and road roughness combination) the filter gains stored in the vehicle computer and secondly, to update the optimum estimates of the non-measurable states at small, discrete steps as time progresses.

Comparisons of the active systems a , b , au and the passive systems at different speeds showed that :

1- Significant improvements in the seat accelerations could be achieved from the active and adaptive passive system when compared with the fixed parameter passive system.

2- The fixed parameter active system au (worst performing active system) was found to perform only slightly better than the adaptive passive system. If the adaptive active systems a and b are employed, further improvements in the seat accelerations could be achieved. However, even these two systems do not represent the best that can be achieved because even further gains can be obtained if the time delay is included in the control law derivation.

Table 8.1 Full and limited state feedback active suspension systems studied.

| System | Full state feedback State vector | Measurements | Control strategy |
|--------|--|--|---|
| a | $[x_i - x_{oj}, \dot{x}_i]^T$ $i = 1, 2, \dots, 8$ $j = 1, 1, 2, 2, 3, 3, 4, 4$ | Perfect measurements of all the states | Full state feedback, integrated white noise case. |
| b | $[x_i, \dot{x}_i, x_{ok}]^T$ $i = 1, 2, \dots, 8$ $k = 1, 2, 3, 4$ | Perfect measurements of all the states | Full state feedback, filtered white noise case. |
| e | $[x_i, \dot{x}_i, x_{ok}, \eta_k]^T$ $i = 1, 2, \dots, 8$ $k = 1, 2, 3, 4$ | Perfect measurements of all the states | Full state feedback with time delay, filtered white noise case. |
| L_a | As in b | Perfect measurements of all states at body/suspension connection points x_i, \dot{x}_i | Gradient search method |
| L_b | As in e | As in L_a | Gradient search method with time delay |
| L_f | $[z_b, \theta, \phi, x_m, z_b, \dot{\theta}, \dot{\phi}, \dot{x}_m, x_{ok}, \eta_k]^T$ $m = 1, 3, 5, 7$ $k = 1, 2, 3, 4$ | Noisy measurements of body/wheel velocities $\dot{x}_j - \dot{x}_{j+1}$ | Kalman filter algorithm with time delay |

Table 8.2 Comparison of the performance of the full state feedback active system e and the limited state feedback active system L_b at 2.5 cm r.m.s. working space.

| Active system | Root mean square values calculated when the road of $R_c = 3 \times 10^{-6}$ was traversed at 30 m/s. | | | | | | |
|---------------|---|----------------------------------|----------------------------------|-----------|-----------|------|------|
| | \ddot{z}_x m/s ² | \ddot{y}_x m/s ² | \ddot{x}_x m/s ² | FDTL N | RDTL N | FDTT | LDTT |
| e | 1.1 | 0.34 | 0.34 | 1262 | 1103 | 0.17 | 0.19 |
| L_b | 1.1 | 0.40 | 0.32 | 1283 | 1383 | 0.20 | 0.14 |

Table 8.3 Reduction in r.m.s. values for adaptive passive system and the active system a , b and au compared with fixed parameter passive system at different vehicle speed.

| Suspension system | Speed m/s | Percentage reduction in r.m.s. values of seat accelerations compared to fixed parameter passive system | | |
|------------------------------------|--------------|--|--------------|--------------|
| | | \ddot{z}_x | \ddot{y}_x | \ddot{x}_x |
| Adaptive passive | 10 | 21 | 16 | 44 |
| | 20 | 25 | 25 | 40 |
| | 30 | 11 | 21 | 3 |
| Non-adaptive active system au | 10 | 23 | 40 | 33 |
| | 20 | 26 | 50 | 28 |
| | 30 | 23 | 50 | 26 |
| Adaptive active system a | 10 | 32 | 54 | 57 |
| | 20 | 35 | 66 | 51 |
| | 30 | 23 | 50 | 26 |
| Adaptive active system b | 10 | 31 | 60 | 55 |
| | 20 | 35 | 73 | 50 |
| | 30 | 27 | 71 | 35 |

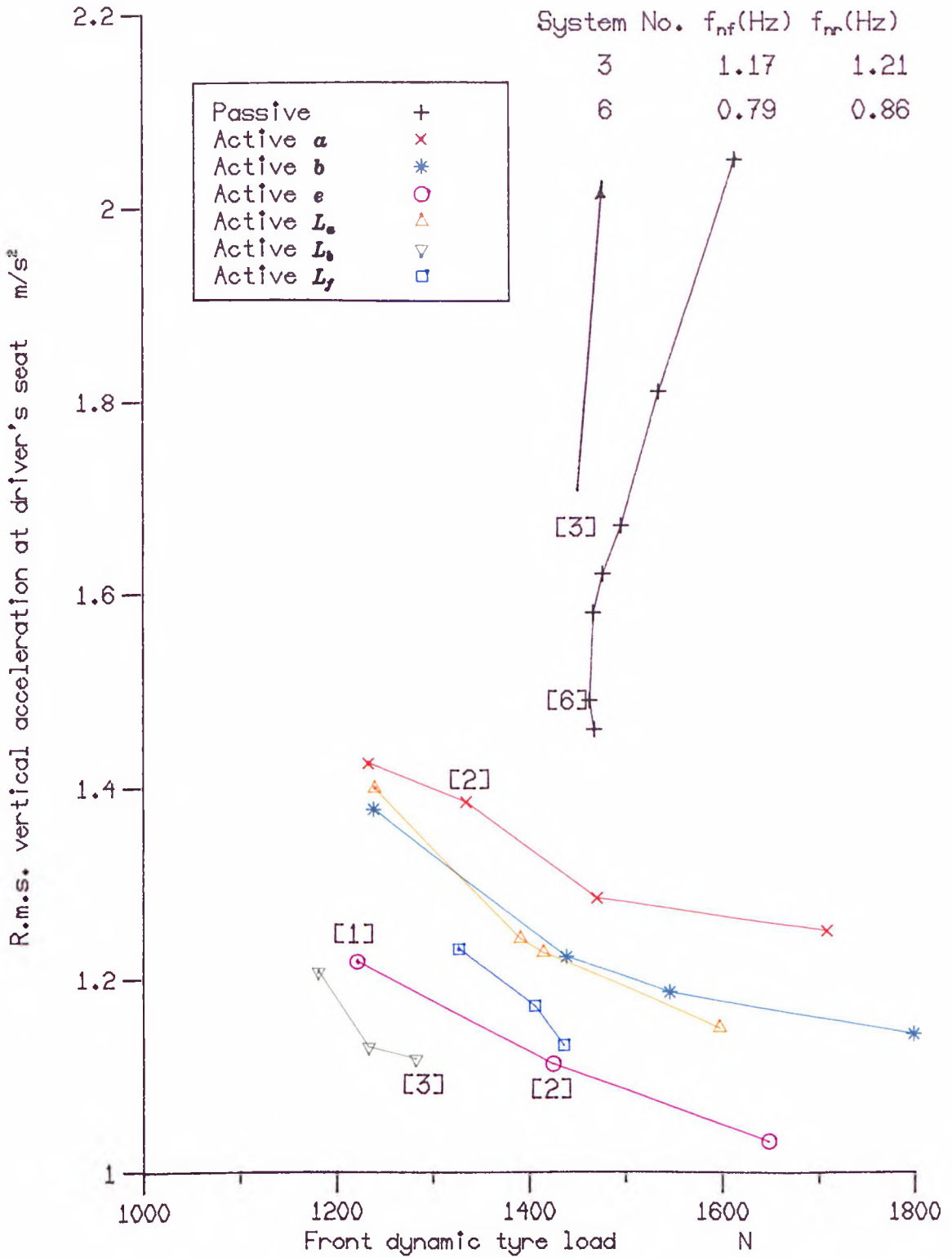


Fig. 8.1 Vertical acceleration results for various suspension types for 2.5 cm. r.m.s. working space at 30 m/s on a road of roughness $R_o = 3 \times 10^{-6}$.

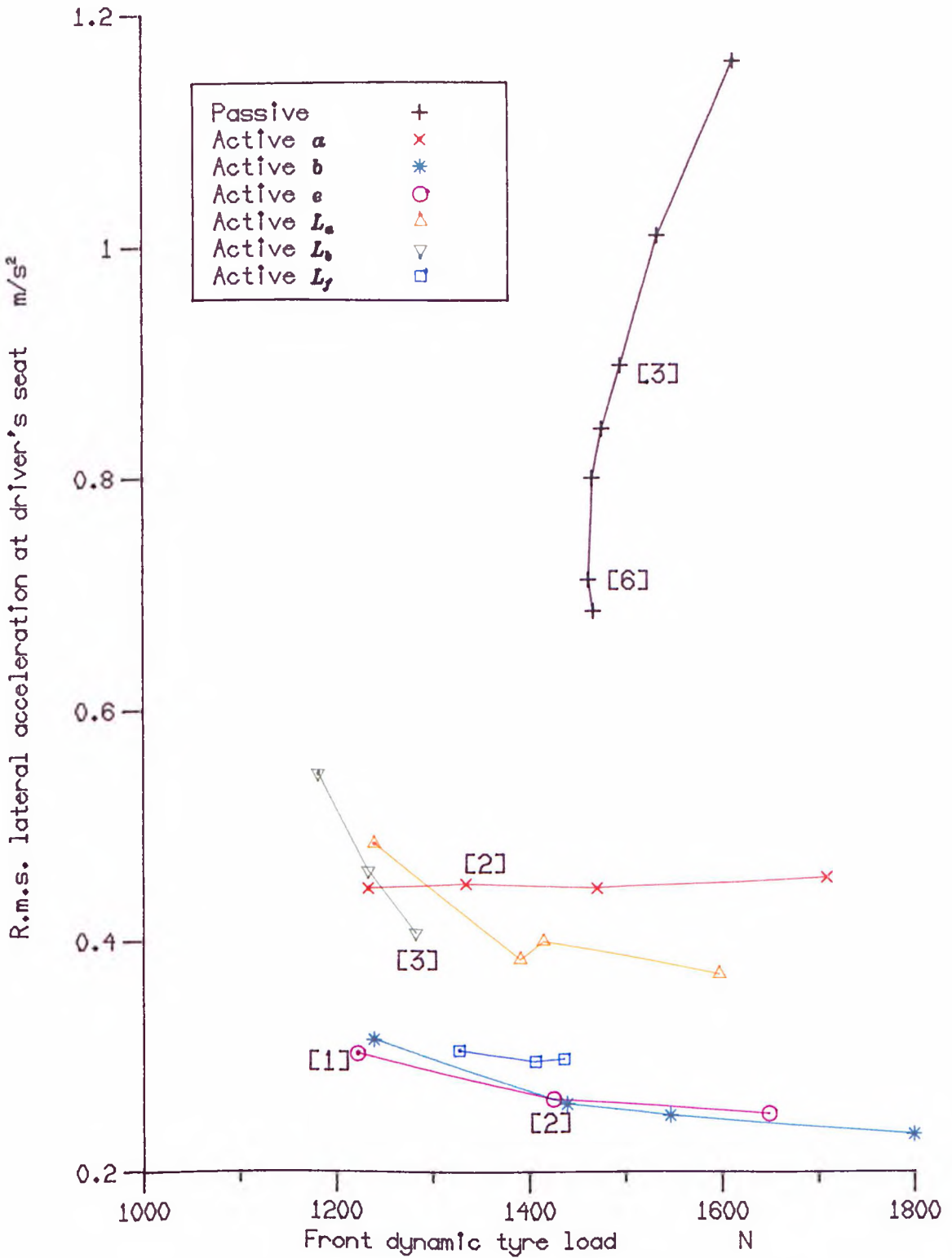


Fig. 8.2 Lateral acceleration results for various suspension types for 2.5 cm. r.m.s. working space at 30 m/s on a road of roughness $R_o = 3 \times 10^{-8}$.

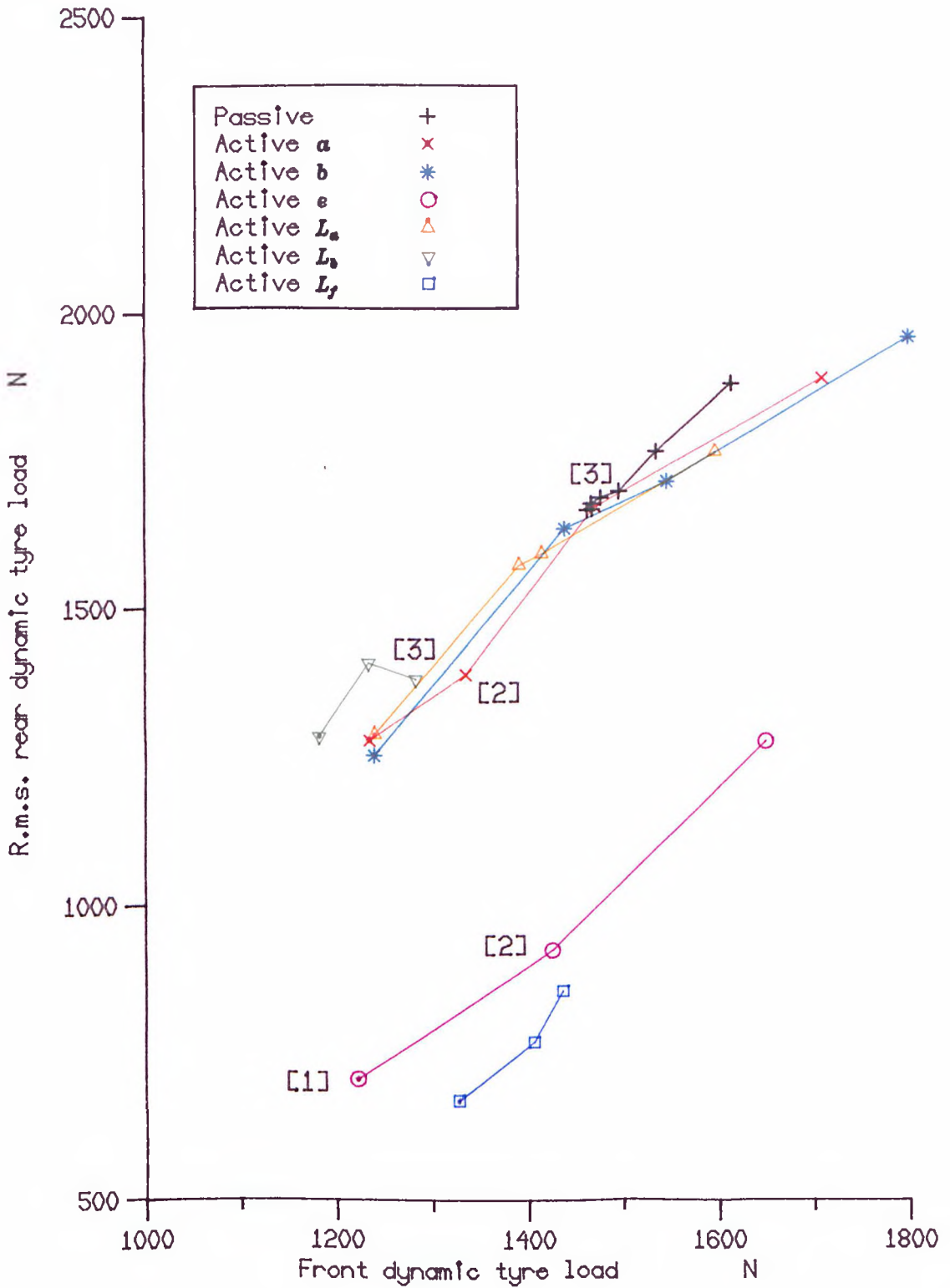


Fig. 8.4 Rear dynamic tyre load results for various suspension types for 2.5 cm. r.m.s. working space at 30 m/s on a road of roughness $R_0 = 3 \times 10^{-3}$.

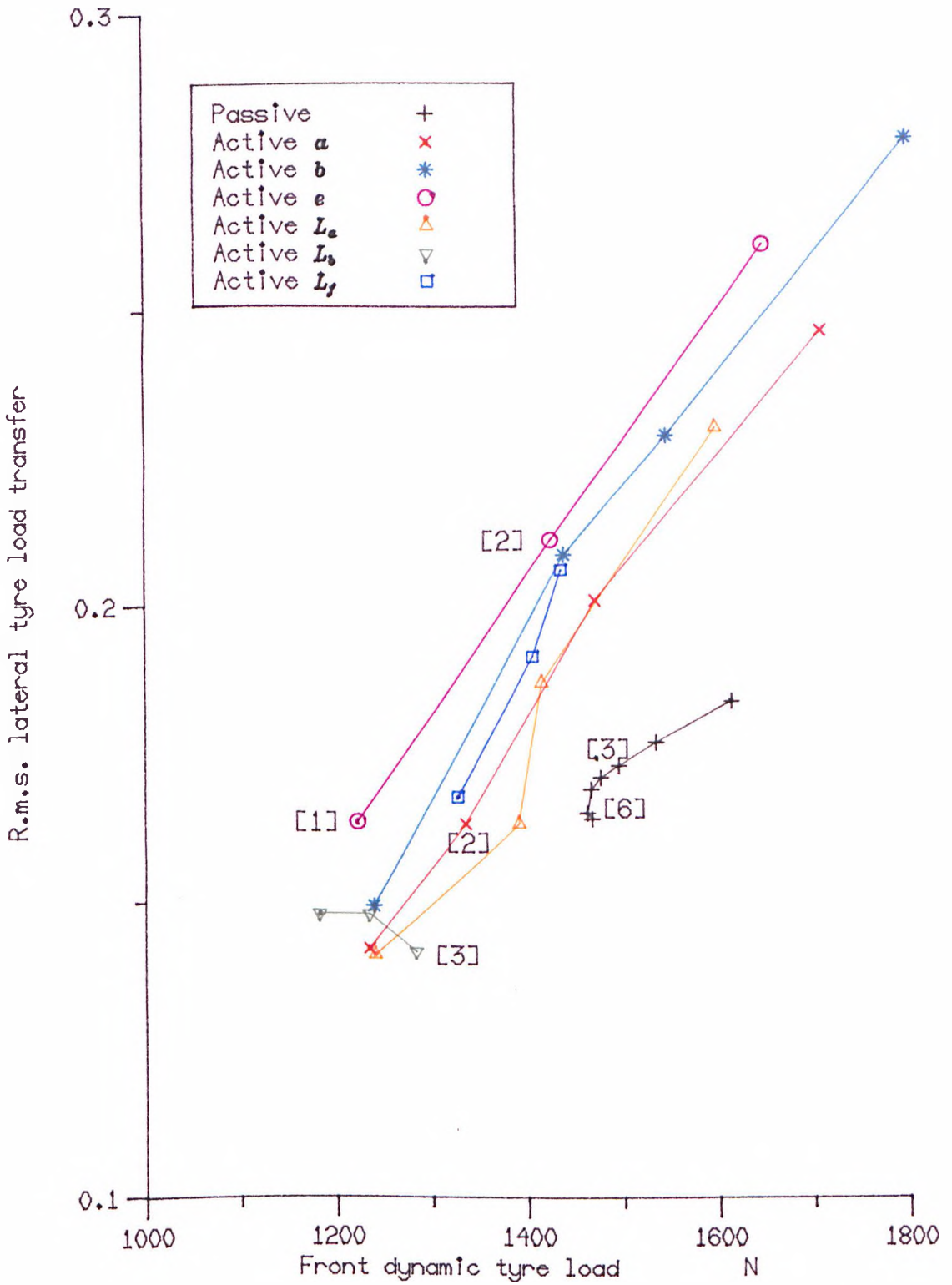


Fig. 8.6 Lateral tyre load transfer results for various suspension types for 2.5 cm. r.m.s. working space at 30 m/s on a road of roughness $R_o = 3 \times 10^{-6}$.

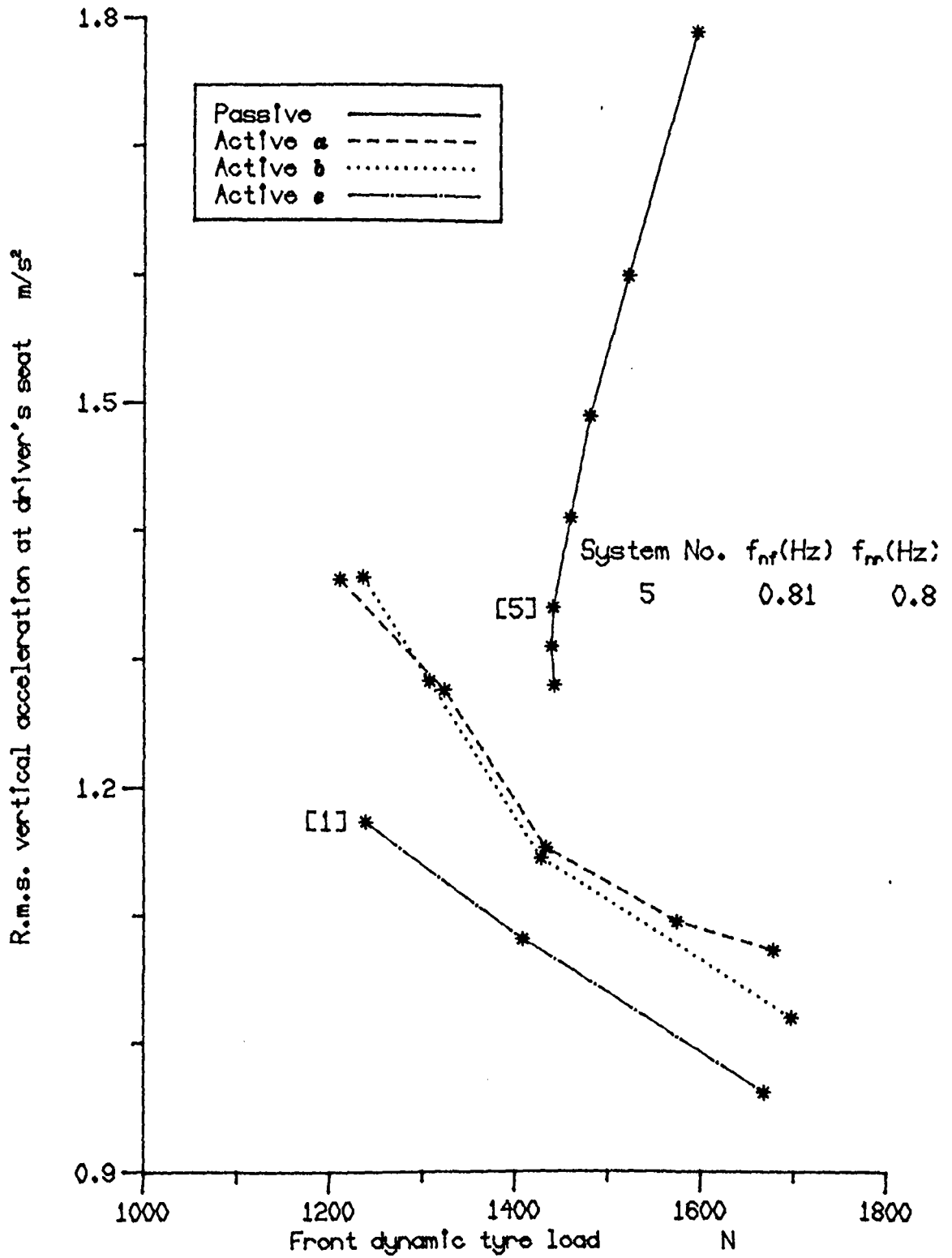


Fig. 8.7 Vertical acceleration results for various suspension types for 3 cm. r.m.s. working space at 30 m/s on a road of roughness $R_0 = 3 \times 10^{-3}$.

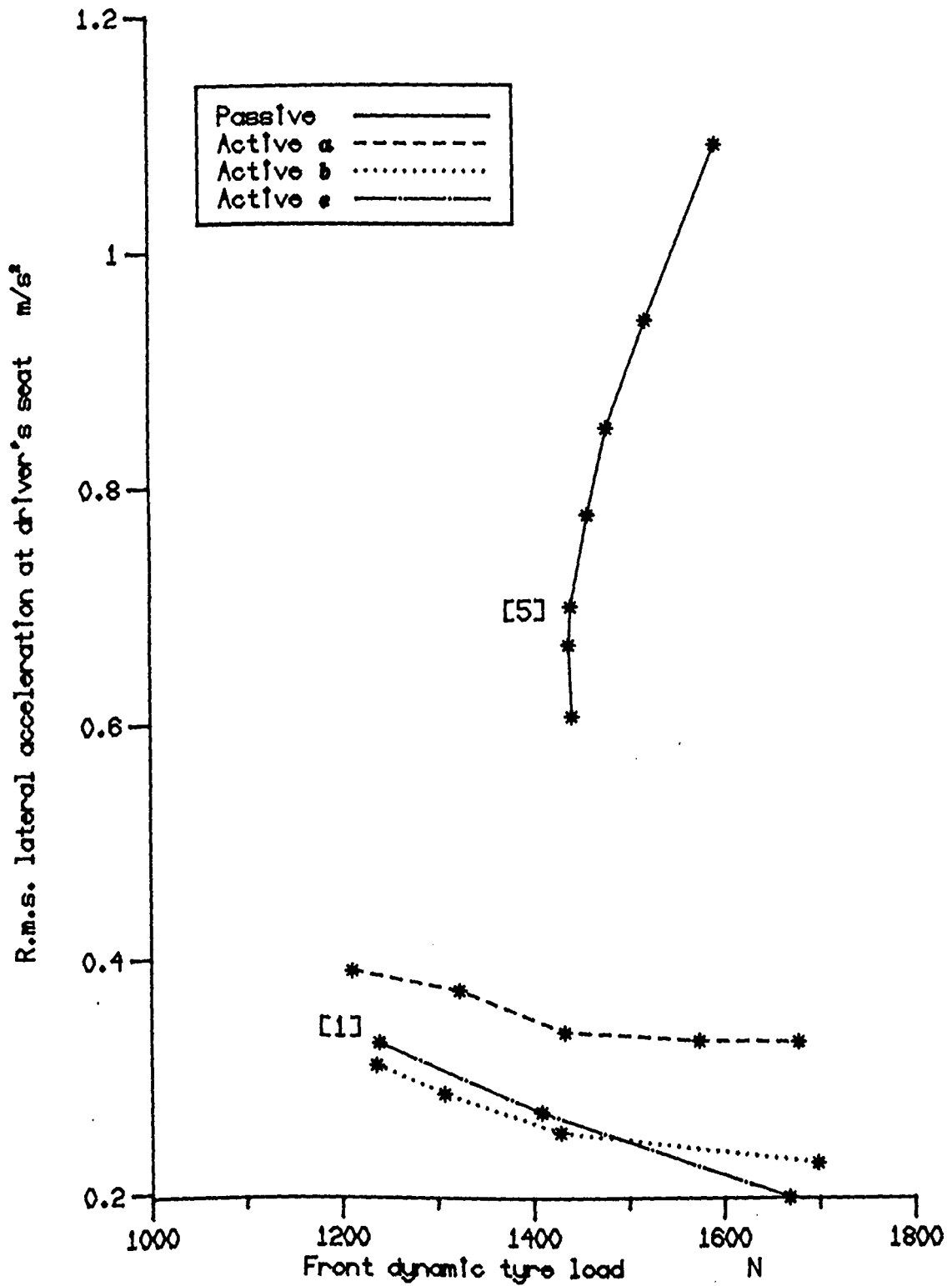


Fig. 8.8 Lateral acceleration results for various suspension types for 2 cm. r.m.s. working space at 30 m/s on a road of roughness $R_s = 3 \times 10^{-6}$.

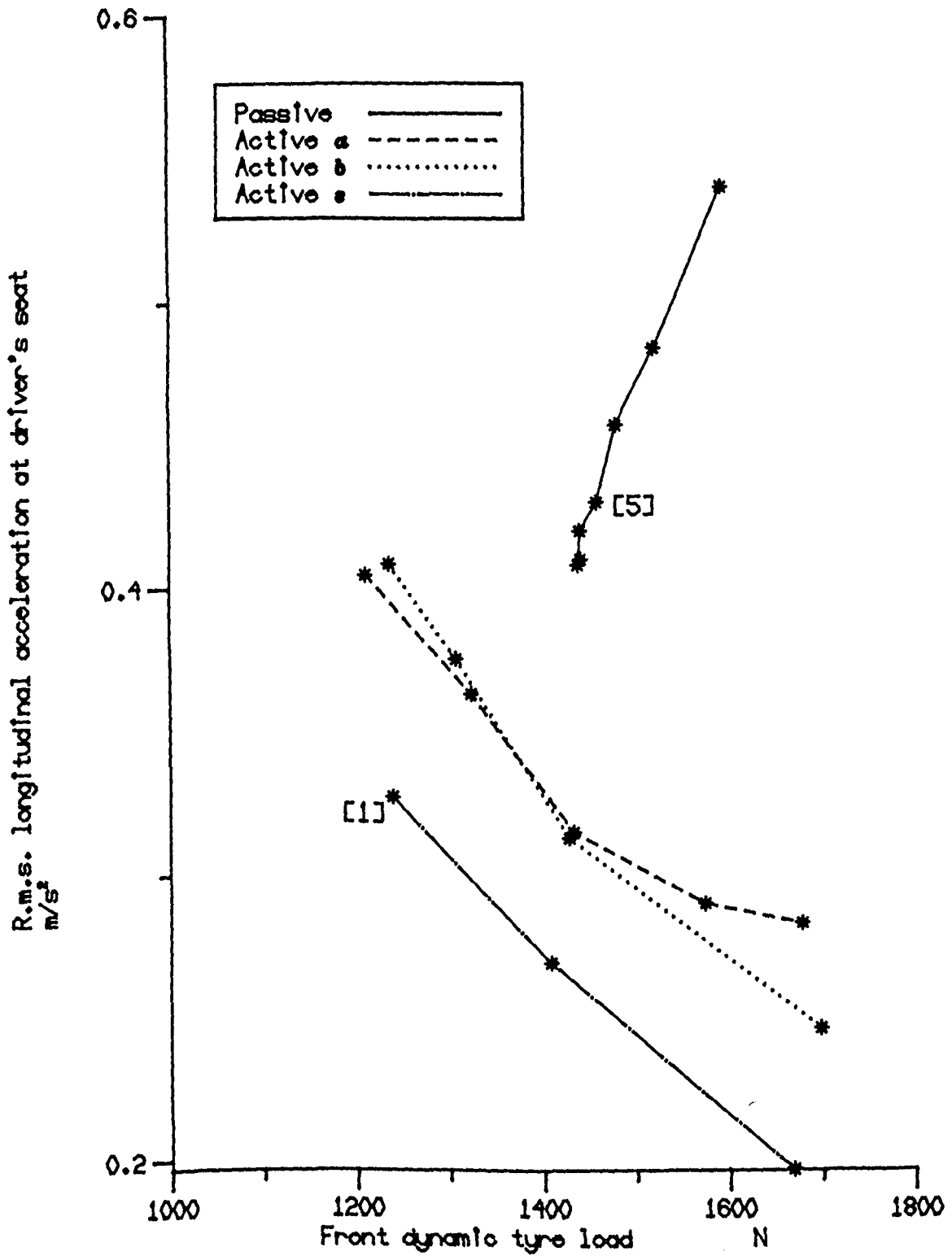


Fig. 8.9 Longitudinal acceleration results for various suspension types for 3 cm. r.m.s. working space at 30 m/s on a road of roughness $R_s = 3 \times 10^{-4}$.

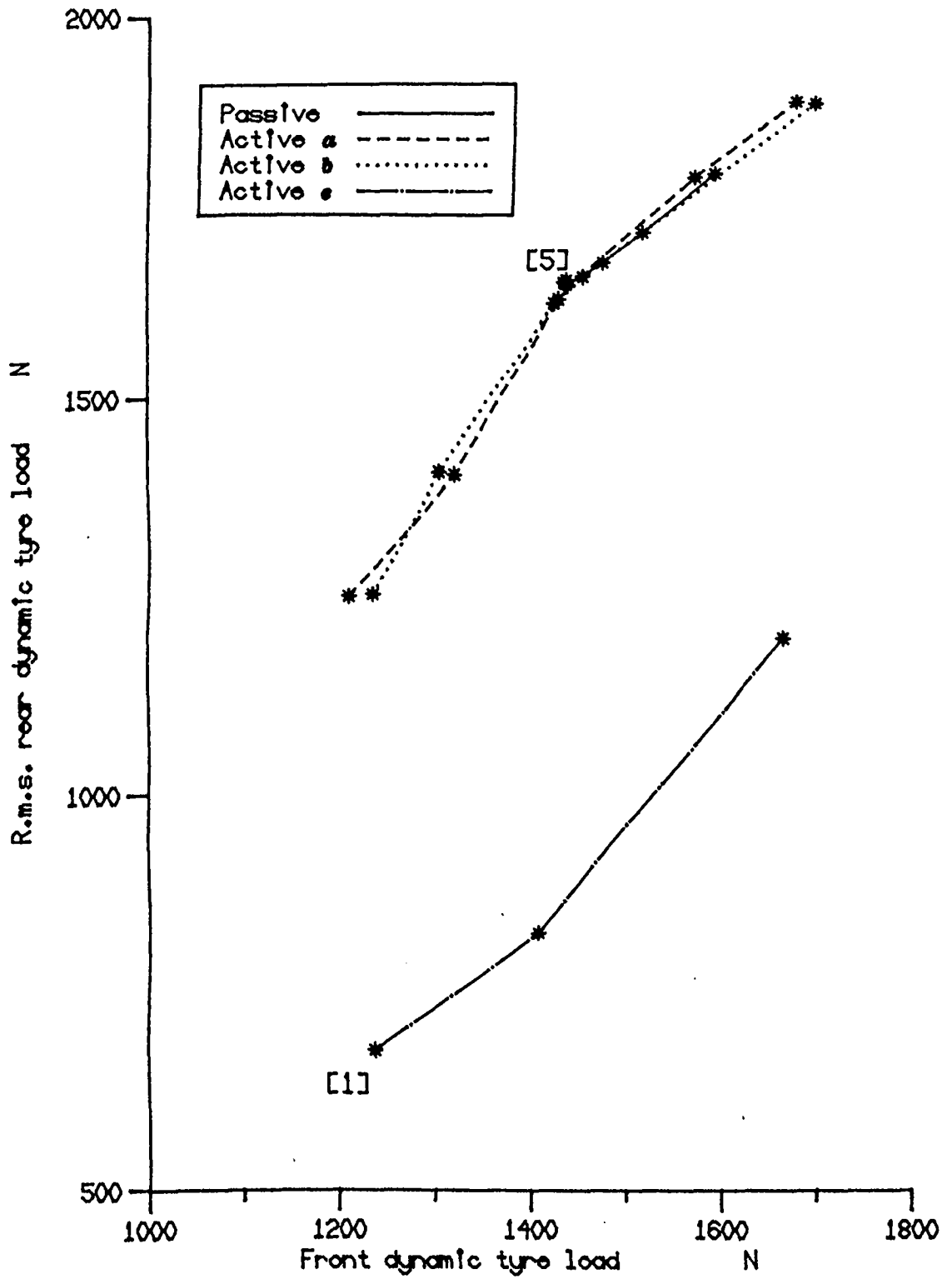


Fig. 8.10 Rear dynamic tyre load results for various suspension types for 3 cm. r.m.s. working space at 30 m/s on a road of roughness $R_0 = 3 \times 10^{-3}$.

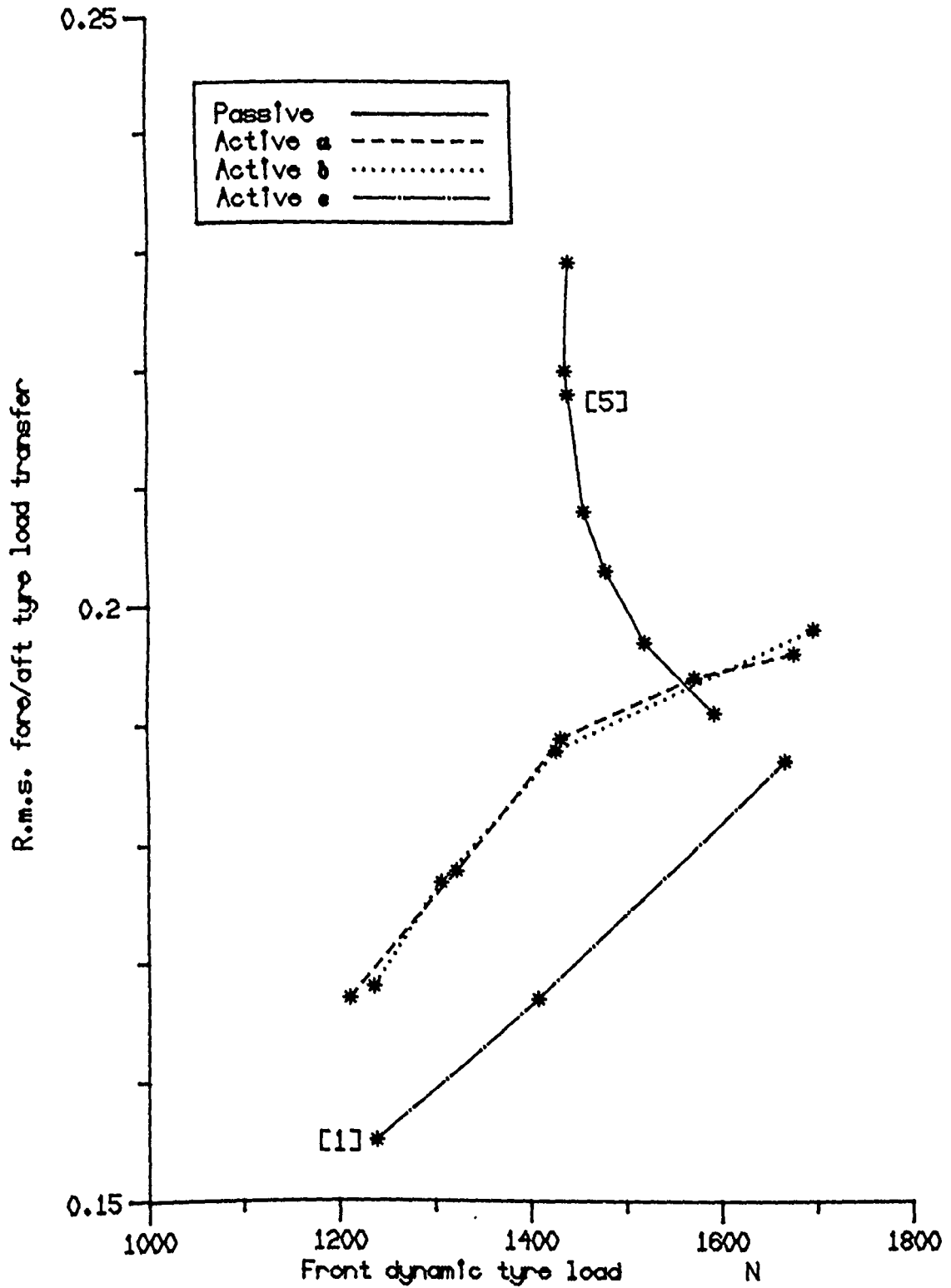


Fig. 8.11 Fore/aft tyre load transfer results for various suspension types for 3 cm. r.m.s. working space at 30 m/s on a road of roughness $R_0 = 3 \times 10^{-6}$.

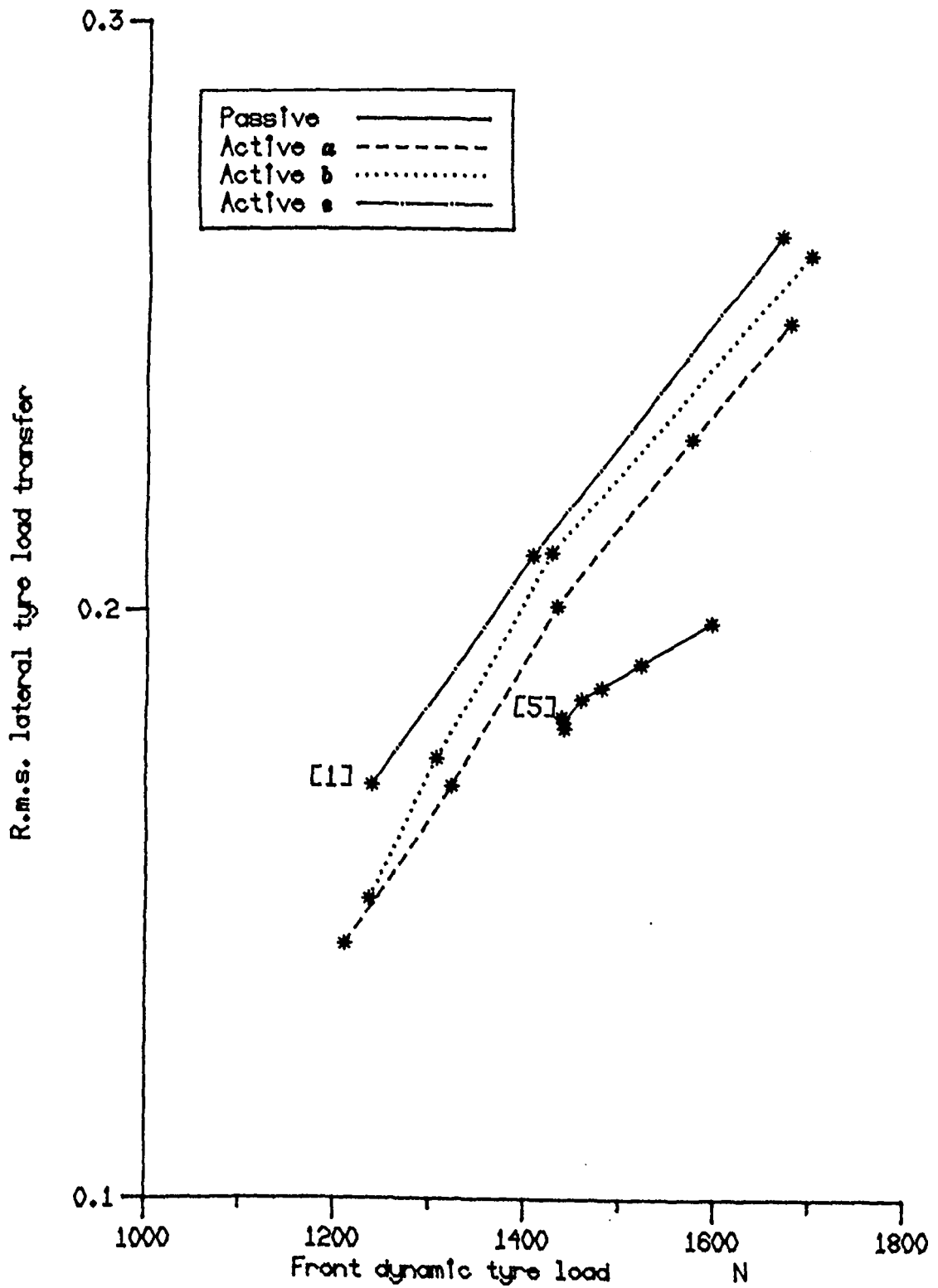


Fig. 8.12 Lateral tyre load transfer results for various suspension types for 3 cm. r.m.s. working space at 30 m/s on a road of roughness $R_0 = 3 \times 10^{-6}$.

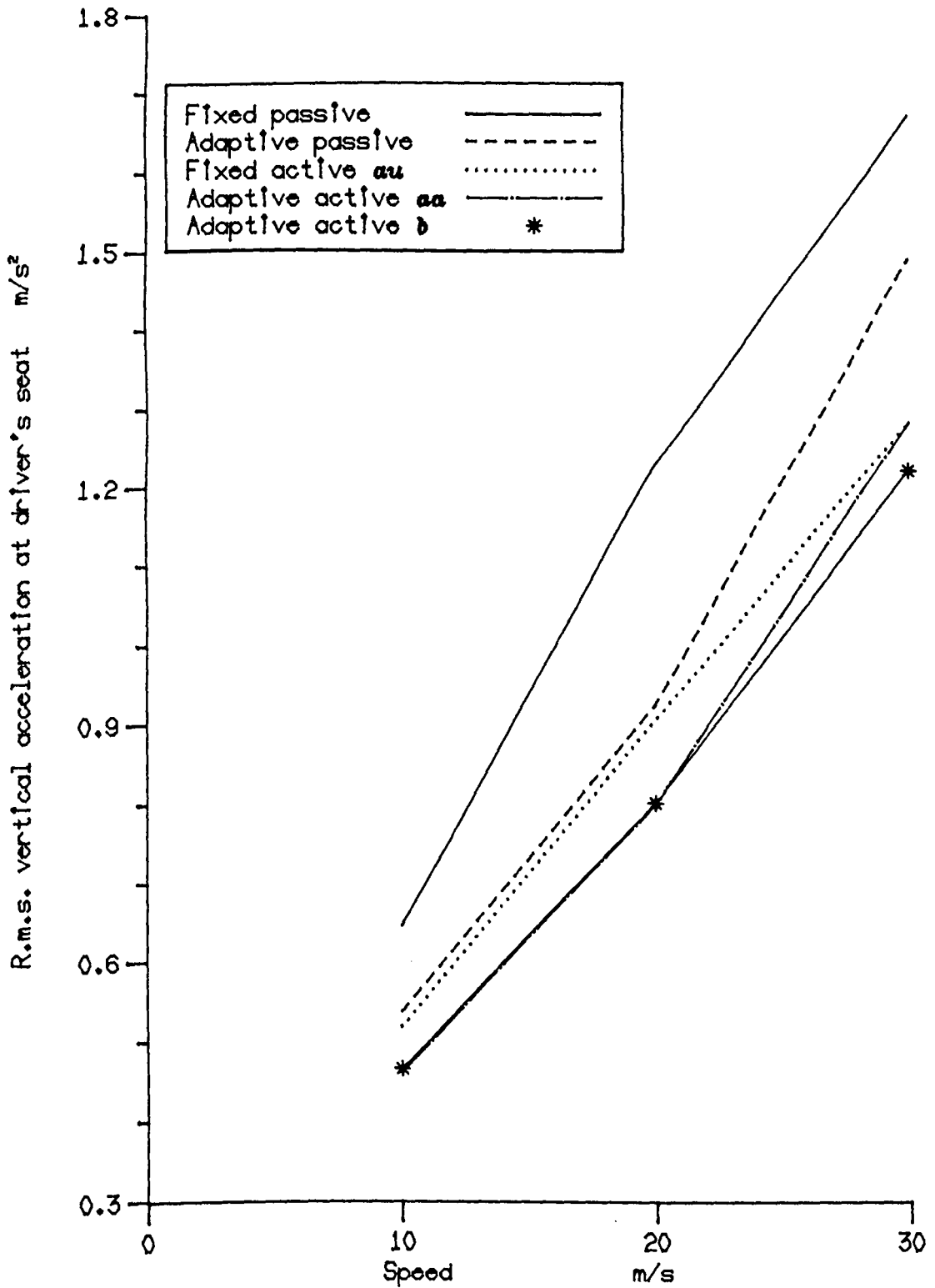


Fig. 8.13 Performance of the fixed parameter and adaptive passive systems and the active systems *aa*, *b* and *au* calculated at different vehicle speeds.

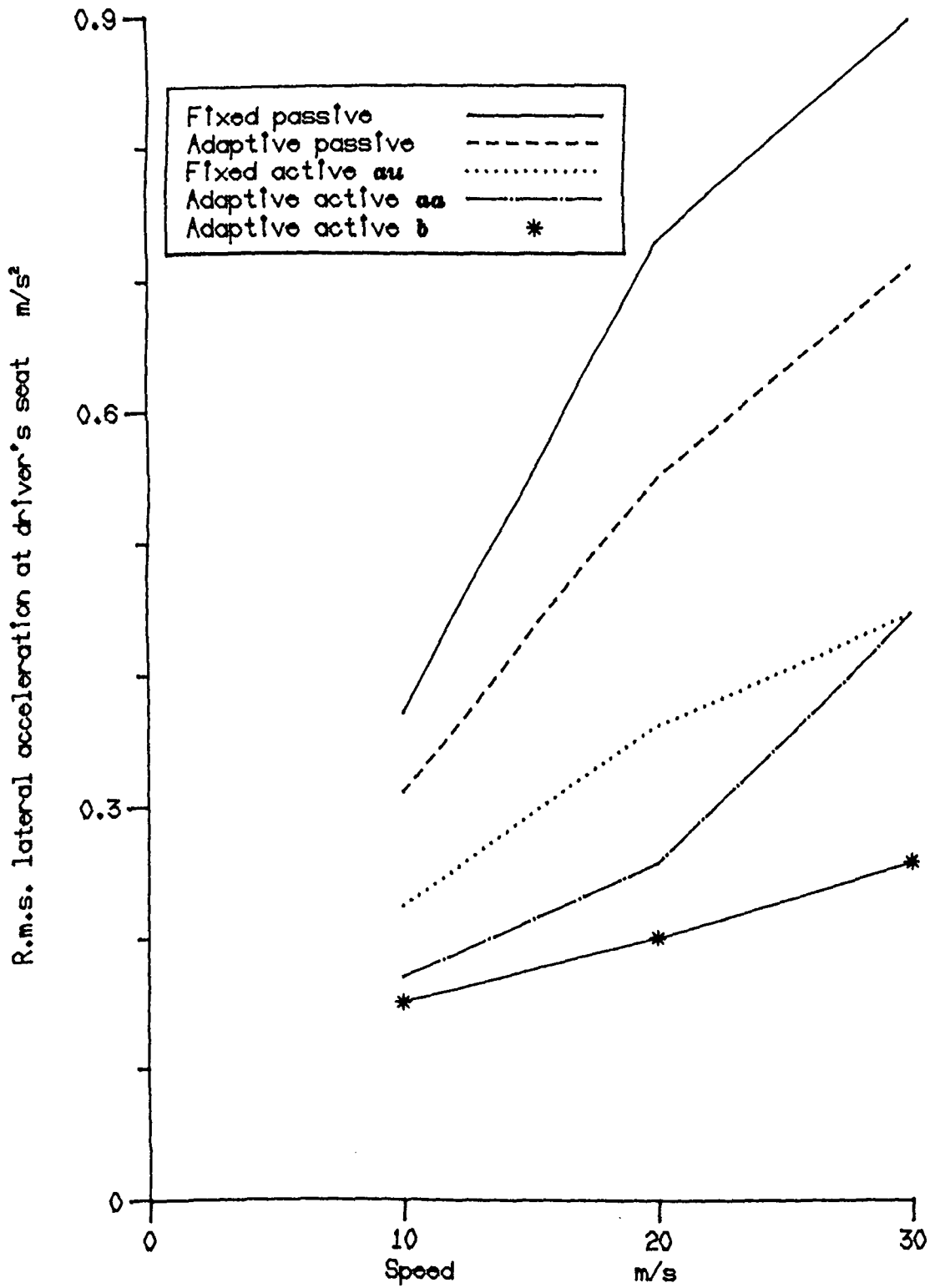


Fig. 8.14 Performance of the fixed parameter and adaptive passive systems and the active systems *aa*, *b* and *au* calculated at different vehicle speeds.

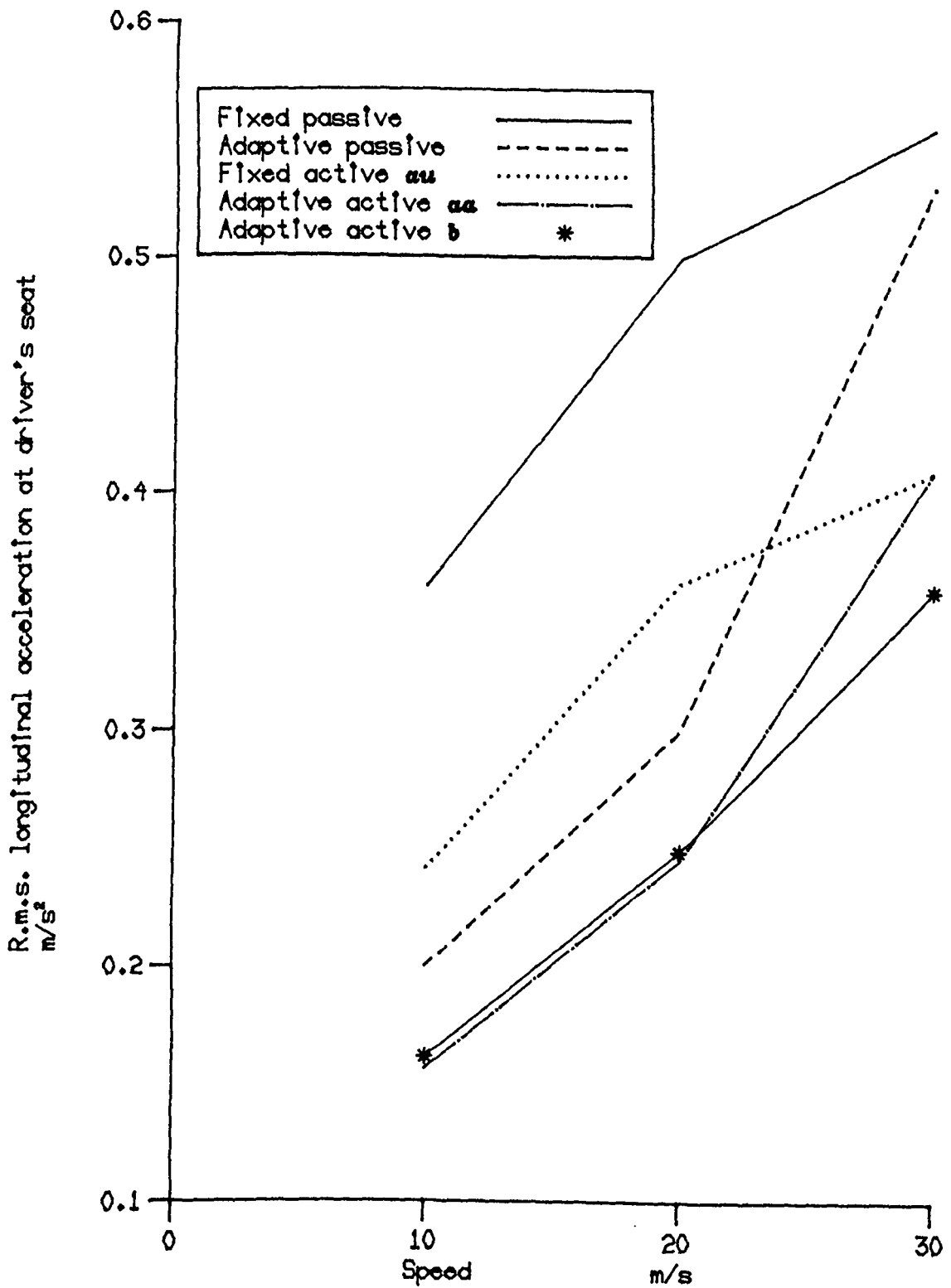


Fig. 8.15 Performance of the fixed parameter and adaptive passive systems and the active systems *aa*, *b* and *aa* calculated at different vehicle speeds.

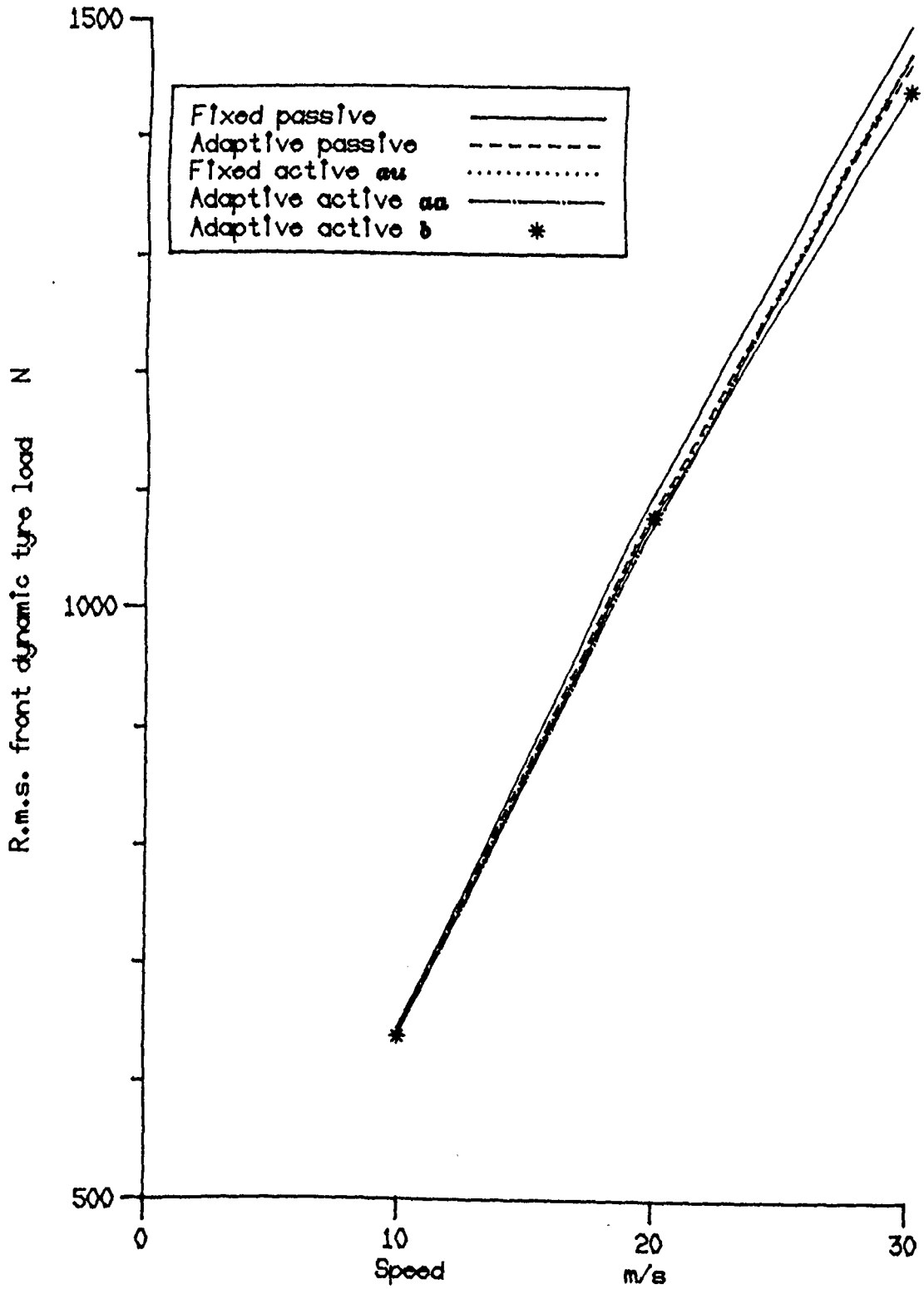


Fig. 8.16 Performance of the fixed parameter and adaptive passive systems and the active systems aa, b and aa calculated at different vehicle speeds.

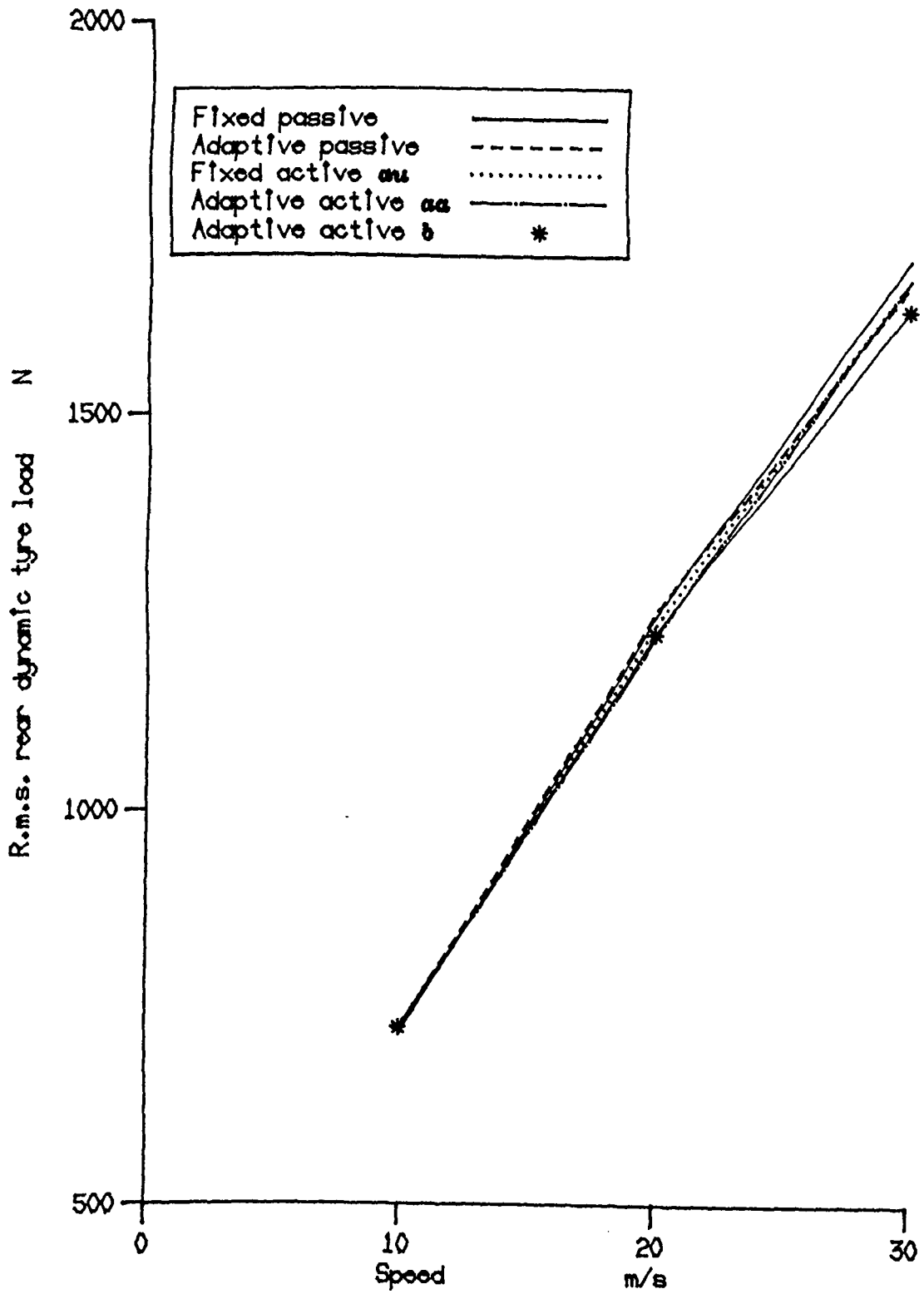


Fig. 8.17 Performance of the fixed parameter and adaptive passive systems and the active systems *aa*, *b* and *au* calculated at different vehicle speeds.

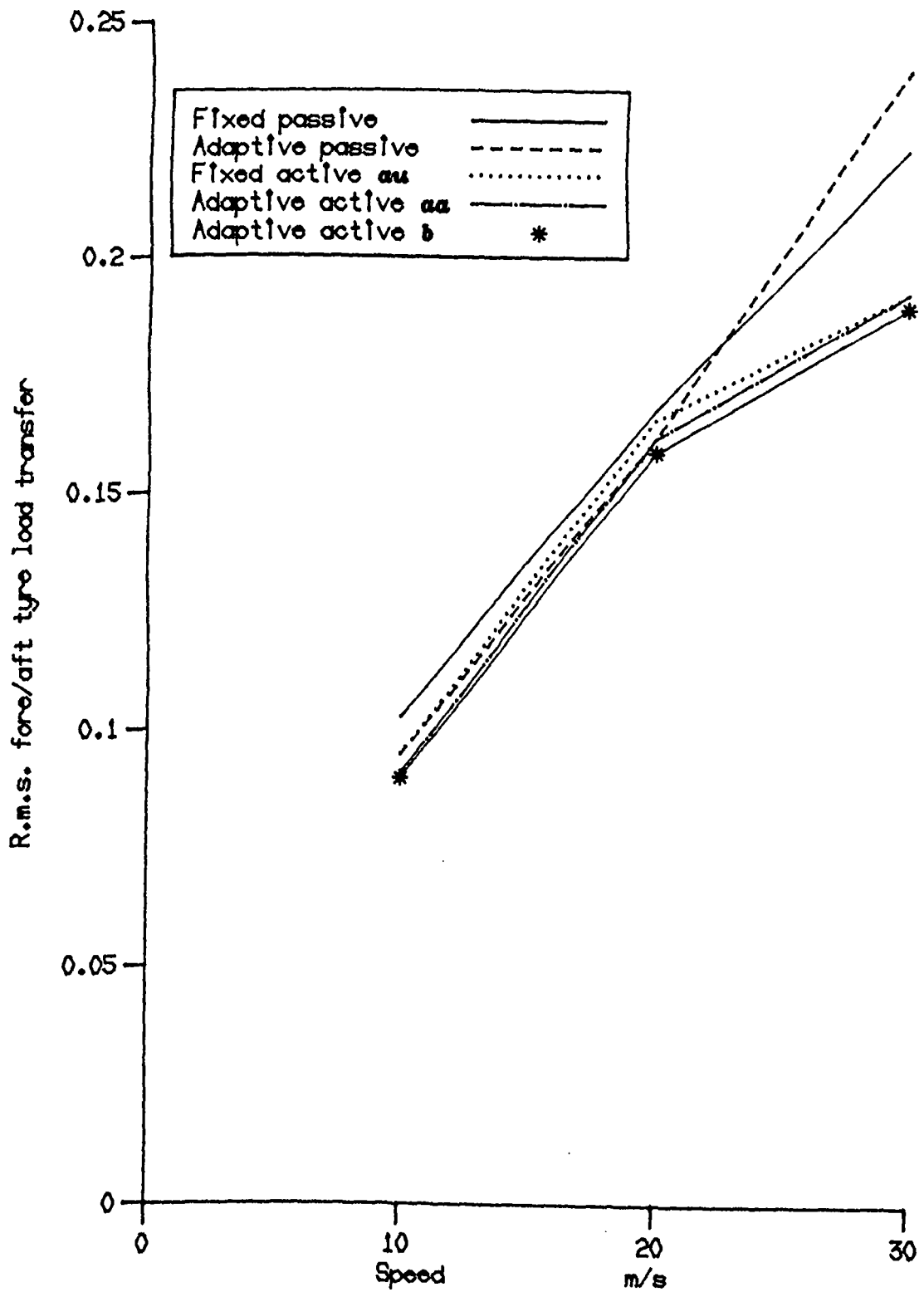


Fig. 8.18 Performance of the fixed parameter and adaptive passive systems and the active systems *aa*, *b* and *aa* calculated at different vehicle speeds.

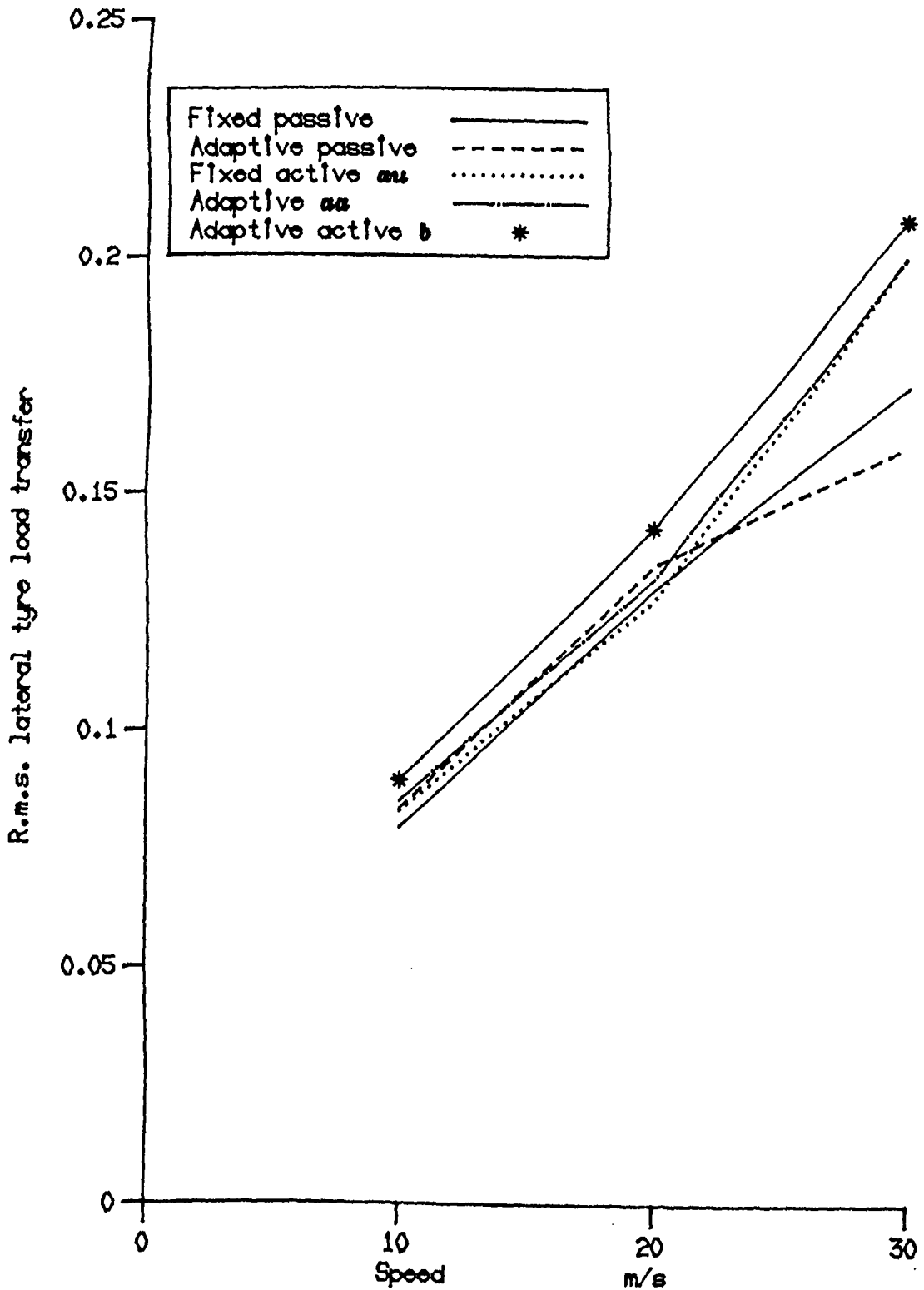


Fig. 8.19 Performance of the fixed parameter and adaptive passive systems and the active systems *aa*, *b* and *aa* calculated at different vehicle speeds.

CHAPTER 9

CONCLUSIONS AND FUTURE WORK

9.1 Conclusions

An attempt is made in the following paragraphs to draw together the conclusions reached in each of the Chapters already presented.

In the literature almost all the efforts to date have been directed towards analyses and optimisations of active systems based on the quarter car model while few investigations based on the three dimensional vehicle model have been published. Of the full model studies published, most have not considered the wheelbase time delay in developing the control laws of the active systems. Hence, the conclusions drawn have not changed much when compared with those obtained from using the quarter car model. Furthermore, most of the control laws in these studies have assumed perfect knowledge of all the state variables. Therefore, a need was identified for a more general study to design control laws for limited state feedback active systems, to include the wheelbase time delay and to examine the effect of the measurement errors on the performance of these systems.

Based on the three dimensional vehicle model, there has been confusion in quantifying the benefits achieved from the active systems over the passive systems. Some authors have claimed

that the active system can dramatically improve the vehicle performance when compared with the passive system. Others, however, have shown that a well designed passive system can perform close to the active one. Therefore, a need has been identified for an equitable basis comparison study to enable the benefits from fitting an active system to a full vehicle model to be quantified clearly.

In Chapter 2, the problem of generating a single profile or two correlated profiles has been briefly reviewed. The equations of motion necessary for ride analysis or for the active system optimisation problem have been explained and an illustrative example based on a 7 d.o.f. vehicle model given. The analyses of linear systems in terms of frequency response or spectral density functions have been discussed and the computational scheme of the difference equation to evaluate the time history of the outputs of interest has been indicated. Overall, therefore, the analytical techniques required for the subsequent chapters are outlined in Chapter 2.

In Chapter 3, a performance analysis of passive suspension systems on a full vehicle model has been presented. The purposes of this analysis were to provide a clear understanding of the performance properties of these systems when a three dimensional vehicle model is employed and to quantify the ride behaviour of these systems so they can be used as a guide in scaling the performance of the active systems.

The most important conclusions reached were as follows:

1- Employing soft suspension with low damping coefficients always improves the ride comfort but at the expense of increasing the working space and the lateral tyre load transfer. On the other hand, the best dynamic tyre load and the fore/aft dynamic tyre load transfer can be obtained by employing a moderate spring stiffness ($f_n = 1$ Hz). However, the requirements of the damping coefficient in each performance category are variable. The fore/aft load transfer requires a low damping coefficient, while the dynamic tyre load requires a moderate damping coefficient.

2- In the above point, the conclusions concerning the ride comfort, dynamic tyre load and the suspension working space agree with those obtained from other studies based on the 2 d.o.f. quarter car model. Hence, the use of this simple model in studying the fundamental ride behaviour of passive suspension systems is justified.

3- In studying the effect of varying the anti-roll bar stiffness, it was found that the r.m.s. values of the vertical and longitudinal seat accelerations, dynamic tyre load and the fore/aft tyre load transfer were not significantly affected by increasing the stiffness of the anti-roll bar. On the other hand, employing front and rear anti roll bars with stiffnesses $K_{r,f} = 36$ kN m/rad and $K_{r,r} = 20$ kN m/rad was found to double the lateral acceleration compared with the case of setting these stiffnesses to zero.

4- The practical limitations of using a suspension system with a soft spring were discussed. The possibility of employing a passive system with soft spring stiffness (to improve the

ride comfort) and with stiff anti-roll bars (to maintain the vehicle attitude during handling manoeuvres) was examined. The comparison of the performance of this system with a system having moderate spring and anti-roll stiffnesses showed that the improvements achieved from the former system in the vertical acceleration are associated with an increase in the lateral acceleration and the lateral dynamic tyre load. Hence, the use of a system with soft spring and stiff anti-roll bars is not worthwhile overall.

In Chapter 4, an outline of the application of linear optimal control theory to the design of the control laws for active suspension systems was given. Both common descriptions of the road surface, either as integrated white noise or filtered white noise, were considered.

The mathematical detail of deriving full and limited state feedback control laws was first reviewed for the case where the correlation between the road inputs is ignored. Modifications to the problem formulation so that the control laws could account for the cross correlation and/or the wheelbase time delay were given. The cross correlation term was presented by means of a first order shaping filter, while the time delay was represented by means of the Pade approximation. With these modifications, the linear control theory was shown to be still applicable to the active suspension problem. The main contribution of this chapter is that it

brings together for the first time a comprehensive review showing the mathematical schemes to generate continuous control laws for a full vehicle model.

Limited state feedback control laws for the correlated road input case were also discussed and a novel strategy based on the gradient search method for deriving practical control laws for a full vehicle was presented.

In Chapter 5, the effect of including the cross correlation in the derivation of the control law is examined by using a 4 d.o.f. bounce and roll single ended vehicle model together with the first order shaping filter introduced by Rill [1983]. It was shown that ignoring the cross correlation does not affect the performance level of the active suspension system.

Two sets of calculations were used to investigate the time delay approximation in the control law. First, for a half vehicle model, the performance index calculated using a 2nd and 4th order Pade approximation was compared with that calculated by Louam et al [1988] based on the discrete optimal control theory. Good agreement between the results obtained based on the 4th order Pade approximation and those obtained from the discrete theory was found for a range of vehicle speeds. Second, the Pade approximation was tested using the passively suspended vehicle. The half vehicle model response calculated using the pure time delay was compared with that obtained from representing the time delay by an N^{th} order Pade approximation. The results confirmed that the 4th order Pade

approximation accurately represented the wheelbase time delay and hence supported the use of this approximation in deriving the control laws.

The results from the decoupled half vehicle model showed that if the time delay is included in the derivation of the control law, dramatic improvements are obtained at the rear suspension compared with its quarter car equivalent version. Hence, the quarter car model may be useful only in case of using sub-optimal control laws. This is an important conclusion because it highlights an aspect of control system performance which is not captured by the quarter car model. Hence, control laws which are optimal for the quarter car model are actually sub-optimal if they are simply extended to the half vehicle case without taking the wheelbase time delay into account.

Based on the 7 d.o.f. vehicle model, the performance analyses of various full and limited state feedback active systems showed that:

1- The methods used to obtain the control laws are restricted to the assumptions that the ground is represented by either integrated or filtered white noise (implying $\kappa=2$ in eqn. 1.1). However, in vehicle performance calculations, the ground surface was modelled by a Gaussian process (eqn. 1.1) with ($\kappa=2.5$ and $\lambda_0 = 0.01$ cycle/m). For these conditions, the assumption of filtered white noise in deriving the control law was found to result in superior performance to that obtained for the integrated white noise case.

2- Feedback of the absolute displacement and velocity of the body bounce, pitch and roll instead of those of the suspension

to body connection points has no influence on the system performance. However, in practice, it is likely that measurement of the absolute displacements and velocities at the connection points is more attractive than the measurements based at the vehicle c.g.

3- Including the wheelbase time delay in deriving the control law was found to improve dramatically the performance of the active systems. For the full state feedback active systems, it is shown that it is possible to reduce the r.m.s. value of the rear dynamic tyre load by 45% with considerable reductions in the vertical and longitudinal accelerations (around 14% and 20% respectively for 3 cm working space).

4- The practical limitations of realising the control laws of these full state feedback systems in practice were discussed. A practical method was suggested to overcome the problems arising from the need to collect information at the rear wheels to derive the front control forces. In this, the optimal control law was replaced with a sub-optimal one which does not depend on this information. This sub-optimal control law causes only a slight increase in the lateral seat acceleration in the case where the working space is most limited. Furthermore, the most practical problem arising in the systems which account for the time delay from introducing new states which can not be measured directly is discussed. It is shown that these states can be calculated on-line providing that accurate road input information and sufficient processing power are available.

The novel application of the gradient search technique in deriving the control law of an active system which incorporates the effect of the time delay showed the following:

1- It is possible to generate control laws which account for the wheelbase time delay without the need to estimate the time delay states (using the Kalman filter algorithm) or to calculate them on line. Furthermore, the road input information is omitted from these control laws. This approach, therefore, results in the most practical control laws proposed to date which account for the wheelbase time delay.

2- The results generated from this approach (Chapter 7), showed that this system significantly improves the seat accelerations and the dynamic tyre load when compared with a limited state feedback active system which requires exactly the same measurements but does not account for the time delay.

The analysis of the performance capabilities of the active systems which have control strategies based on the Kalman filter algorithm showed the following:

1- As the measurement errors increased, the suspension performance deteriorated. For example, in system L_c (which requires measurements of wheel to ground displacements and body to wheel displacements and velocities), as sensor random error increased from 0.001 to 0.00408, the vertical, lateral and longitudinal accelerations are increased by 8%, 21% and 16% respectively.

2- The results showed that these active systems are more sensitive to the measurement errors than the number of the states to be measured.

3- A practical method to overcome the problems arising from the need to measure the wheel-ground relative displacements in system L_c and L_e has been proposed. In this method, the measurement system is modified to allow these relative displacements to be estimated after measuring the vertical acceleration of the body and wheel connection points.

4- The effect of including the wheelbase time delay in deriving the control laws for the case of noisy measurements was obtained. The results showed that the inclusion of the time delay substantially improves the performance of the active system. This improvement was not affected significantly as the sensor random error increased.

In Chapter 8, the performance analyses of the systems considered at 30 m/s showed that:

1- The full state feedback active system e (filtered white noise case with time delay) was found to give the best overall performance.

2- Active systems show a greater percentage improvement over the passive system as the available working space is reduced.

3- The limited state feedback active system L_b (which uses gradient search method with time delay and only requires measurements of the body and wheel absolute displacements and velocities) has a performance level approaching that of the full state feedback active system e .

4- For the limited state feedback active system L_f (which is based on the Kalman filter algorithm, only requires measurements of the wheel-body relative velocities and accounts for the time delay) it was found that this system

also performed very closely to the full state feedback active system e . In contrast with the limited state feedback system L_b , the system L_f has two additional requirements: firstly, an estimate of the sensor random error and its subsequent use to select (based on the vehicle speed and road roughness combination) the filter gains stored in the vehicle computer and secondly, an updating of the optimum estimates of the non-measurable states at small, discrete steps as time progresses. Although these requirements can in principle be realised in practice (see section 7.5), active system L_b still looks less complicated from a practical viewpoint.

Results generated to study the effect of the system adaptation (Chapter 3, 6 and 8) showed that:

- 1- Significant improvements in the seat accelerations could be achieved from the active and adaptive passive system when compared with the fixed parameter passive system.
- 2- The fixed parameter active system au (worst performing active system) was found to perform only slightly better than the adaptive passive system. If the adaptive active systems a and b (which involve the integrated white noise and filtered white noise case respectively and do not account for the time delay) are employed, further improvements in the seat accelerations could be achieved. However, even these two systems do not represent the best that can be achieved because even further gains can be obtained if the time delay is included in the control law derivation.
- 3- In general, suspension adaptation is a dominant feature behind the overall performance improvements available with

controlled suspensions. However, whereas it is, in principle at least, a simple matter to make the active system adaptive - it relies typically on changing gains in the microprocessor controller - it is a much bigger problem to make the passive system adaptive. In particular, an attractive method of varying the stiffness without producing high dynamic forces is required.

9.2 Future work

In order to obtain further insight into the design of control strategies and the analysis of the performance capabilities of other active systems, further investigation still remains. The list of such work includes the following:

- 1- From a practical viewpoint, the concept of using slow and semi active suspension systems looks attractive. In the literature, control strategies for these systems which consider the time delay between the front and rear inputs have not yet received attention.
- 2- Almost all the studies carried out on the active systems have been concerned with the ride behaviour. Theoretical studies to investigate the performance of active systems in providing vehicle stability and directional control during handling manoeuvres should be given more attention.
- 3- The use of preview information appears very promising in providing further improvements. However, most of the strategies available are difficult to realise in practice because of the large amount of information which must be calculated on-line within a short period of time. Further

work is needed, therefore, in this field.

4- It is not known yet, whether the improvements achieved from including the time delay in deriving the control will be associated with a reduction or increase in actuator power. In future studies, the performance indices should be extended to identify the power required in the actuators of various active systems.

5- Experimental investigations based on the quarter car model test rigs are important for judging sub-optimal active systems, but systems on full cars involve further considerations. Further testing and experimentation on such systems is likely to involve fitting prototype systems to practical vehicles and generating results in response to laboratory, or road inputs.

NOMENCLATURE

The following is a set of symbols used throughout the thesis. The meanings of all other symbols are defined explicitly within the text.

| Symbol | Description |
|-----------------------------------|--|
| a, b, c, d, e, g | full state feedback active systems |
| A | state matrix in first-order equations of motion |
| a_0, a_1, \dots, a_N | Pade approximation constants |
| A_η, B_η, C_η | Pade approximation matrices in the state space representation |
| B | coefficient matrix in first-order equations of motion |
| B_2, B_3, B_w | input matrices in first-order equations of motion |
| B_4 | coefficient matrix of non-linear forces in first-order equations of motion |
| C, H | output matrices in first order equations of motion |
| C_f, C_r | front and rear damping coefficients $kN.s/m$ |
| d_s | displacements across connecting elements |
| D | wheelbase time delay s |
| $d_1, d_2, g_1, g_2, S_0, \alpha$ | constants of the shaping filter |
| DR | damping ratio |

| | |
|---|--|
| e_r | vector of estimation error |
| E | excitation amplitude vector |
| f | frequency cycle/sec (Hz) |
| F_{DTL} | r.m.s. front dynamic tyre load N |
| F_{DTT} | r.m.s. fore/aft dynamic tyre load transfer |
| fn | natural frequency Hz |
| F_p | vector of passive suspension and tyre forces |
| f_t | vector of non-linear forces |
| I | identity matrix |
| I_p | pitch moment of inertia kgm^2 |
| IPL | input profile length m |
| I_r | roll moment of inertia kgm^2 |
| J | performance index |
| $K, K_H, K_x, K_{x_0}, \hat{K}_{x_0}, K_\eta$ | matrices of feedback gains |
| K_1 | modified Bessel function of the second kind |
| K_f, K_r | front and rear stiffness coefficients of the passive suspension springs kN/m |
| K_k | matrix of Kalman filter gains |
| K_{rf}, K_{rr} | front and rear stiffness coefficients of the anti-roll bars kN/m |
| K_t | tyre spring stiffness kN/m |
| L | vehicle wheelbase m |
| $L_a, L_b, L_c, L_d, L_e, L_f$ | limited state feedback active systems |
| $LDTT$ | r.m.s. lateral dynamic tyre load transfer |

| | |
|------------------|---|
| M_b | sprung mass kg |
| M_c, M_k | matrices containing damping and stiffness coefficients respectively in second-order equations of motion |
| M_f, M_{f1} | connection matrices in second-order equations of motion |
| M_U, M_{UD} | input matrices in second-order equations of motion |
| M_{wf}, M_{wr} | front and rear unsprung masses kg |
| M_X, M_{XD} | matrices of stiffness and damping coefficients in second-order equations of motion |
| M_{XDD} | matrix of masses and inertias in second-order equations of motion |
| n | system order in second-order equations of motion |
| N | Pade approximation order |
| n_1 | system order in first-order equations of motion |
| N_p | number of points in the input profile |
| P_o | filter error covariance matrix |
| $psd(\lambda)$ | amplitude spectral density of ground profile as a function of wave number, λ |
| q | road intensity |
| Q, R | weighting matrices |
| R_c | road roughness coefficient |
| $RDTL$ | r.m.s. rear dynamic tyre load N |
| r.m.s. | root mean square |

| | |
|-------------------------------------|---|
| S_u | input spectral density matrix |
| S_x | output spectral density matrix |
| sws | r.m.s. suspension working space cm |
| sws_f, sws_r | r.m.s. front and rear suspension working spaces cm |
| T | sampling time sec |
| t_s | half suspension track m |
| $T_U, T_{UD}, T_X, T_{XD}, T_{XDD}$ | output matrices in second-order equations of motion |
| t_w | wheel track m |
| u | vector of control forces |
| V | vehicle speed m/s |
| v_f, v_r | front and rear white noise signals |
| v_a | vector of measurement error |
| V_a | covariance matrix of the vector v_a |
| w | vector of white noise processes |
| W | covariance matrix of the white noise vector w |
| w_a | horizontal distance from body centre to front wheels m |
| w_b | horizontal distance from body centre to rear wheels m |
| x | state vector in first-order equations of motion |
| x_1, x_3 | vertical displacement of the front unsprung masses |
| x_2, x_4 | vertical displacement of the sprung mass at the front connection points |

| | |
|--------------------------------------|---|
| x_5, x_7 | vertical displacement of the rear unsprung masses |
| x_6, x_8 | vertical displacement of the sprung mass at the rear connection points |
| x_a | vector of the state variables x combined with the road inputs x_o |
| X_a | covariance matrix of the vector x_a |
| \hat{x}_a | optimal estimates of the state variables x_a |
| x_o | vector of road inputs |
| x_{o_1}, x_{o_2} | front road input displacements |
| x_{o_3}, x_{o_4} | rear road input displacements |
| X_s, Y_s, Z_s | horizontal, lateral and vertical distances from driver's seat position to the vehicle body centre |
| $\ddot{x}_x, \ddot{y}_x, \ddot{z}_x$ | r.m.s. longitudinal, lateral and vertical seat accelerations |
| y | output vector in first order equations of motion |
| y_z | output vector in second order equations of motion |
| z | state vector in second order equations of motion |
| z_b | vertical motion of the sprung mass c.g. |
| z_r | the series of spot heights at regular intervals along the track |
| $Z(\omega)$ | matrix of the frequency responses |
| γ_c | coherence function |

| | |
|---------------------|---|
| ζ_f, θ_f | uncorrelated random functions resulting from the application of first order shaping filters in generating road profiles |
| η | time delay states |
| θ | pitch motion of the sprung mass <i>rad</i> |
| θ_k | a set of independent random phase angles uniformly distributed between 0 and 2π . |
| κ | road surface exponent |
| λ | wave number <i>cycle/m</i> |
| λ_o | cutoff wave number <i>cycle/m</i> |
| ϕ | roll motion of the sprung mass <i>rad</i> |
| ω | frequency <i>rad/sec</i> |
| Ω | spatial frequency <i>rad/m</i> |

List of references

- Abdel Hady, M.B.A. and Crolla, D.A. [1989]** "Theoretical analysis of active suspension performance using a four-wheel vehicle model". Proc. Instn. Mech. Engrs Vol 203 pp. (125-135).
- ADAMS [1984]** "Users guide, fifth edition".
- Athans, M., and Falb, P.L. [1966]** "Optimal control". McGraw-Hill, New York
- Barak, P. and Sachs, H. [1985]** "On the optimal ride control of a dynamic model for an automotive vehicle system". Proc. 9th IAVSD Symposium on the Dynamics of Vehicles on Roads and on Railway Tracks (Ed.O.Nordstrom), pp. (15-29).
- Barak, P. and Hrovat, D. [1988]** "Application of the LQG approach to design of an automotive suspension for three-dimensional vehicle models". International Conference on Advanced suspensions, London, October, pp. (11-26).
- Bryson, Jr. and A. E.; Yu-Chi Ho, [1975]** "Applied Optimal Control", John Wiley and Sons.
- Cebon, D. and Newland, E.D. [1983]** "The artificial generation of road surface topography by the inverse FFT method". Proc. 8th IAVSD Symposium on Dynamics of Vehicles on Roads and on Railway Tracks (Ed. J.K.Hedrick), Cambridge, MA, pp. (29-42).
- Chalasanani, R. M. [1986 a]** "Ride performance potential of active suspension systems- Part I : simplified analysis based on a quarter car model". ASME symposium on simulation and control of ground vehicle and transportation systems (Eds L. Segel, J.Y. Wong, E.H. Law and D. Hrovat), papers AMD-Vol. 80, DSC-Vol 2, pp. (187-204).
- Chalasanani, R. M. [1986 b]** "Ride performance potential of active suspension systems- Part I : comprehensive analysis based on a full-car model". ASME symposium on simulation and

control of ground vehicle and transportation systems (Eds L. Segel, J.Y. Wong, E.H. Law and D. Hrovat), papers AMD-Vol. 80, DSC-Vol 2, pp. (187-204).

Crolla, D.A. and Abouel-Nour, A.M.A. [1988] "Theoretical comparison of various active suspension systems in terms of performance and power requirements". International Conference on Advanced Suspensions, London, October, pp. (1-9).

Fruhauf, F., Kasper, R. and Luckel, J. [1985] "Design of an active suspension for a passenger vehicle model using input processes with time delays". Proc. 9th IAVSD Symposium on the Dynamics of Vehicles on Roads and on Railway Tracks (Ed.O.Nordstrom), pp. (126-136).

Goodall, R.M. and Kortum, W. [1983] "Active controls in ground transportation - a review of the state-of-the-art and future potential". Vehicle System Dynamics, vol. 12, pp. (225-257).

Golub, G.H., Nash, S. and Van Loan, C. [1979] "A Hessenburg-Schur method for the problem $ax + xb = c$ ". IEEE Transactions on Automatic Control, Vol AC-24, No. 6, pp. (909-913).

Hac, A. [1985] "Suspension optimisation of a 2-DOF vehicle model using a stochastic optimal control technique". J. Sound and Vibration, 100(3), pp. (343-357).

Hac, A. [1987] "Active control of vehicle suspension". Vehicle System Dynamics, vol. 16, pp. (57-74).

Healey, A.J., Nathman, E. and Smith, C.C. [1977] "An analytical and experimental study of automobile dynamics with random roadway input". Transaction of the ASME, Journal of Dynamic Systems, Measurement, and Control, December, pp. (284-292).

Hearn, A.C. [1985] "REDUCE user's manual", version 3.2. The Rand Corporation CA 90406.

Hedrick, J. K. and Firouztash, H. [1974] "The covariance propagation equation including time-delayed inputs". IEEE Transactions on Automatic Control, Vol AC-19, No. 5, pp. (587-589).

Hedrick, J. K. and Wormley, D. N. [1975] "Active suspension for ground transportation vehicles- A state-of-the-art review". Mechanics of Transportation Systems, AMD, Vol. 15, ASME, pp. (21-40).

Horton, D., [1986] "An introduction to ride analysis in vehicle dynamics". Research Report DAC12, Dept. of Mechanical Engineering, Leeds University.

International Standard ISO 2631, [1974], [1978], [1978/A1], [1982] "Guide for the evaluation of human exposure to whole-body vibrations", International Standards Organization.

Kalman, R. E. and Bucy, R. S. [1961] "New results in linear filtering and prediction theory". Trans. ASME, J. Basic Eng. 83, pp. (95-101).

Kuo, B.C. [1981] "Automatic control systems". Prentice - Hall

Louam, N., Wilson, D.A. and Sharp, R.S. [1988] " Optimal control of a vehicle suspension incorporating the time delay between front and rear wheel inputs". Vehicle System Dynamics, 17, pp. (317-336).

Malek, K. M. and Hedrick, J. K. [1985] "Decoupled active suspension design for improved automotive ride quality/handling performance". Proc. 9th IAVSD Symposium on the Dynamics of Vehicles on Roads and on Railway Tracks (Ed.O.Nordstrom), pp. (383-398).

MEDYNA [1986] "An interactive analysis and design program for flexible multibody vehicle systems". Proc. of the 3rd ICTS Course and Seminar on Advanced Vehicle System Dynamics, Amalfi, Italy

Morman, K. N. and Giannopoulos, F. [1982] "Recent advances in the analytical and computational aspects of modelling active and passive vehicle suspensions". ASME Applied Mechanics Symposia, AMO Vol. 50 Computational Methods in Ground Transportation Vehicles, Ed. M. Kamal and J. Wolf.

Muller, P.C. [1982] "Mathematical methods in vehicle dynamics". Dynamics of High Speed Vehicle, CISM Courses and Lectures No. 274, (Ed W.O.Schiehlen), pp. (50-81)

NAG. [1987] "The numerical algorithms group Fortran library - mark 13". Europe and elsewhere, excluding North America and Australia. NAG Ltd, Wilkinson House, Jordan Hill Road, Oxford, U.K. OX2 8DR.

Newland, D.E. [1984] "An introduction to random vibrations and spectral analysis". Second Edition, Longman.

Rill, G. [1983] "The influence of correlated random road excitation processes on vehicle vibration". Proc. 8th IAVSD Symposium on the Dynamics of Vehicles on Roads and on Railway Tracks, pp. (449-459).

Robson, J.D. [1979] "Road surface description and vehicle response". International J. of Vehicle Design, vol. 1, pp. (25-35).

Ryba, D. [1974 a] "Improvements in dynamics characteristics of automobile suspension systems, (Part I, Two Mass System)". Vehicle System Dynamics, 3, pp. (17-46).

Ryba, D. [1974 b] "Improvements in dynamics characteristics of automobile suspension systems, (Part II, Three Mass System)". Vehicle System Dynamics, 3, pp. (55-98).

Sharp, R.S. and Hassan, S.A. [1984] "The fundamentals of passive automotive suspension system design". Society of Environmental Engineers Conference on Dynamics in Automotive Engineering, Cranfield Inst. Tech., pp. (104-115).

Sharp, R.S. and Hassan, S.A. [1986 a] "The relative performance capabilities of passive, active and semi-active car suspension systems". Proc. Instn. Mech. Engrs, 200, D3, pp. (219-228).

Sharp, R.S. and Hassan, S.A. [1986 b] "An evaluation of passive automotive suspension systems with variable stiffness and damping parameters". Vehicle System Dynamics, 15, pp. (335-350)

Sharp, R.S. and Crolla, D.A. [1987a] "Road vehicle suspension design - a review". Vehicle System Dynamics, 16, pp. (167-192).

Sharp, R.S. and Crolla, D.A. [1987b] "Intelligent suspension for road vehicles - current and future developments". Proc. E.A.E.C. Conference on New Developments in Power Train and Chassis Engineering, Strasbourg, 2, pp. (579-601).

Sharp, R.S. and Hassan, S.A. [1987 a] "On the performance capabilities of active automobile suspension systems of limited bandwidth". Vehicle System Dynamics, 16, pp. (213-225).

Sharp, R.S. and Hassan, S.A. [1987 b] "Performance and design considerations for dissipative semi-active suspension systems for automobiles". Proc. Instn. Mech. Engrs, 201(D2), pp. (1-5).

Sharp, R.S. and Wilson, D.A. [1989] "The generation of control laws for active and semi-active vehicle suspension systems via linear optimal control theory". Proc. of Inst of Math. and its Applications Conf. on Math. in the Automotive Industry, University of Warwick.

Thompson, A.G. [1976] "An active suspension with optimal linear state feedback". Vehicle System Dynamics, 5, pp. (187-203).

Thompson, A.G. and Pearce, C.E.M. [1979] "An optimal suspension for an automobile on a random road, Society of Automotive Engineers paper 790478.

Thompson, A.G. [1984] " Optimal and sub-optimal linear active suspensions for road vehicles". Vehicle System Dynamics, 13, pp. (61-72).

VDAS [1988] Horton, D. " Vehicle dynamic analysis software". Version 2.1, Dept. of Mechanical Engineering, Leeds University.

Wilson, D.A., Sharp, R.S. and Hassan, S.A. [1986] "Application of linear optimal control theory to the design of automobile suspensions". Vehicle System Dynamics, 15, pp. (105-118).

Wilson, D.A., Sharp, R.S. and Hassan, S.A. [1987] "Reply to comments by A.G. Thompson on the paper: Application of linear optimal control theory to the design of automobile suspensions, Vehicle System Dynamics, 15, pp. (105-118)". Vehicle System Dynamics, 16, pp. 105